

General Disclaimer

One or more of the Following Statements may affect this Document

- This document has been reproduced from the best copy furnished by the organizational source. It is being released in the interest of making available as much information as possible.
- This document may contain data, which exceeds the sheet parameters. It was furnished in this condition by the organizational source and is the best copy available.
- This document may contain tone-on-tone or color graphs, charts and/or pictures, which have been reproduced in black and white.
- This document is paginated as submitted by the original source.
- Portions of this document are not fully legible due to the historical nature of some of the material. However, it is the best reproduction available from the original submission.

(NASA-TM-X-73208-Vol-2) AEROX: COMPUTER
PROGRAM FOR TRANSONIC AIRCRAFT AERODYNAMICS
TO HIGH ANGLES OF ATTACK. VOLUME 2:
COMPARISONS OF TEST CASES WITH EXPERIMENT
(NASA) 140 p HC A07/MF A01

N77-20023

Unclas
22810

CSCL 01A G3/02

**NASA TECHNICAL
MEMORANDUM**

NASA TM X-73,208

NASA TM X-73,208

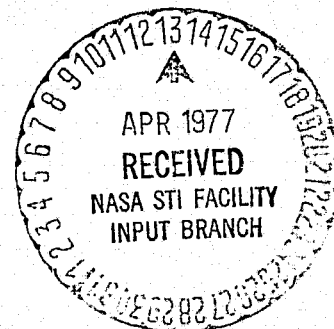
AEROX - COMPUTER PROGRAM FOR TRANSONIC AIRCRAFT

AERODYNAMICS TO HIGH ANGLES OF ATTACK

VOLUME II - COMPARISONS OF TEST CASES WITH EXPERIMENT

John A. Axelson

**Ames Research Center
Moffett Field, Calif. 94035**



February 1977

1. Report No. TM X-73,208	2. Government Accession No.	3. Recipient's Catalog No.	
4. Title and Subtitle AEROX — COMPUTER PROGRAM FOR TRANSONIC AIRCRAFT AERODYNAMICS TO HIGH ANGLES OF ATTACK VOLUME II — COMPARISONS OF TEST CASES WITH EXPERIMENT		5. Report Date	
		6. Performing Organization Code	
7. Author(s) John A. Axelson		8. Performing Organization Report No. A-6927	
		10. Work Unit No. 505-06-19	
9. Performing Organization Name and Address Ames Research Center Moffett Field, Calif. 94035		11. Contract or Grant No.	
		13. Type of Report and Period Covered Technical Memorandum	
12. Sponsoring Agency Name and Address National Aeronautics and Space Administration Washington, D. C. 20546		14. Sponsoring Agency Code	
		15. Supplementary Notes	
16. Abstract The theory, users' guide, test cases, and program listing are presented in the three volumes. The AEROX program estimates lift, induced-drag and pitching moments to high angles of attack (typ. 60°) for wings and for wing-body combinations with or without an aft horizontal tail. Minimum drag coefficients are not estimated, but may be input for inclusion in the total aerodynamic parameters which are output in listed and plotted formats.			
17. Key Words (Suggested by Author(s)) Aerodynamics Computer programming and software		18. Distribution Statement Unlimited STAR Categories — 02.	
19. Security Classif. (of this report) Unclassified	20. Security Classif. (of this page) Unclassified	21. No. of Pages 140	22. Price* \$5.75

TABLE OF CONTENTS — VOLUME II

SUMMARY	1
Test Cases	2
Data Presentation	2
DISCUSSION	2
Accuracy	2
Applicability	4
CONCLUSION	4
NOMENCLATURE	5
REFERENCES	8
TABLES I-IX. INPUTS FOR TEST CASES	9-17
FIGURES	
Figure 1.- Flow zones, and models indicated for test cases . . .	18-20
Figure 2.- F-4 aerodynamic estimates and data	21-25
Figure 3.- F-5 " " " "	26-32
Figure 4.- Model L " " " "	33-41
Figure 5.- Model A-1 " " " "	42-56
Figure 6.- Model A-2 " " " "	57-71
Figure 7.- Model A-3 " " " "	72-86
Figure 8.- Model A-4 " " " "	87-101
Figure 9.- Model A-5 " " " "	102-116
Figure 10.- Shuttle Orbiter	117-137

- A E R O X -

COMPUTER PROGRAM FOR TRANSONIC AIRCRAFT AERODYNAMICS
TO HIGH ANGLES OF ATTACK

VOLUME II

COMPARISONS OF TEST CASES WITH EXPERIMENT

John A. Axelson
Ames Research Center

Summary

The present Volume II presents comparisons of the estimated and experimental aerodynamics for nine aircraft configurations over a wide range of angles of attack and Mach numbers. The aerodynamic theory formulated for the AEROX program is documented in Volume I. Program operators should consult pages 15 through 19 of Volume I. A program listing and sample output tables and plots are shown in Volume III.

AEROX provides estimates of the lift, induced-drag and pitching-moment coefficients for wings, bodies, and for wing-body combinations with or without an aft horizontal tail. Both trimmed and untrimmed characteristics are estimated. Zero-lift drag coefficients (including friction, wave and propulsion-system additive drags) are not evaluated in AEROX, but may be input for inclusion in the output values of total drag coefficient and lift/drag ratio. The method is based on new, explicit aerodynamic formulations accounting for compressibility, transonic flow with strong shock waves and separation, and supersonic flow with detached leading-edge shock waves. The transonic airfoil mathematical model incorporates the Laitone limit Mach number criterion, with the chordwise location of the shock as an input parameter rather than an extracted solution. A new lift equation derived from the integration of downwash momentum is used for nonpotential flow regimes. The directness of this new, overall approach and the rapid execution time of the corresponding AEROX program are ideally suited for use in computerized aircraft preliminary designs and optimizations, and in activities dealing with aerodynamic instruction and research.

Test Cases

Validation of the AEROX program is presented in the form of comparisons of the estimated and experimental longitudinal aerodynamics for nine different aircraft configurations over the broad flight envelope shown in figure 1(a). Sketches of each configuration appear in figures 1(b) through 1(j), and the dimensional inputs are summarized in Tables I through IX. The test cases include the F4; the F5; a light-weight fighter configuration designated Model L; five related research models identified as A-1 through A-5; and the shuttle orbiter.

Data Presentation

The experimental results presented in figures 2 through 10 consist of static aerodynamic coefficients measured in wind tunnels and reported in references 1 through 7. Shown in the figures are lift curves (C_L versus α), drag polars (C_L versus C_D), and pitching-moment coefficients (C_m versus α or C_L). The AEROX program includes the option for estimating trimmed characteristics (ITRIM=1) up to 25° angle of attack. Comparisons of the AEROX trimmed estimates with the limited amount of available, trimmed-flight data indicate the same good agreement as displayed here with the estimated and measured static aerodynamics. The small numbers appearing on the plots identify the flow regime (fig. 1(a)) and the particular equations (vol. I) used in the estimation. Two sets of symbols for the same model identify different test conditions or model supports.

DISCUSSION

Accuracy

The formulations in the AEROX program constitute the only known analytical method for estimating transonic aircraft aerodynamics to maximum lift. No estimates are included for the effects of the propulsion system, such as the inlets, nacelles, nozzles or power-induced effects. Approximations are included for the contributions of the nose, afterbody, horizontal tail and wing leading-edge

chord extensions or strakes. In view of the complexity of the problem, and in light of the simplifications required in arriving at a rapid, practicable computer program, the goal for accuracy is realistically set at ± 5 percent of the maximum values of lift and drag coefficient, and ± 5 percent CBARW in the aerodynamic center location used in evaluation of the pitching-moment coefficients. Over 90 percent of the 117 pages of data comparisons presented here meet the goal. There is generally good agreement at all angles of attack.

Test points which differ from the estimates by greater than ± 5 percent do not necessarily infer errors in the program, but rather these differences can often be attributed to test procedure or model contours not appropriate to the present analysis. For example, the reduced lift measured for model L at the higher angles of attack at a Mach number of 1.8, (fig. 4(d)) is believed to stem in part from the relatively large model (1.5 ft. span) in the 4-foot supersonic wind tunnel.

Subsonic experimental lift coefficients which are well below the estimates are shown in figures 6(a,c), 7(a,c), and 8(a,c) for the related models A-2, A-3 and A-4. These lower experimental lift coefficients above 10° angle of attack can be attributed to the poor subsonic characteristics normally associated with the type of airfoil used on these models. For simplicity of construction, the sections were double beveled, flat airfoils with four essentially sharp ridge lines, which would tend to promote separation at subsonic speeds (but not at supersonic speeds). Note that in the case of model A-3, tail off, (fig. 7(a)), the flow apparently re-established itself above 30° angle of attack, and good agreement with estimate resulted. There was agreement at all angles of attack for models A-1 and A-5 at 0.6 Mach number (figs. 5(a), 9(a)). These models had the highest sweep angles for the leading edges and the ridge lines and experienced relatively little separation.

Because of the sharp ridge lines and almost sharp leading edges on the wings of models A-1 through A-5, the airfoil designator was set at ALELJ=1 for subsonic speeds. The small bluntness of the leading edges would promote detached bow shocks at supersonic speeds, so the value of ALELJ used was 5 for the supersonic estimates. The leading-edge radius has strong influence at transonic

speeds, but at supersonic conditions with detached bow shocks, it exerts no direct influence on lift in the present program. The leading-edge radius at these conditions (i.e., $Z=6$) continues to influence the wave drag and the C_{D0} values entered on the input sheets (Tables I - IX).

Applicability

The AEROX program provides estimates of longitudinal aerodynamics through maximum lift at all Mach numbers above those where low-speed, viscous stall predominates. The separate or combined characteristics of wings, bodies and tails are estimated. The program should also prove useful for augmenting, correlating, and validating limited or questionable samples of experimental data. Because of the low cost and versatility of the AEROX program and its parameterization capability, it constitutes a valuable aid for design, instruction and research activities.

CONCLUSION

The AEROX computer program provides estimates of lift and induced drag coefficients for aircraft (including maximum lift) at transonic and supersonic speeds with an accuracy generally within ± 5 percent of the maximum values. The accuracy for the estimated pitching-moment coefficients is generally within ± 5 percent of the wing mean aerodynamic chord for the aerodynamic center location. The AEROX program provides a valuable tool for estimating, correlating, augmenting and validating aerodynamic characteristics and is ideally suited to computerized design, instruction and research activities.

Nomenclature

The symbols appearing on the input and output listings of AEROX and on the enclosed figures are defined as follows:

ALJLJ,J	Input integer identifying type of airfoil ($1 \leq J \leq 5$). See AXE listing.
ALFTR	trimmed angle of attack (ITRIM=1), deg.
ALPHA,	angle of attack of wing reference plane, deg.
ALTV	input altitude, ft.
APLAN	plan area of nose, sq. ft.
ARH	input aspect ratio of horizontal tail
ARW	input aspect ratio of wing
ASECT	nose maximum cross-sectional area, sq. ft.
BDMAX	input body diameter, ft.
CBARW	wing mean aerodynamic chord, ft.
CDHOR	horizontal tail induced drag coefficient (ref. to wing area)
CDN	nose or body induced drag coefficient (ref. to wing area)
CD0	input wing minimum drag coefficient
CDOB	input additive drag coefficient (body, tail, propulsion system)
CDSEP	wing separation drag coefficient ($Z=4$)
CDTOT,CD	total drag coefficient
CDW	wing induced drag coefficient
CLHOR	horizontal tail lift coefficient (ref. to wing area)
CLN	nose or body lift coefficient (ref. to wing area)
CLO	input wing lift coefficient at zero angle of attack (subsonic)
CLOB	input additive lift coefficient (body, propulsion system)
CLTOT,CL	total lift coefficient
CLW	wing lift coefficient
CLWL	lift coefficient for wing lower surface
CLWU	lift coefficient for wing upper surface
CM,C _m	pitching-moment coefficient
CMO	input wing pitching-moment coefficient at zero angle of attack
CMOB	input additive pitching-moment coefficient (body, propulsion)
CROOT	wing root (C_r) chord, ft.
CTIP	wing tip chord, ft.
DALTR	increment of angle of attack to maintain C_L during trim, deg.

DELH	increment of tail deflection to trim, deg.
DLWING	wing lift-curve slope, per rad.
DWASH	downwash angle at horizontal tail, deg.
FTOTL	multiplying factor to change lift coefficient reference area
FTOTD	" " " " drag " " "
FCM	" " " " pitching-moment coefficient reference area or length
ICDO	input control integer for minimum drag; 0, CDO omitted; 1, input wing CDO included.
IFLEX	input control integer for strake bluntness; 0, sharp; 1, blunt.
ITRIM	input control integer for trim; 0, untrimmed; 1, trimmed ($\alpha \pm 25^\circ$)
IT	input horizontal tail incidence, deg.
IXCD	input control integer for limit shock position; 0, constant X/C; 1, limit shock sweep angle SHK specified from XCD at airplane centerline.
J,ALELJ	input integer identifying airfoil. See AXE listing.
L/D	lift/drag ratio when ICDO=1.
LE	tail length from moment center or center of gravity, ft.
LT	tail length from C _{BARW} /4, ft.
M,SMN	Mach number
RNLOC	Reynolds number per foot.
ROC	input leading-edge radius-to-chord ratio for J=5 airfoils.
SEXT	input area of forward wing-chord extensions (strakes), sq. ft.
SHK	input sweep angle of limit shock when IXCD=1), deg.
SHOR	input horizontal tail area, sq. ft.
SMN,M	Mach number
SPANW	wing span, ft.
SQH	input sweep angle of horizontal tail C/4 line, deg.
SQW	input sweep angle of wing C/4 line, deg.
SWING	input wing reference area, sq. ft.
SWPWLE	sweep angle of wing leading edge, rad.
TCRW	input thickness-to-chord ratio of wing root (C_r) chord
TCTW	input thickness-to-chord ratio of wing tip chord.
TRW	input wing taper ratio,
XCD	input designated chordwise location of limit shock, Z=4.
XCG	input longitudinal station of moment center or center-of-gravity, ft.
XEXT	input longitudinal station of centroid of wing chord extension SEXT, ft.

XLB input body length, ft.
XLN input nose length, ft.
XQHOR input longitudinal station of horizontal tail $C/4$, ft.
XQMAC input longitudinal station of wing $CBARW/4$, ft.
YHOR input horizontal tail height from wing chord plane, positive for
 high tail, ft.
Z integer identifying flow zone.

References

1. Woods, A. R., "Performance Data and Substantiation" McDonnell Aircraft Corporation, Dec. 1973.
2. Ackerman, N. G., and Warren, B. L., "F-5 Basic Aerodynamic Drag Data", Norair Report NOR 64-2, Northrop Corporation, January, 1964.
3. Levin, A. D., and Petroff, D. N., "An Experimental Investigation of Single and Double-Hinged Leading-Edge Flaps on a Model of an F-5A Aircraft at Transonic Mach Numbers", TMX-62,095, Jan. 1972, NASA.
4. Dollyhigh, S. M., "Subsonic and Supersonic Stability and Control Characteristics of an Aft-Tail Fighter Configuration with Cambered and Uncambered Wings and Uncambered Fuselage", NASA TMX-3078, 1974.
5. Jorgensen, L. H., and Nelson, E. R., "Experimental Aerodynamic Characteristics for Slender Bodies with Thin Wings and Tail at Angles of Attack from 0° to 58° and Mach Numbers from 0.6 to 2.0", TMX-3310, March 1976, NASA.
6. Esparza, V., and Embury, W. R., "Results of Investigations on an 0.015-Scale 140 A/B Configuration Space Shuttle Vehicle Orbiter Model (49-0) in the LTV 4- by 4-Foot High-Speed Wing Tunnel", NASA Contract NAS9-13247, DMS-DR-2037, NASA CR-134,405, August 1974.
7. Gillins, R. L., "Results of Investigations (OA77 and OA78) on an 0.015-Scale 140 A/B Configuration Space Shuttle Vehicle Orbiter Model 49-0 in the AEDC VKF B and C Wind Tunnels", NASA Contract NAS9-13247, DMS-DR-2134, NASA CR-134,429, January 1975.

TABLE I

INPUT FOR F4 TEST CASE (Fig. 2a-e)

(TITLE UP TO 56 CHARACTERS LONG) F4 TEST CASE (OVERPRINT)

KARRAYS

NSMN = 6

SHN = 0.40 , 0.90 , 1.00 , 1.20 , 1.60 , 1.95 ,

ICDD = 1

CDD = .0190 , .0200 , .0310 , .0420 , .0415 , .0410 ,

CMD = 6.*0. ,

CLOB = 6.*0. ,

CDOB = 6.*0. ,

CHOB = 6.*0. ,

ITRIM = 0 ,

BEND

SWINGIN

ALELJ = 3

MNARM = 2.82 , MXARM = 2.82 , INARM = 1.0 ,

MNTRM = 0.167 , MXTRM = 0.167 , INTRM = 1.0 ,

MNSOW = 45.0 , MXSOW = 45.0 , INSOW = 1.0 , CLO = 0.0 ,

SWING = 530.0 , SPANW = 38.41 , CRODT = 23.5 , CTIP = 3.117 ,

TCBW = 0.064 , TCTW = 0.030 , XOMAC = 25.763 , CBARM = 16.442 ,

ROC = 0 , SEXT = 0 , XEXT = 0 , IPLEX = 0 ,

BEND

KHOSEIN

BDMAX = 5.7 , XLN = 20.0 , XLB = 44.0 , XCG = 26.565 ,

BEND

KTAILIN

SHOR = 96.23 , XOMOR = 50.13 , ARM = 3.23 , SQH = 35.5 ,

YHOR = 1.75 , IT = 0 ,

BEND

KFLOWIN

MNALF = 2 , MXALF = 40 , INALF = 2 ,

MNXCDD = 0.35 , MXXCDD = 1.0 , INXCDD = 0.325 ,

IXCDD = 0 , SHK = 0 ,

ALTV = 35000 ,

BEND

KFACTOR

PTOTL = 1.0 , PTOTD = 1.0 , PCM = 1.0 ,

BEND

KOUTPUT

IDATA = 1 , ITABL = 1 ,

IPLOT = 1 , PPLOT = 1 ,

LDISP = 1 , 1 , 1 , 1 , 1 ,

DDISP = 1 , 1 , 1 , 1 ,

BEND

TABLE II
INPUT FOR F5 TEST CASE (Fig. 3a-g)

(TITLE UP TO 56 CHARACTERS LONG) ← F5 TEST CASE

BARARRAYS

NSMN = 5

SHN = 0.6 , 0.9 , 1.1 , 1.2 , 1.4 ,

ICDD = 1

CDD = 0.0212 , 0.0225 , 0.0470 , 0.0485 , 0.0490 ,

CHD = 5.*0. ,

CLO = 5.*0. ,

CDOR = 5.*0. ,

CHOB = 5.*0. ,

ITRIM = 0

SEND

SWINGIN

ALELJ = 1

MNARW = 3.75 , MXARW = 3.75 , INARW = 1.0 ,

MNTRW = 0.2 , MXTRW = 0.2 , INTRW = 1.0 ,

MNSQW = 24.0 , MXSQW = 24.0 , INSQW = 1.0 , CLO = 0.0 ,

SWING = 170. , SPANW = 25.25 , CRODT = 11.221 , CTIP = 2.244 ,

TCDW = 0.048 , TCTW = 0.045 , XOMAC = 25.99 , CDARW = 7.73 ,

ROC = 0. , SEXT = 0. , XEXT = 0. , IFLEX = 0 ,

SEND

ENDSEIN

BDMAX = 4.3 , XLN = 22.5 , XLB = 44.0 , XCG = 25.14 ,

SEND

STATLIN

SHOR = 59.0 , XOMOR = 38.96 , ARH = 2.88 , SQH = 25.0 ,

YHOR = 0.0 , IT = 0.0 ,

SEND

BFLOWIN

MNALF = 2.0 , MXALF = 40.0 , INALF = 2.0 ,

MNXCD = 0.35 , MXXCD = 0.675 , INXCD = 0.325 ,

IXCD = 0 , SHK = 0. ,

ALTV = 35000. ,

SEND

FACTOR

PTOTL = 1.0 , PTOTD = 1.0 , FCM = 1.0 ,

SEND

OUTPUT

IDATA = 1 , ITABL = 1 ,

IPLOY = 1 , PPLOY = 1 ,

LDISP = 1 , 1 , 1 , 1 , 1 , 1 ,

DDISP = 1 , 1 , 1 , 1 ,

SEND

TABLE III

INPUT FOR MODEL L TEST CASE (Fig.4a-i)

(TITLE UP TO 56 CHARACTERS LONG) ← MODEL L

BARAYS

NSMN = 4

SRN = 0.5 , 0.8 , 1.2 , 1.8 ,

ICDO = 1

CDD = 0.0210 , 0.0200 , 0.0360 , 0.0210

CHO = 4.*0.

CLOB = 4.*0.

COOB = 4.*0.

CHOB = 4.*0.

ITRM = 0

SEND

SWINGIN

ALEJ = 3

MNARW = 2.75

MXARW = 2.75

INARW = 1.0

MNTRW = 0.2

MXTRW = 0.2

INTRW = 1.0

MNSOW = 43.53

MXSOW = 43.53

INSOW = 1.0

CLO = 0.0

SWING = 752.398

SPANW = 45.552

CRODT = 27.5

CTIP = 5.504

TCRW = 0.045

TCTW = 0.045

XOMAC = 32.2

CBARW = 19.185

ROC = 0

SEXT = 0

XEXT = 0

IFLEX = 0

SEND

EMOSEIN

EDMAX = 5.8

XLN = 25.0

XLB = 62.07

XCG = 37.4

SEND

KYATLIN

SHOR = 256.2

XOMOR = 12.8

ARH = 2.912

SGH = 37.5

YHOR = -2.286

IT = 0

SEND

EFLOWIN

MNALF = 2.0

MXALF = 40.0

INALF = 3.0

MNXCD = 0.35

MXXCD = 0.675

INXCD = 0.325

IXCD = 0

SHK = 0

ALTV = 35000

SEND

EFACOR

PTOTL = 1

PTOTD = 1

FCM = 1

SEND

ROUTPUT

IDATA = 1

ITABL = 1

IPLOT = 1

PPLOT = 1

LDISP = 1

1 , 1 , 1 , 1 , 1

DDISP = 1

1 , 1 , 1

SEND

ORIGINAL PAGE IS
OF POOR QUALITY

TABLE IV
INPUT FOR MODEL A-1 (Fig. 5a-0)

(TITLE UP TO 56 CHARACTERS LONG) ← MODEL A-1

ARRAYS

NSMN = 5 ,
SMN = 0.6 , 0.9 , 1.2 , 1.5 , 2.0 ,
ICDO = 1
† CDO = 0.0180 , 0.0200 , 0.050 , 0.0400 , 0.0340 ,
CMO = 5.*0. ,
CLO = 5.*0. ,
CDO = 5.*0. ,
CHOB = -0.01 , 0.0 , 0.0 , 0.0 , 0.0 ,
ITRM = 0
END

SWINGIN

* ALEJ = 1;5 ,
MNARW = 4.0 , MXARW = 4.0 , INARW = 1.0 ,
MNTRW = 0.0 , MXTRW = 0.0 , INTRW = 1.0 ,
MNSOW = 36.87 , MXSOW = 36.87 , INSOW = 1.0 , CLO = 0.0 ,
SWING = 108.16 , SPANW = 20.80 , CRODT = 10.4 , CTIP = 0.0 ,
TCBW = 0.0138 , TCTW = 0.100 , XOMAC = 13.0 , CBARW = 6.933 ,
* ROC = 0. ; 0.002 , SEXT = 0. , XEXT = 0. , IFLEX = 0 ,
END

ENDSETN

BDMAX = 2.6 , XLN = 9.1 , XLB = 26.0 OFF
21.58 , XCG = 13.0 ,
END

BTAILIN

SHOR = 42.25 , XOMOR = 22.4 , ARH = 4.0 , SQH = 22.5 ,
VHOR = 0.0 , IT = 0.0 ,
END

BFLOWIN

MNALF = 2.0 , MXALF = 40.0 , INALF = 2.0 ,
MNXCDO = 0.3 , MXXCDO = 0.9 , INXCDO = 0.3 ,
IXCDO = 0 , SHK = 0. ,
ALTV = 30000. ,
END

FACTOR

PTOTL = 1. , PTOTD = 1. , FCM = 1. ,
END

OUTPUT

IDATA = 1. , ITABL = 1. ,
IPLOT = 1 , PPLOT = 1 ,
LDISP = 1 , 1 , 1 , 1 , 1 , 1 ,
DDISP = 1 , 1 , 1 , 1 ,
END

4 DATA SETS CALCULATED (2 JS for Tail on & Tail off) FOR MODELS A-1 THRU A-5

* For J=1 ROC=0

J=5 ROC=.002

† TAIL ON CDO VALUE 2 SHOWN ABOVE. TAIL OFF CDO=.012,.014,.024,.023,.022.
SHOR=0.

TABLE V
INPUT FOR MODEL A-2 (Fig. 6a-0)

```

TITLE UP TO 56 CHARACTERS LONG ← MODEL A-2
BARRAYS
NSMN = 5
SHN = 0.6 , 0.9 , 1.2 , 1.5 , 2.0 ,
ICDO = 1.
CDO = 0.018 , 0.022 , 0.050 , 0.042 , 0.040 ,
CMO = 5. * 0. ,
CLO = 5. * 0. ,
COO = 5. * 0. ,
CMOB = 5. * 0. ,
ITRM = 0
BEND
BINGIN
ALELJ = 1.5 ,
MARM = 4.0 , MXARM = 4.0 , INARM = 1.0 ,
MTRW = 0.25 , MXTRW = 0.25 , INTRW = 1.0 ,
MNSQW = 24.23 , MXSQW = 24.23 , INSQW = 1.0 , CLO = 0.0 ,
SWING = 108.16 , SPANW = 20.80 , CRODT = 8.32 , CTIP = 2.28 ,
TCRW = 0.0172 , TCTW = 0.0688 , XOMAC = 13.832 , CBARW = 5.824 ,
ROC = 0.0 ; 0.002 , SEXT = 0. , XEXT = 0. , IFLEX = 0 ,
BEND
BNOSEIN
BDMAX = 2.6 , XLN = 10.65 , XLB = 20.0 10.5 , XCG = 12.832 ,
BEND
BYAILEIN
SHOR = 42.25 , XOMOR = 23.4 , ARM = 4.0 , SQH = 22.5 ,
YHOR = 0. , IT = 0. ,
BEND
BFLOWIN
MNALF = 2.0 , MXALF = 40.0 , INALF = 2.0 ,
MNXCD = 0.3 , HXXCD = 0.9 , INXCD = 0.3 ,
IXCD = 0 , SHK = 0. ,
ALTV = 30000 ,
BEND
BFACTOR
PTOTL = 1 , PTOTD = 1 , PCM = 1 ,
BEND
BOUTPUT
IDATA = 1 , ITABL = 1 ,
IPLOT = 1 , PPLOT = ,
LDISP = 1 , 1 , 1 , 1 , 1 , 1 ,
DDISP = 1 , 1 , 1 , 1 ,
BEND

```

TAIL OFF CDO = .012 , .012 , .027 , .024 , .025
SHK = 0.

TABLE VI
INPUT FOR MODEL A-3 (Fig. 7a-0)

TITLE UP TO 56 CHARACTERS LONG ← MODEL A-3

PARAMS

NSMN = 5,
SMN = 0.6 , 0.9 , 1.2 , 1.5 , 2.0 ,
ICDO = 1
CDO = 0.019 , 0.022 , 0.050 , 0.042 , 0.040 ,
CHO = 5.*0.,
CLOB = 5.*0.,
CDOB = 5.*0.,
CHOB = 5.*0.,
ITRM = 0
END

SWINGIN

ALEJ = 1, 5 ,
MARM = 4.0 , MXRM = 4.0 , INRM = 1.0 ,
MTRM = 0.5 , MTRM = 0.5 , INTRM = 1.0 ,
MNSW = 14.03 , MXSW = 14.03 , INSW = 1.0 , CLO = 0.0 ,
SWING = 102.16 , SPANW = 20.80 , CRODT = 6.93 , CTIP = 3.467 ,
TCRM = 0.0206 , TCTW = 0.0414 , XOMAC = 14.157 , CBARW = 5.311 ,
ROC = 0, 0.002 , SECT = 0 , XEXT = 0 , IFLEX = 0 ,
END

KNOWIN

BDMAX = 2.6 , XLN = 11.7 , XLB = 26.0 OFF
21.58 ON , XCG = 14.157 ,
END

VTAILIN

SHOR = 42.25 , XOMOR = 23.4 , ARM = 4.0 , SQH = 22.5 ,
YHOR = 0 , IT = 0 ,
END

FLOWIN

MNALF = 2.0 , MXALF = 40.0 , INALF = 2.0 ,
MNXCD = 0.3 , MXXCD = 0.9 , INXCD = 0.3 ,
IXCD = 0 , SHK = 0 ,
ALTV = 30.000 ,
END

FACTOR

PTOTL = 1 , PTOTD = 1 , FCM = 1 ,
END

OUTPUT

IDATA = 1 , ITABL = 1 ,
IPLOT = 1 , PPLOT = 1 ,
LDISP = 1 , 1 , 1 , 1 , 1 , 1 ,
DDISP = 1 , 1 , 1 , 1 ,
END

TAIL OFF CDO = 0.013 , 0.016 , 0.033 , 0.035 , 0.028 ,
SHOR = 0 ,

TABLE VII
INPUT FOR MODEL A-4 (Fig. 8a-0)

TITLE UP TO 56 CHARACTERS LONG ← MODEL A-4

BARARRAYS

NSMN = 5

SMN = 0.6 , 0.9 , 1.2 , 1.5 , 2.0 ,

ICDD = 1

CDD = 0.018 , 0.024 , 0.05 , 0.042 , 0.040 ,

CHD = 5 * 0 ,

CLOS = 5 * 0 ,

CDOS = 5 * 0 ,

CHOS = 5 * 0 ,

ITRIM = 0

END

SWINGIN

ALEJ = 1.5

MNARM = 5.0 , MXARM = 5.0 , INARM = 1.0 ,

MNTRW = 0.25 , MXTRW = 0.25 , INTRW = 1.0 ,

MNSOW = 19.8 , MXSOW = 19.8 , INSOW = 1.0 , CLO = 0.0 ,

SWING = 108.16 , SPANW = 23.26 , CRODT = 7.14 , CTIP = 1.86 ,

TCHW = 0.0192 , TCTW = 0.077 , XOMAC = 14.294 , CBARW = 5.208 ,

ROC = 0.0002 , SECT = 0 , XEXT = 0 , IFLEX = 0 ,

END

ENDSEIN

BDMAX = 2.6 , XLN = 11.38 , XLB = 26.7 ^{26.7} _{21.58} , XCG = 14.51 ,

END

STATLIN

SHOR = 42.25 , XOHOR = 23.4 , ARH = 4.0 , SQH = 22.5 ,

YHOR = , IT = ,

END

FLOWIN

MNALF = 2.0 , MXALF = 40.0 , INALF = 2.0 ,

MNXCD = 0.3 , MXXCD = 0.9 , INXCD = 0.3 ,

IXCD = 0 , SHK = 0 ,

ALTY = 30.000

END

FACTOR

PTOTL = 1 , PTOTD = 1 , FCM = 1 ,

END

OUTPUT

IDATA = 1 , ITABL = 1 ,

IPLOT = 1 , PPLOT = 1 ,

LDISP = 1 , 1 , 1 , 1 , 1 , 1 ,

DDISP = 1 , 1 , 1 , 1 ,

END

TAILOFF CDD = 0.013 , 0.016 , 0.034 , 0.036 , 0.028
SHOR = 0

TABLE VIII
INPUT FOR MODEL A-5 (Fig. 9a-o)

TITLE UP TO 56 CHARACTERS LONG ← MODEL A-5

KEYWORDS

NSHN = 5

SHN = 0.6 , 0.9 , 1.2 , 1.5 , 2.0 ,

ICDD = 1

CDD = 0.016 , 0.018 , 0.050 , 0.040 , 0.035 ,

CHD = 5 * 0 ,

CLOB = 5 * 0 ,

COOR = 5 * 0 ,

CHOB = 5 * 0 ,

ITRIM = 0

END

SWINGIN

ALEJ = 1.5

MNARM = 3.0 , MXARM = 3.0 , INARM = 1.0 ,

MNTRW = 0.25 , MXTRW = 0.25 , INTRW = 1.0 ,

MNSOW = 31.0 , MXSOW = 31.0 , INSOW = 1.0 , CLO = 0.0 ,

SWING = 108.16 , SPANW = 18.0 , CRODT = 9.6 , CTIP = 2.4 ,

TCHW = 0.0149 , TCTW = 0.0595 , XOMAC = 13.16 , CBARW = 6.72 ,

ROC = 0.0002 , SEXT = 0 , XEXT = 0 , IFLEX = 0 ,

END

ENDSEIN

BDMAX = 2.6 , XLN = 9.63 , XLB = 26.0 OFF ON 21.58 ON , XCG = 13.16 ,

END

STATIN

SHOR = 42.25 , XOMOR = 23.4 , ARM = 4.0 , SQH = 22.5 ,

YHOR = 0 , IT = 0 ,

END

FLOWIN

MNALF = 2.0 , MXALF = 40.0 , INALF = 2.0 ,

MNXCDD = 0.3 , MXXCDD = 0.9 , INXCDD = 0.3 ,

IXCDD = 0 , SHK = 0 ,

ALTY = 30000 ,

END

FACTOR

PTOTL = 1 , PTOTD = 1 , PCN = 1 ,

END

OUTPUT

IDATA = 1 , ITABL = 1 ,

IPLOT = 1 , PPLOT = 1 ,

LDISP = 1 , 1 , 1 , 1 , 1 ,

DDISP = 1 , 1 , 1 ,

END

TAIL OFF CDD=0.010,0.012,0.025,0.025,0.022,

SHOR=0.

TABLE IX
INPUT FOR SHUTTLE (Fig. 10a-u)

TITLE UP TO 56 CHARACTERS LONG ← SHUTTLE ORBITER

PARAMS

NSMN = 7.

SMN = 0.6 , 0.9 , 1.2 , 1.6 , 2.0 , 4.0 , 7.0 ,

ICDD =

COO = 0.064 , 0.086 , 0.176 , 0.160 , 0.143 , 0.093 , 0.065 ,

CHO = 7.0 ,

CLOS = -0.1 , -0.1 , -0.06 , -0.04 , -0.06 , -0.07 , 0.0 ,

COOR = 7.0 ,

CHOB = 0.06 , 0.08 , 0.08 , 0.04 , 0.02 , -0.01 , 0.0 ,

ITRIM = 0

END

EWINGIN

ALELJ = 2

MNARM = 2.26 , MXARM = 2.26 , INARM = 1. ,

MNTRW = 0.2 , MXTRW = 0.2 , INTRW = 1. ,

MNSOW = 35.2 , MXSOW = 35.2 , INSOW = 1. , CLO = 0.0 ,

SWING = 87.16 , SPANW = 14.05 , CROOT = 10.327 , CTIP = 2.062 ,

TCHW = 0.11 , TCTW = 0.11 , XOMAC = 13.49 , CBARW = 7.2 ,

ROC = 0. , SEXT = 37.7 , XEXT = 6.5 , IFLEX = 1 ,

END

ENDSEIN

BDMAX = 2.0 , XLN = 0. , XLB = 0. , XCG = 12.58 ,

END

KTATLIN

SHOR = 0.0 , XOMOR = 19.0 , ARH = 0. , SQH = 0. ,

YHOR = 0. , IT = 0. ,

END

EFLOWIN

MNALF = 2.0 , MXALF = 40.0 , INALF = 2.0 ,

MNXC0 = 0.5 , MXXC0 = 1.0 , INXC0 = 0.25 ,

IXC0 = 0 , SHK = 0. ,

ALTY = 50000 ,

END

EFACOR

PTOTL = 1. , PTOTD = 1. , PCN = 1. ,

END

OUTPUT

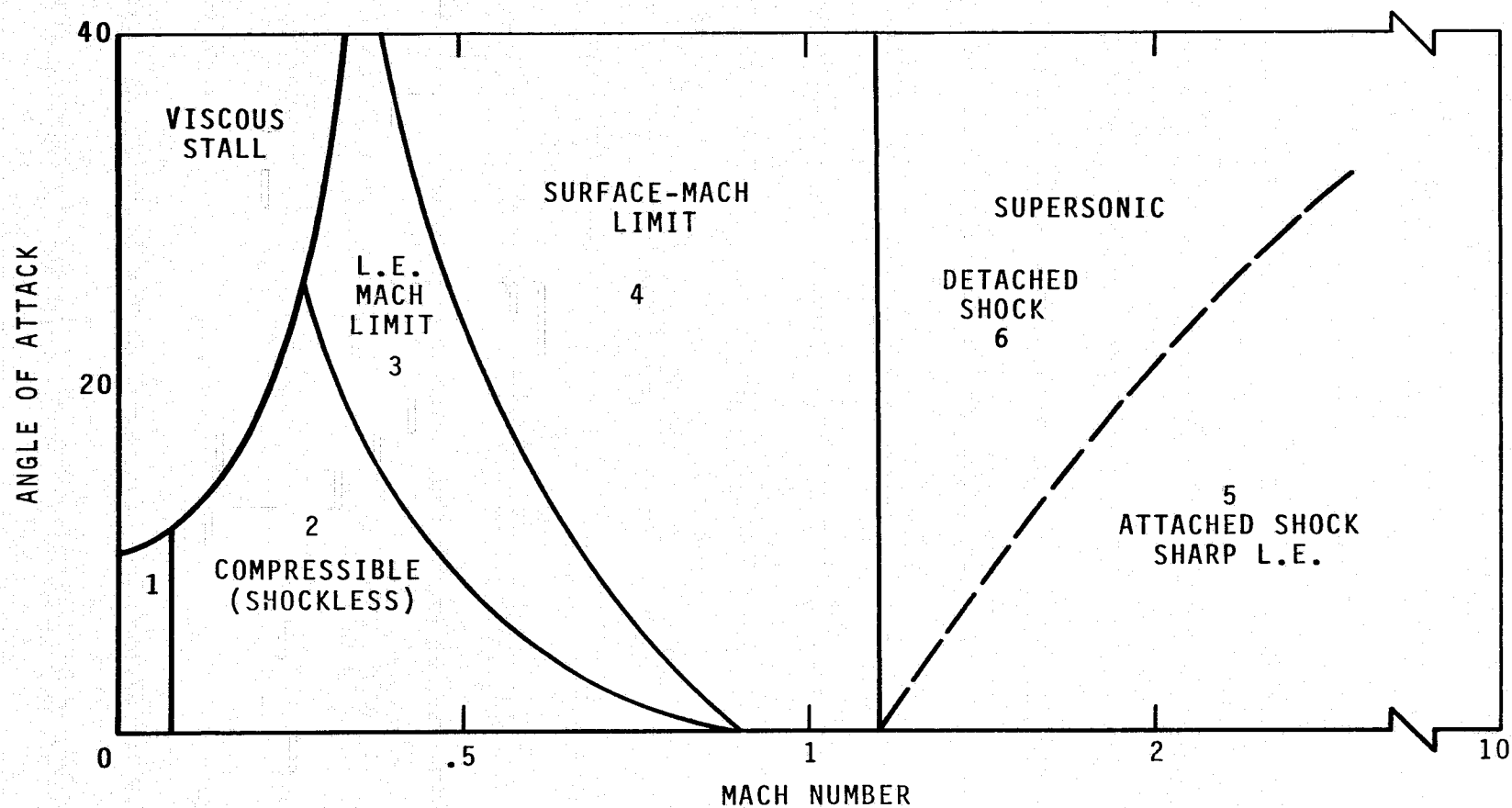
IDATA = 1 , ITABL = 1 ,

IPLOT = 1 , PFLDT = 1 ,

LDISP = 1 , 1 , 1 , 1 , 1 , 1 ,

DDISP = 1 , 1 , 1 , 1 ,

END



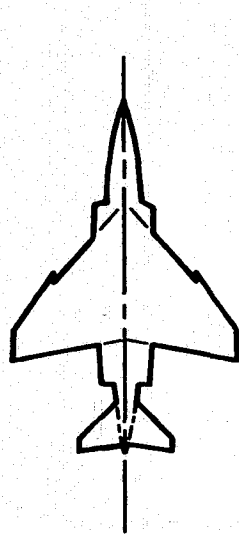
(a) FLOW ZONES.

FIGURE 1.- FLOW ZONES AND MODELS INDICATED FOR TEST CASES.

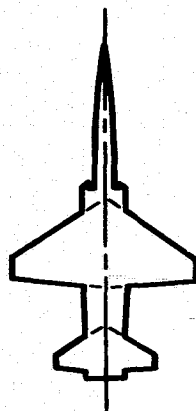
MODEL	F4	F5	L	A1	A2	A3	A4	A5	SHUTTLE
REFERENCE	1	2, 3	4	← 5 →					6, 7
INPUT TABLE	I	II	III	IV	V	VI	VII	VIII	IX
DATA FIGURE	2(a-e)	3(a-g)	4(a-i)	5(a-o)	6(a-o)	7(a-o)	8(a-o)	9(a-o)	10(a-u)
WING ASPECT RATIO	2.82	3.75	2.75	4.00	4.00	4.00	5.00	3.00	2.26
WING TAPER RATIO	0.17	0.20	0.20	0.00	0.25	0.50	0.25	0.25	0.20
NOMINAL α - RANGE	0° to 32°	0° to 22°	0° to 20°	← 0° to 60° →					0° to 33°
MACH NUMBERS	0.9, 1.2	0.6, 0.9, 1.1, 1.2	0.5, 0.8, 1.2, 1.8	← 0.6, 0.9, 1.2, 1.5, 2.0 →					0.6, 0.9, 1.2, 1.6, 2.0, 4.0, 8.0

(b) TEST CASE SUMMARY.

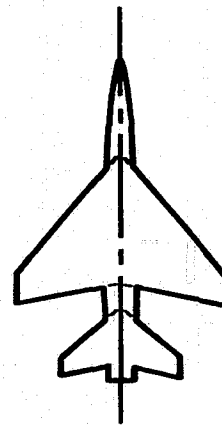
FIGURE 1.- CONTINUED.



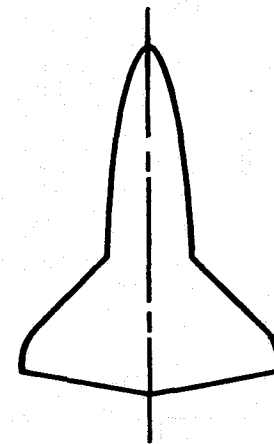
F4



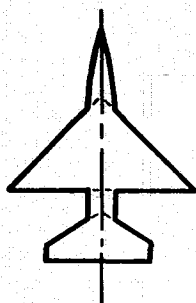
F5



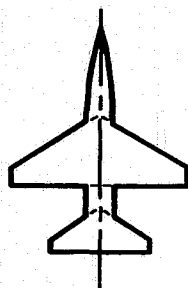
L



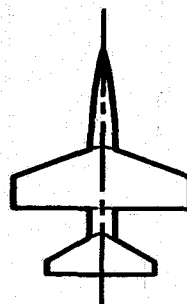
SHUTTLE



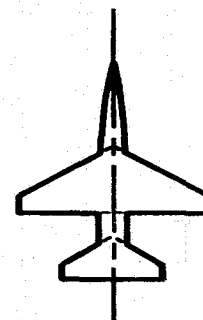
A1



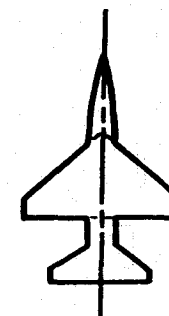
A2



A3



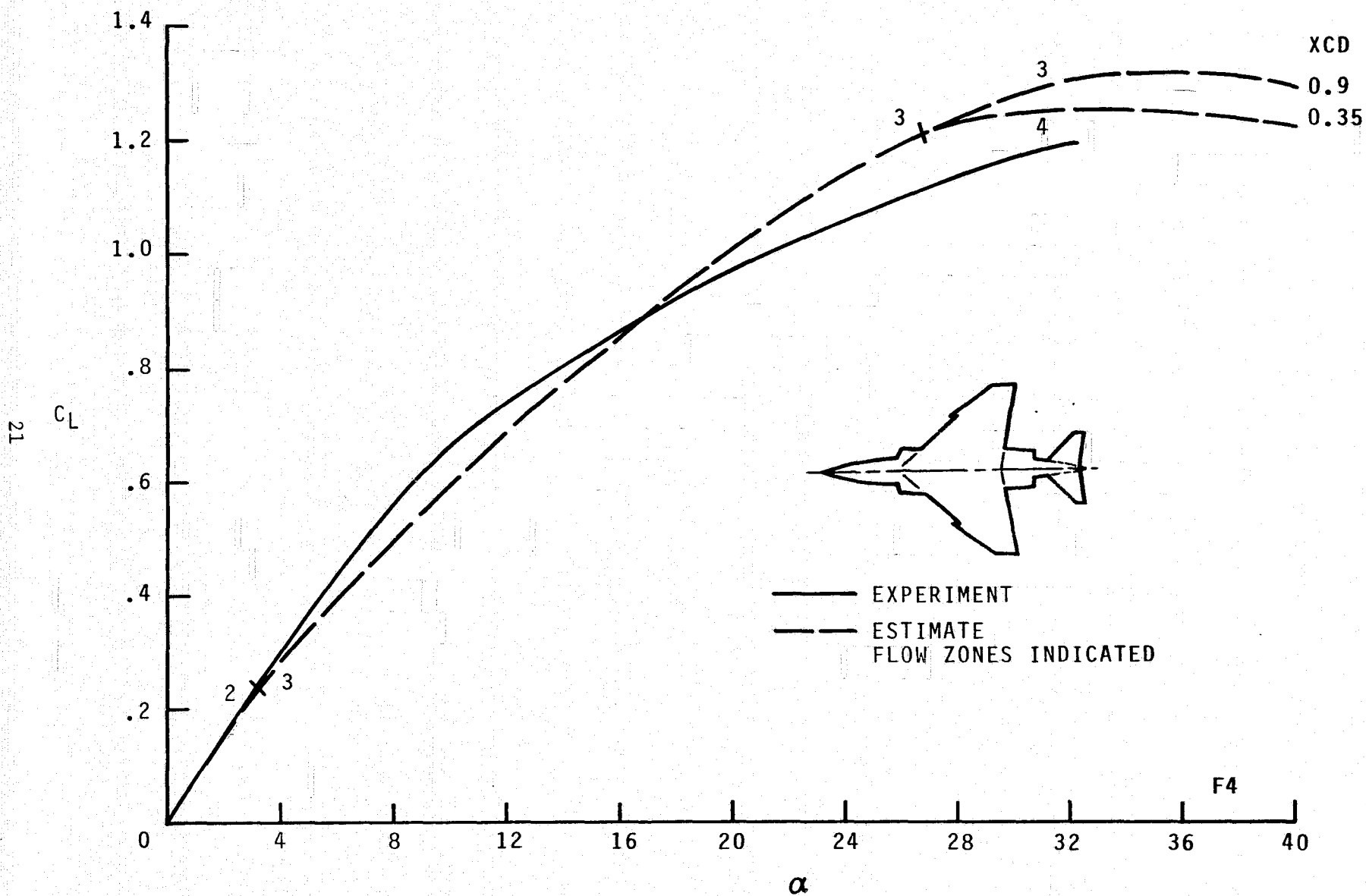
A4



A5

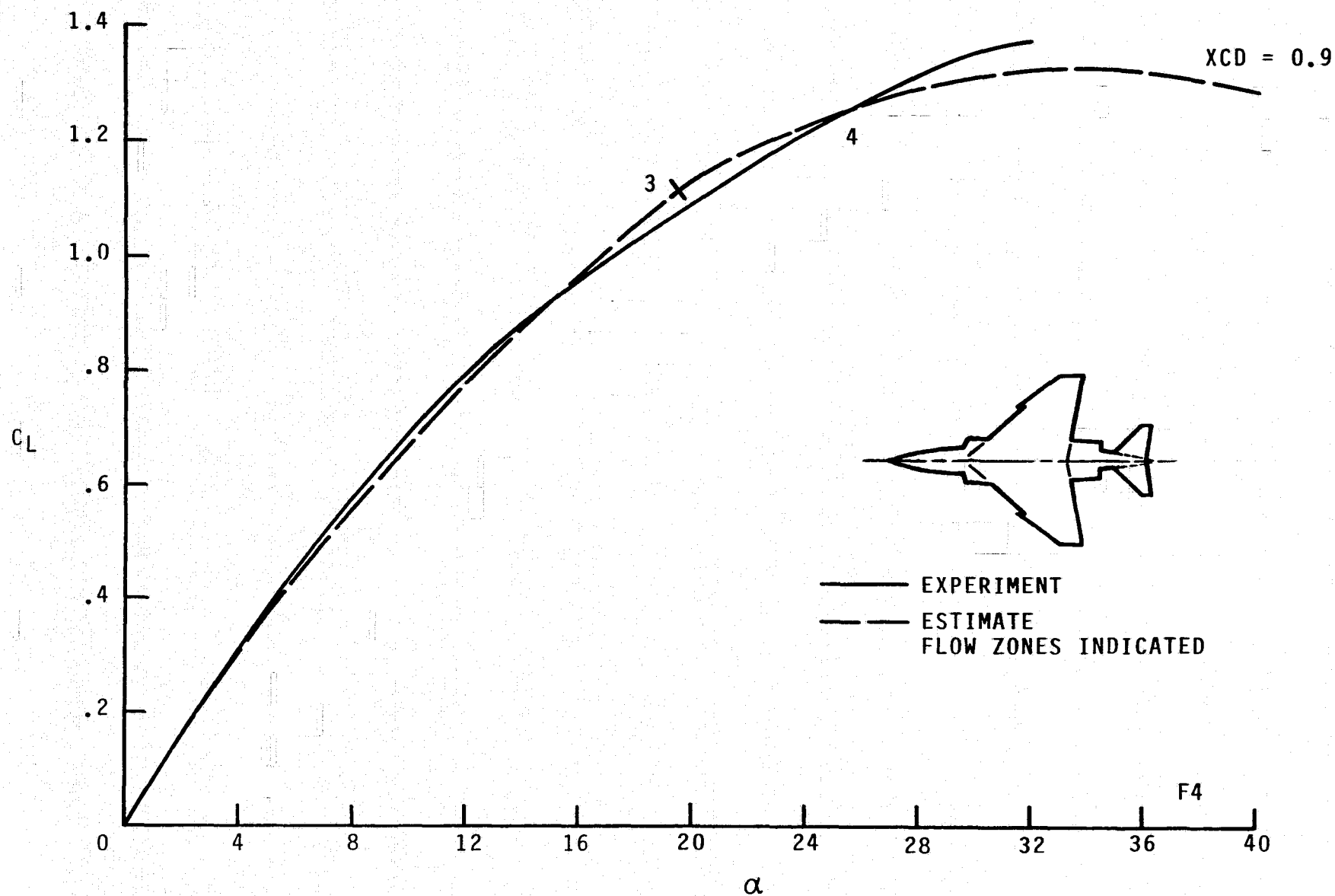
(c) MODEL SKETCHES.

FIGURE 1.- CONCLUDED.



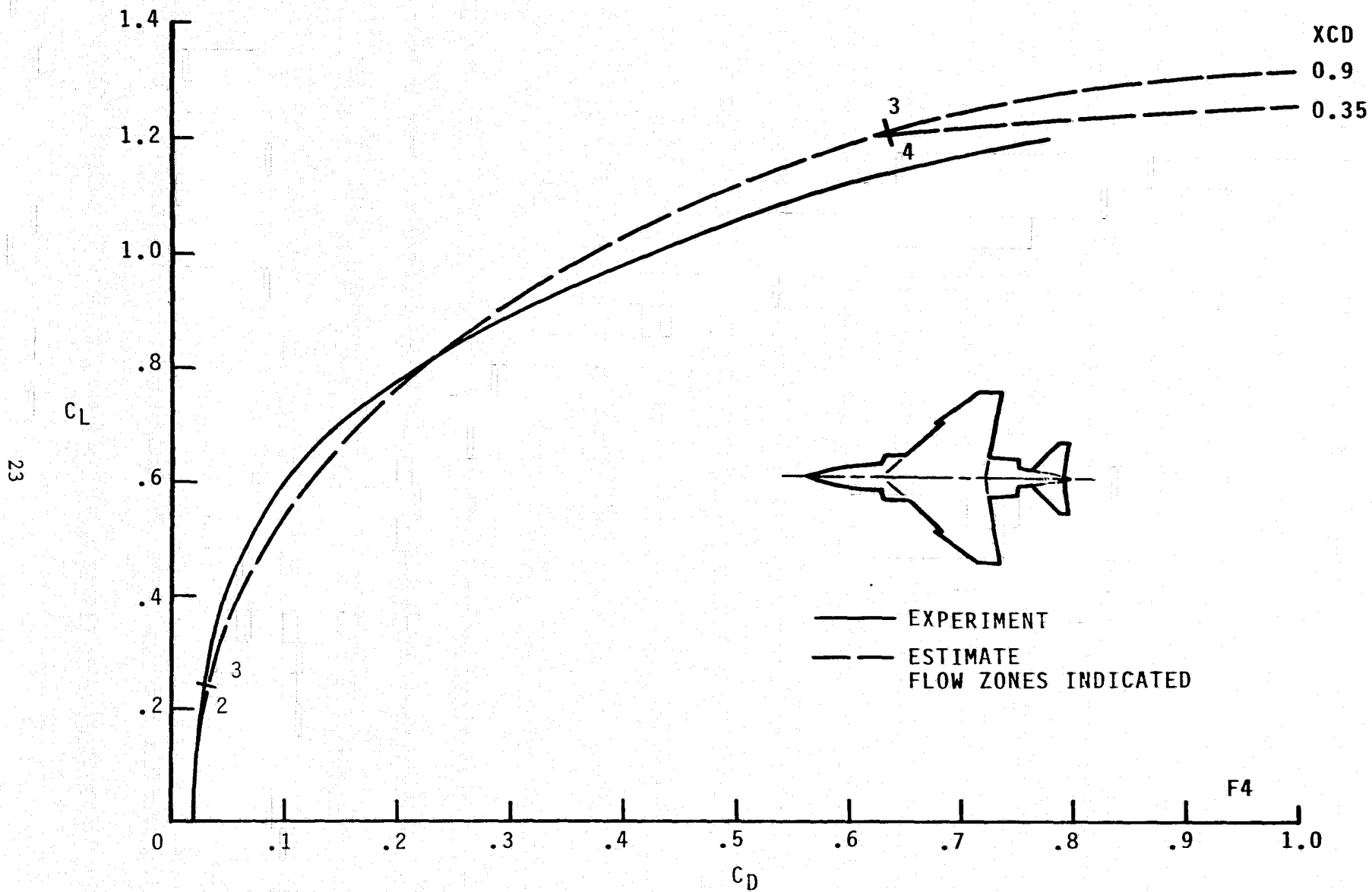
(a) C_L VERSUS α ; $M = 0.9$.

FIGURE 2.- AERODYNAMICS FOR THE F4; $J = 3$.



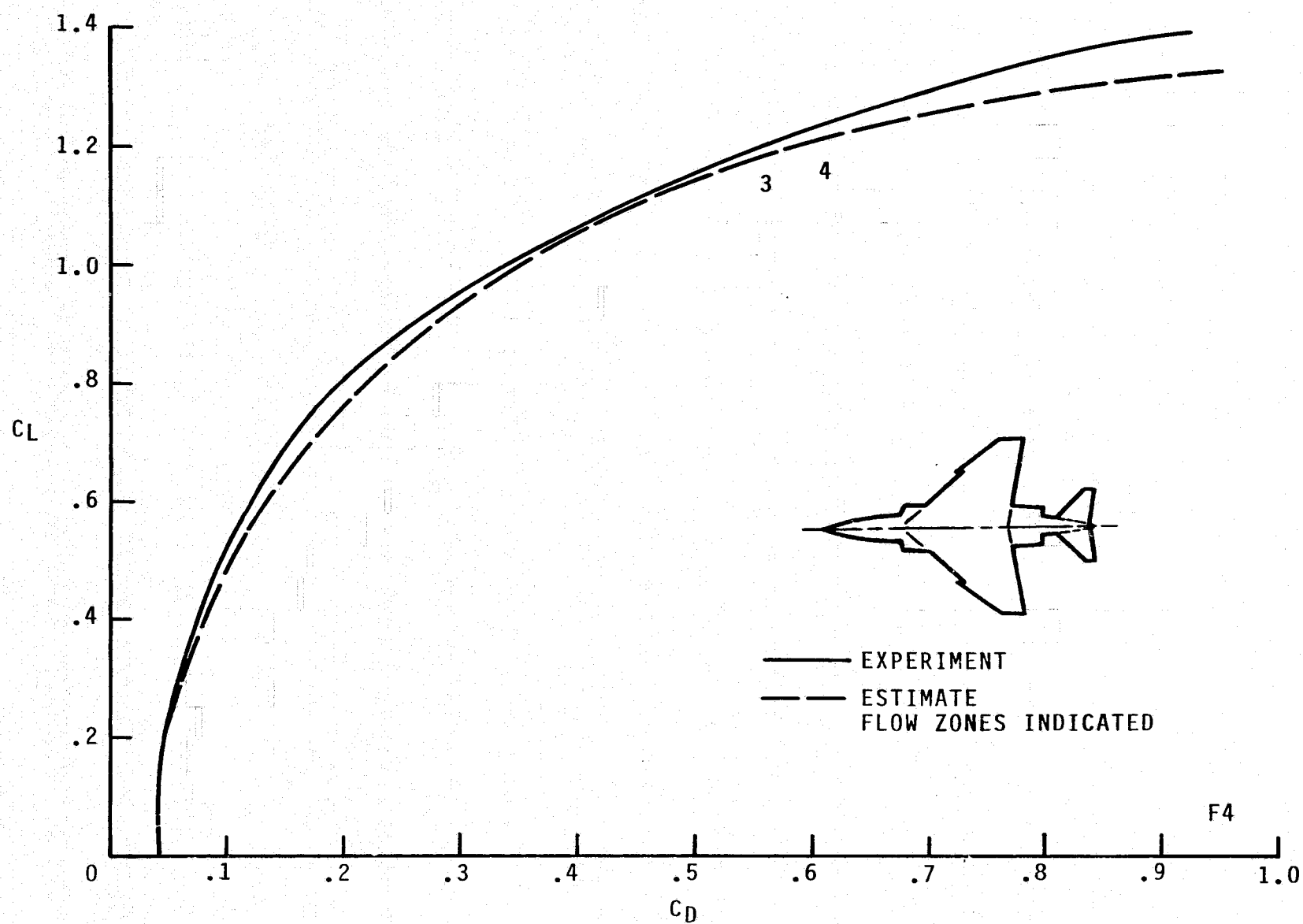
(b) C_L VERSUS α ; $M = 1.2$.

FIGURE 2.- CONTINUED.



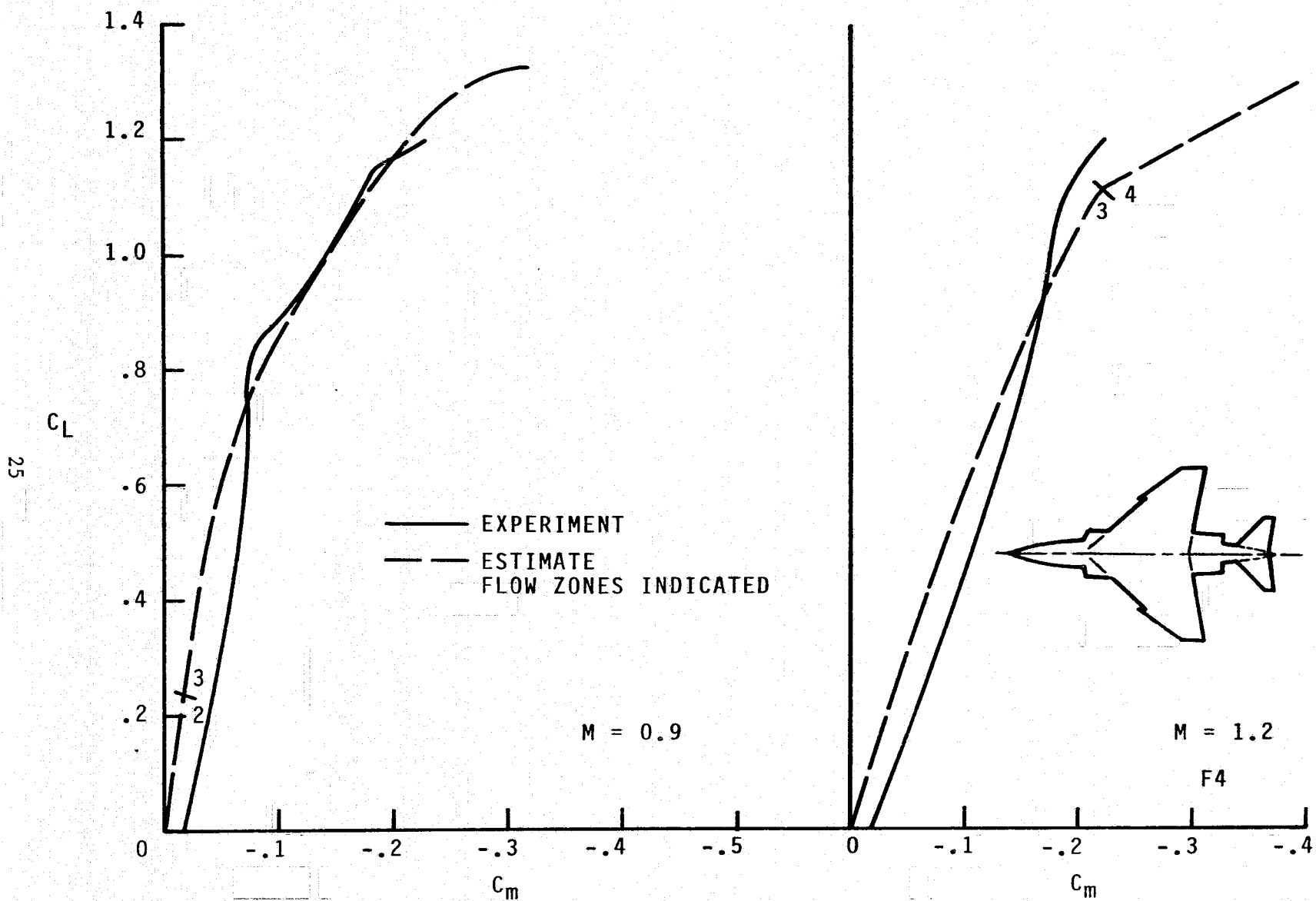
(c) C_L VERSUS C_D ; $M = 0.9$.

FIGURE 2.- CONTINUED.



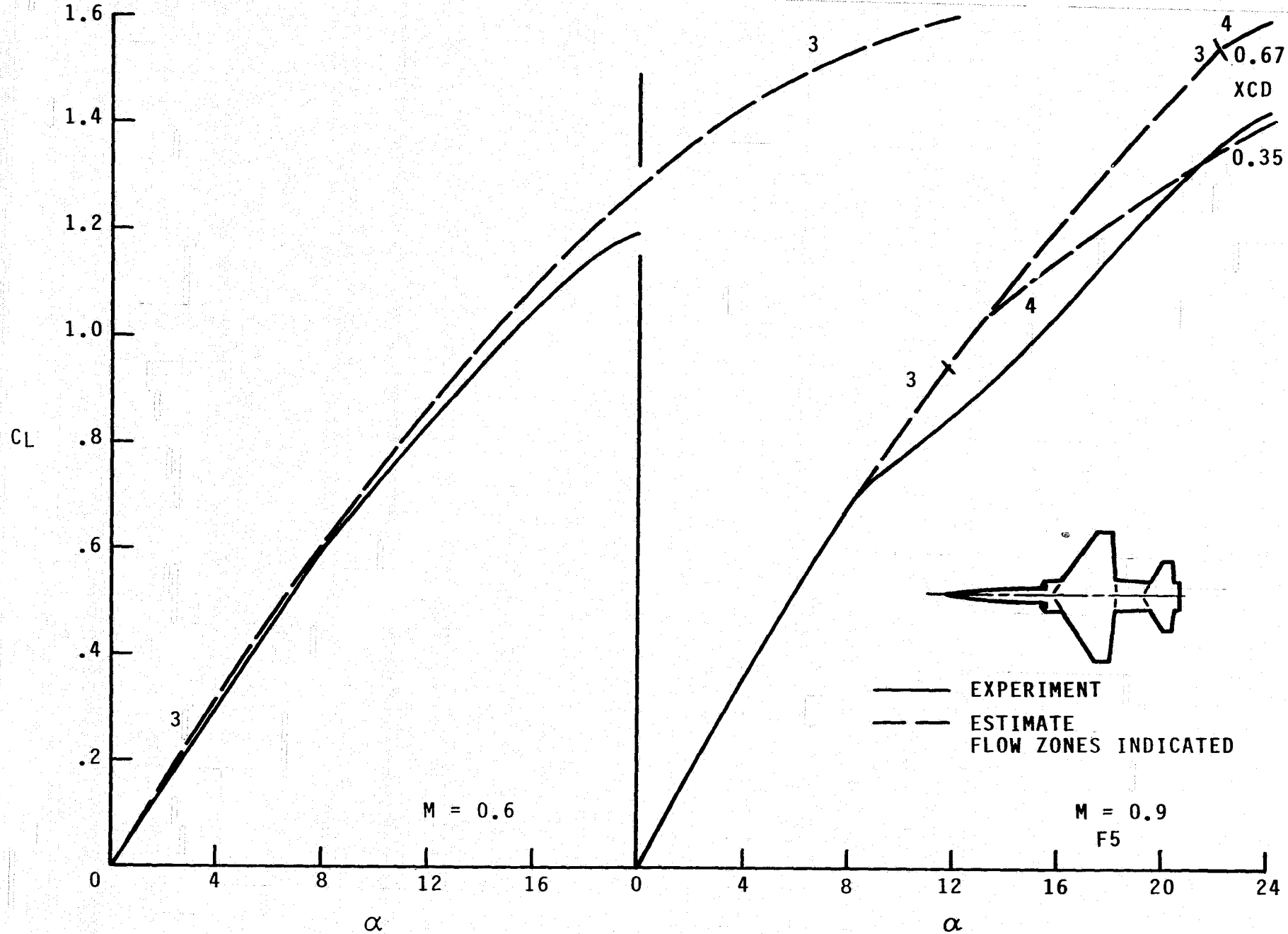
(d) C_L VERSUS C_D ; $M = 1.2$.

FIGURE 2.- CONTINUED.



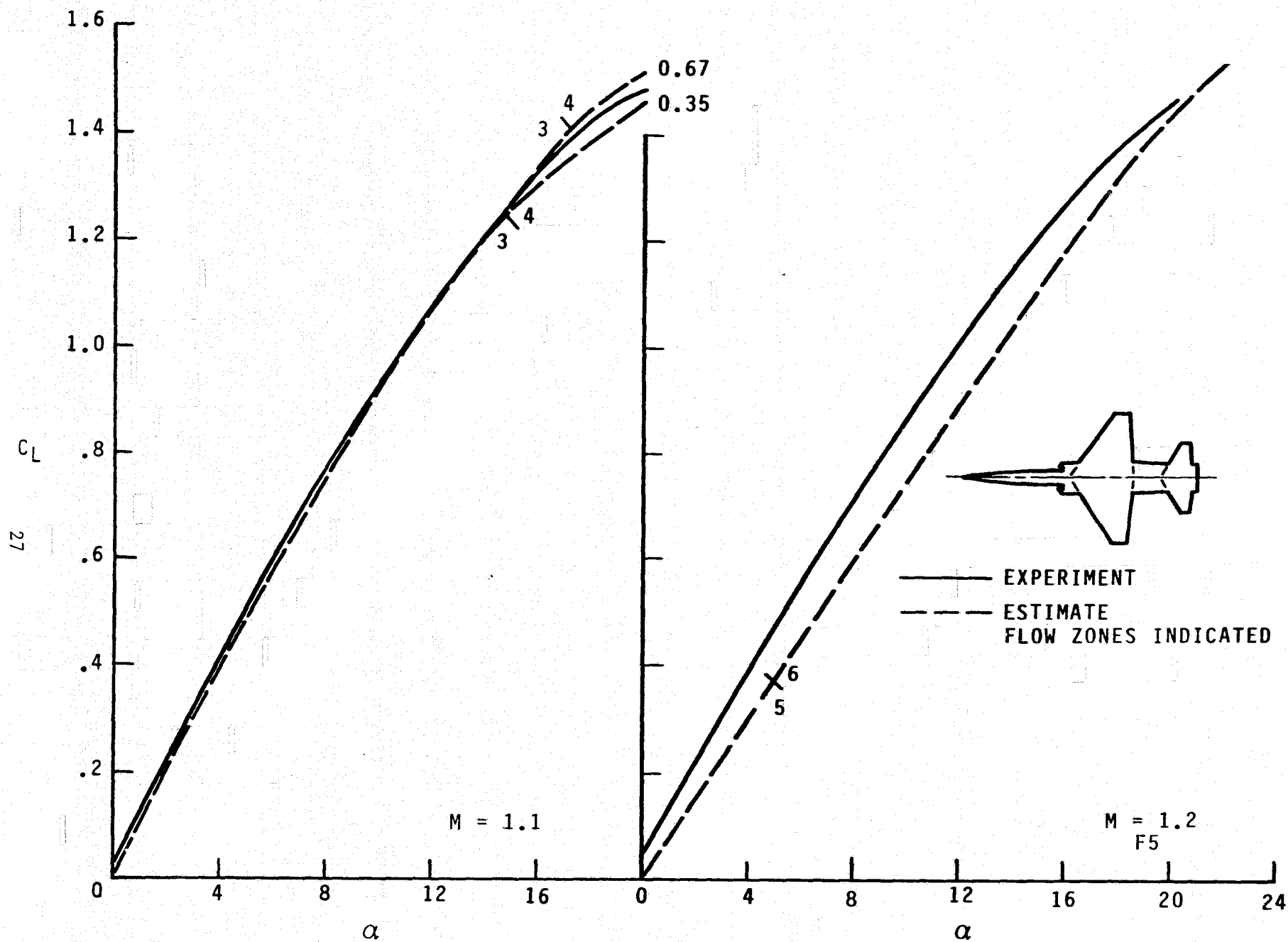
(e) C_L VERSUS C_m ; $M = 0.9, 1.2$.

FIGURE 2.- CONCLUDED.



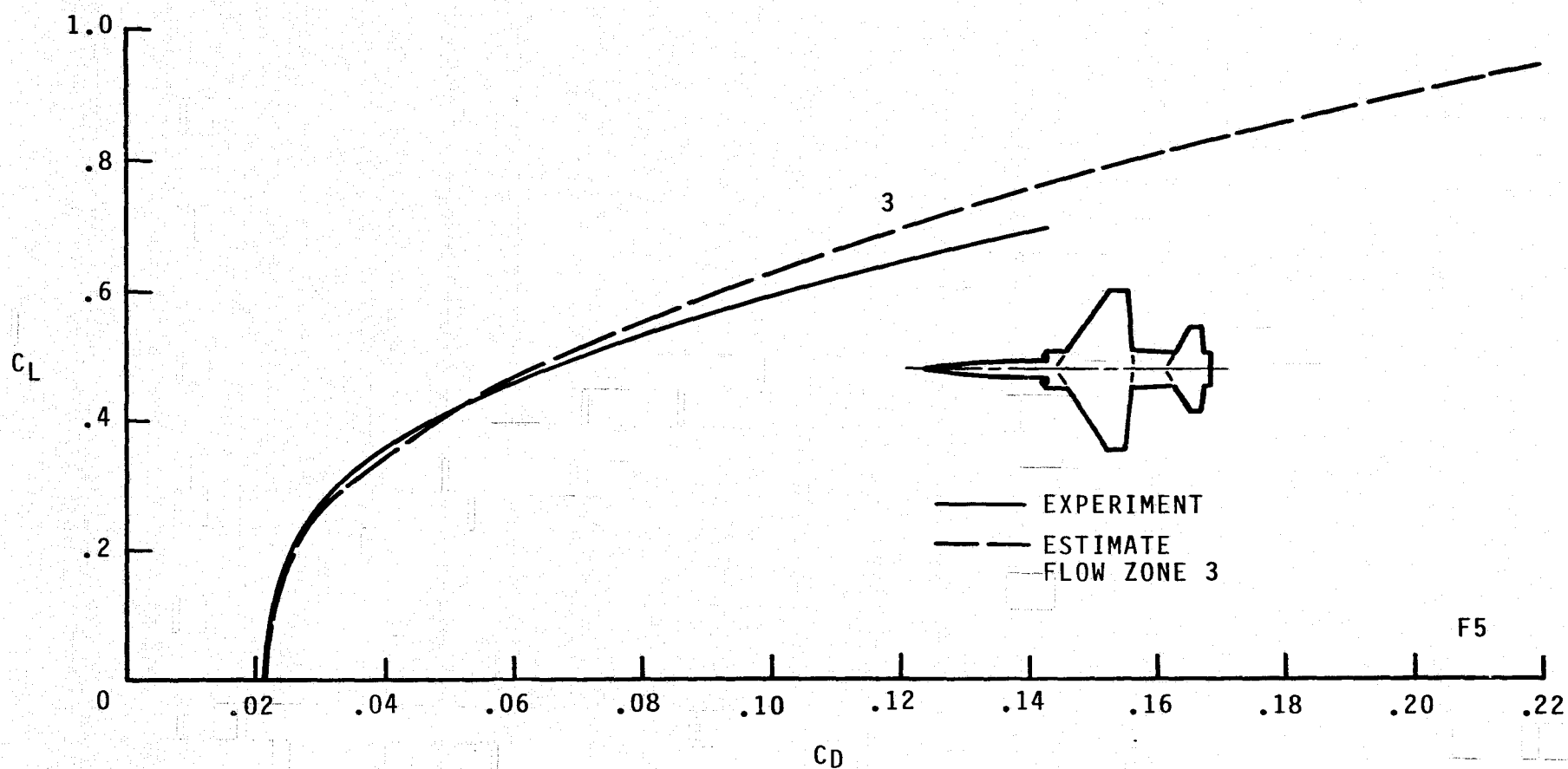
(a) C_L VERSUS α ; $M = 0.6, 0.9$.

FIGURE 3.- AERODYNAMICS FOR THE F5, $J = 1$.



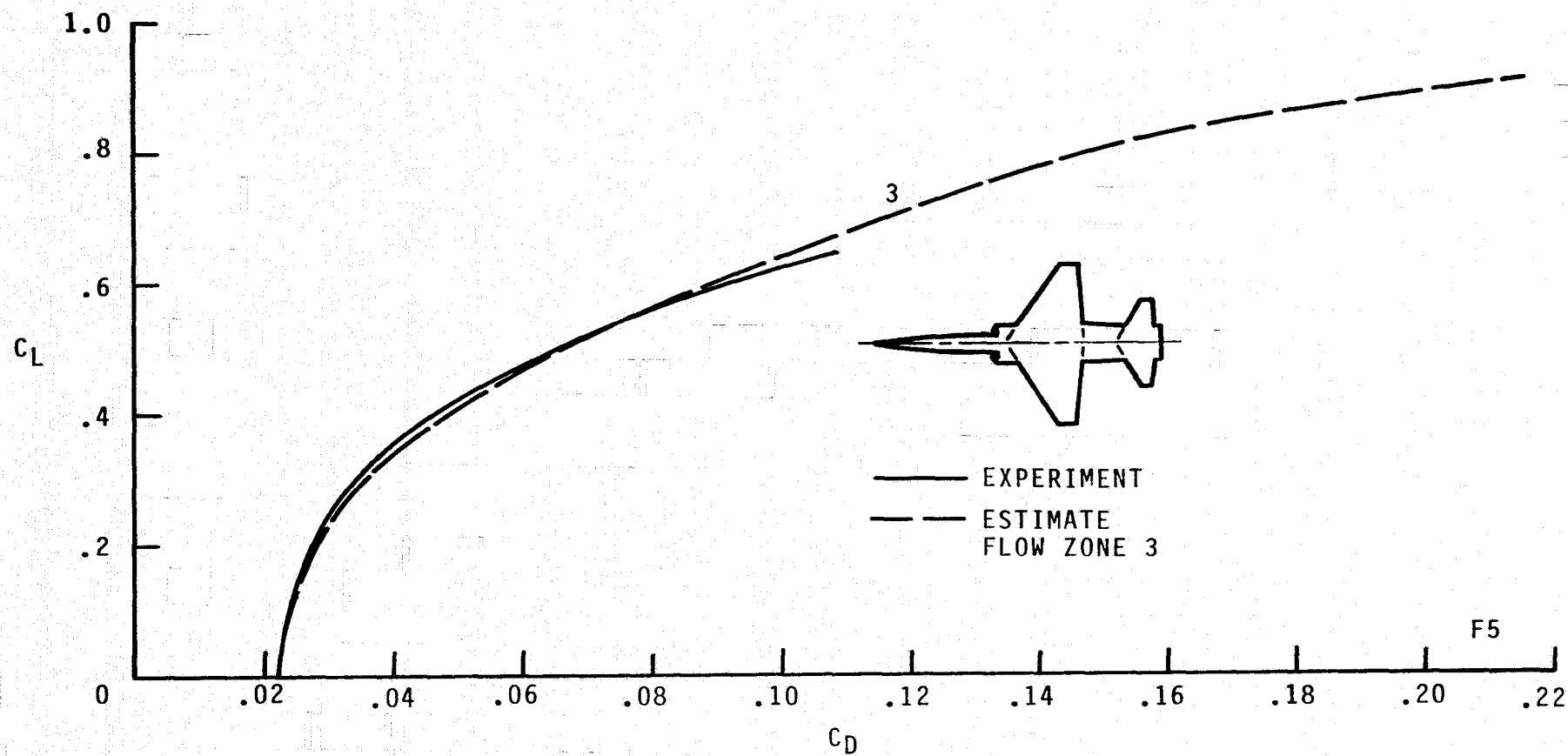
(b) C_L VERSUS α ; $M = 1.1, 1.2$.

FIGURE 3.- CONTINUED.



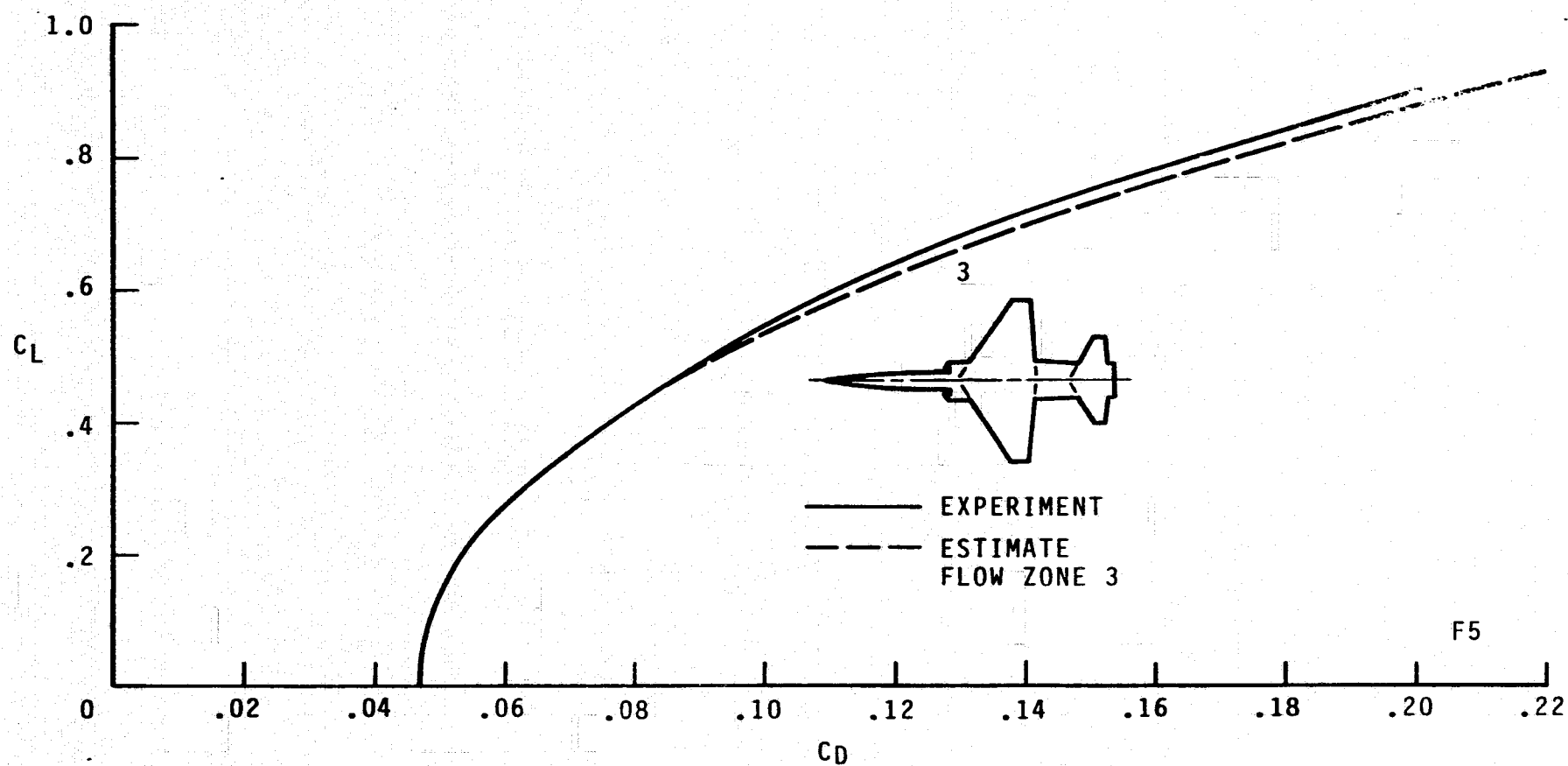
(c) C_L VERSUS C_D ; $M = 0.6$.

FIGURE 3.- CONTINUED.



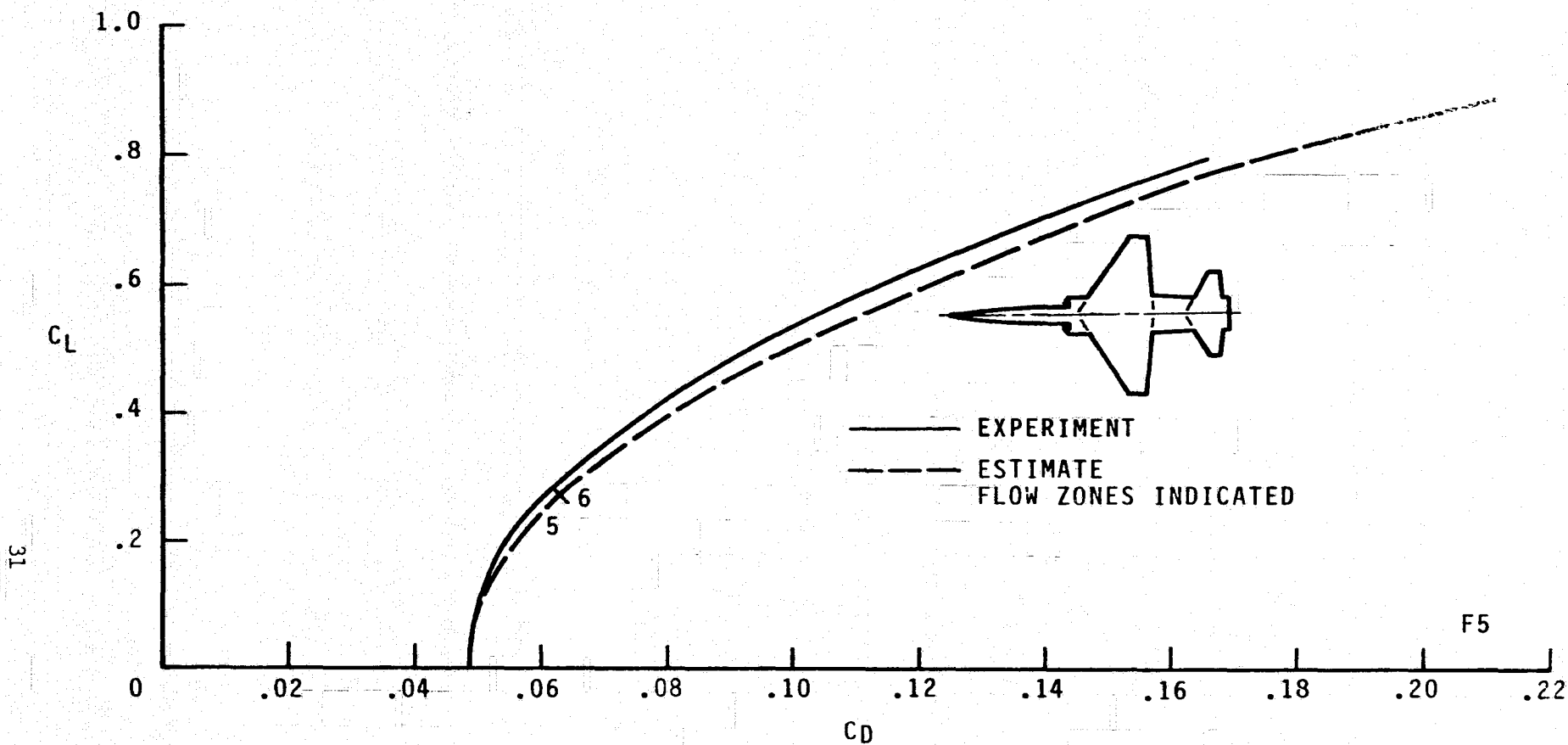
(d) C_L VERSUS C_D ; $M = 0.9$.

FIGURE 3.- CONTINUED.



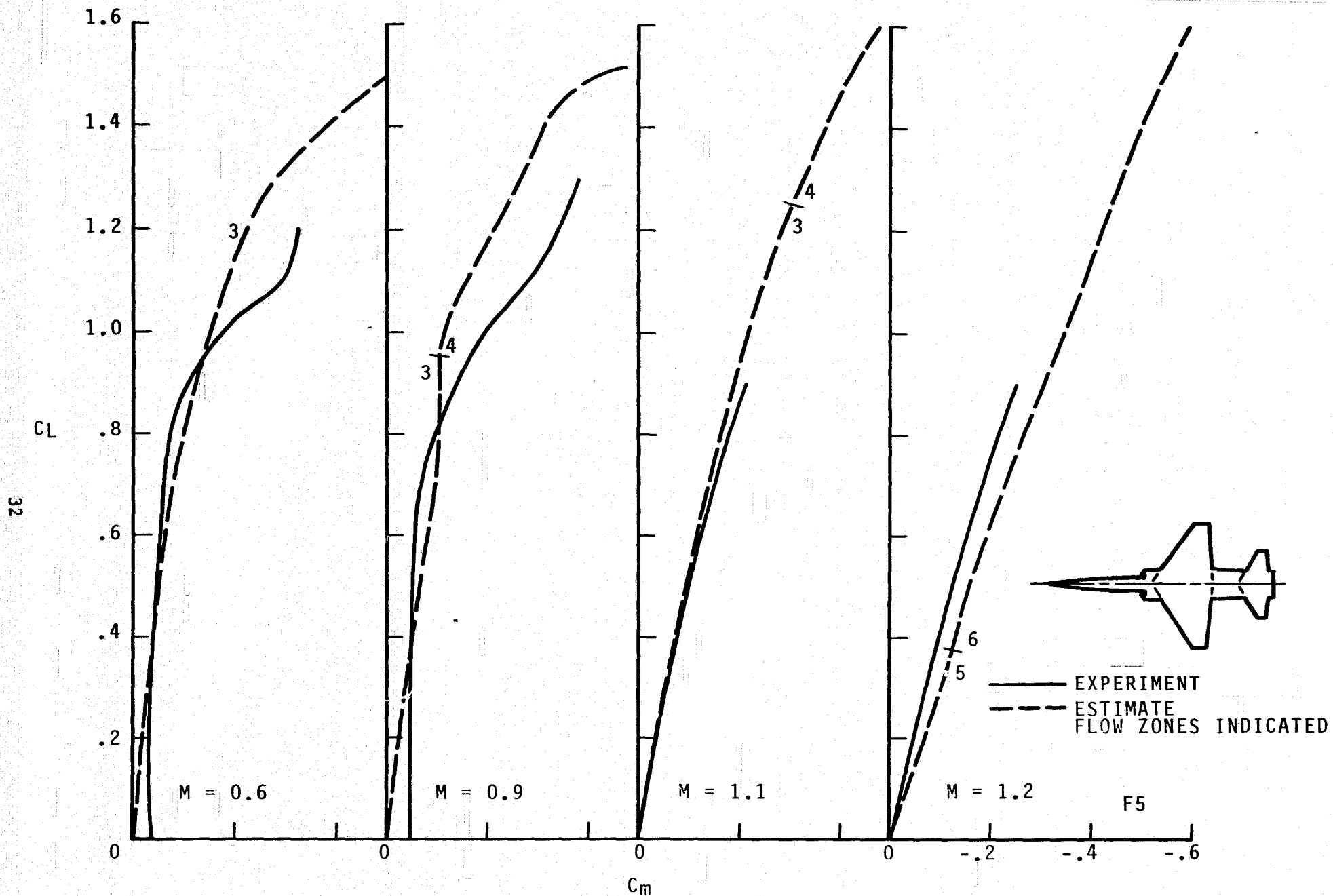
(e) C_L VERSUS C_D ; $M = 1.1$.

FIGURE 3.- CONTINUED.



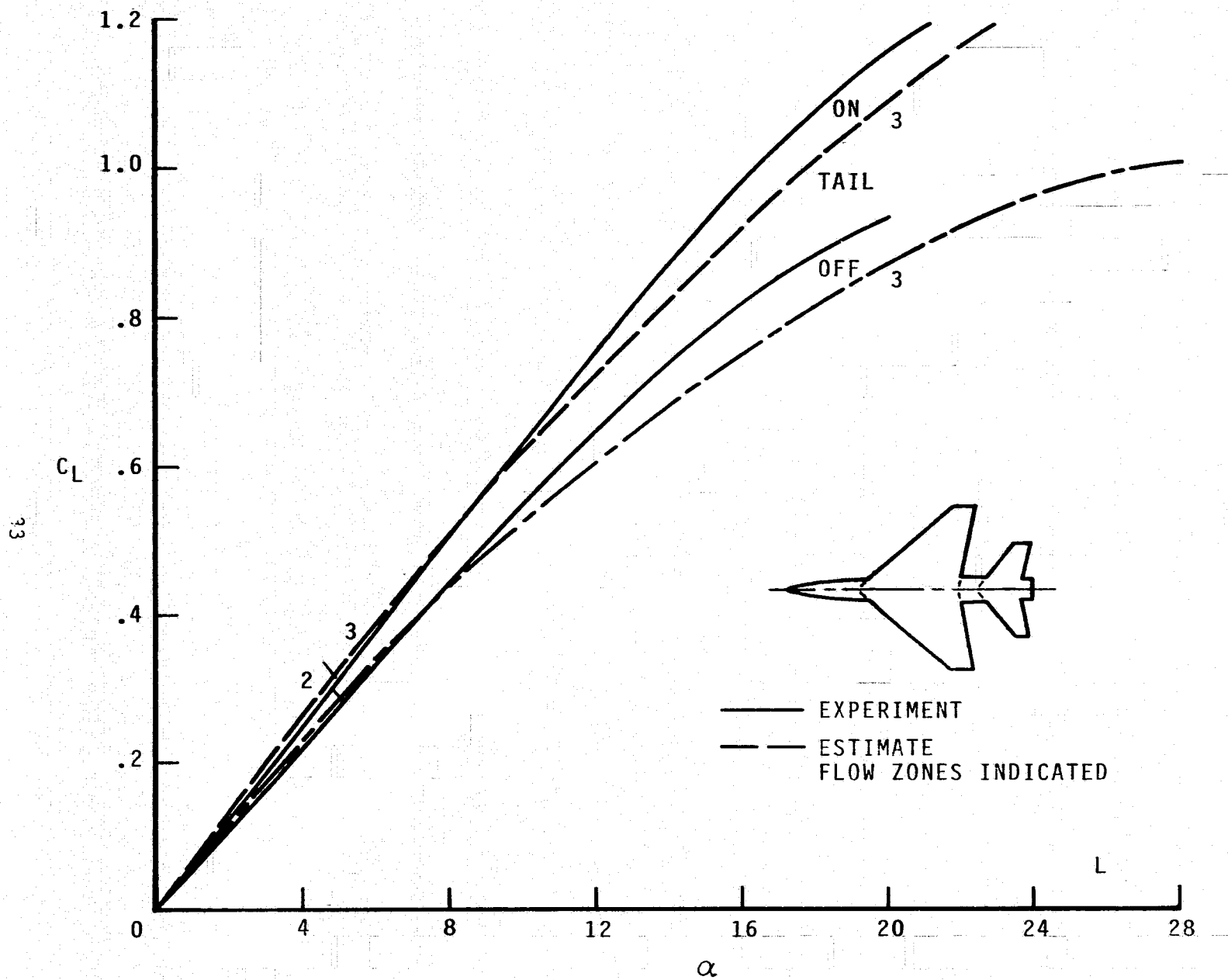
(f) C_L VERSUS C_D ; $M = 1.2$.

FIGURE 3.- CONTINUED.



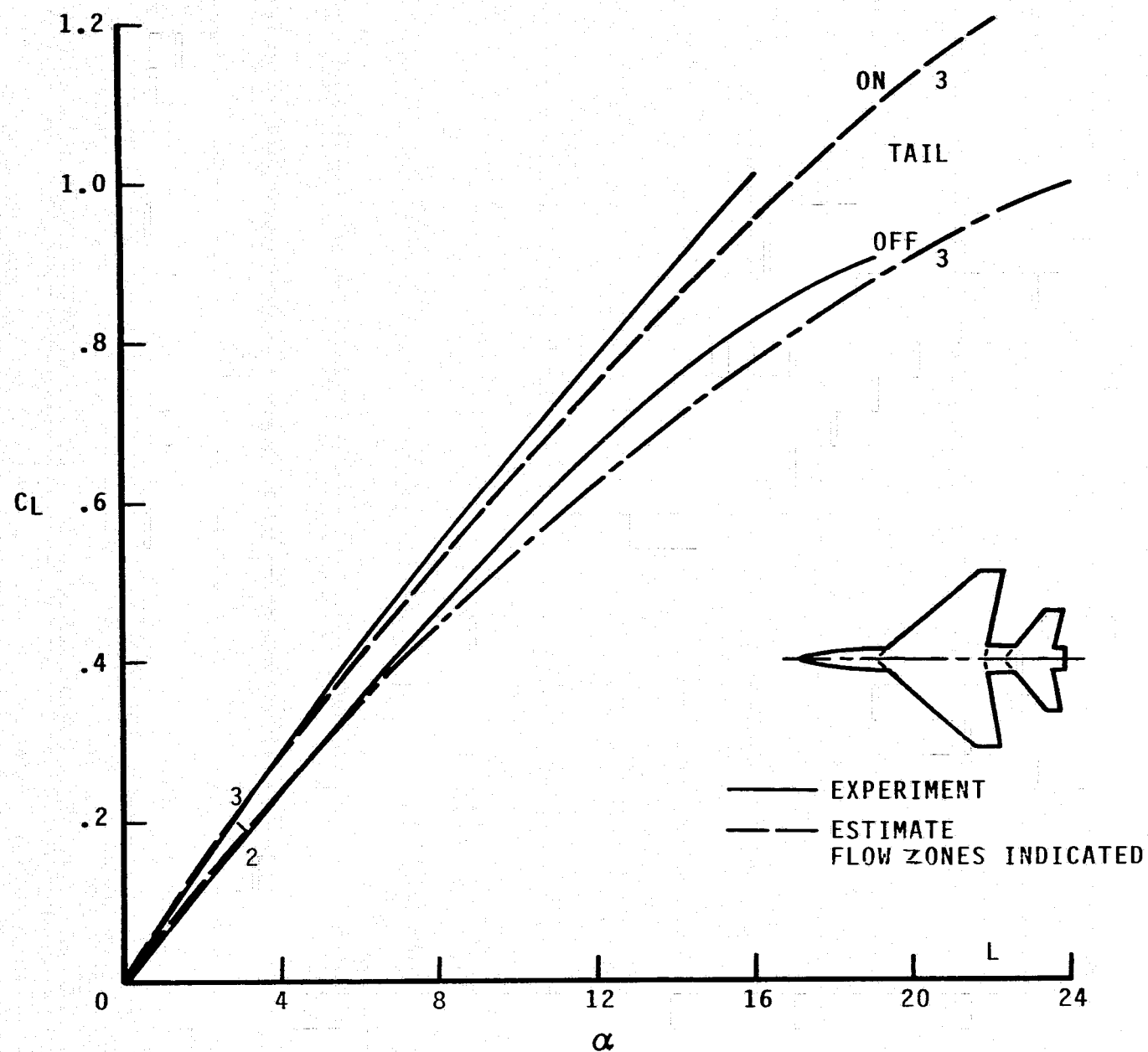
(g) C_L VERSUS C_m ; $M = 0.6, 0.9, 1.1, 1.2$.

FIGURE 3.- CONCLUDED.



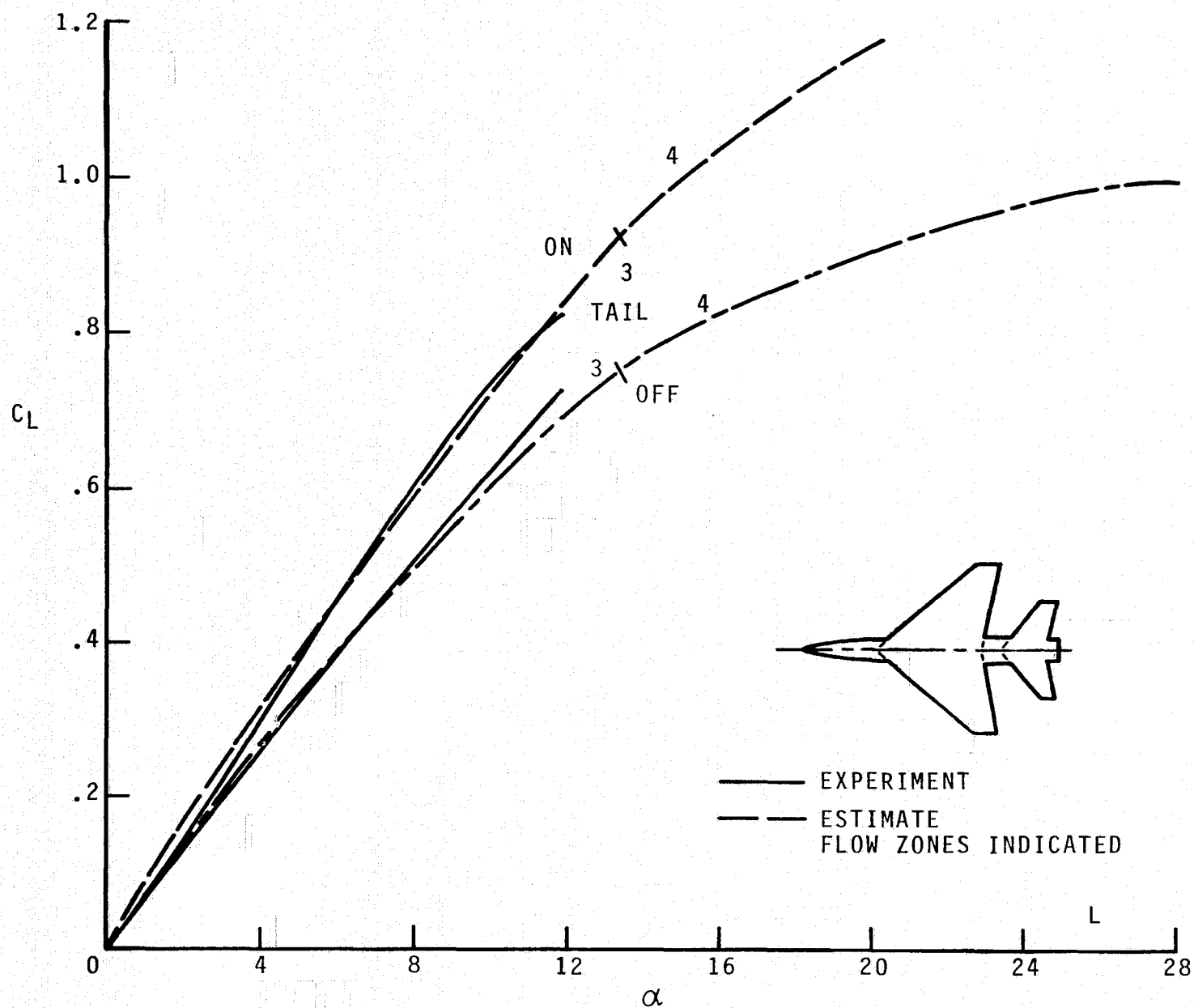
(a) C_L VERSUS α ; $M = 0.5$.

FIGURE 4.- AERODYNAMICS FOR MODEL L; $J = 3$.



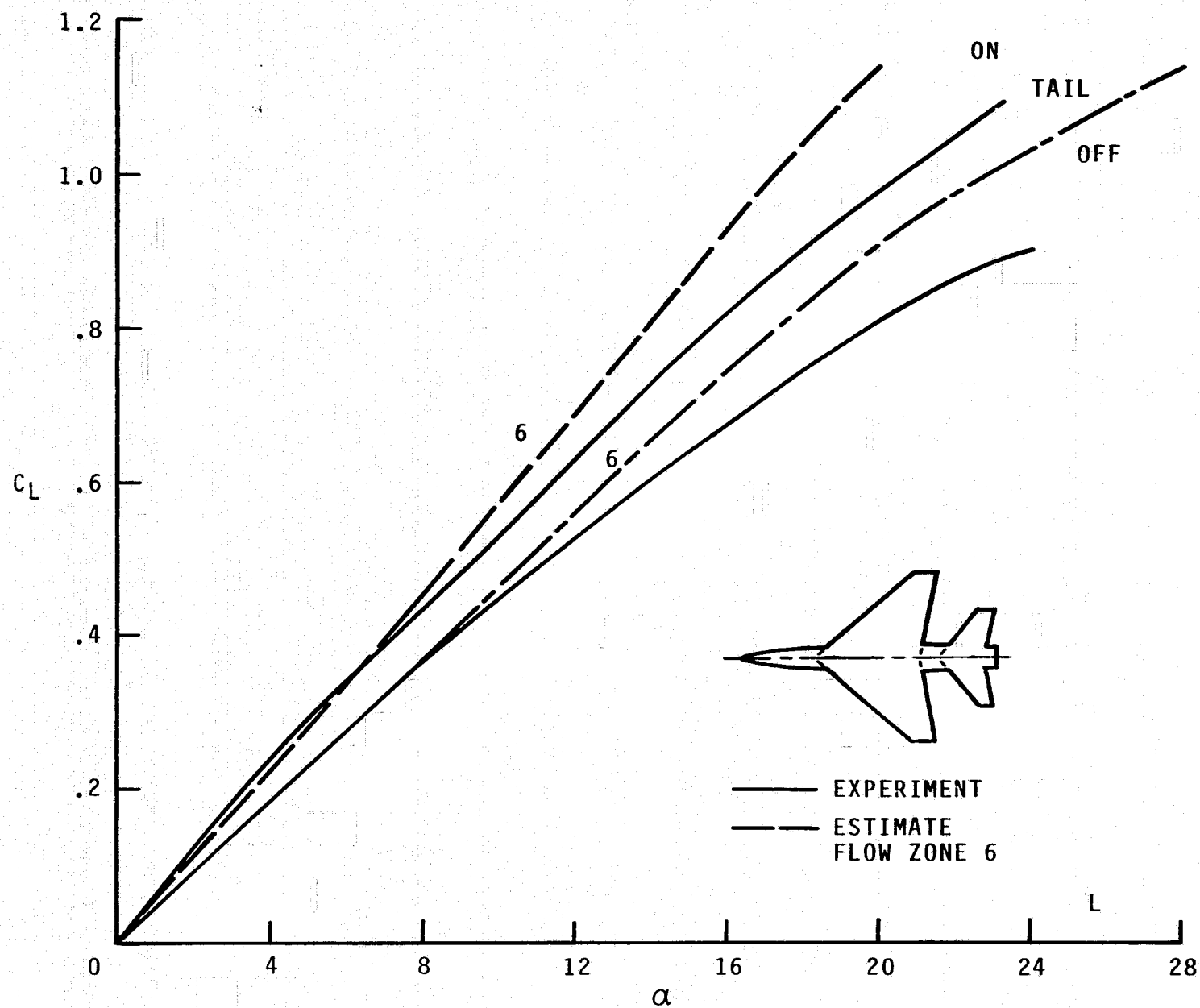
(b) C_L VERSUS α ; $M = 0.8$.

FIGURE 4.- CONTINUED.



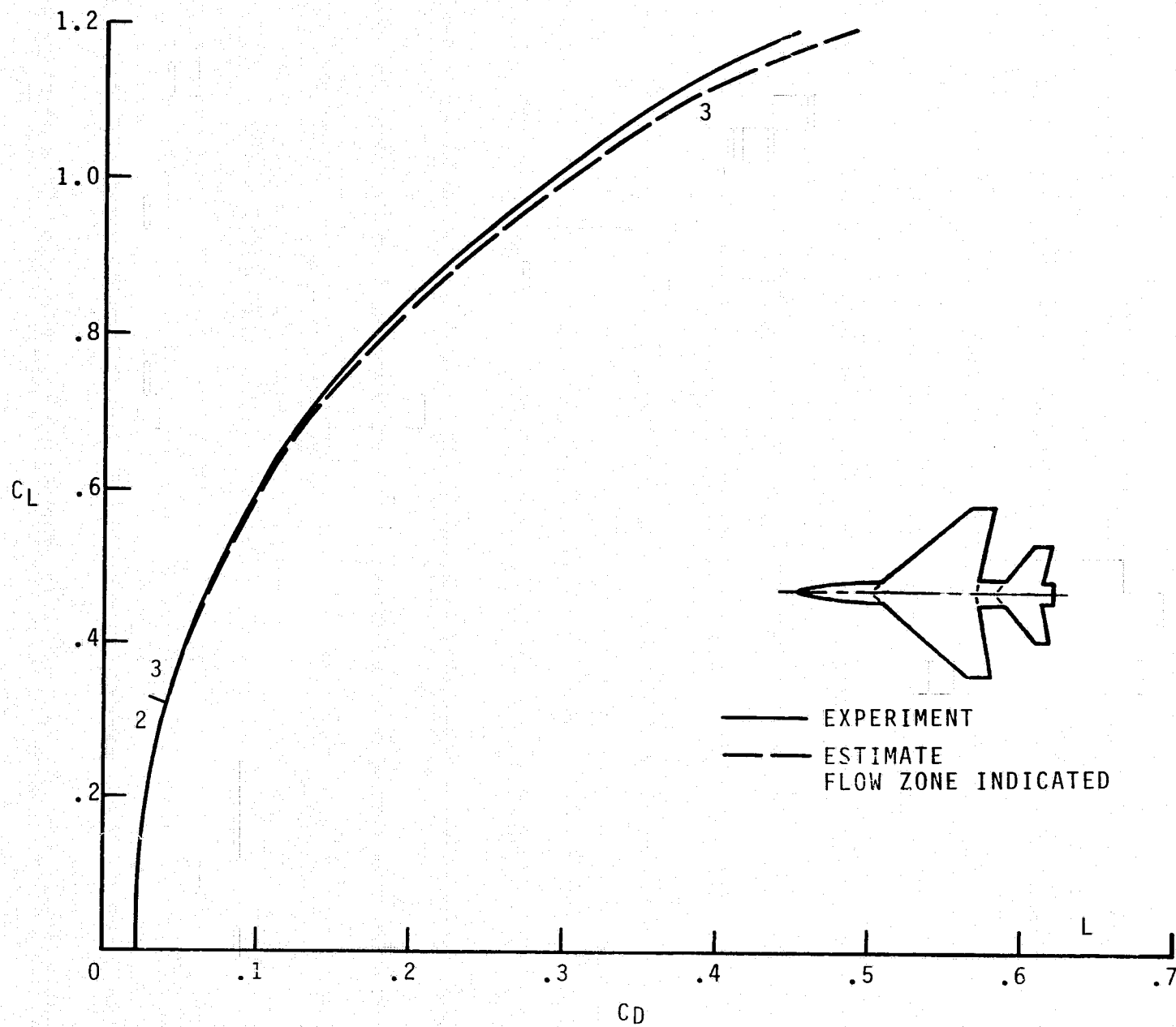
(c) C_L VERSUS α ; $M = 1.2$.

FIGURE 4.- CONTINUED



(d) C_L VERSUS α ; $M = 1.8$.

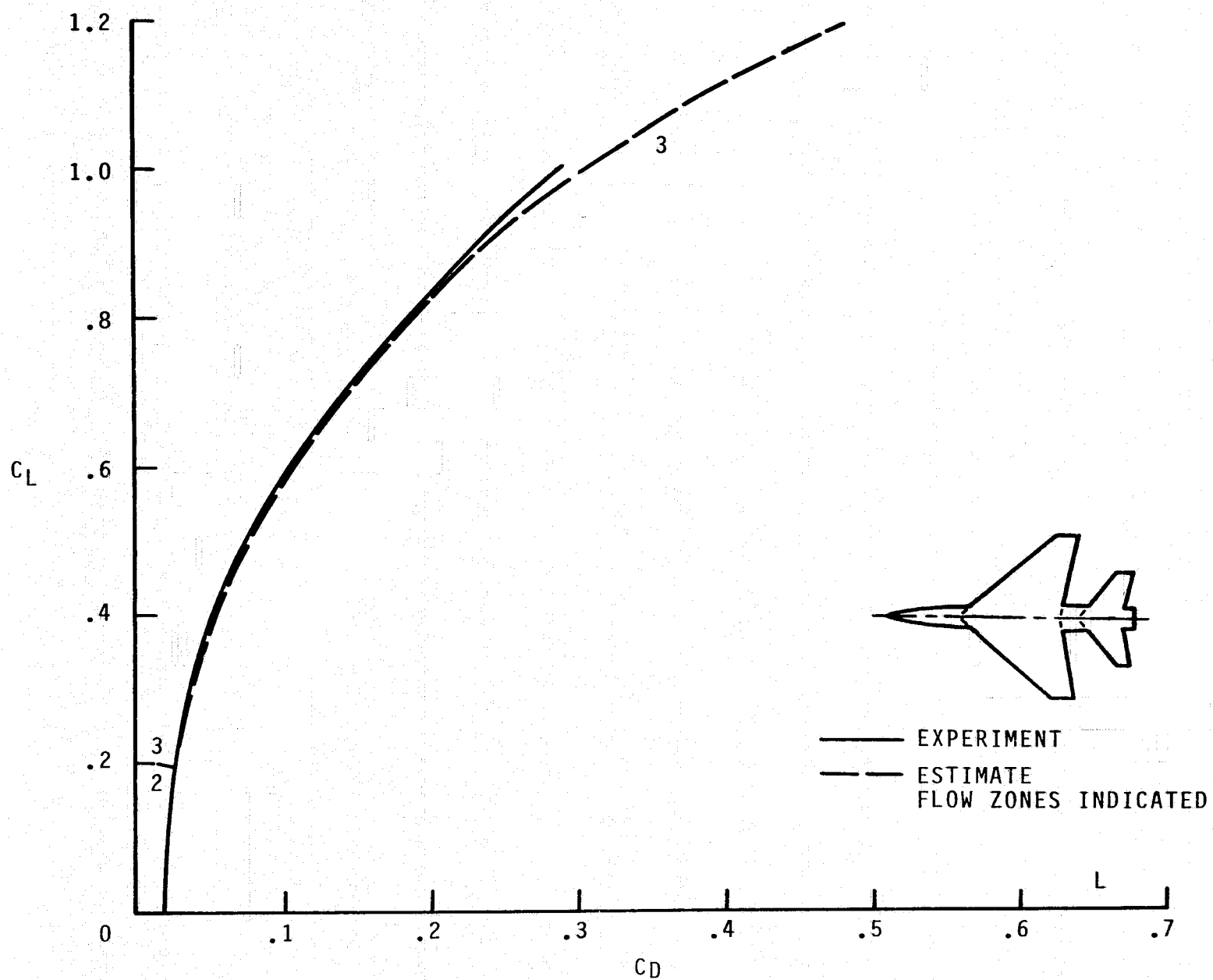
FIGURE 4.- CONTINUED.



(e) C_L VERSUS C_D ; $M = 0.5$.

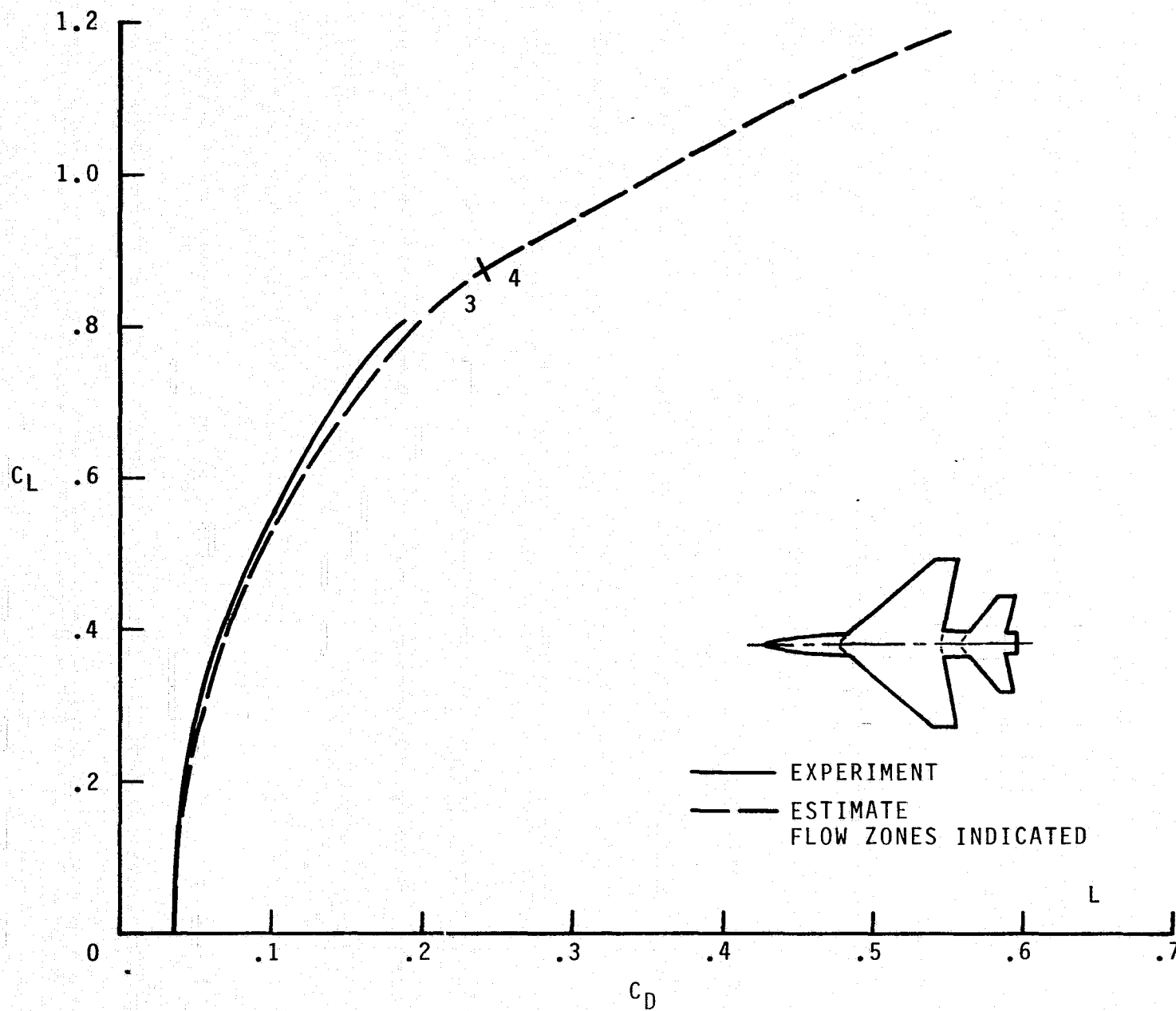
FIGURE 4.- CONTINUED.

38



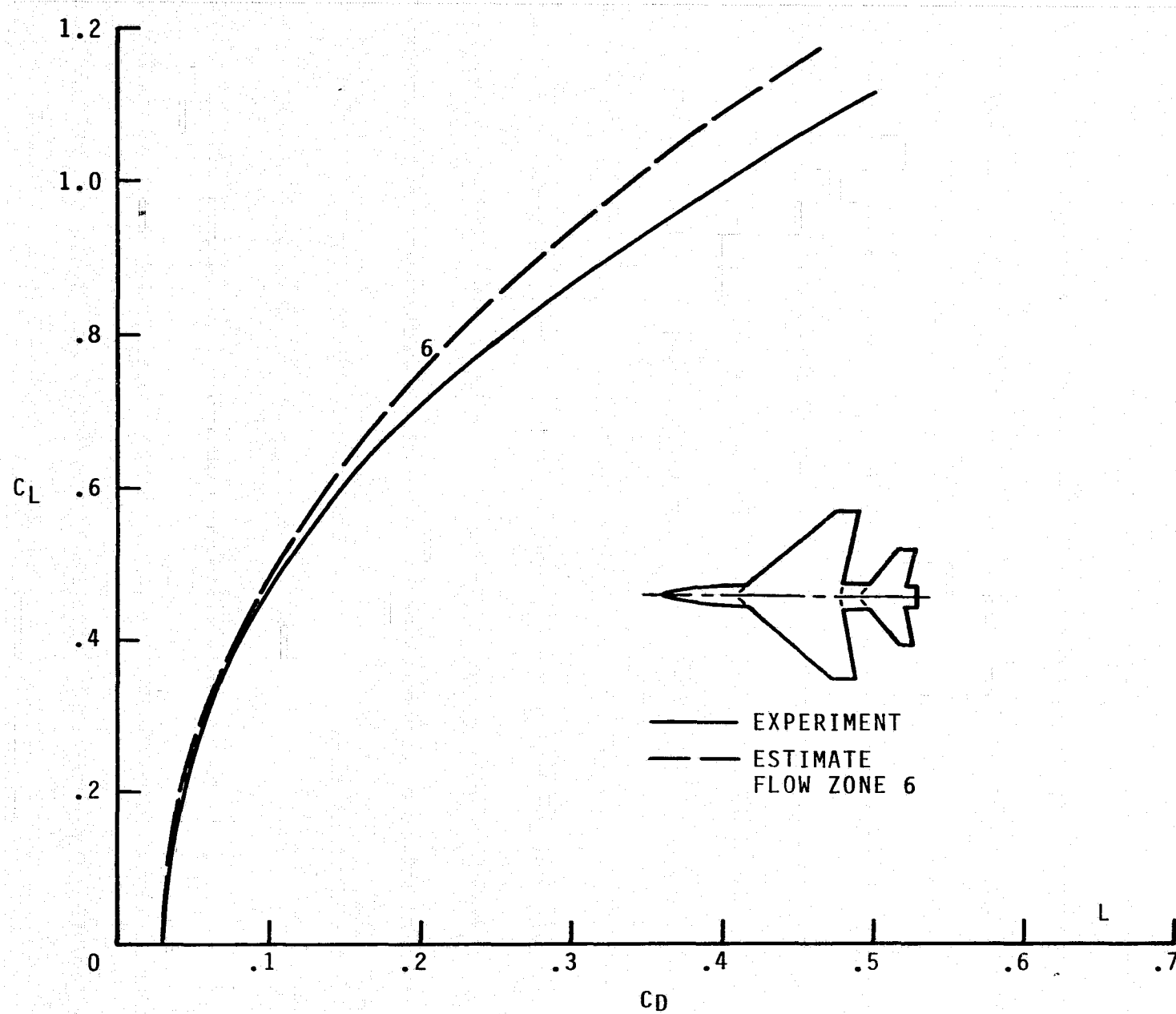
(f) C_L VERSUS C_D ; $M = 0.8$.

FIGURE 4.- CONTINUED.



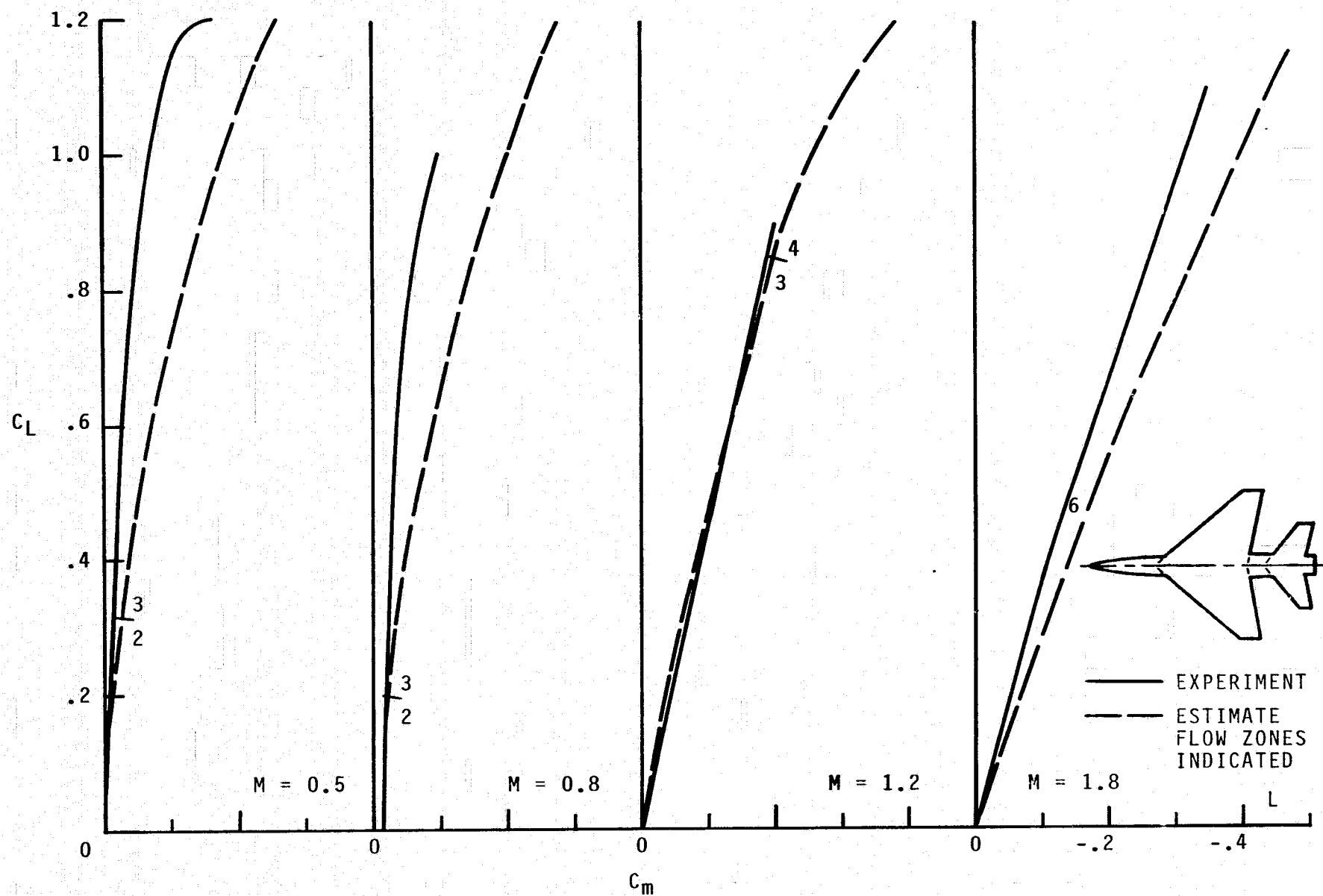
(g) C_L VERSUS C_D ; $M = 1.2$.

FIGURE 4.- CONTINUED.



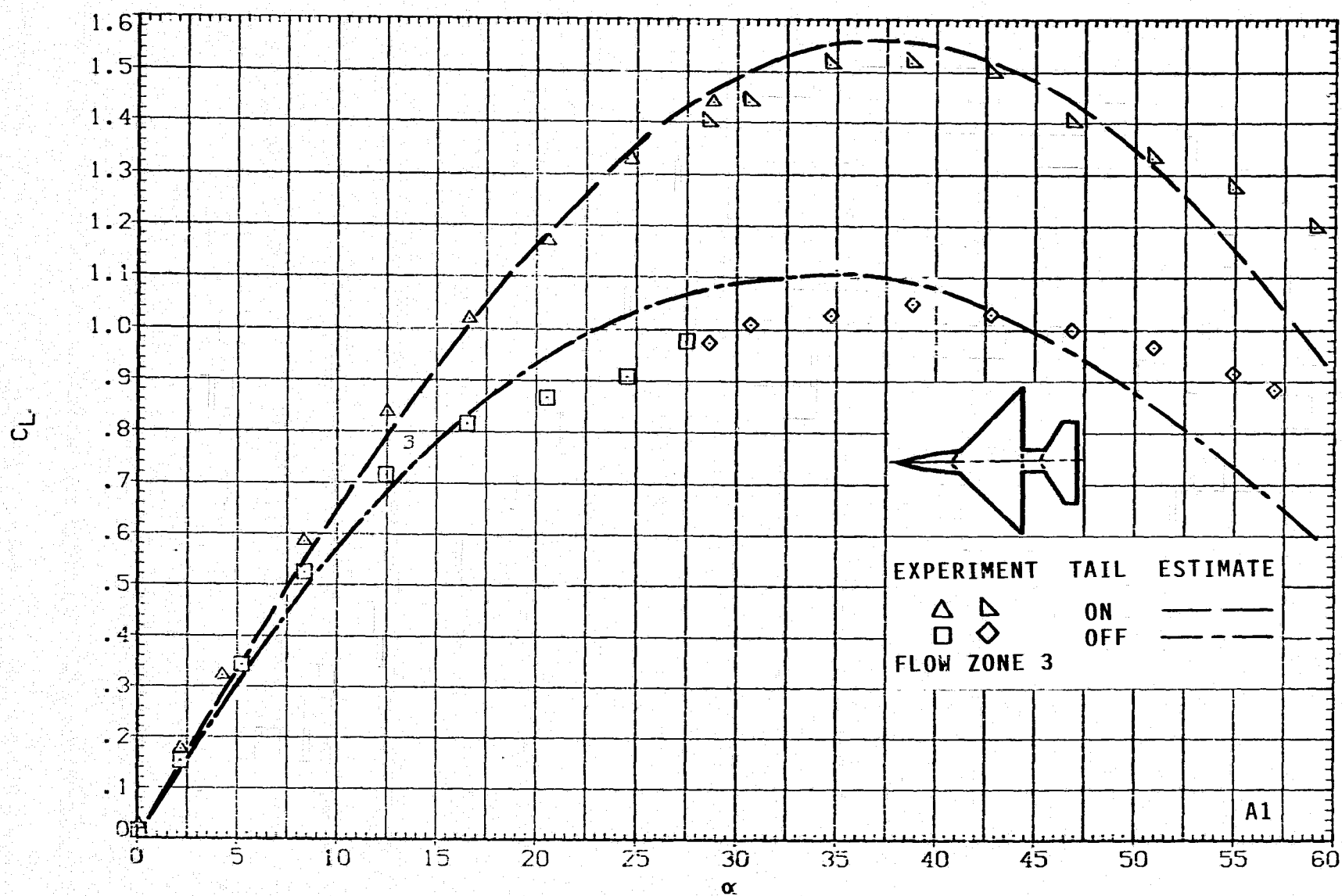
(h) C_L VERSUS C_D ; $M = 1.8$.

FIGURE 4.- CONTINUED.



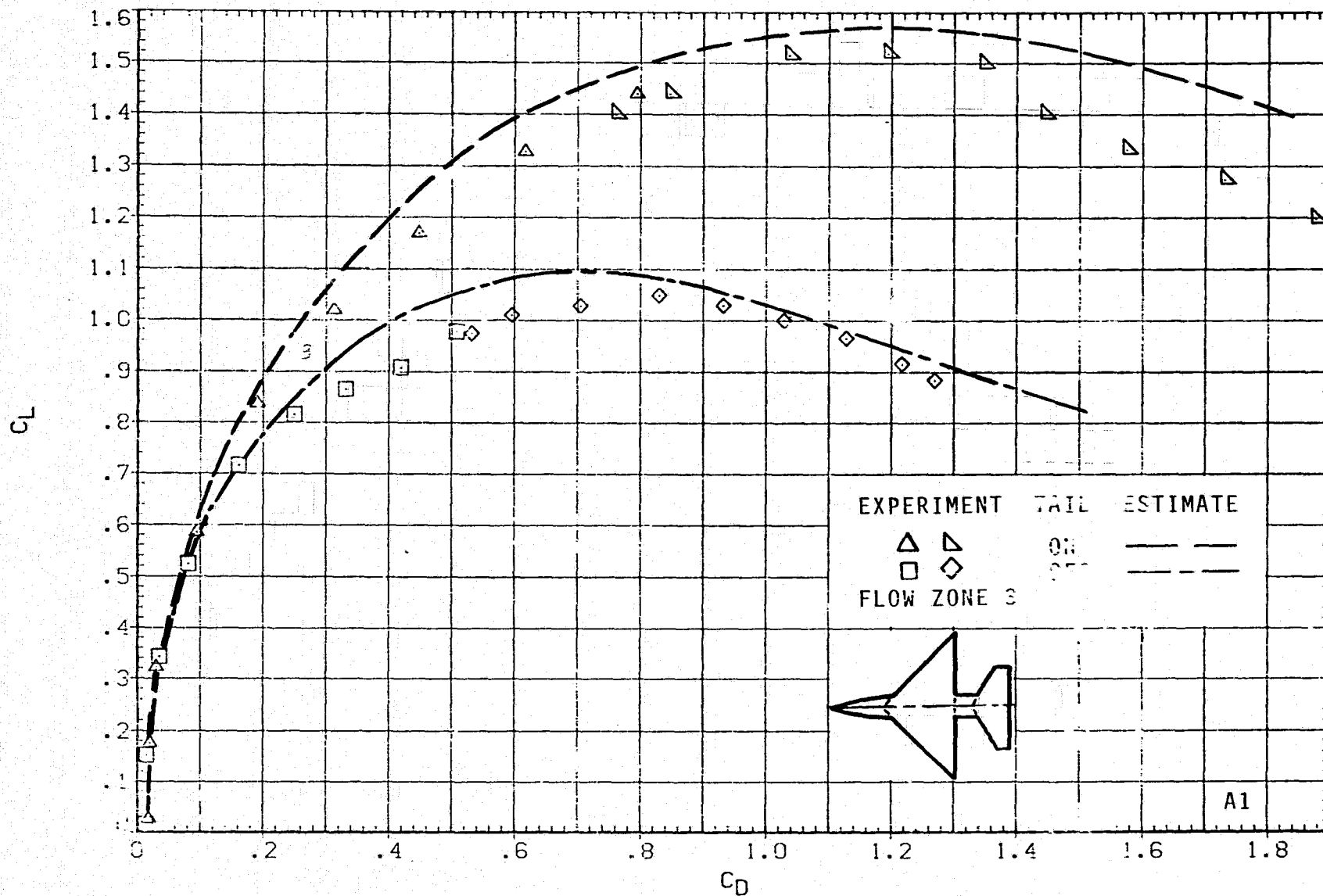
(i) C_L VERSUS C_m ; $M = 0.5, 0.8, 1.2, 1.8$.

FIGURE 4.- CONCLUDED.



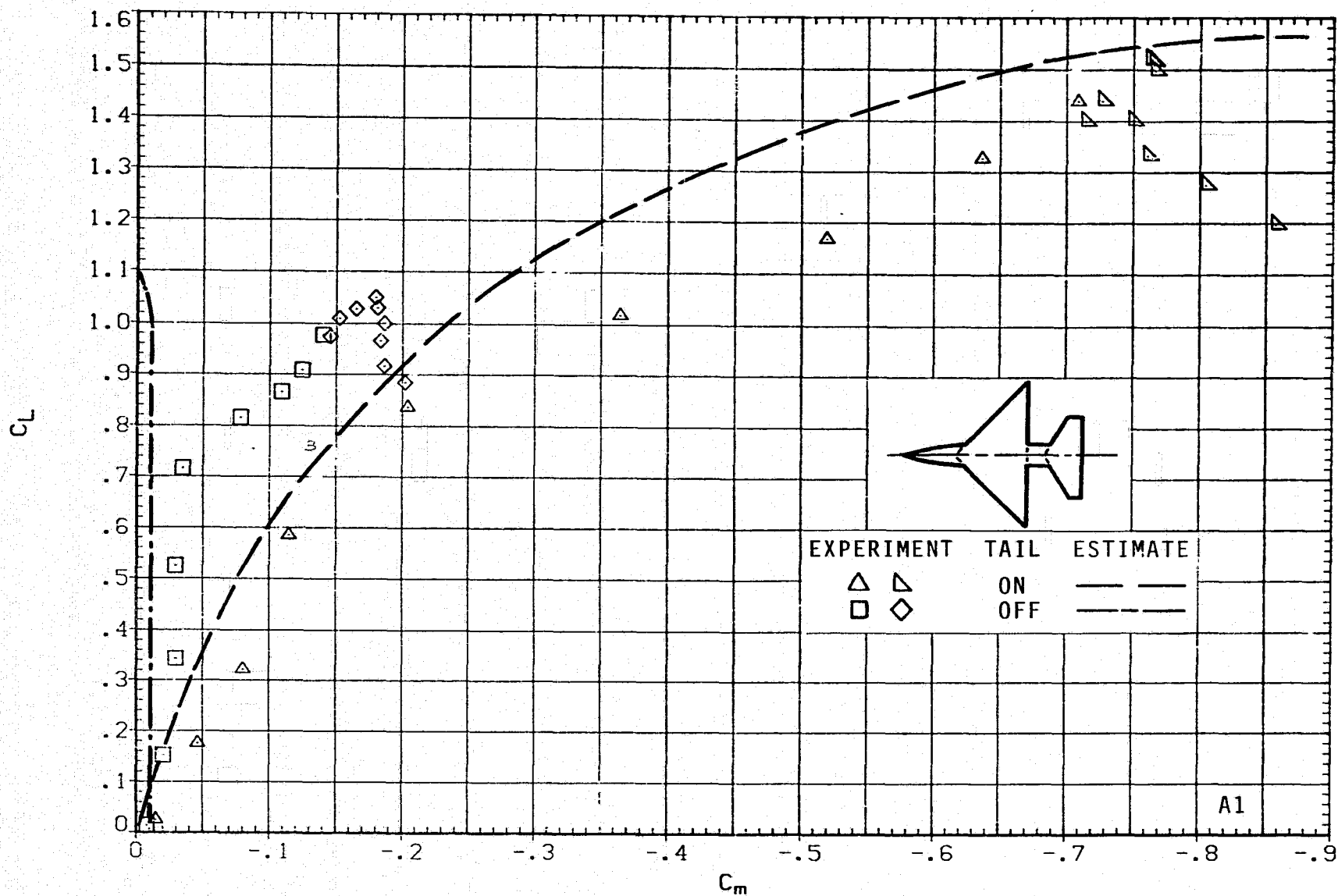
(a) C_L VERSUS α ; $M = 0.6$, $J = 1$.

FIGURE 5.- AERODYNAMICS FOR MODEL A1; $ARW = 4$, $TRW = 0$.



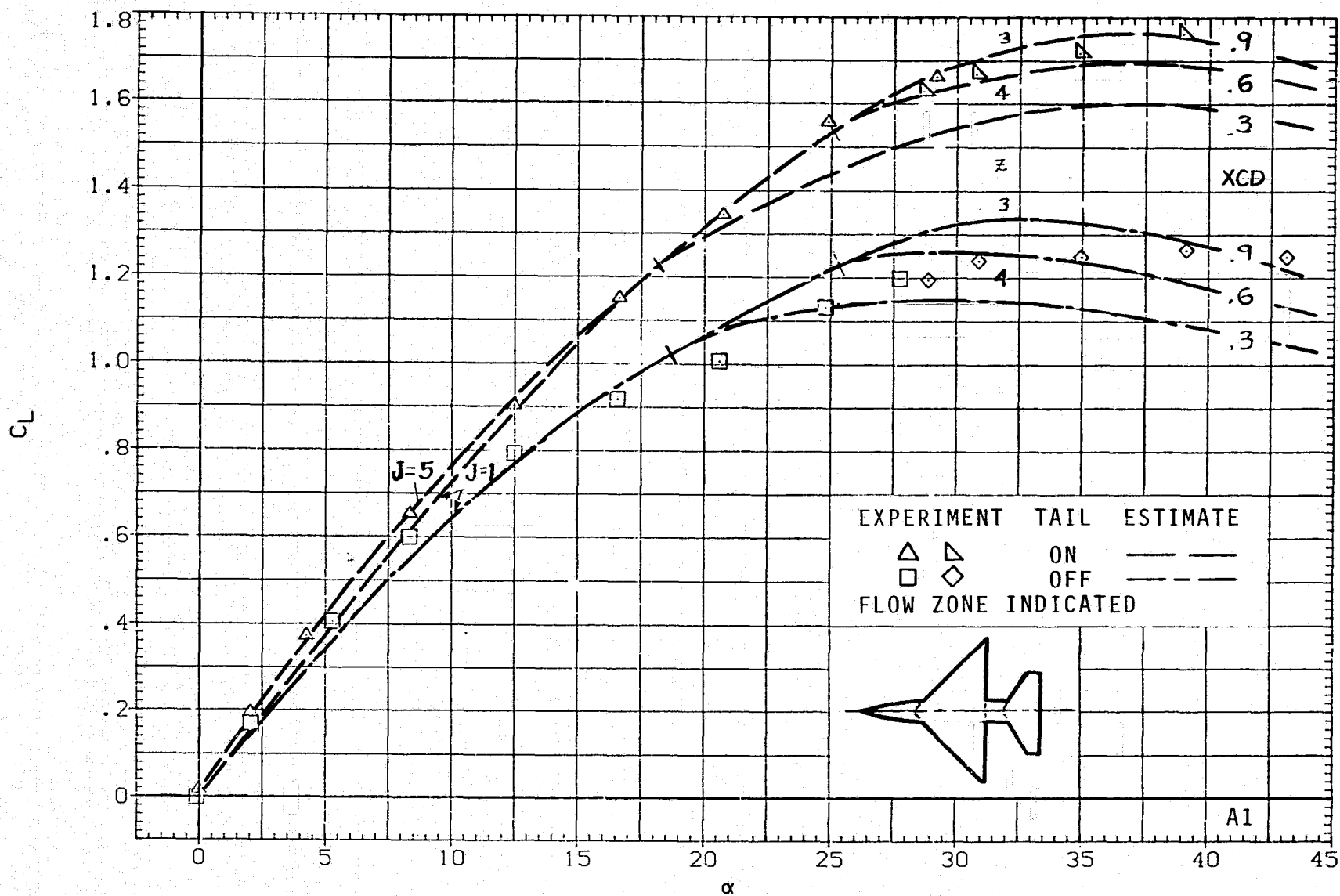
(b) C_L VERSUS C_D ; $M = 0.6$, $J = 1$.

FIGURE 5.- CONTINUED.



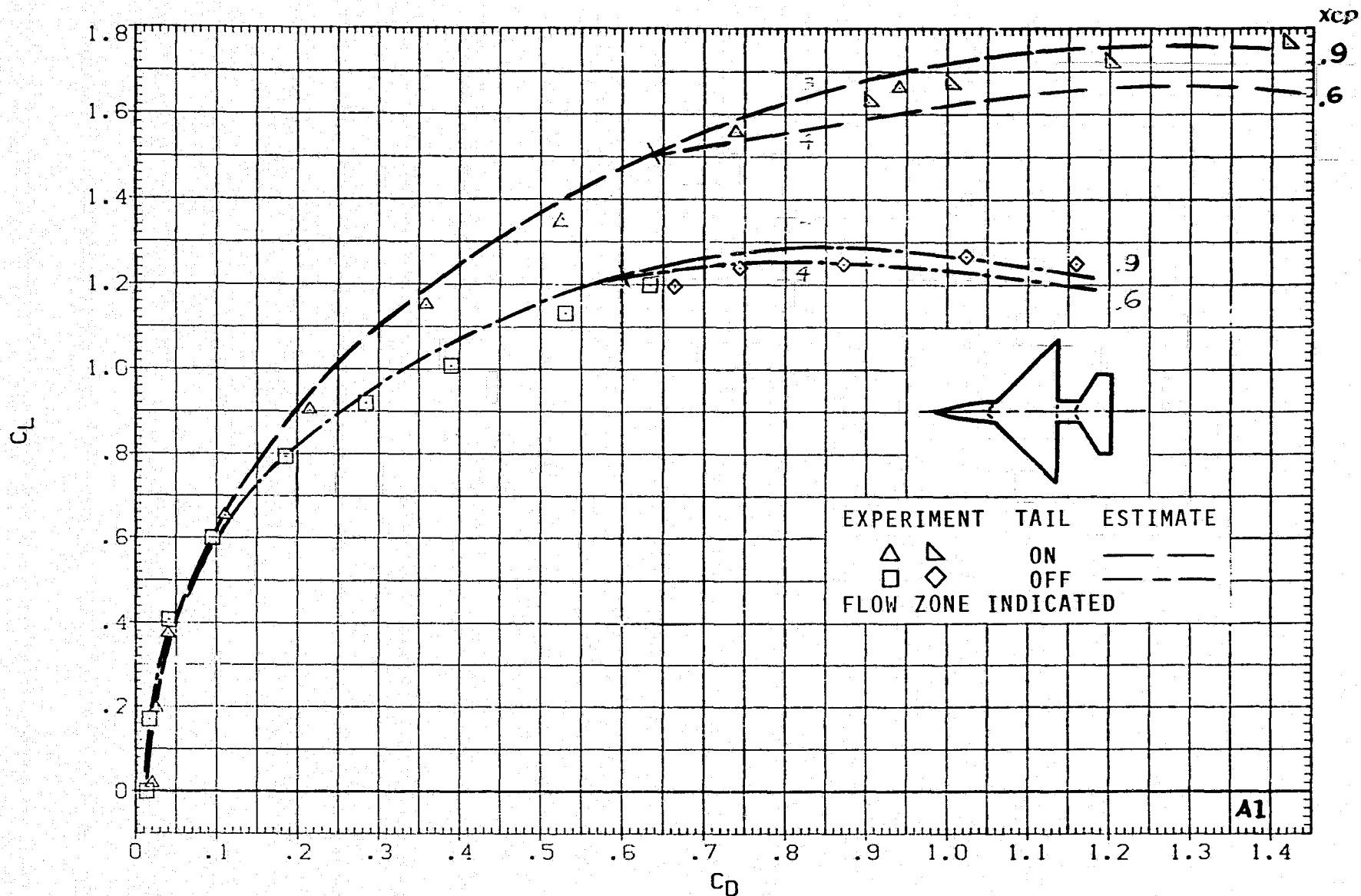
(c) C_L VERSUS C_m ; $M = 0.6$, $J = 1$.

FIGURE 5.- CONTINUED.



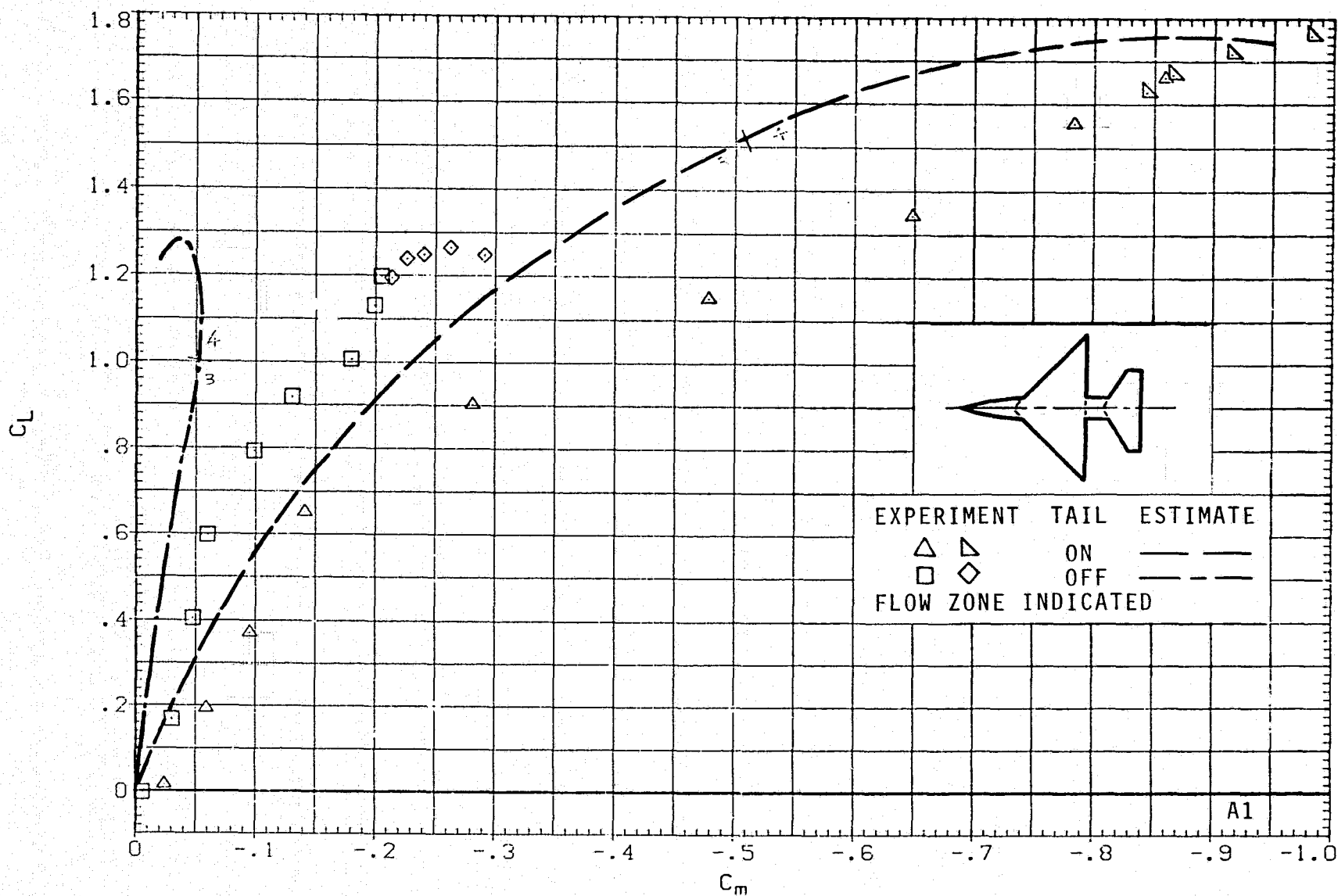
(d) C_L VERSUS α ; $M = 0.9$, $J = 1$.

FIGURE 5.- CONTINUED.



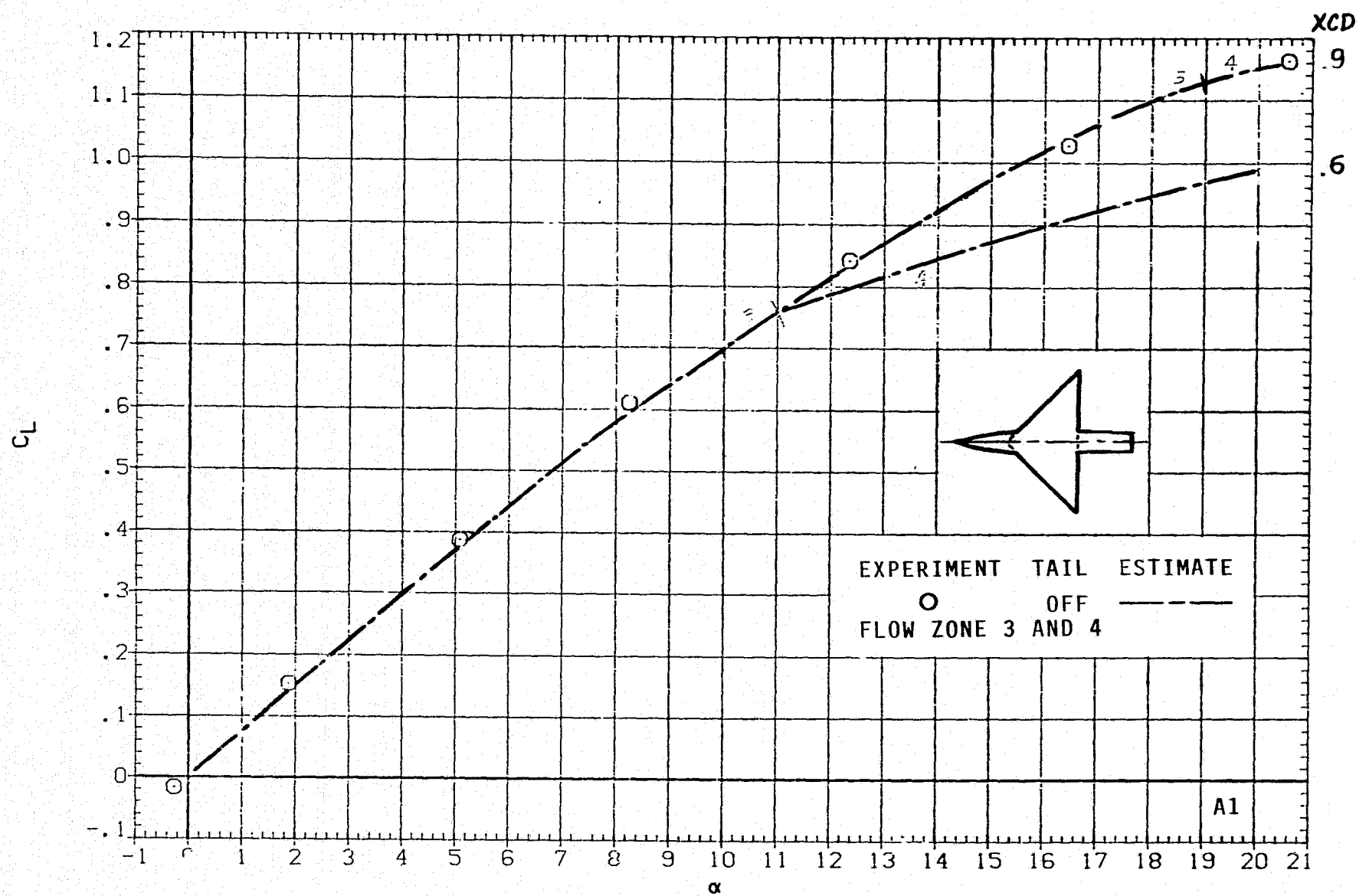
(e) C_L VERSUS C_D ; $M = 0.9$, $J = 1$.

FIGURE 5.- CONTINUED.



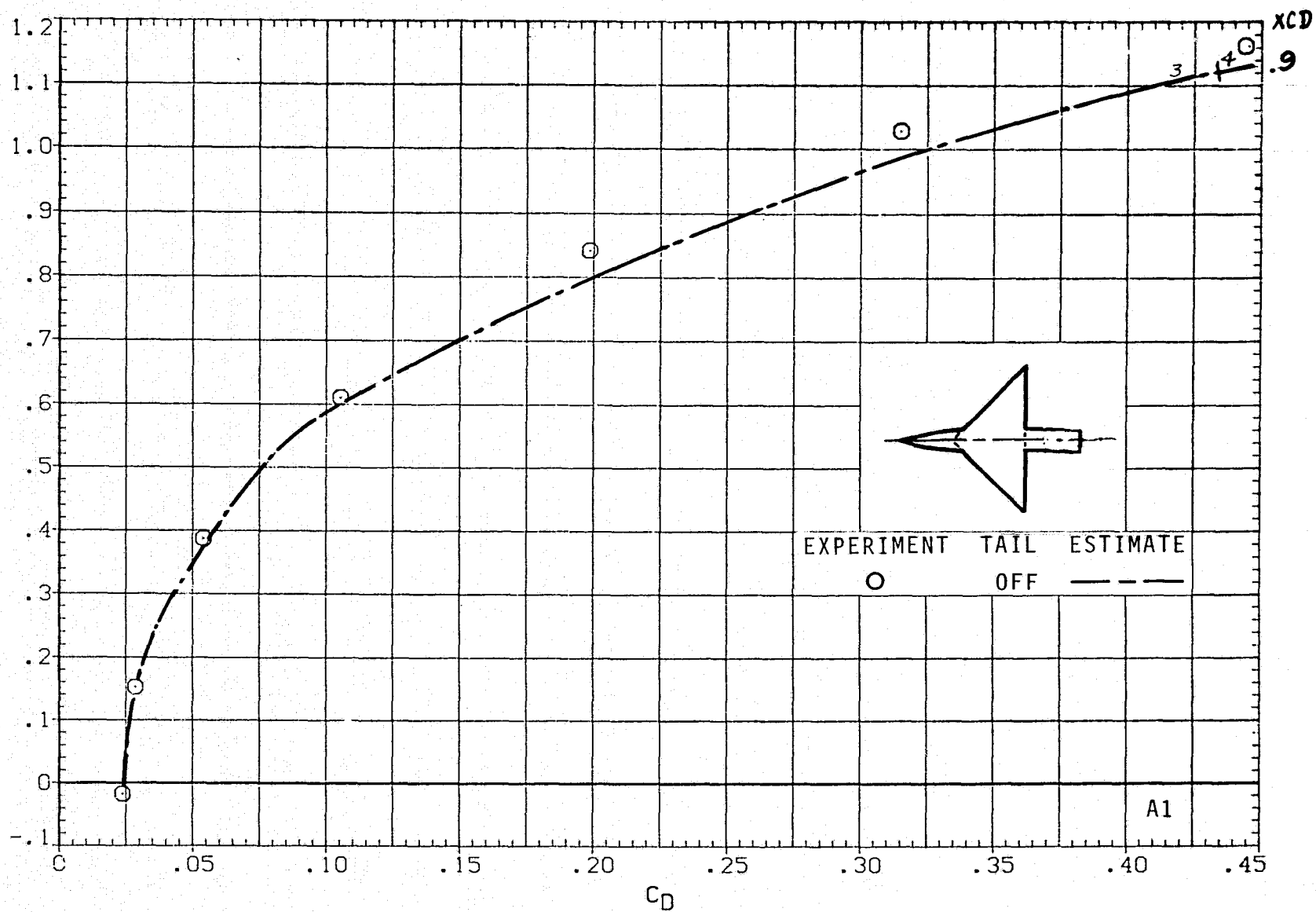
(f) C_L VERSUS C_m ; $M = 0.9$, $J = 1$.

FIGURE 5.- CONTINUED.



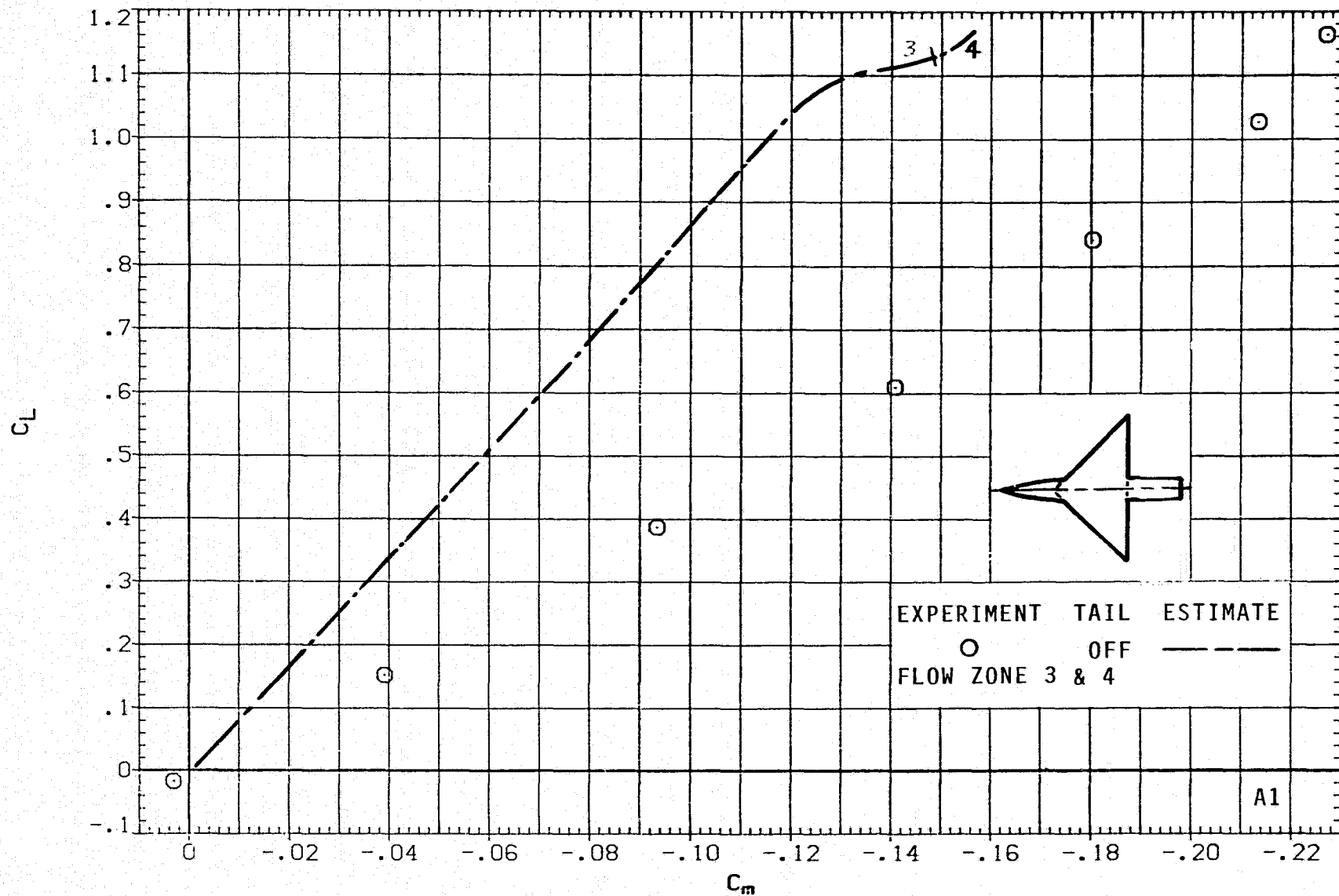
(g) C_L VERSUS α ; $M = 1.2$, $J = 1$.

FIGURE 5.- CONTINUED.



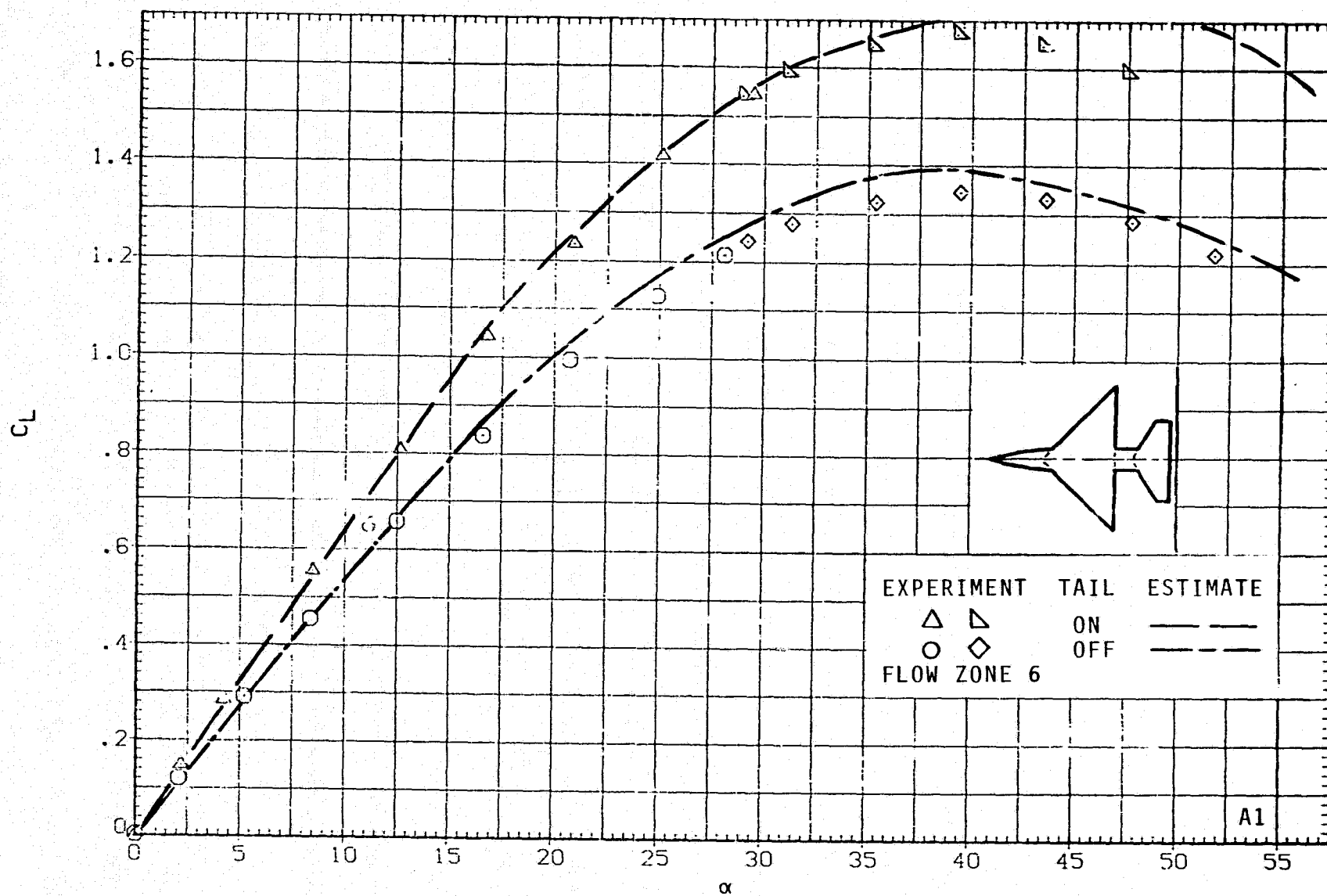
(h) C_L VERSUS C_D ; $M = 1.2$, $J = 1$.

FIGURE 5.- CONTINUED.



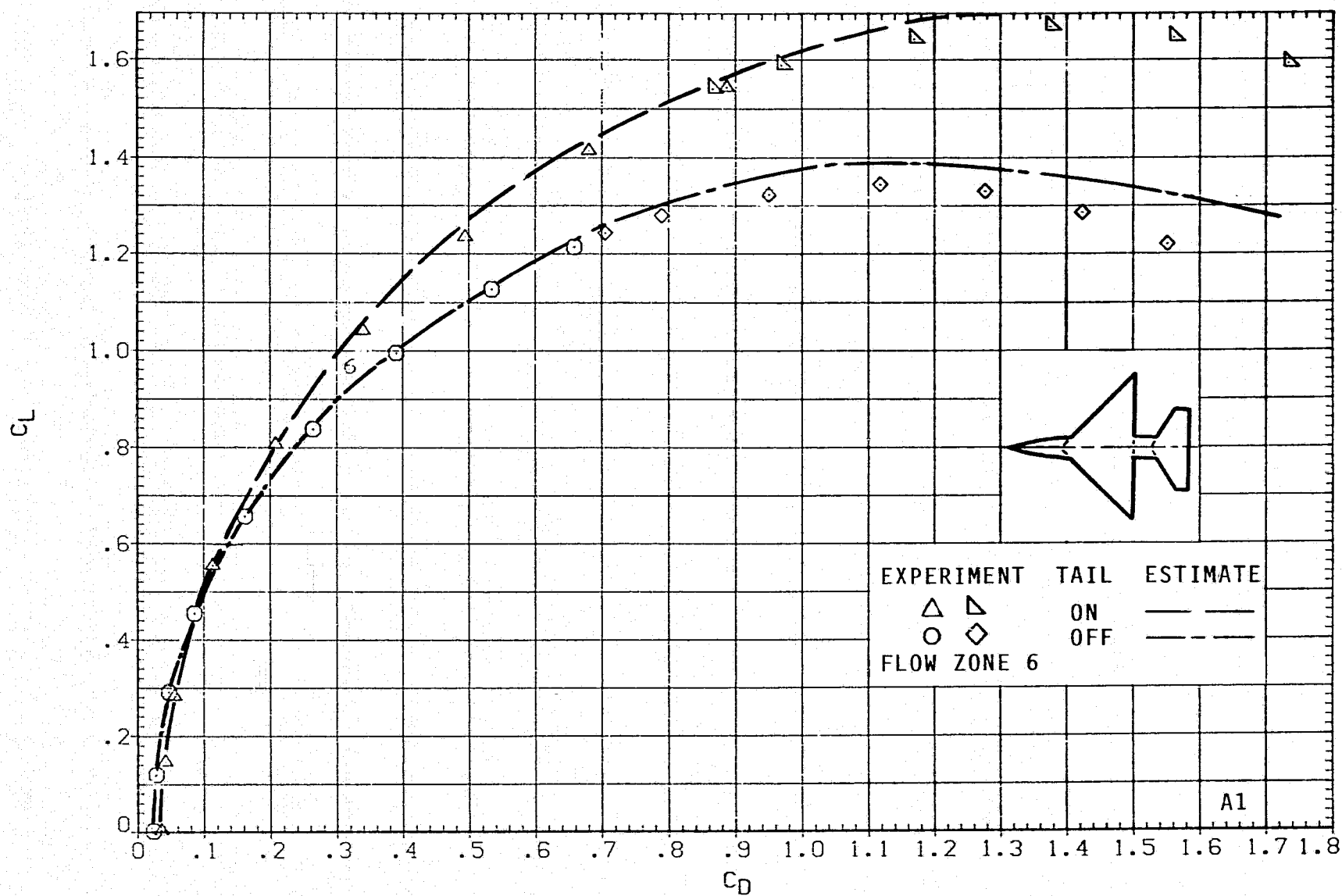
(i) C_L VERSUS C_m ; $M = 1.2$ $J = 1$.

FIGURE 5.- CONTINUED.



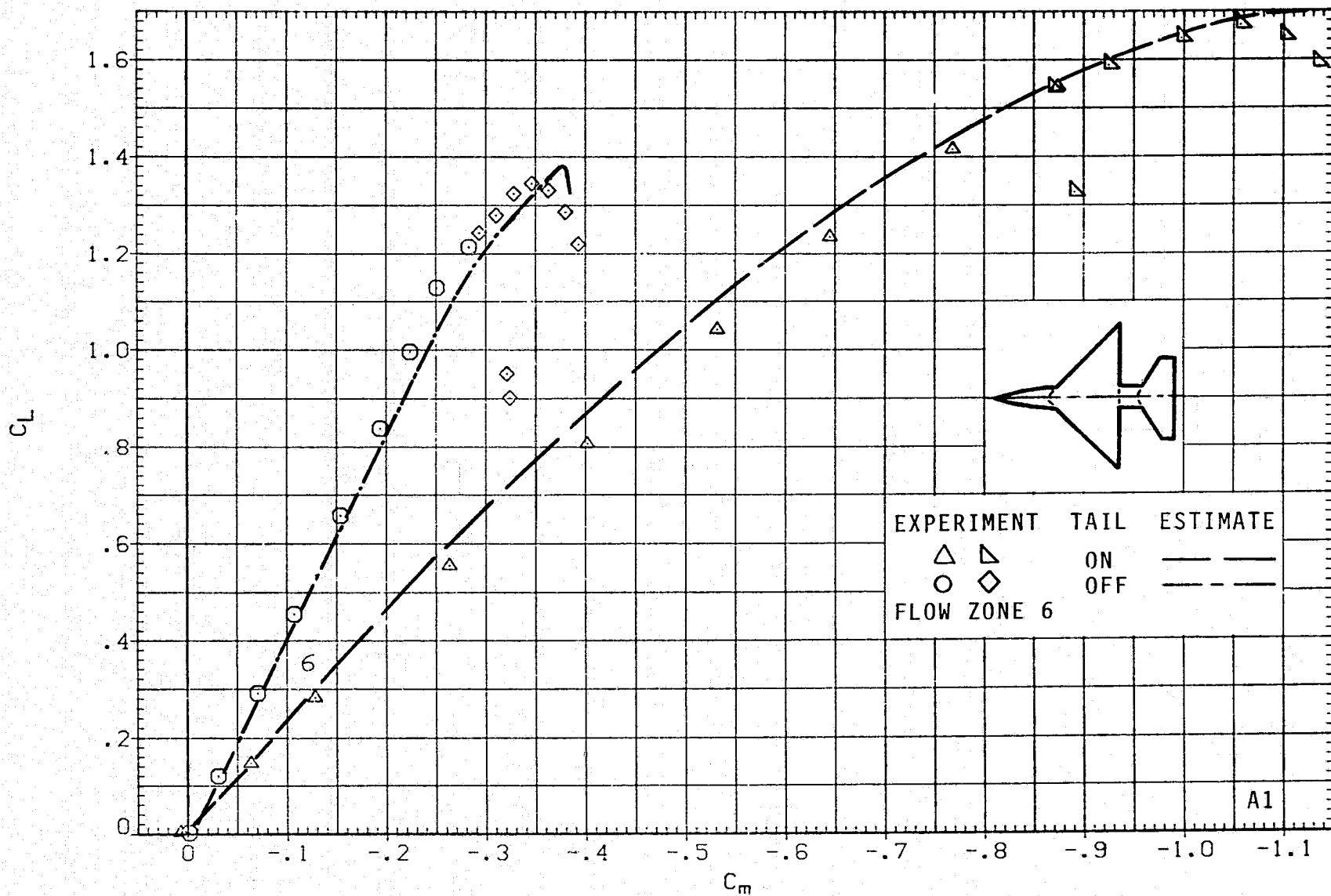
(j) C_L VERSUS α ; $M = 1.5$, $J = 5$.

FIGURE 5.- CONTINUED.



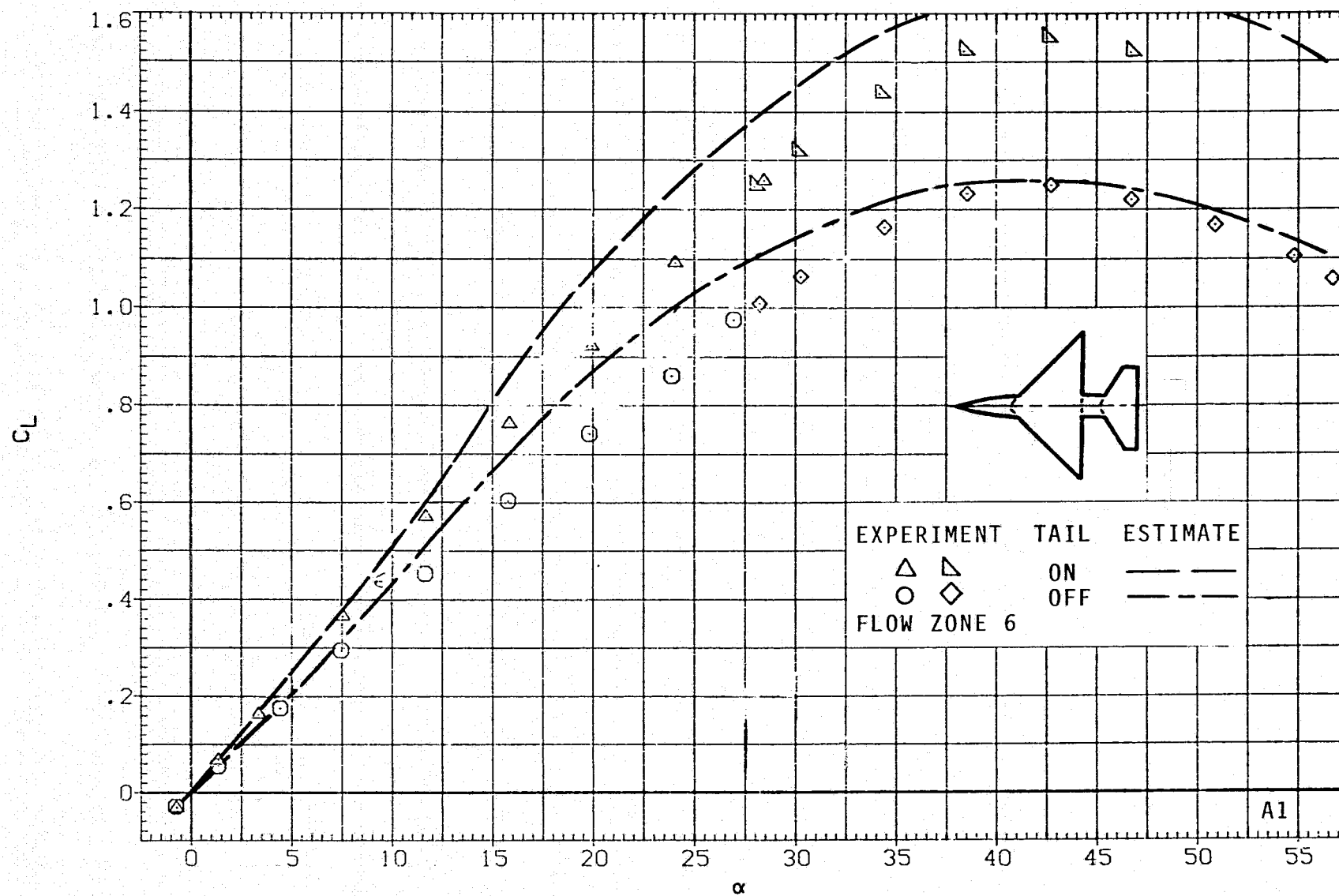
(k) C_L VERSUS C_D ; $M = 1.5$, $J = 5$.

FIGURE 5.- CONTINUED.



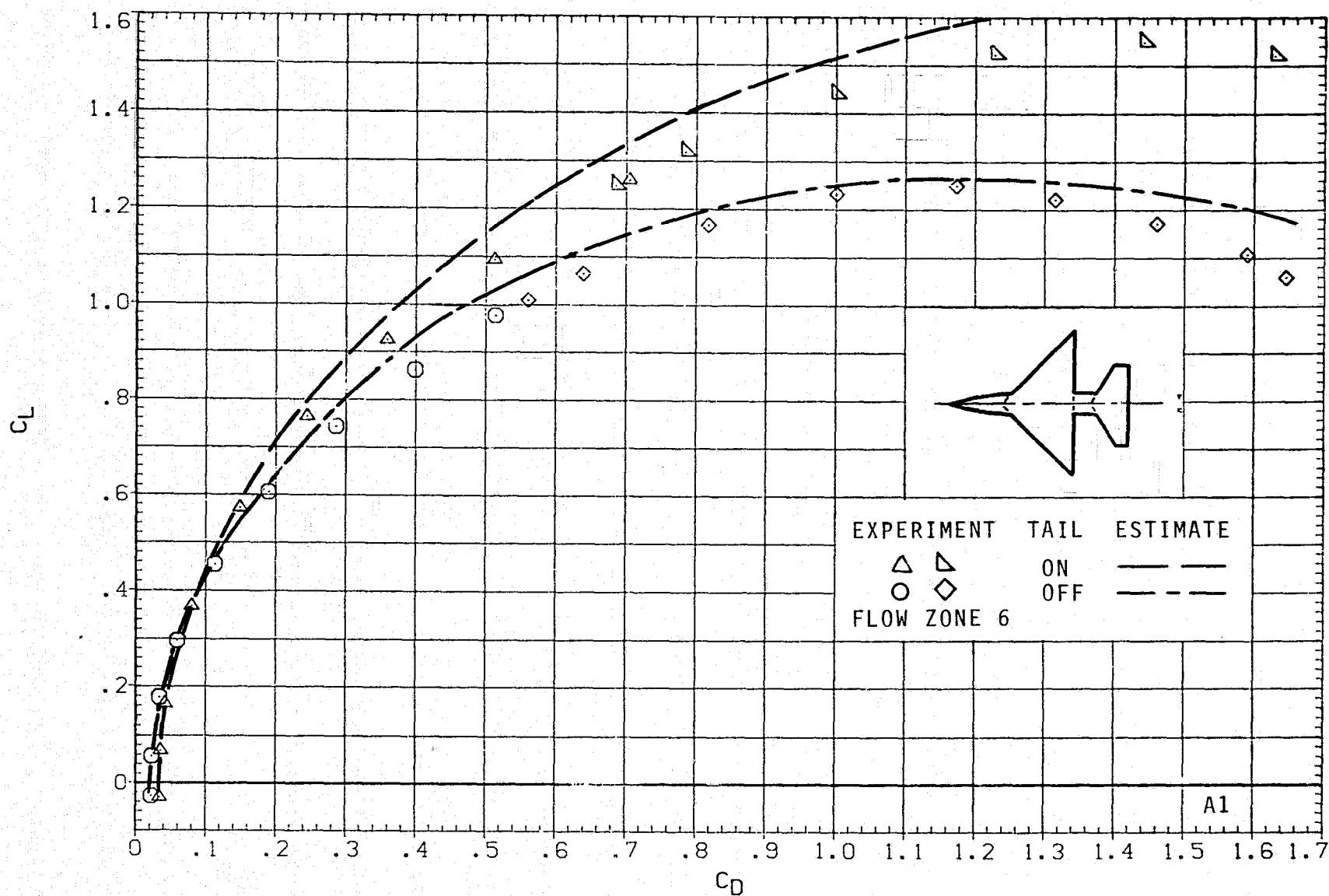
(1) C_L VERSUS C_m ; $M = 1.5$, $J = 5$.

FIGURE 5.- CONTINUED.



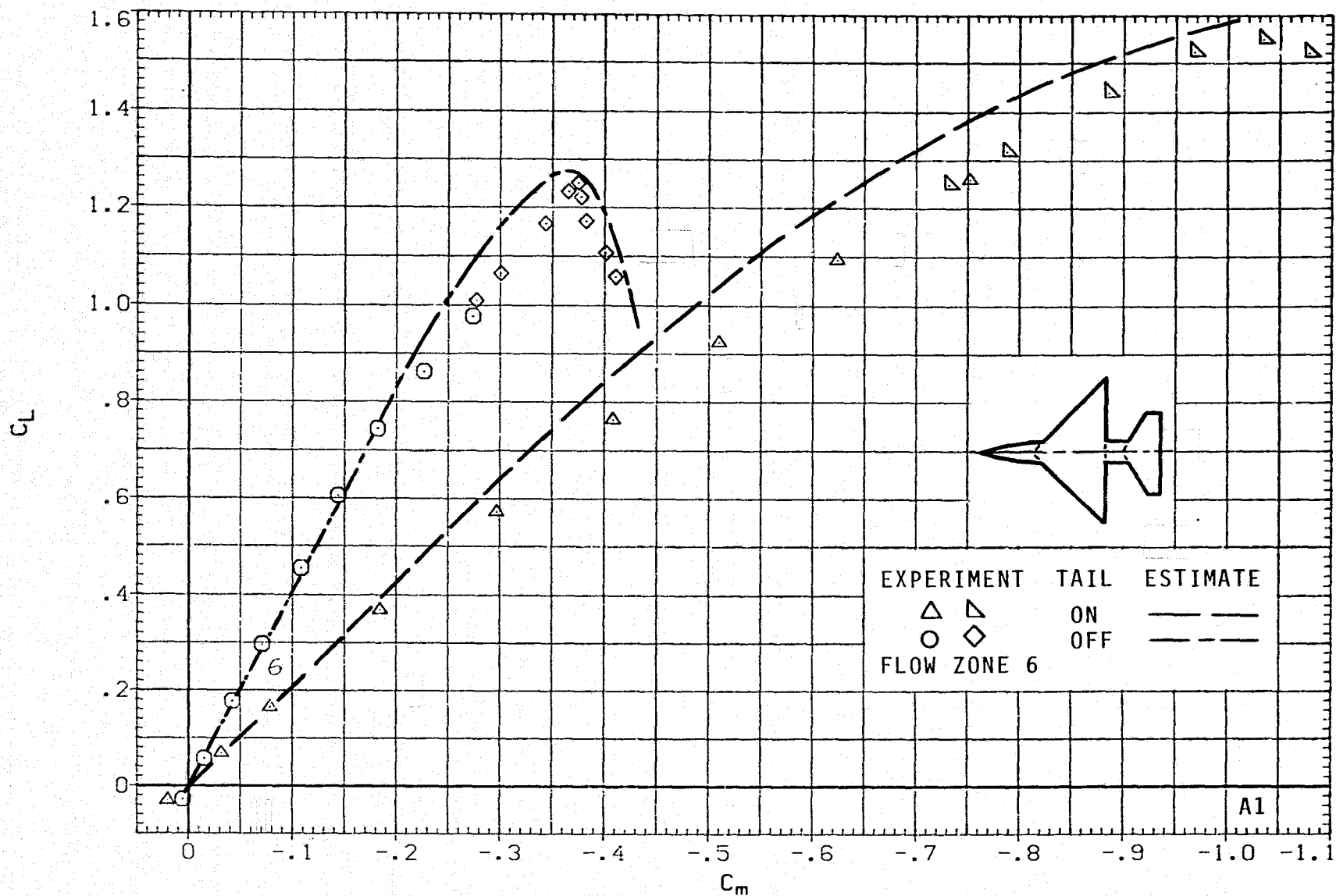
(m) C_L VERSUS α ; $M = 2.0$, $J = 5$.

FIGURE 5.- CONTINUED.



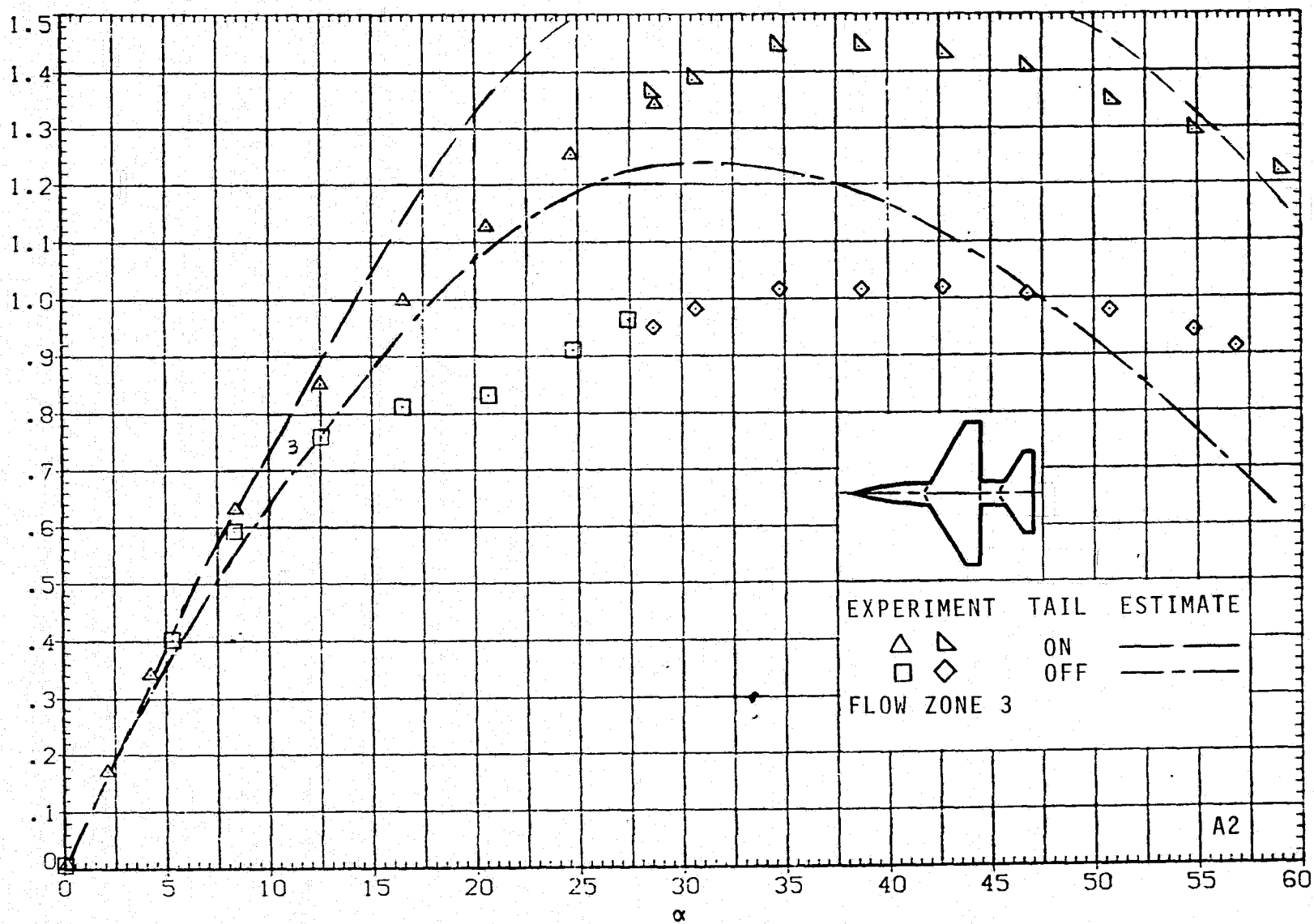
(n) C_L VERSUS C_D ; $M = 2.0$, $J = 5$.

FIGURE 5.- CONTINUED.



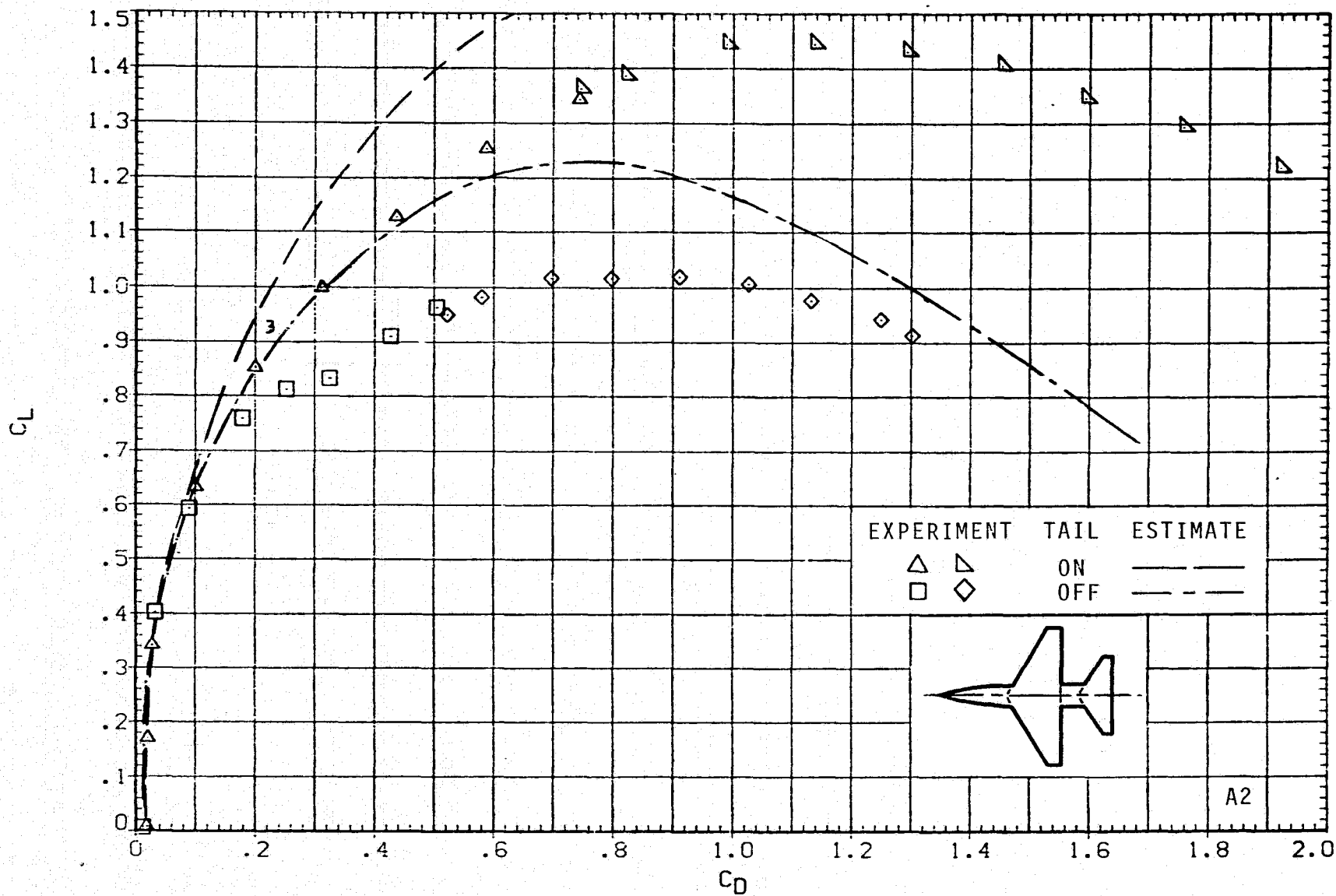
(o) C_L VERSUS C_m ; $M = 2.0$, $J = 5$.

FIGURE 5.- CONCLUDED.



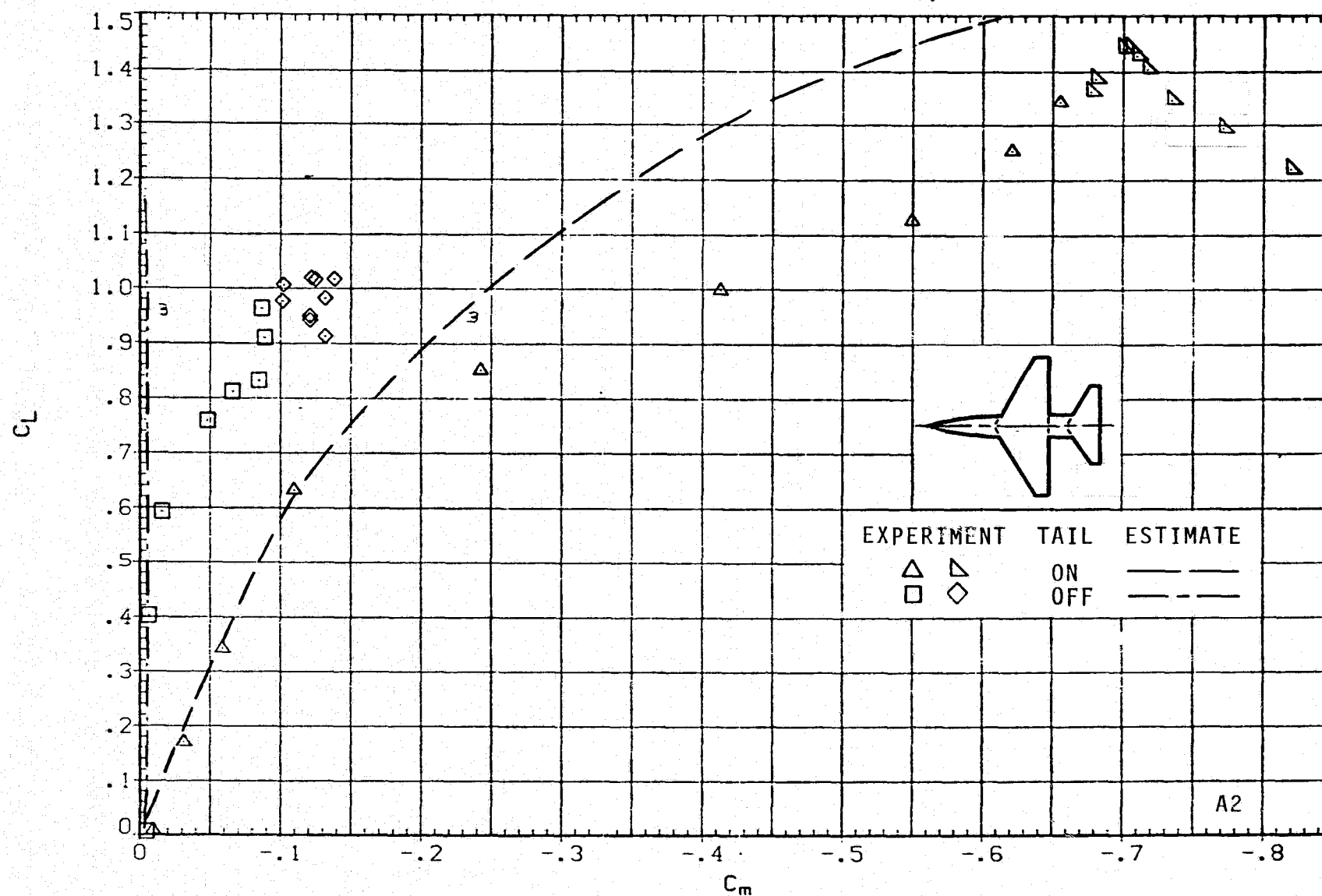
(a) C_L VERSUS α ; $M = 0.6$, $J = 1$.

FIGURE 6.- AERODYNAMICS FOR MODEL A2; ARW = 4, TRW = 0.25.



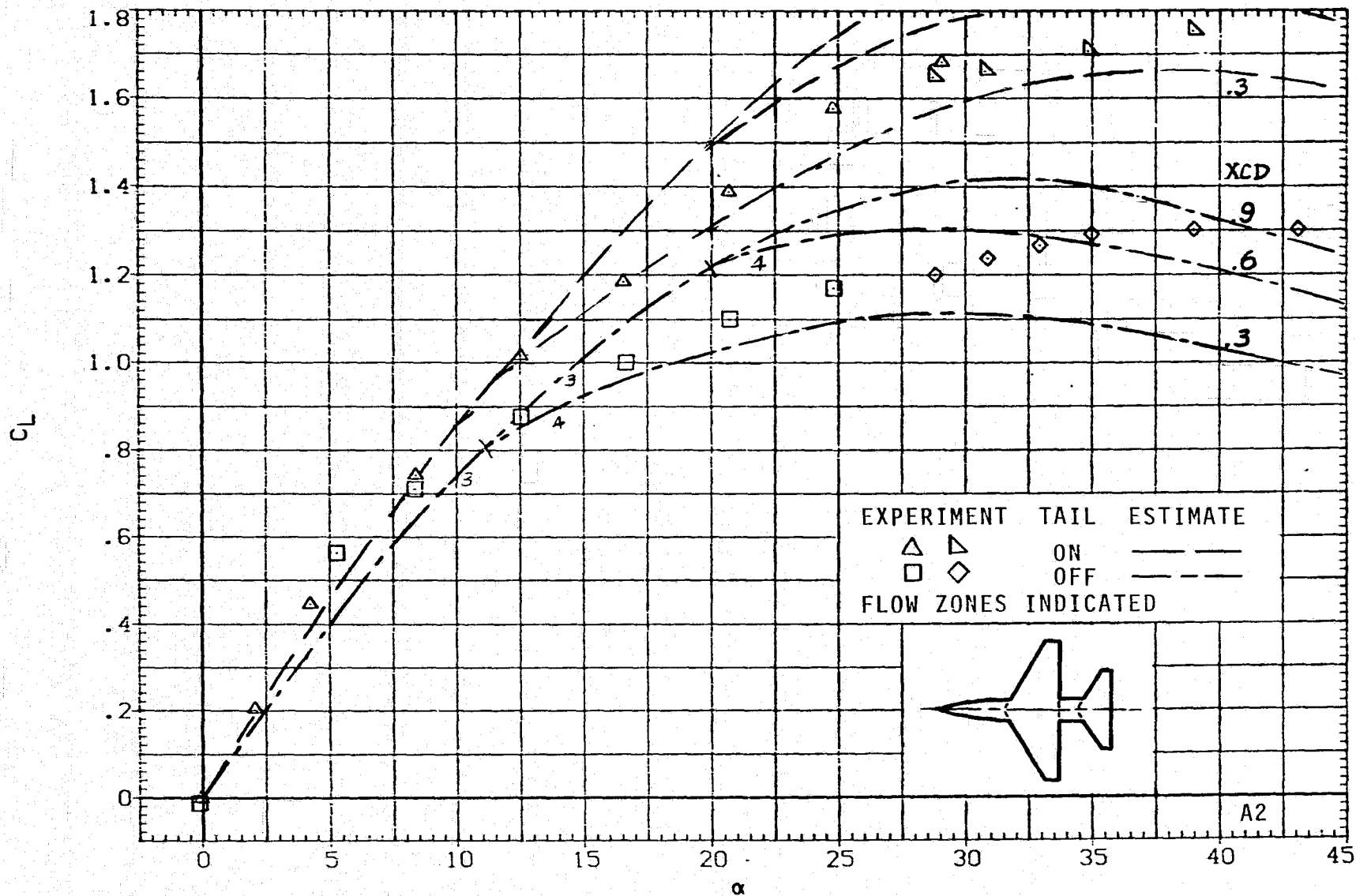
(b) C_L VERSUS C_D ; $M = 0.6$, $J = 1$.

FIGURE 6.- CONTINUED.



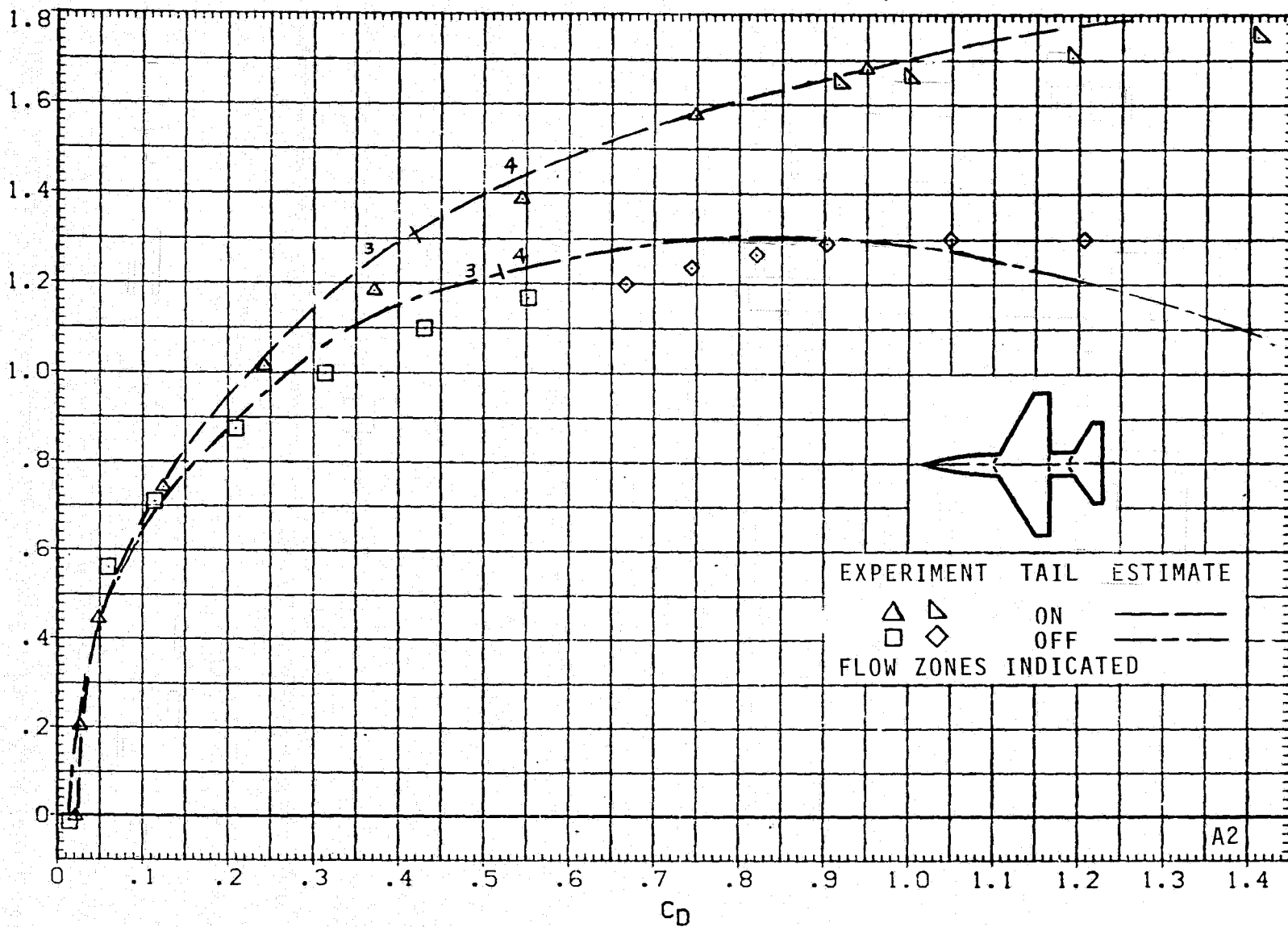
(c) C_L VERSUS C_m ; $M = 0.6$, $J = 1$.

FIGURE 6.- CONTINUED.



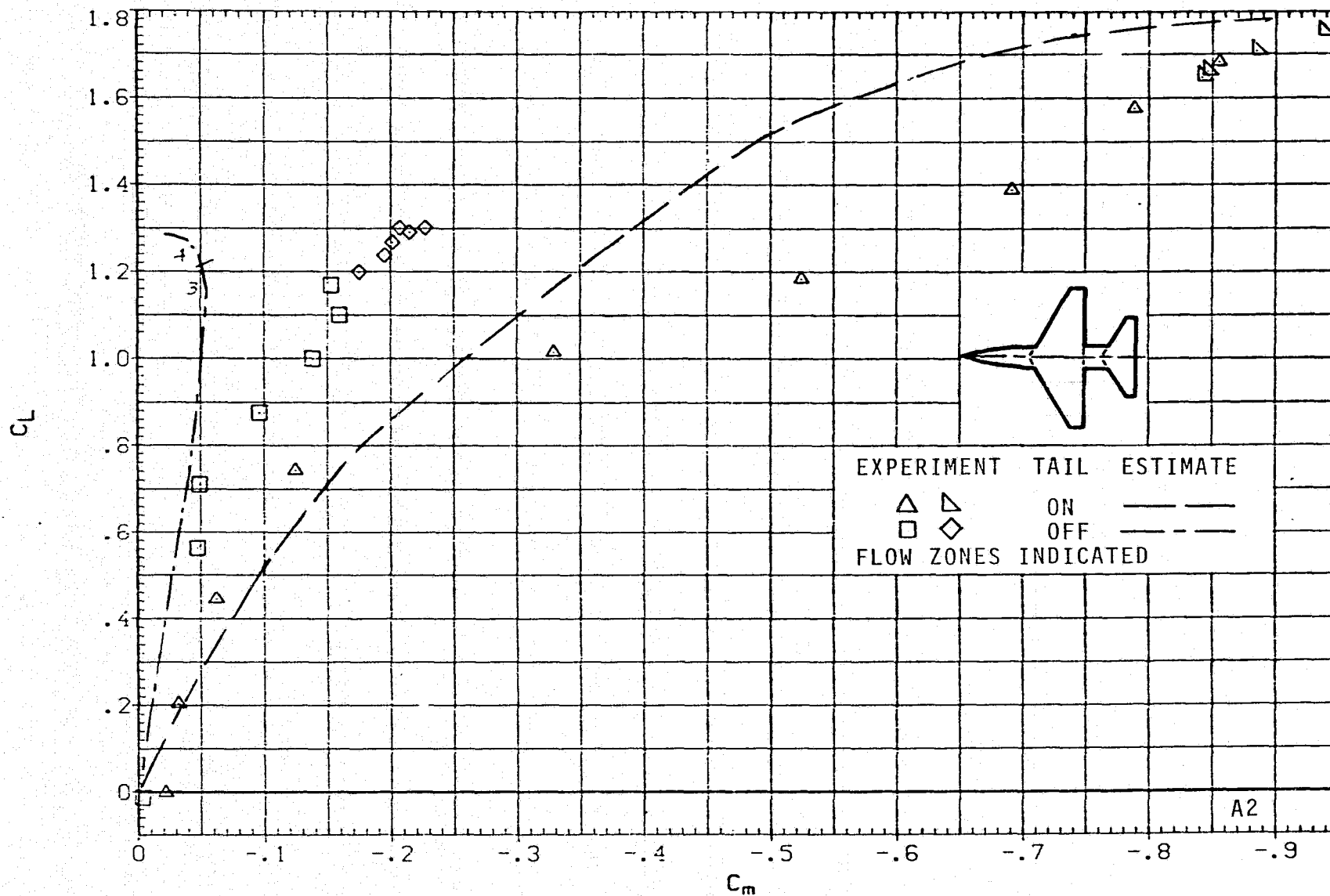
(d) C_L VERSUS α ; $M = 0.9$, $J = 1$.

FIGURE 6.- CONTINUED.



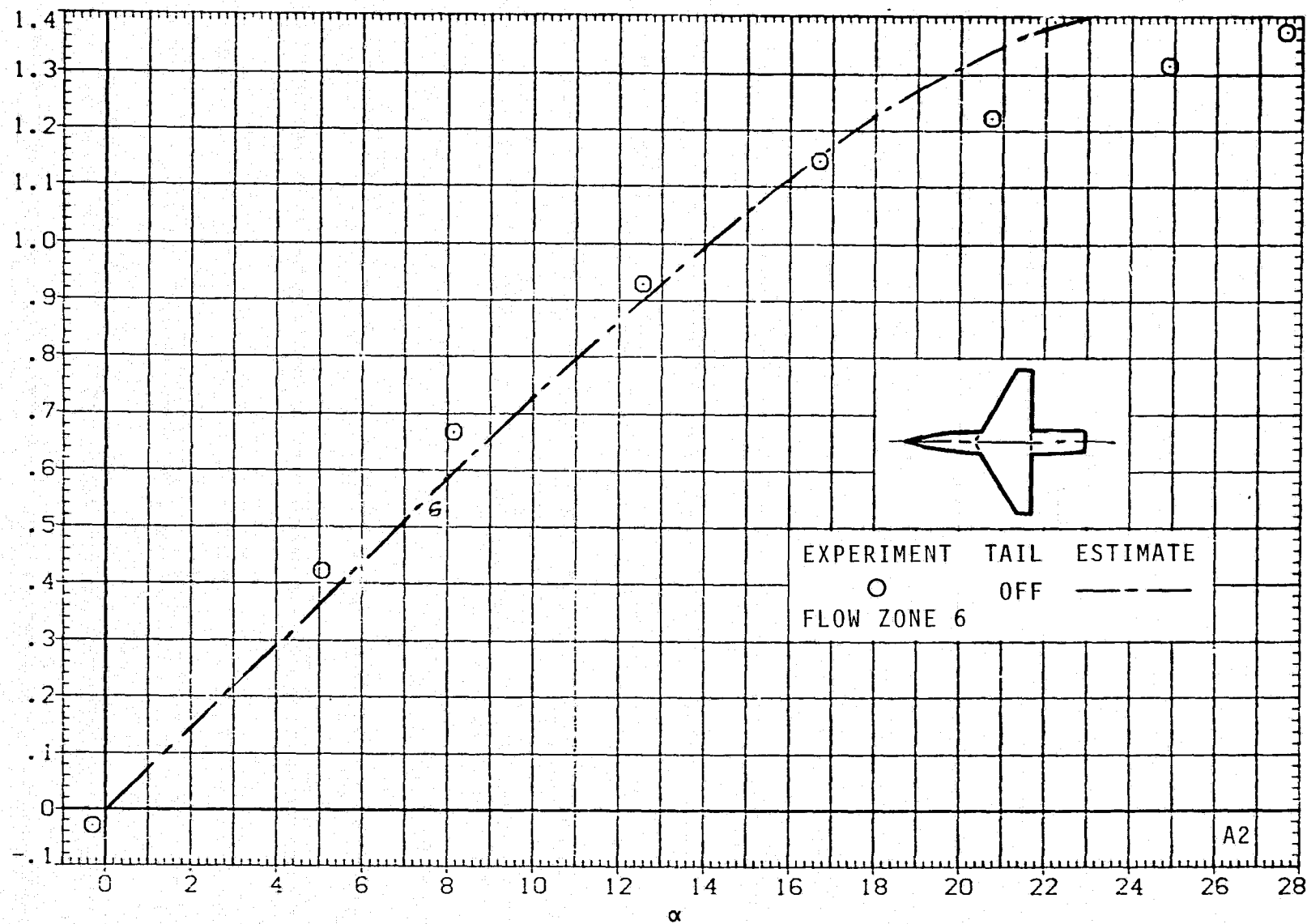
(e) C_L VERSUS C_D ; $M = 0.9$, $J = 1$.

FIGURE 6.- CONTINUED.



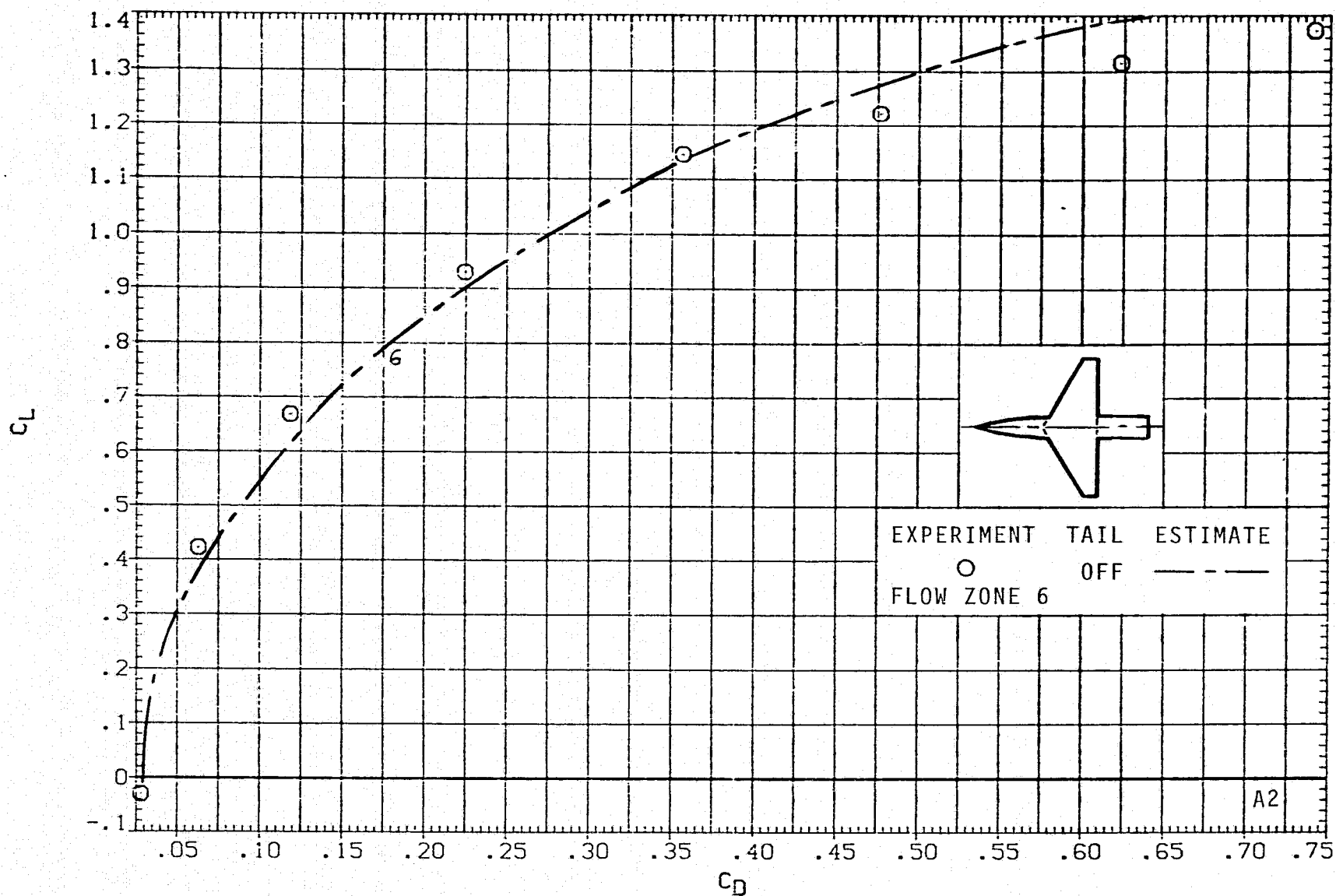
(f) C_L VERSUS C_m ; $M = 0.9$, $J = 1$.

FIGURE 6.- CONTINUED.



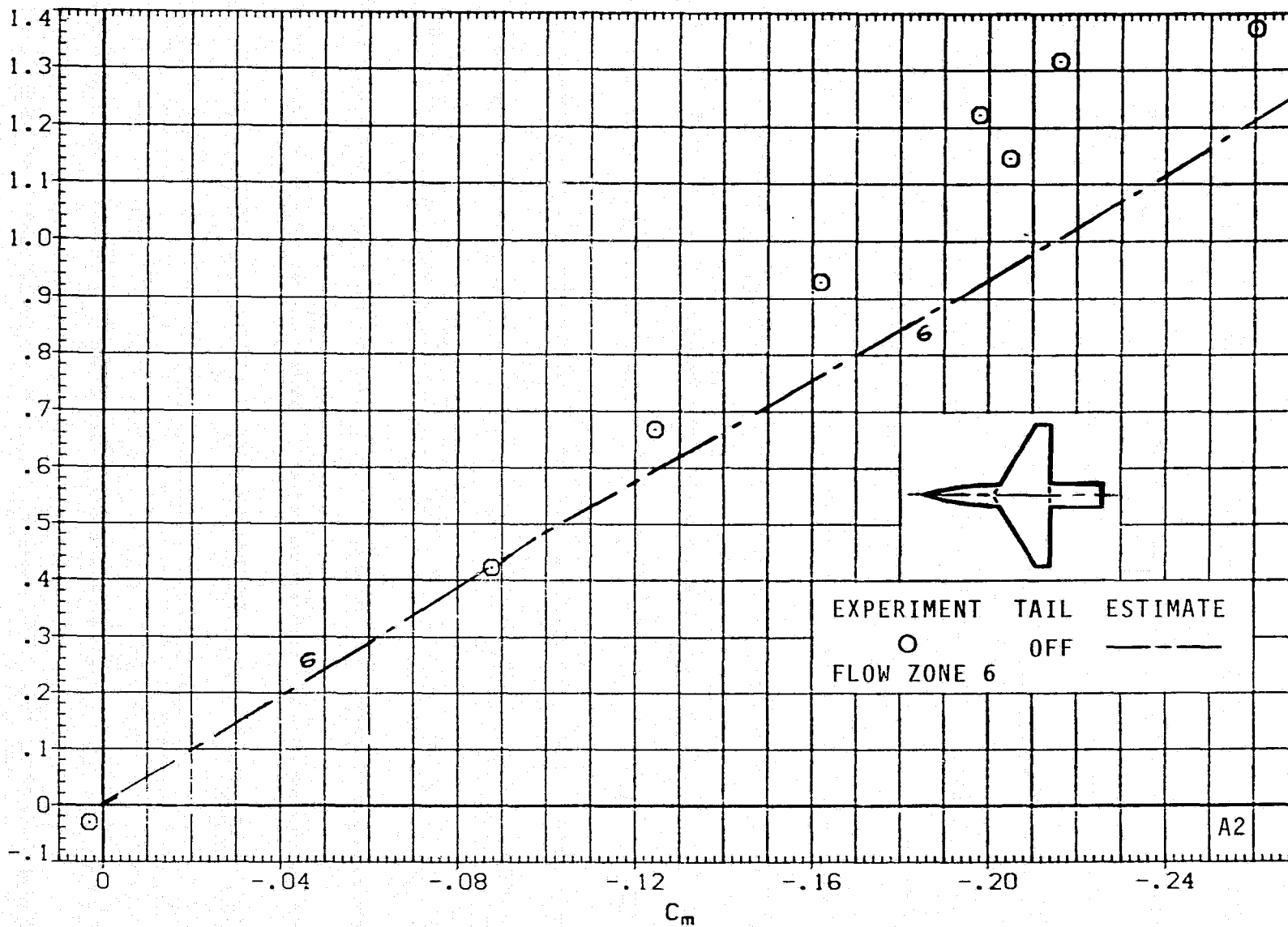
(g) C_L VERSUS α ; $M = 1.2$, $J = 5$.

FIGURE 6.- CONTINUED.



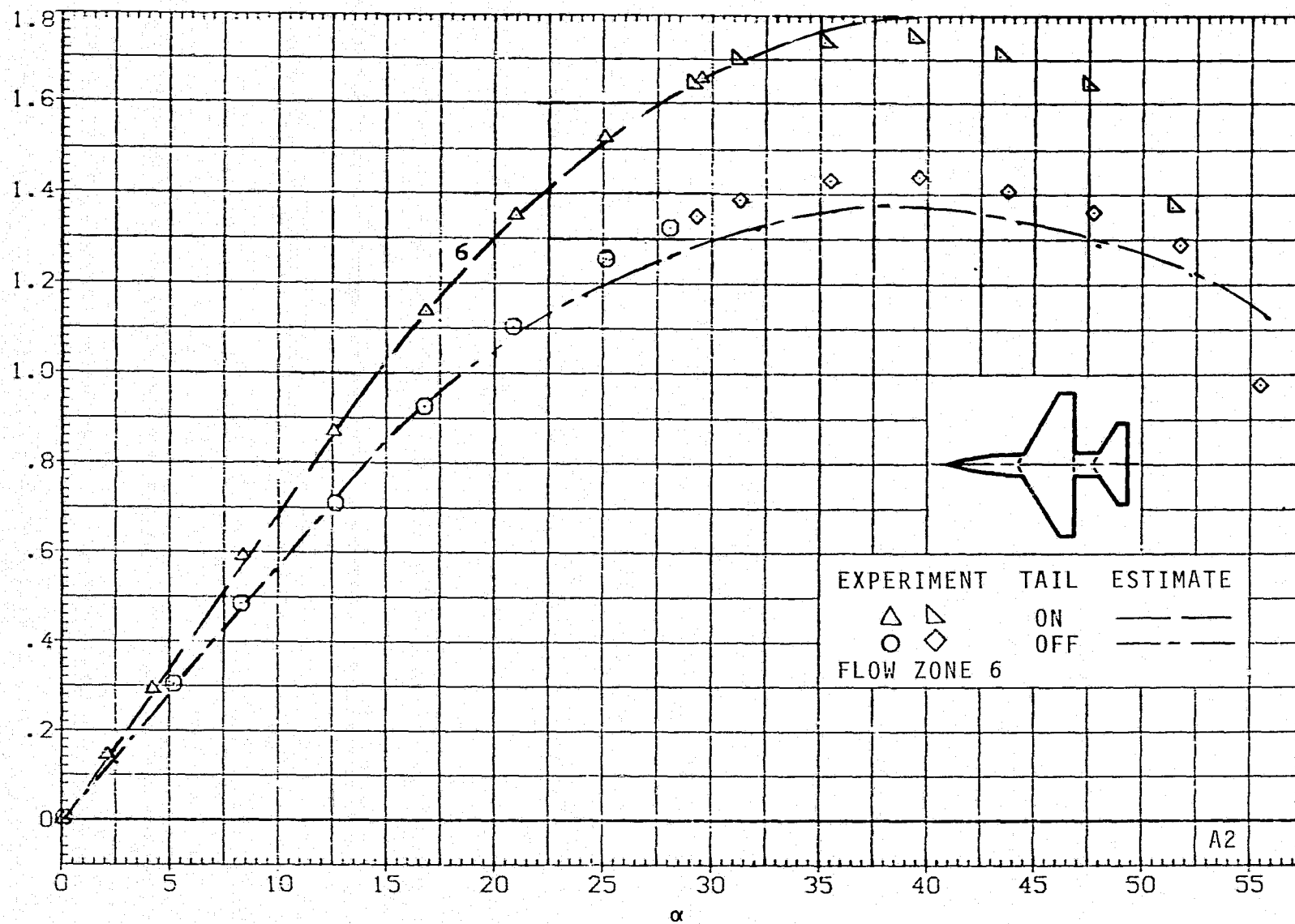
(h) C_L VERSUS C_D ; $M = 1.2$, $J = 5$.

FIGURE 6.- CONTINUED.

C_L 

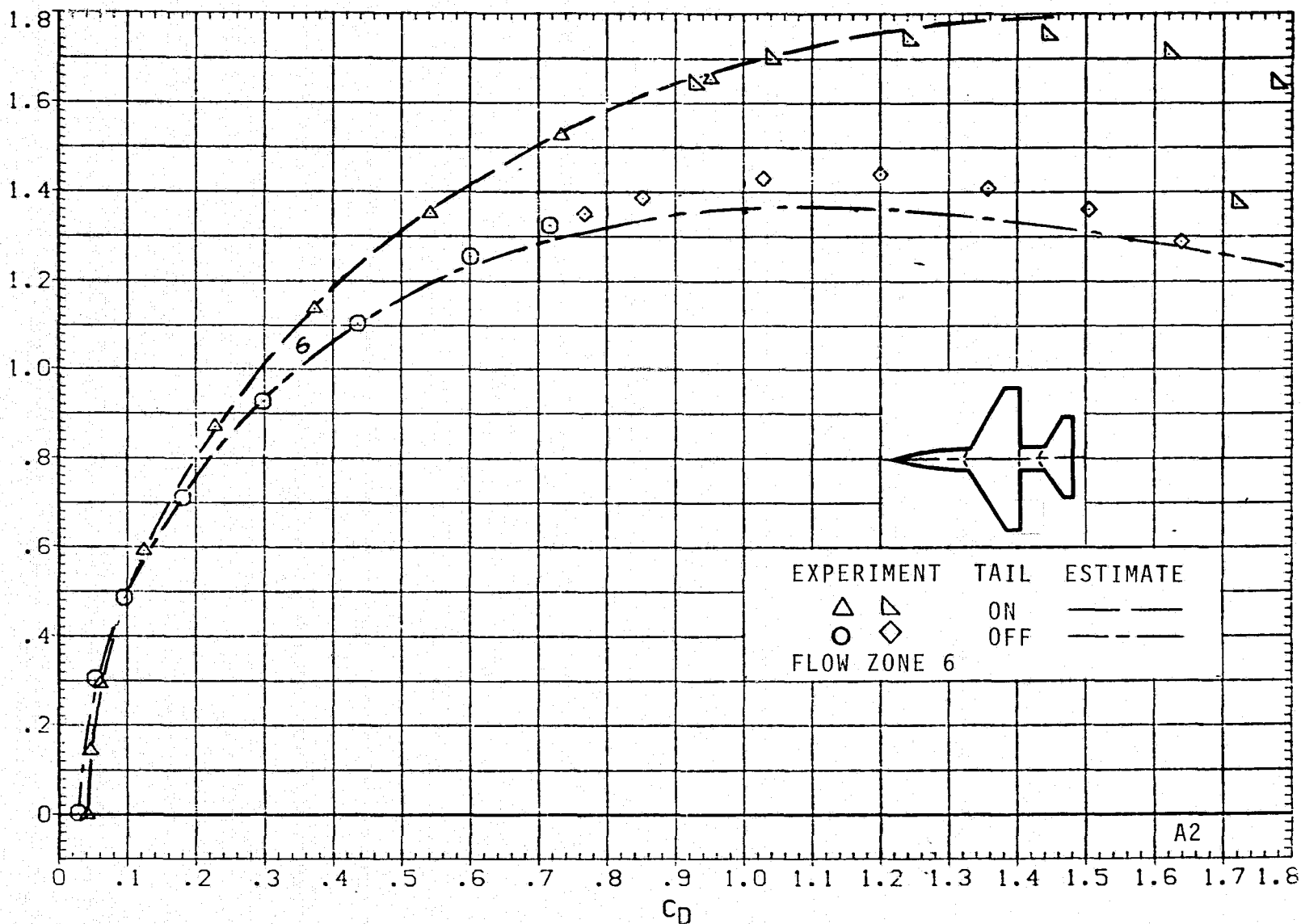
(i) C_L VERSUS C_m ; $M = 1.2$, $J = 5$.

FIGURE 6.- CONTINUED.



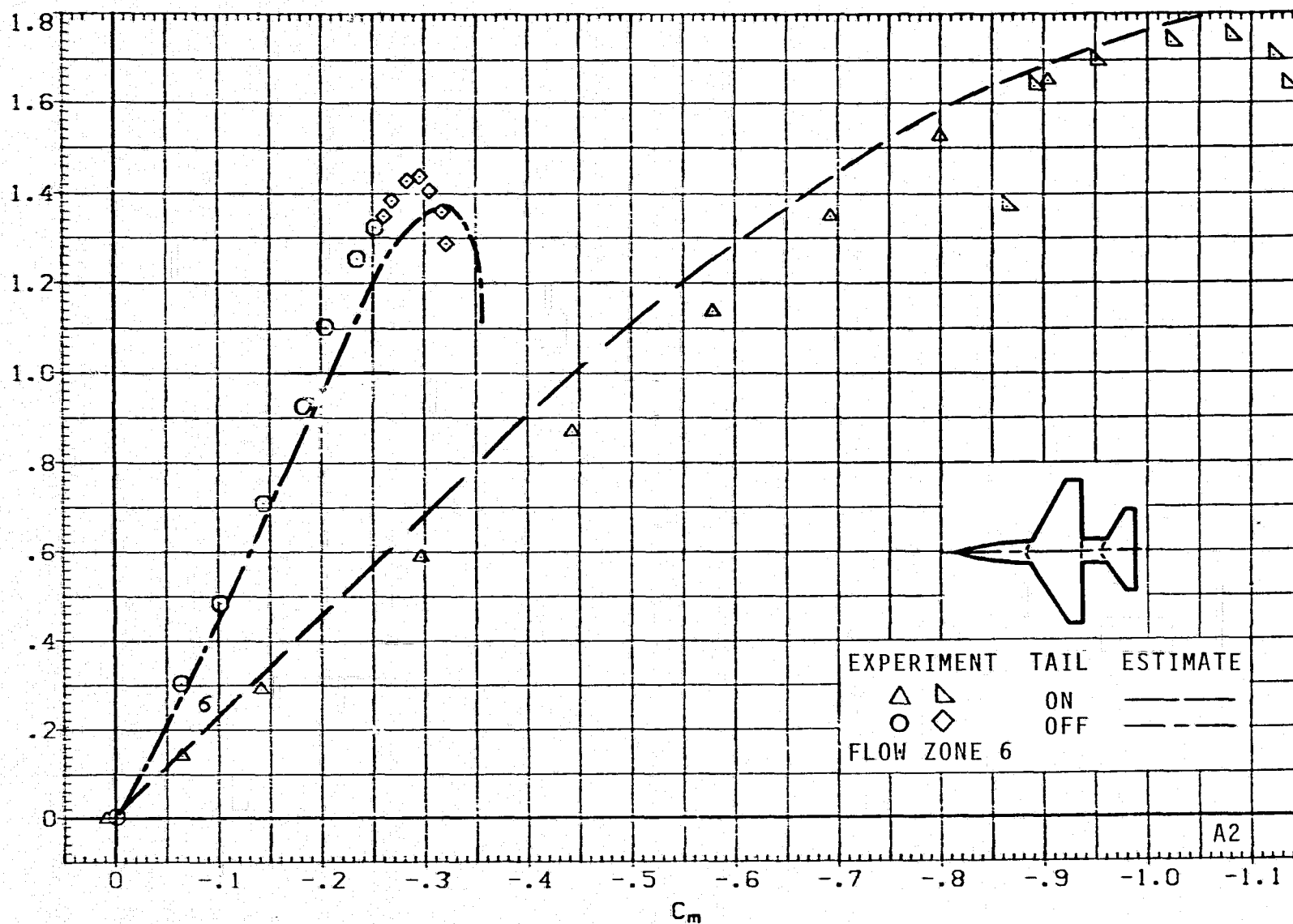
(j) C_L VERSUS α ; $M = 1.5$, $J = 5$.

FIGURE 6.- CONTINUED.

C_L 

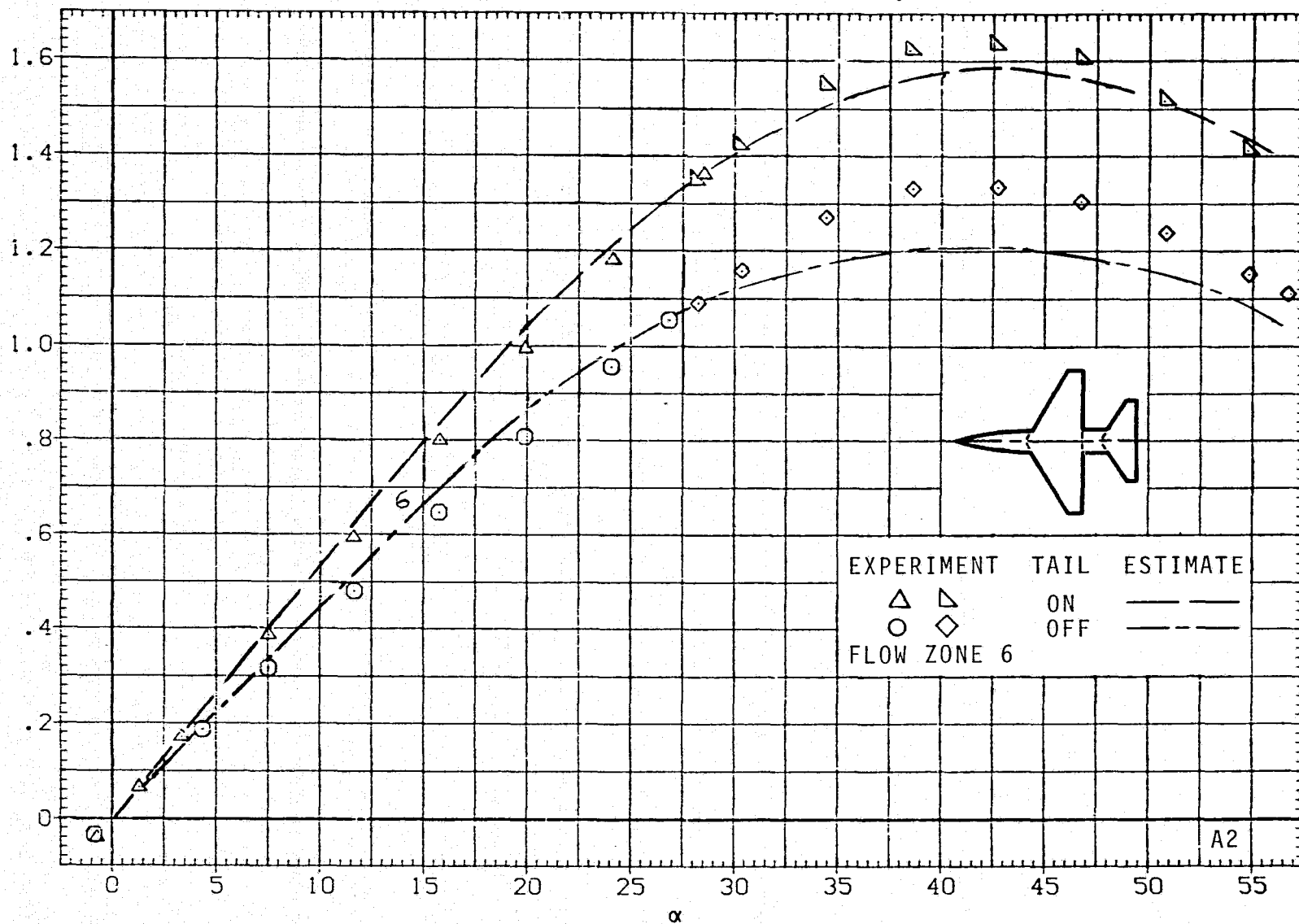
(k) C_L VERSUS C_D ; $M = 1.5$, $J = 5$.

FIGURE 6.- CONTINUED.

C_L 

(1) C_L VERSUS C_m ; $M = 1.5$, $J = 5$.

FIGURE 6.- CONTINUED.

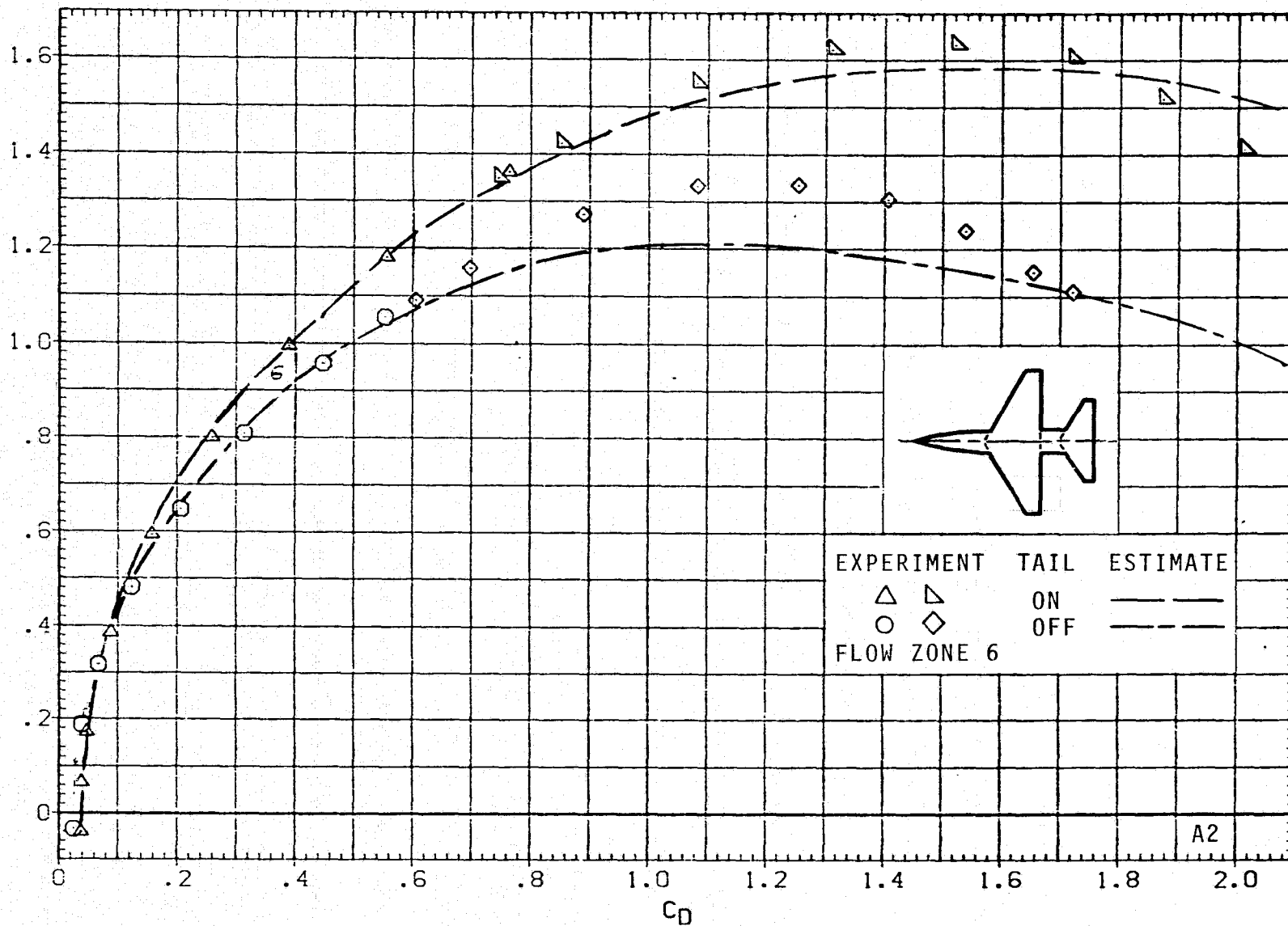
C_L 

(m) C_L VERSUS α ; $M = 2.0$, $J = 5$.

FIGURE 6.- CONTINUED.

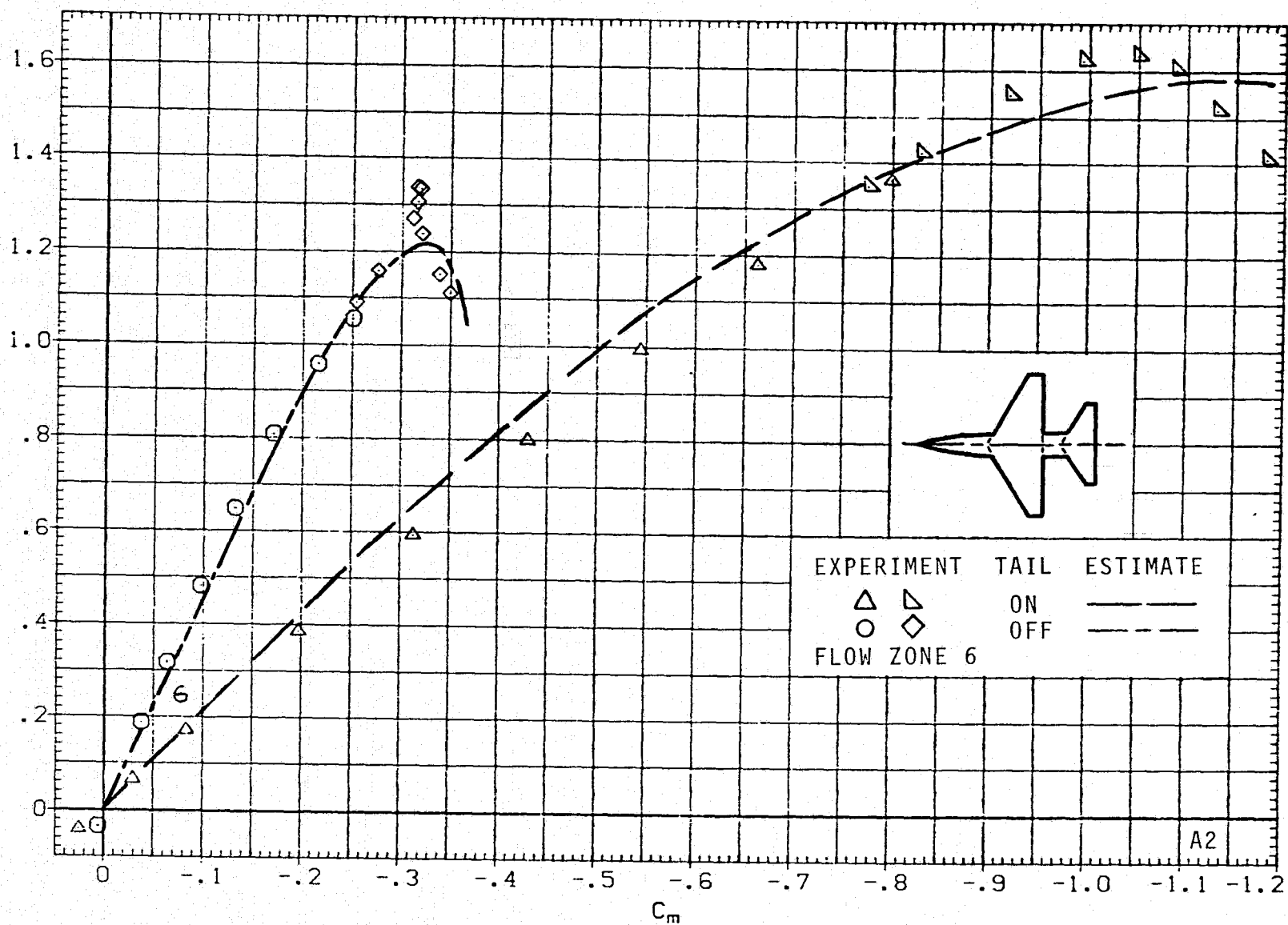
C_L

70



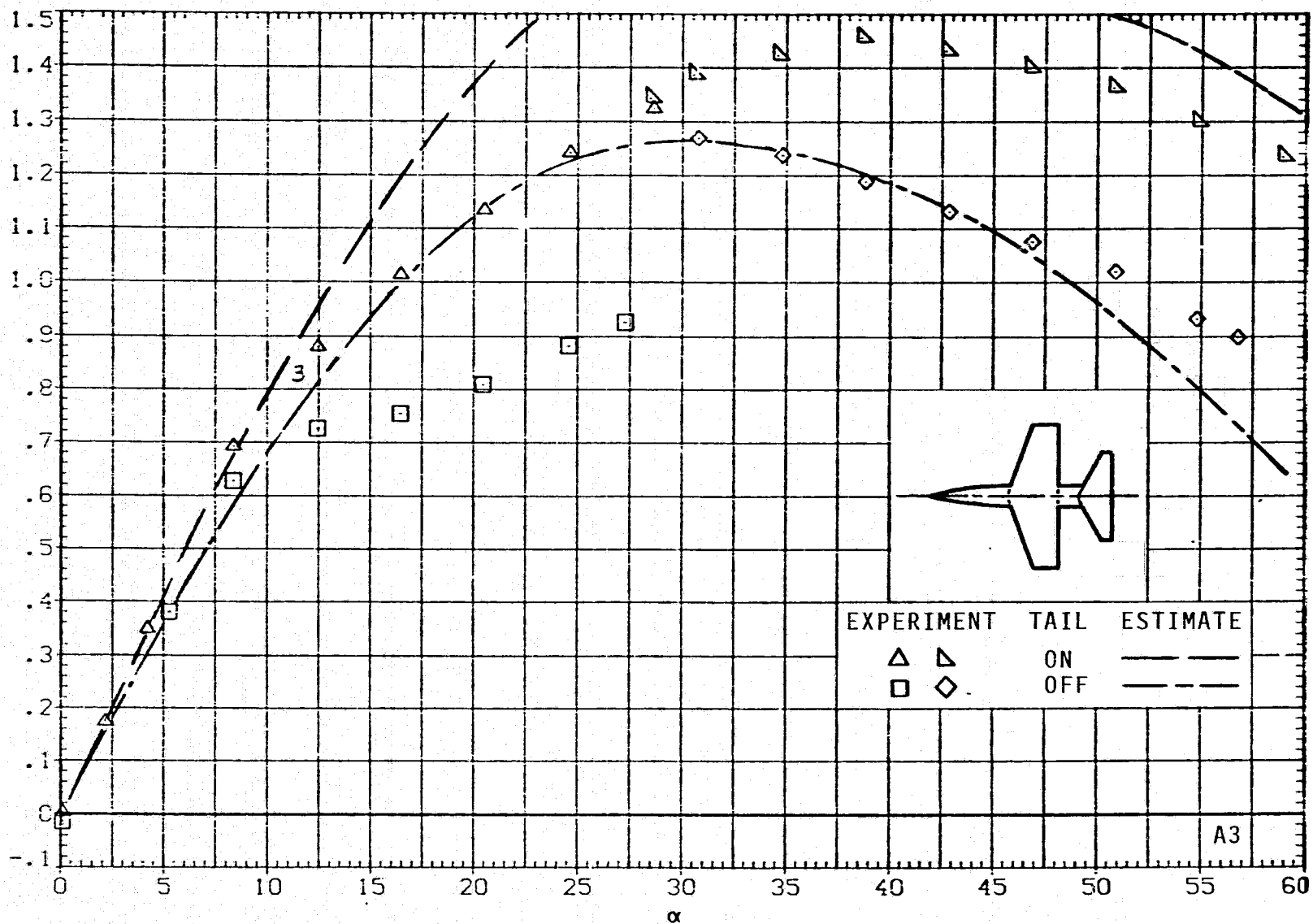
(n) C_L VERSUS C_D ; $M = 2.0$, $J = 5$.

FIGURE 6.- CONTINUED.



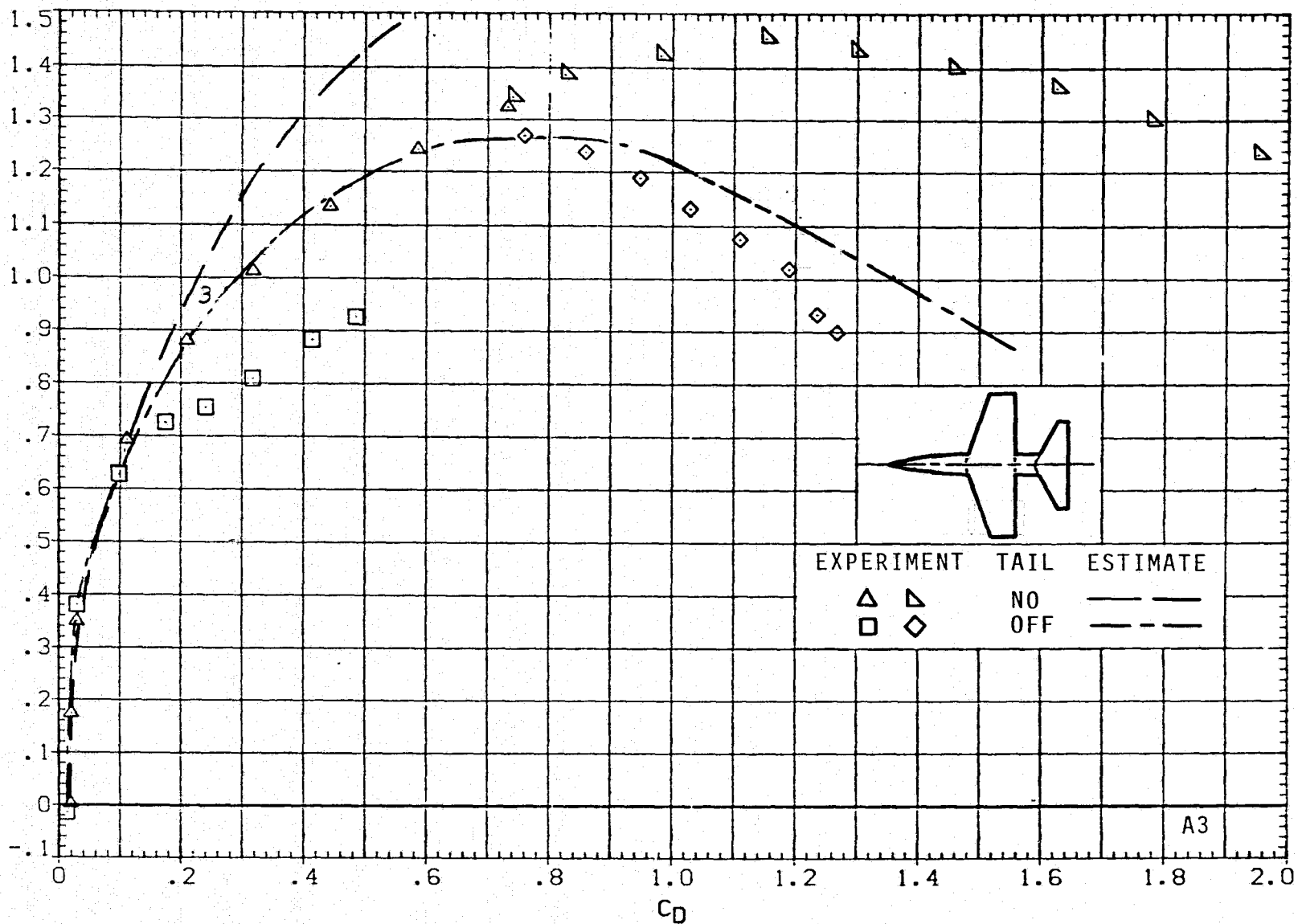
(o) C_L VERSUS C_m ; $M = 2.0$, $J = 5$.

FIGURE 6.- CONCLUDED.



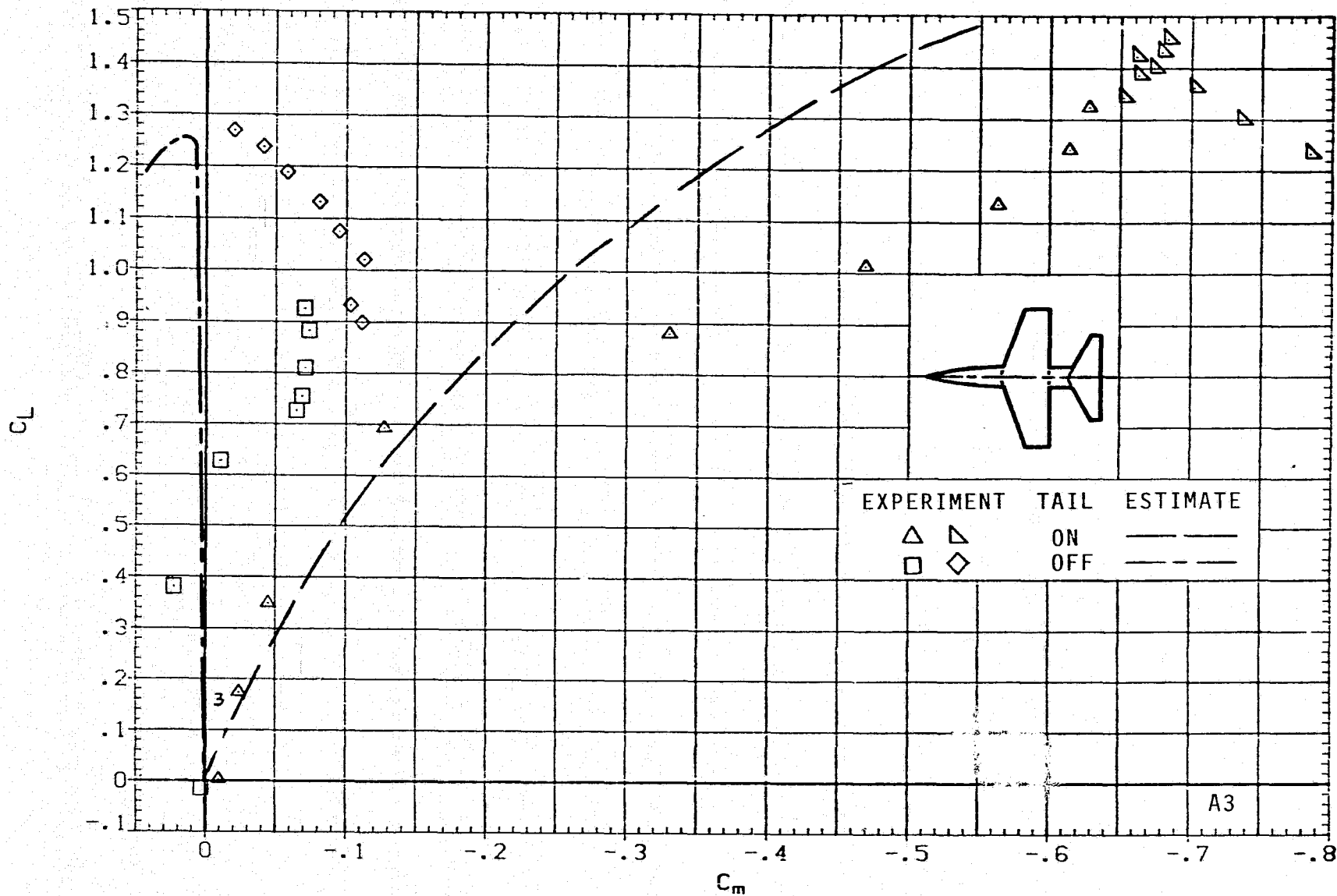
(a) C_L VERSUS α ; $M = 0.6$; $J = 1$.

FIGURE 7.- AERODYNAMICS FOR MODEL A3; ARW = 4, TRW = 0.25.



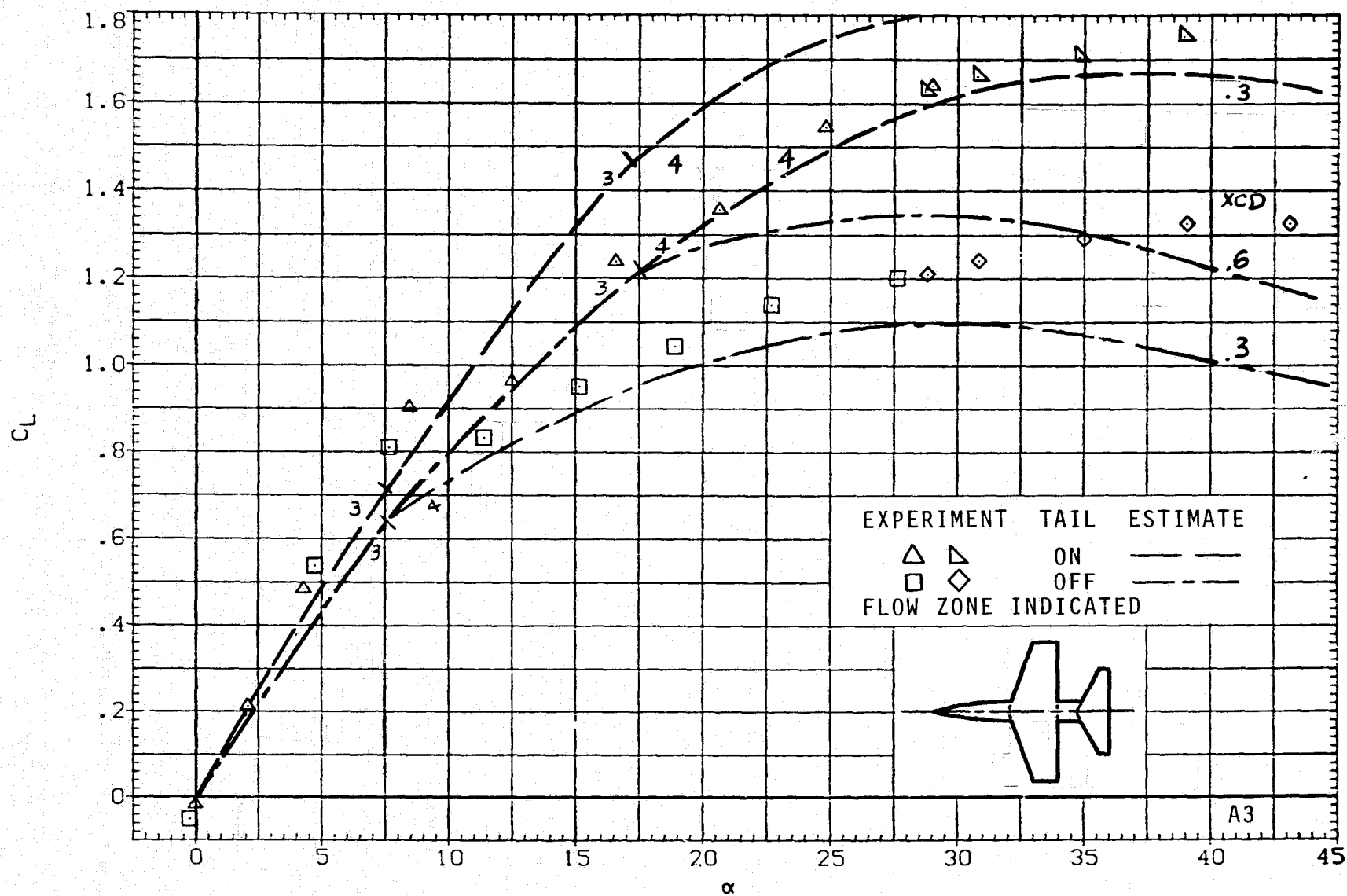
(b) C_L VERSUS C_D : $M = 0.6$, $J = 1$.

FIGURE 7-. CONTINUED.



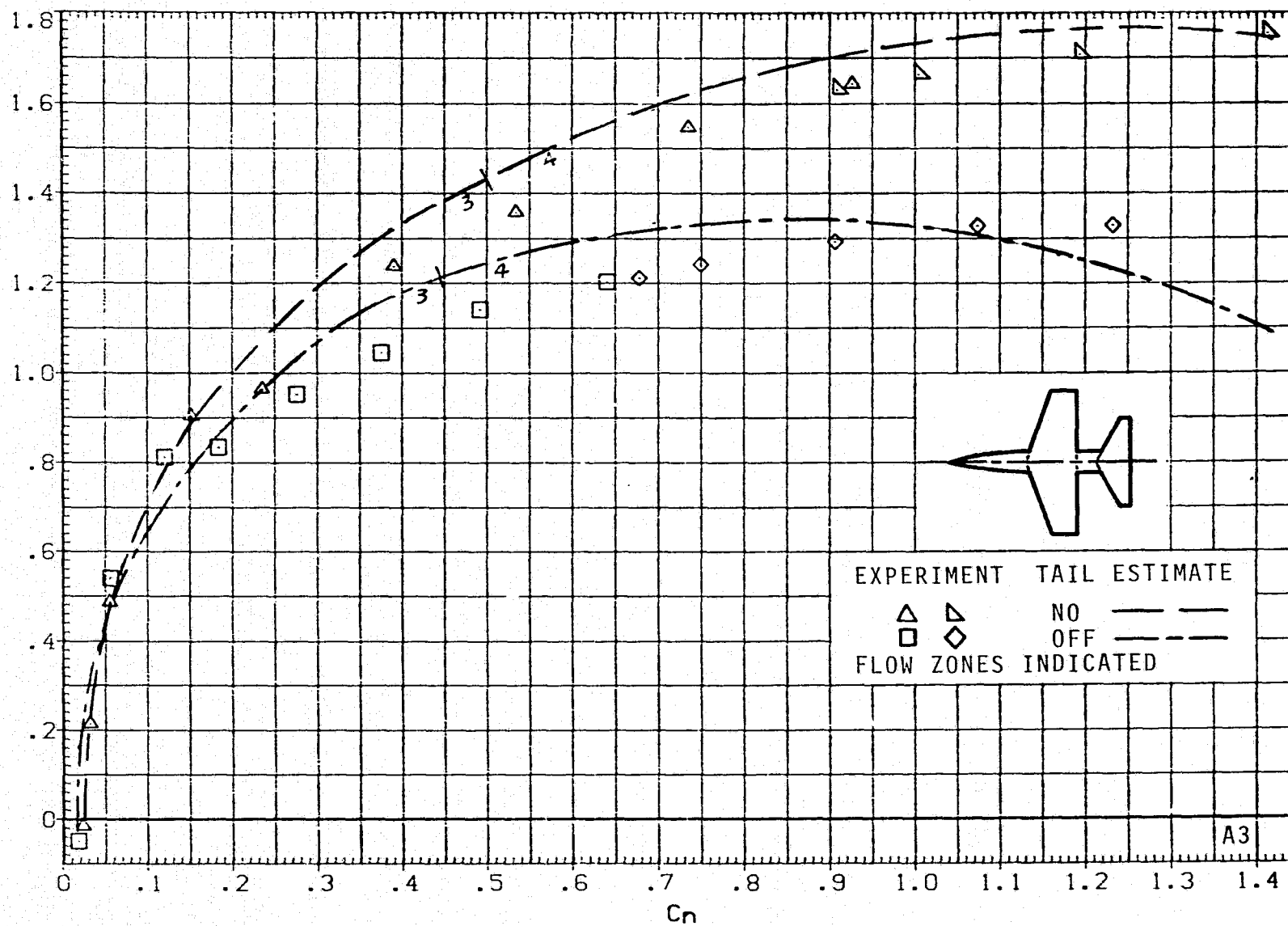
(c) C_L VERSUS C_m ; $M = 0.6$, $J = 1$.

FIGURE 7.- CONTINUED.



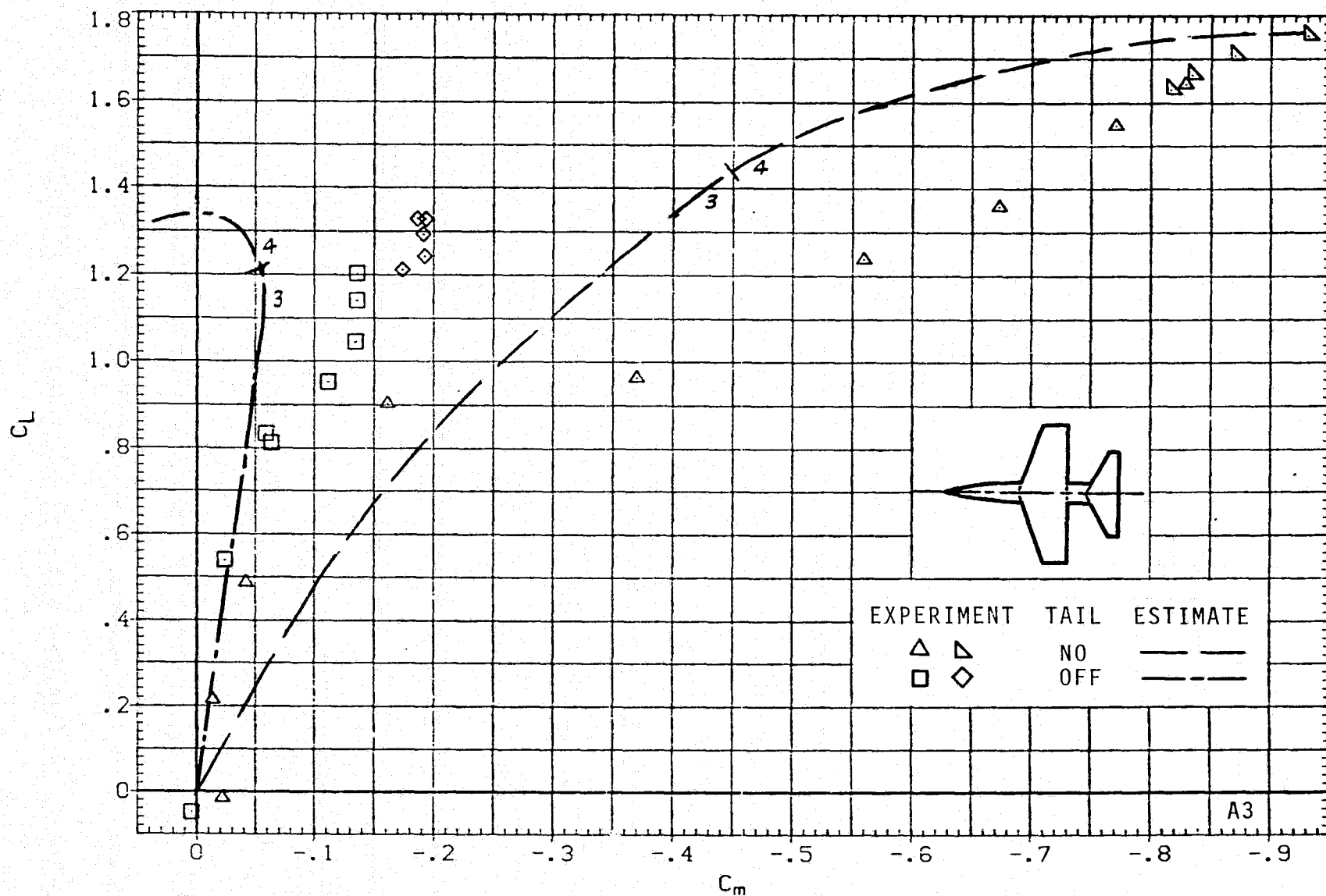
(d) C_L VERSUS α ; $M = 0.9$, $J = 1$.

FIGURE 7.- CONTINUED.



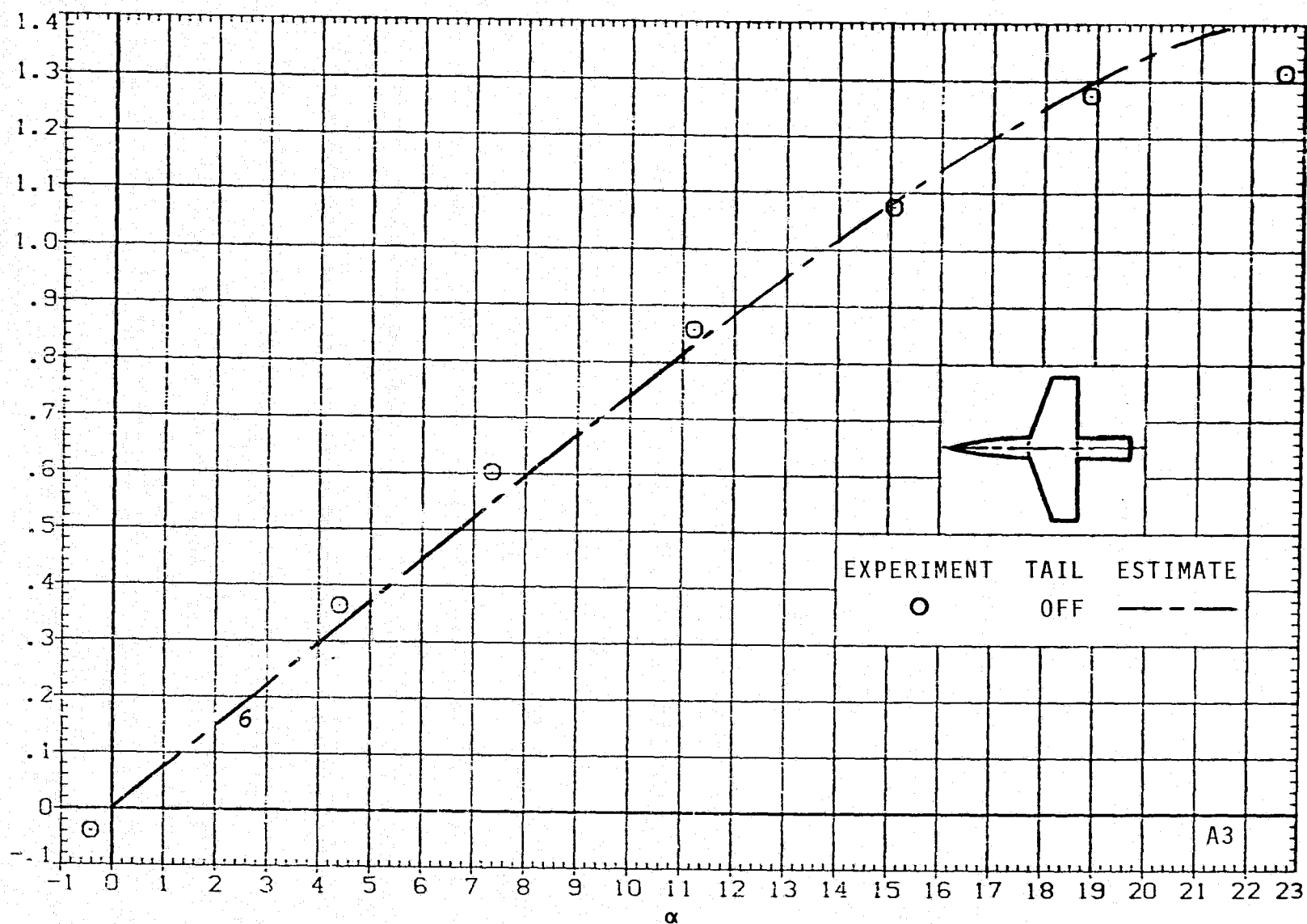
(e) C_L VERSUS C_D ; $M = 0.9$, $J = 1$.

FIGURE 7.- CONTINUED.



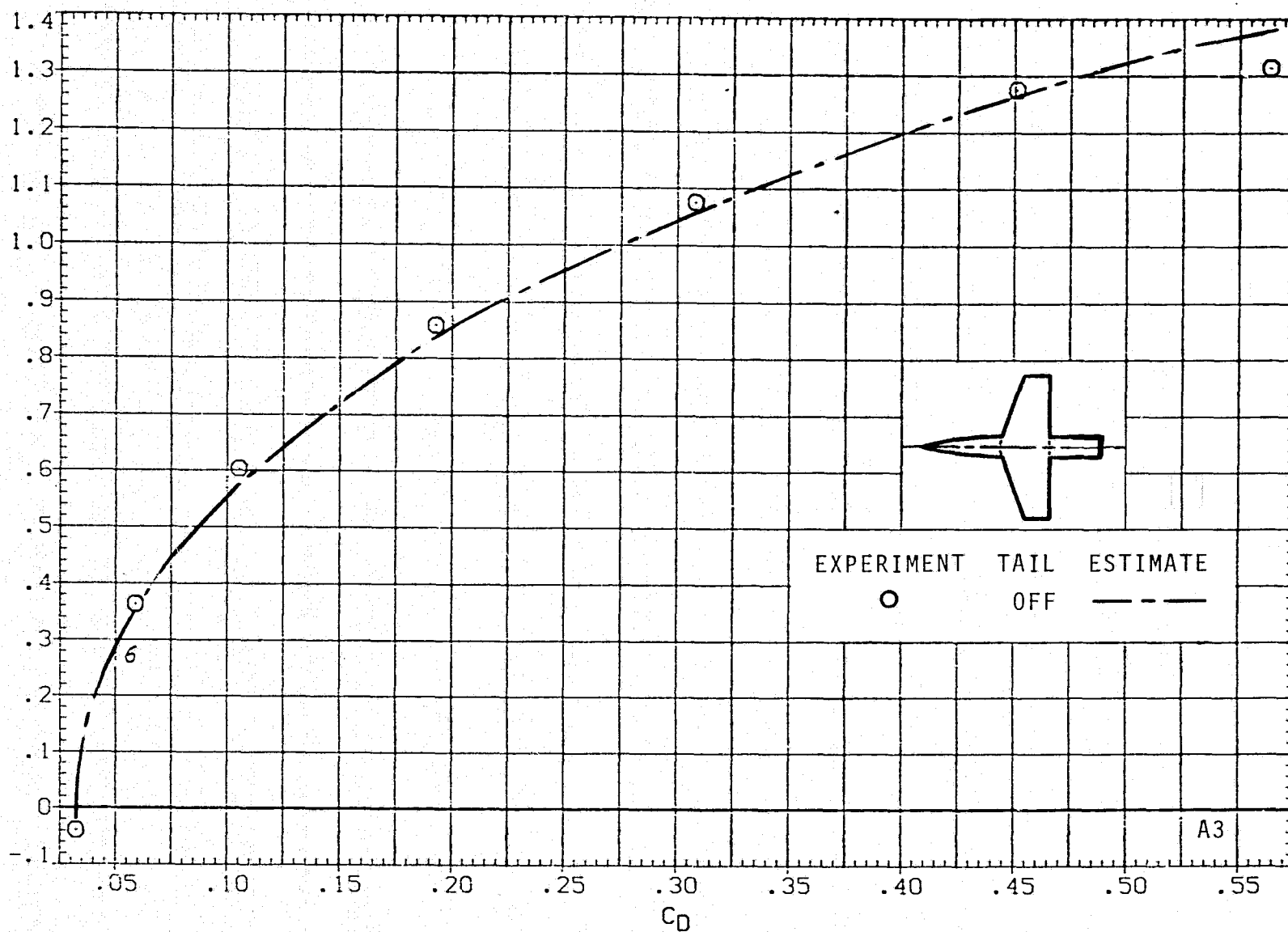
(f) C_L VERSUS C_m ; $M = 0.9$, $J = 1$.

FIGURE 7.- CONTINUED.



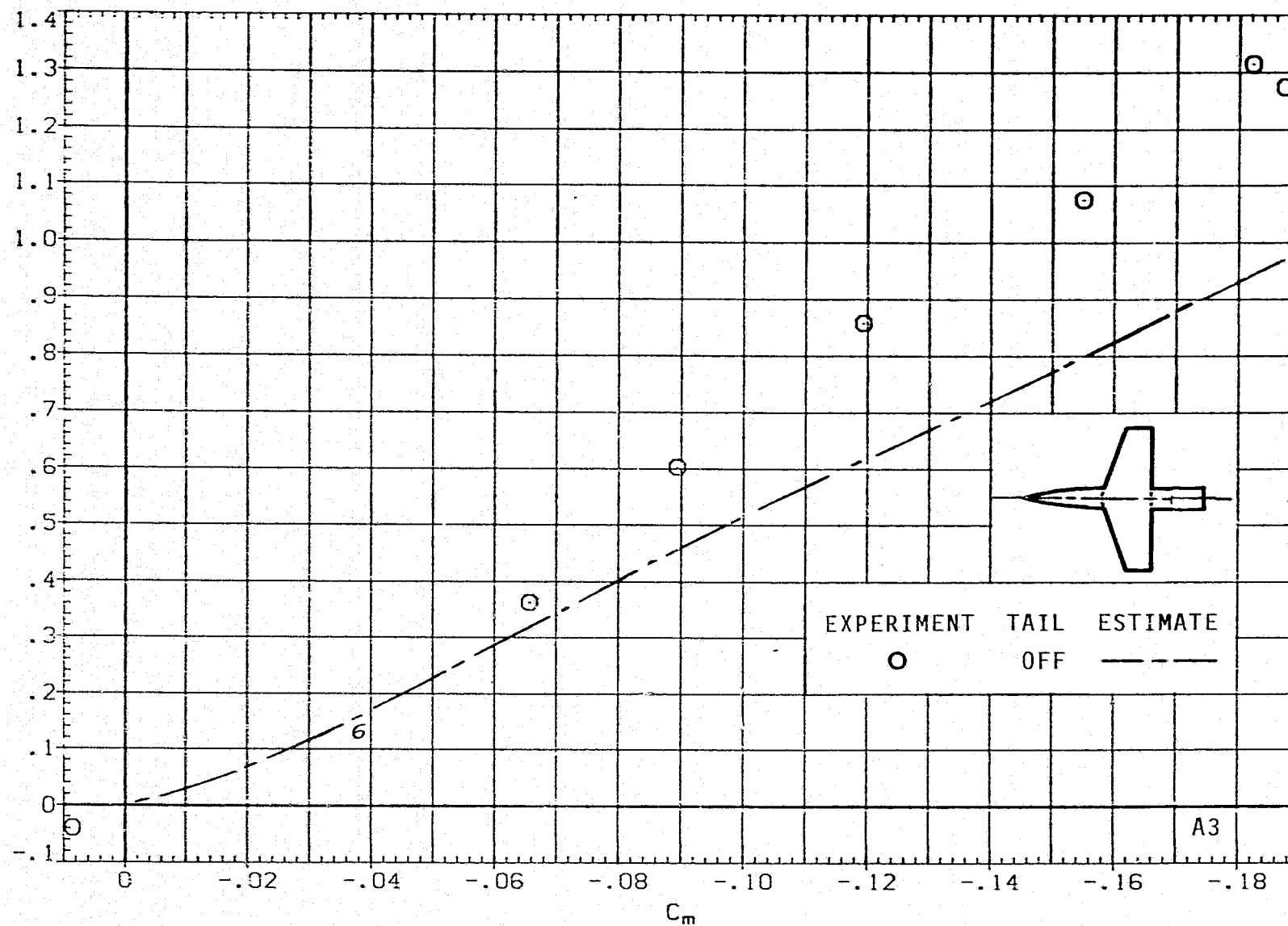
(g) C_L VERSUS α ; M 1.2, J = 5.

FIGURE 7.- CONTINUED.



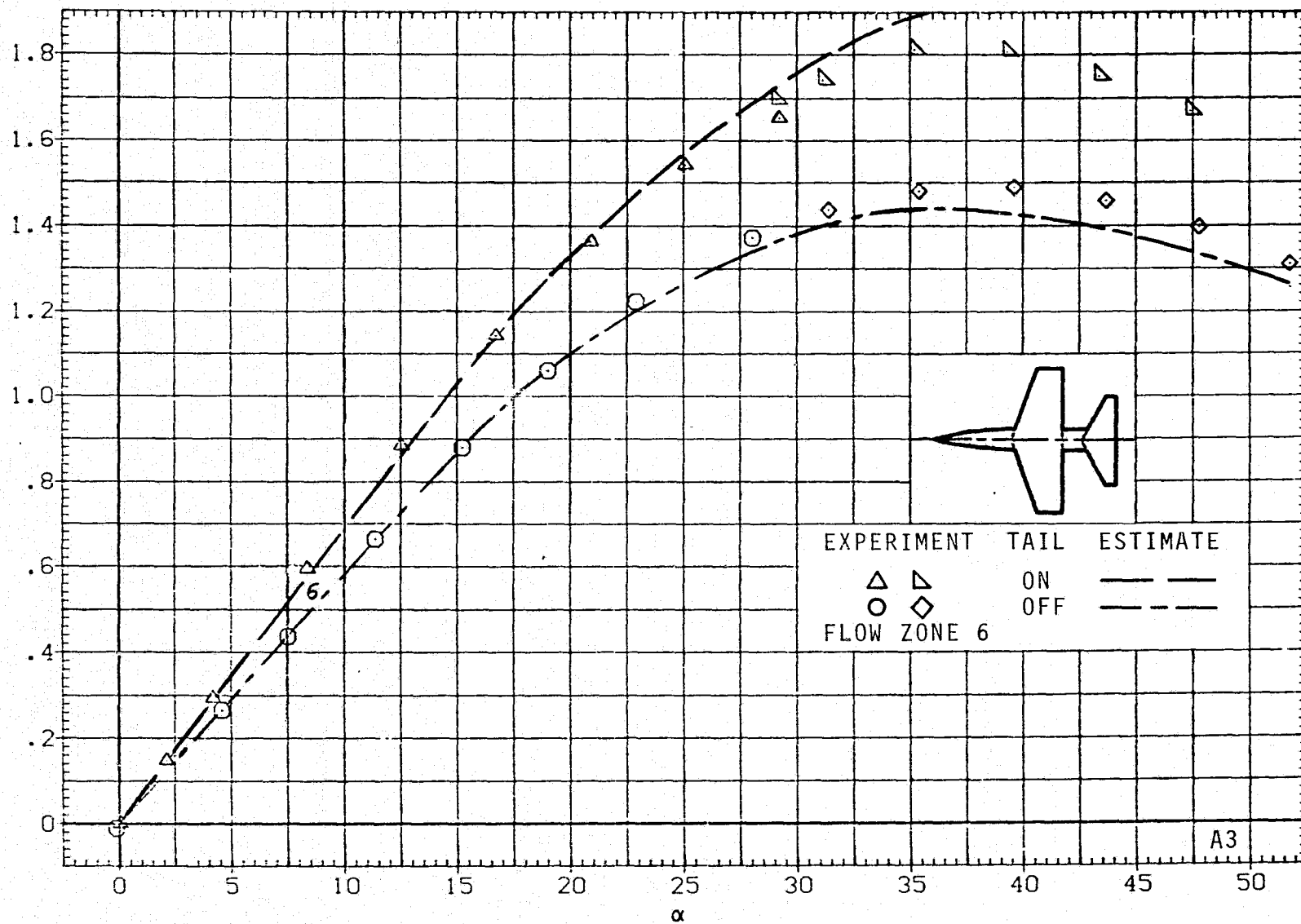
(h) C_L VERSUS C_D ; $M = 1.2$, $J = 5$.

FIGURE 7.- CONTINUED.



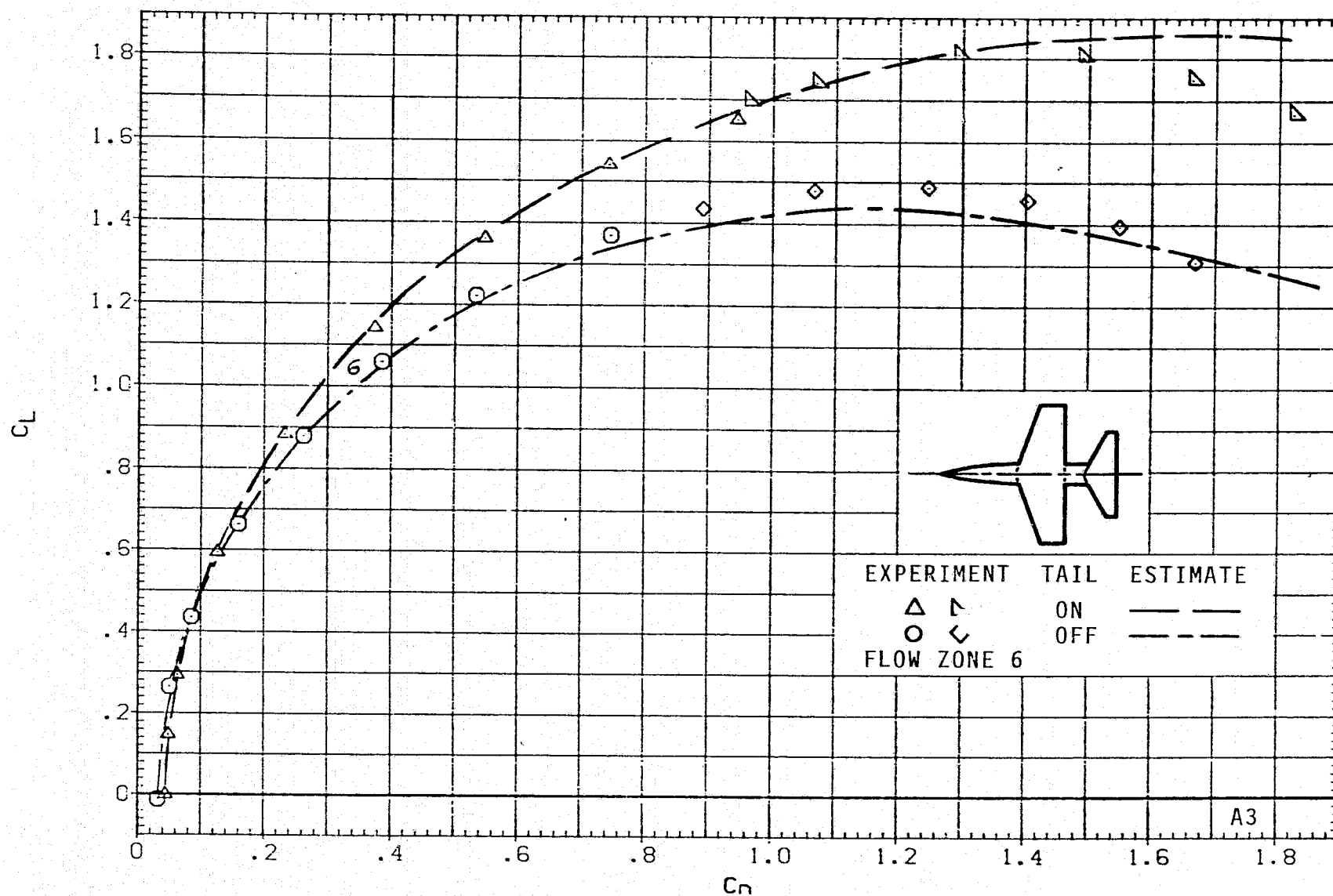
(i) C_L VERSUS C_m ; $M = 1.2$, $J = 5$.

FIGURE 7.- CONTINUED.



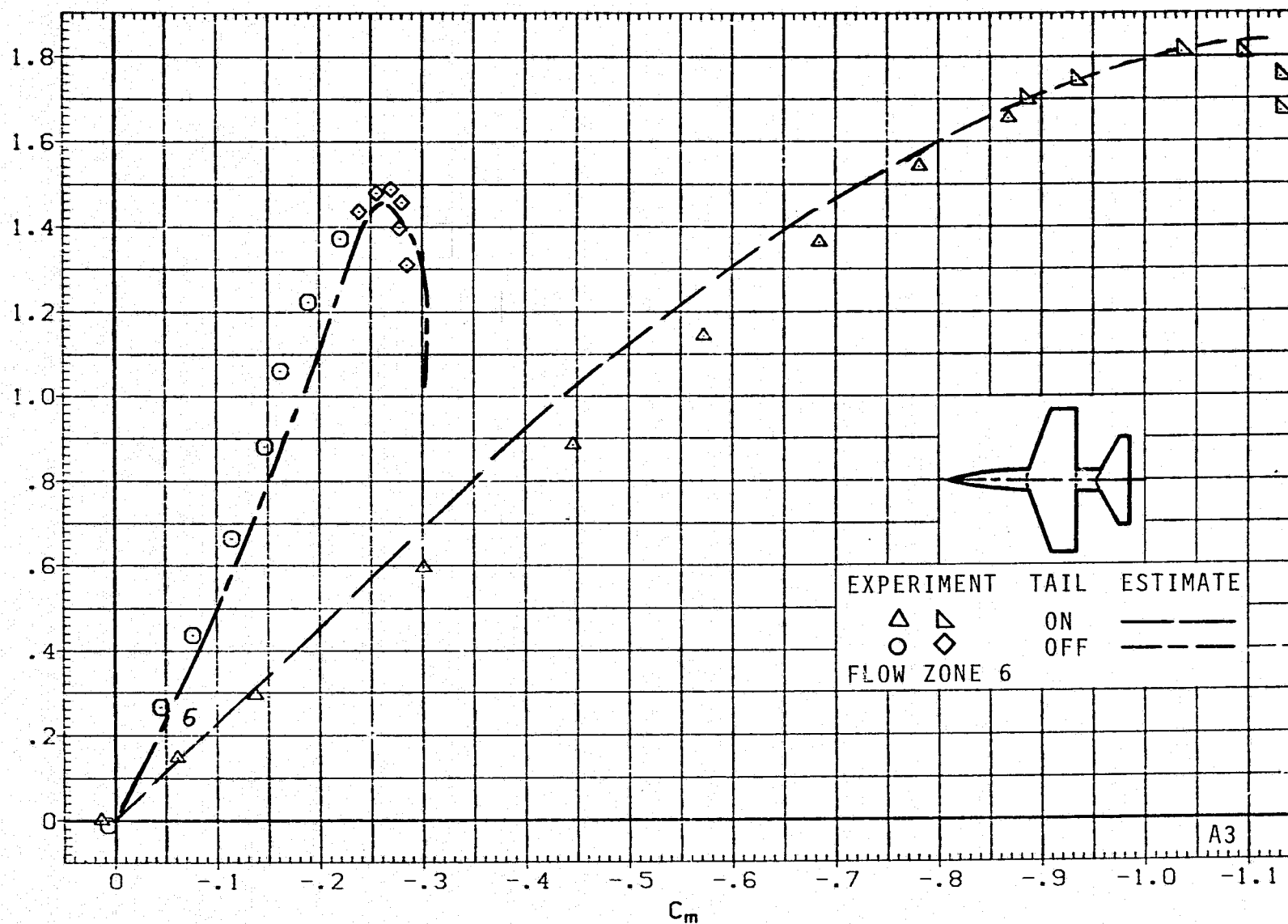
(j) C_L VERSUS α ; $M = 1.5$, $J = 5$.

FIGURE 7.- CONTINUED.



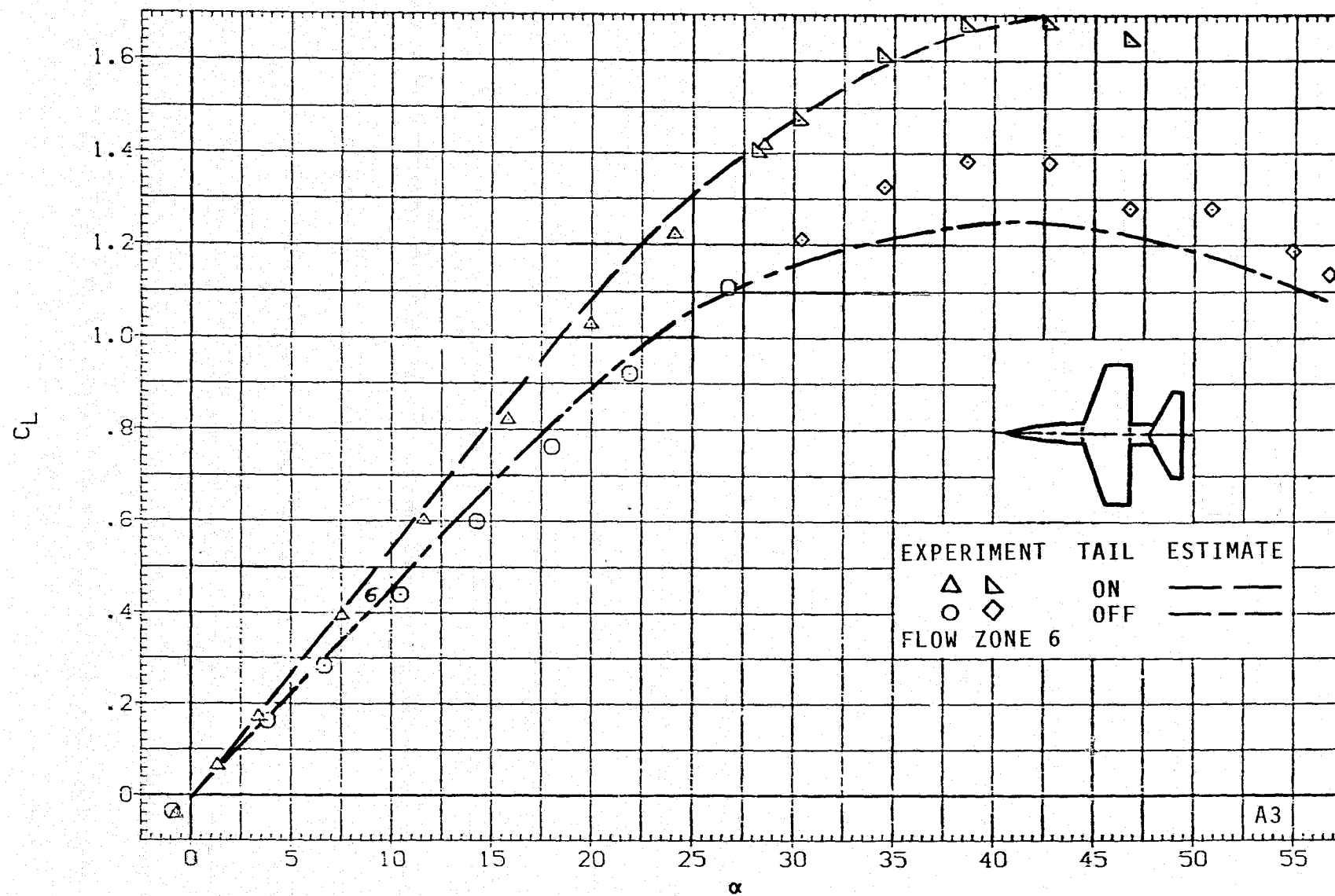
(k) C_L VERSUS C_D ; $M = 1.5$, $J = 5$.

FIGURE 7.- CONTINUED.



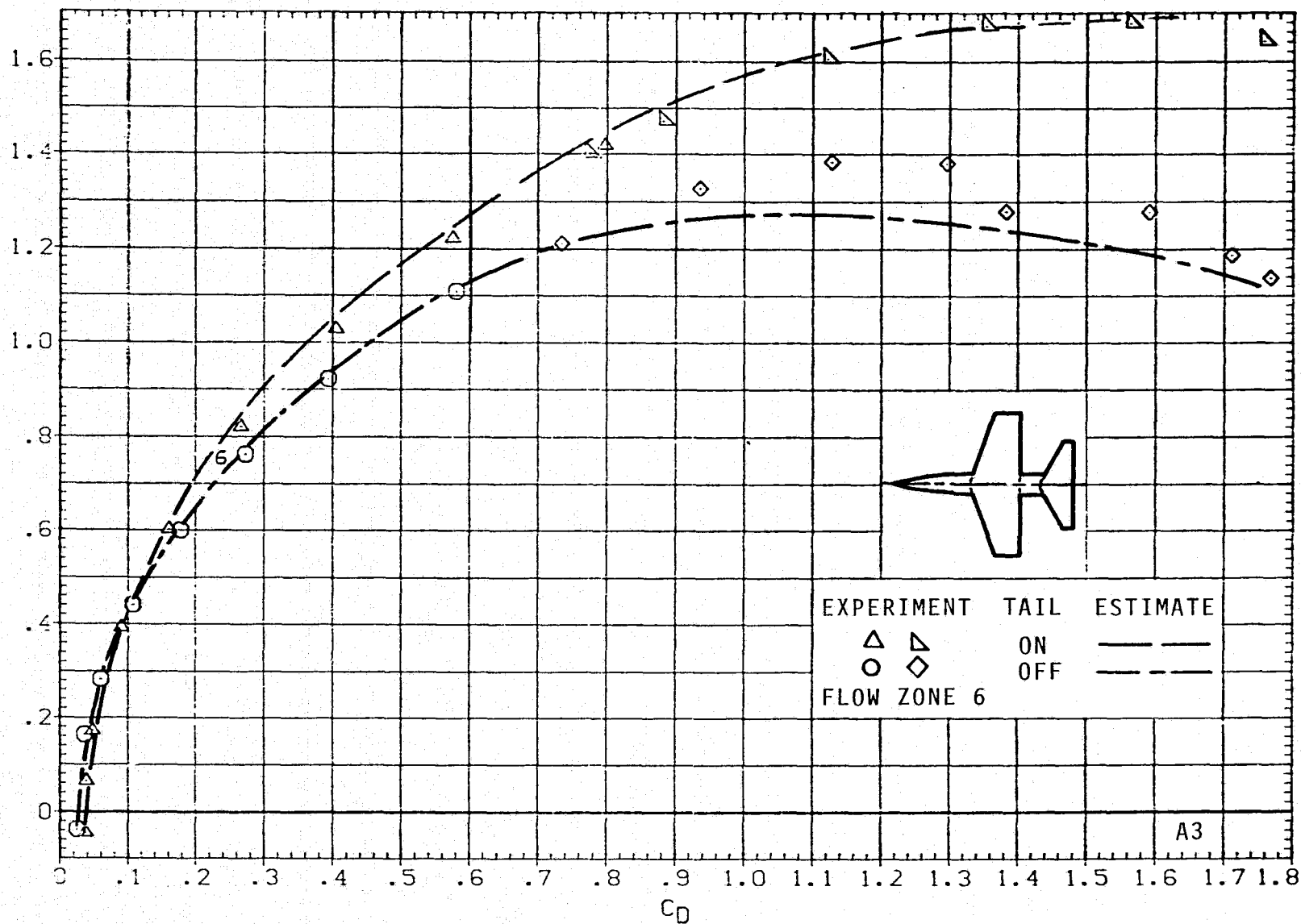
(1) C_L VERSUS C_m ; $M = 1.5$, $J = 5$.

FIGURE 7.- CONTINUED.



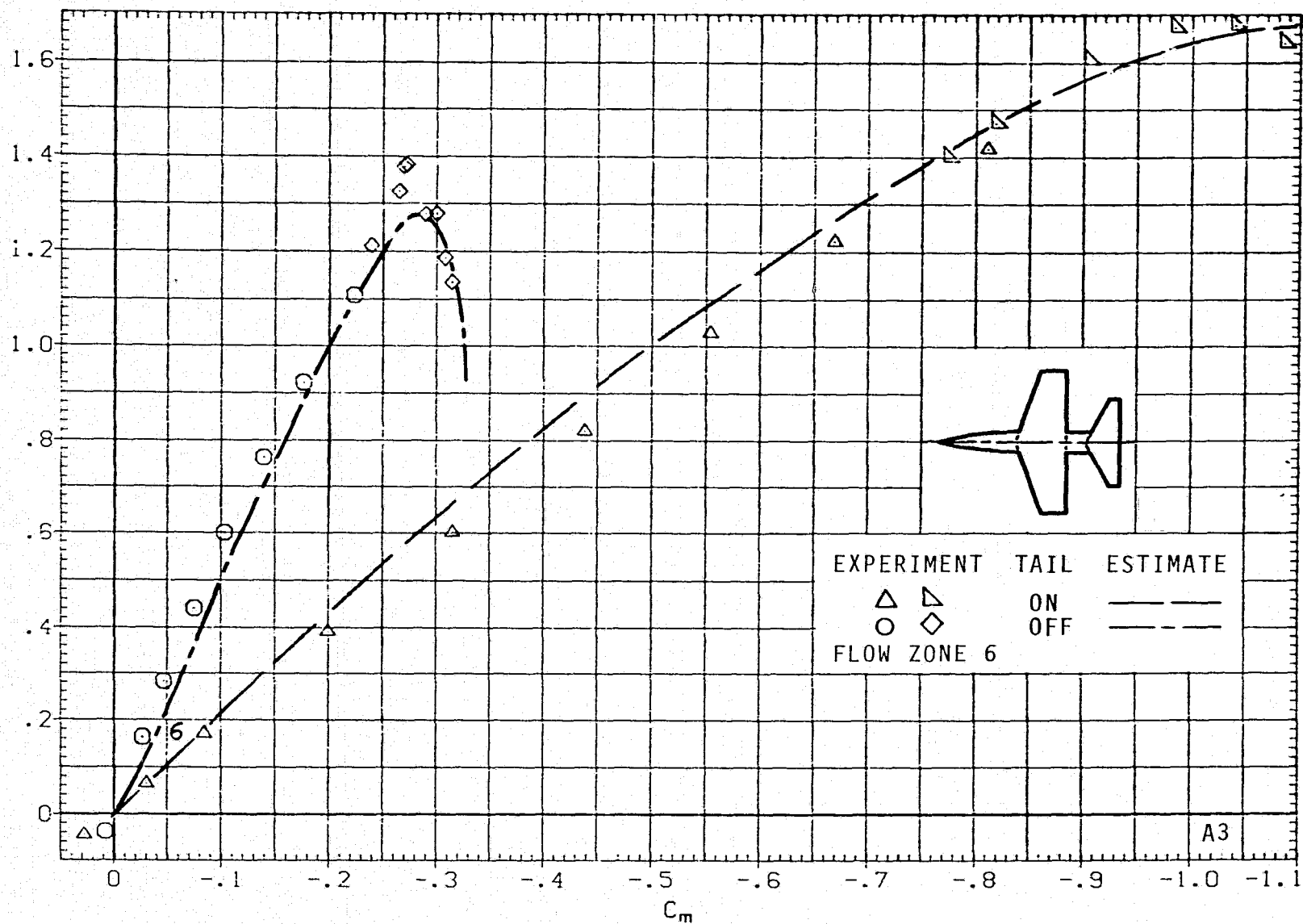
(m) C_L VERSUS α ; $M = 2.0$, $J = 5$.

FIGURE 7.- CONTINUED.

C_L 

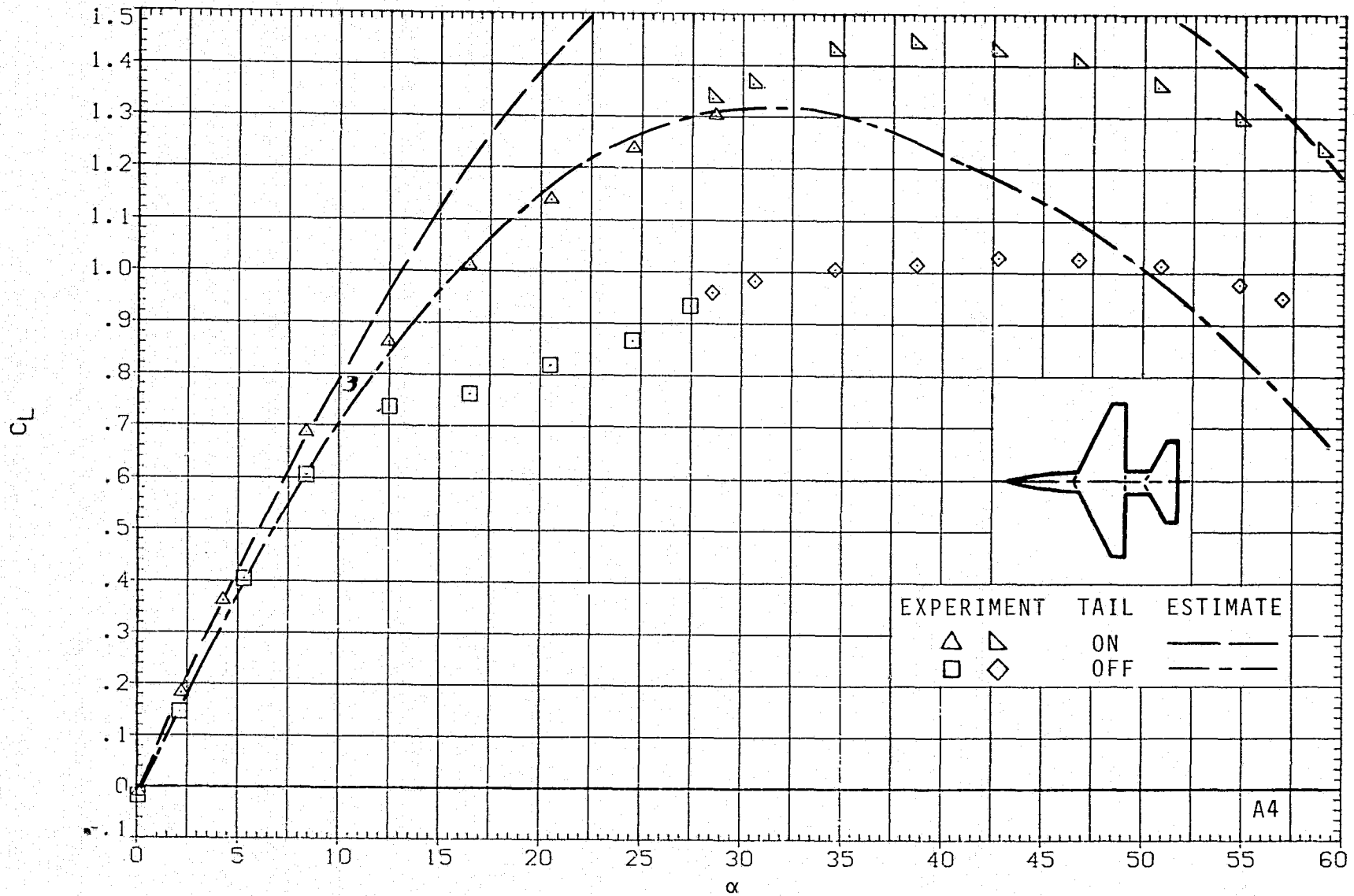
(n) C_L VERSUS C_D ; $M = 2.0$, $J = 5$.

FIGURE 7.- CONTINUED.



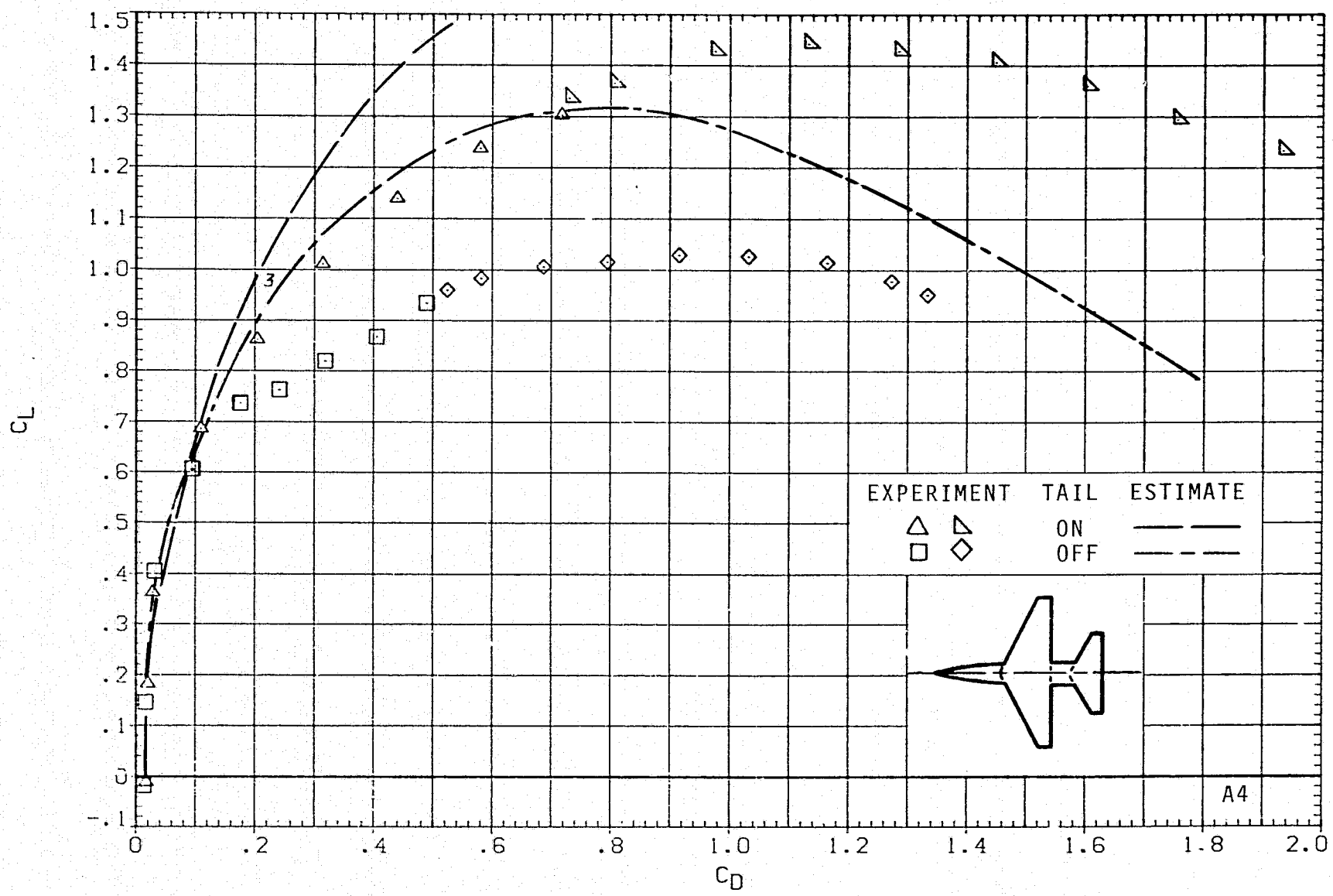
(o) C_L VERSUS C_m ; $M = 2.0$, $J = 5$.

FIGURE 7.- CONCLUDED.



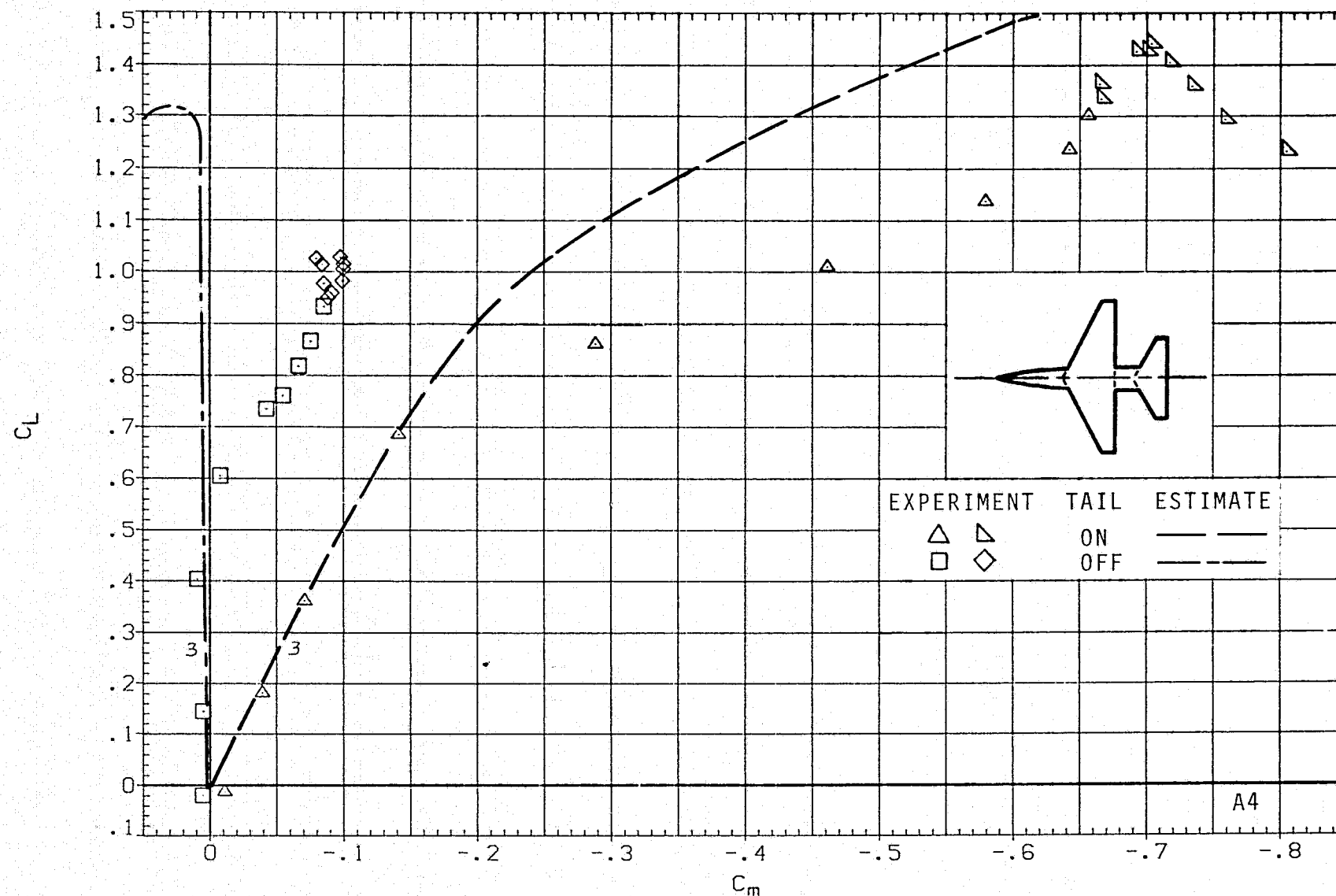
(a) C_L VERSUS α ; $M = 0.6$, $J = 1$.

FIGURE 8.- AERODYNAMICS FOR MODEL A4; ARW = 5, TRW = 0.25.



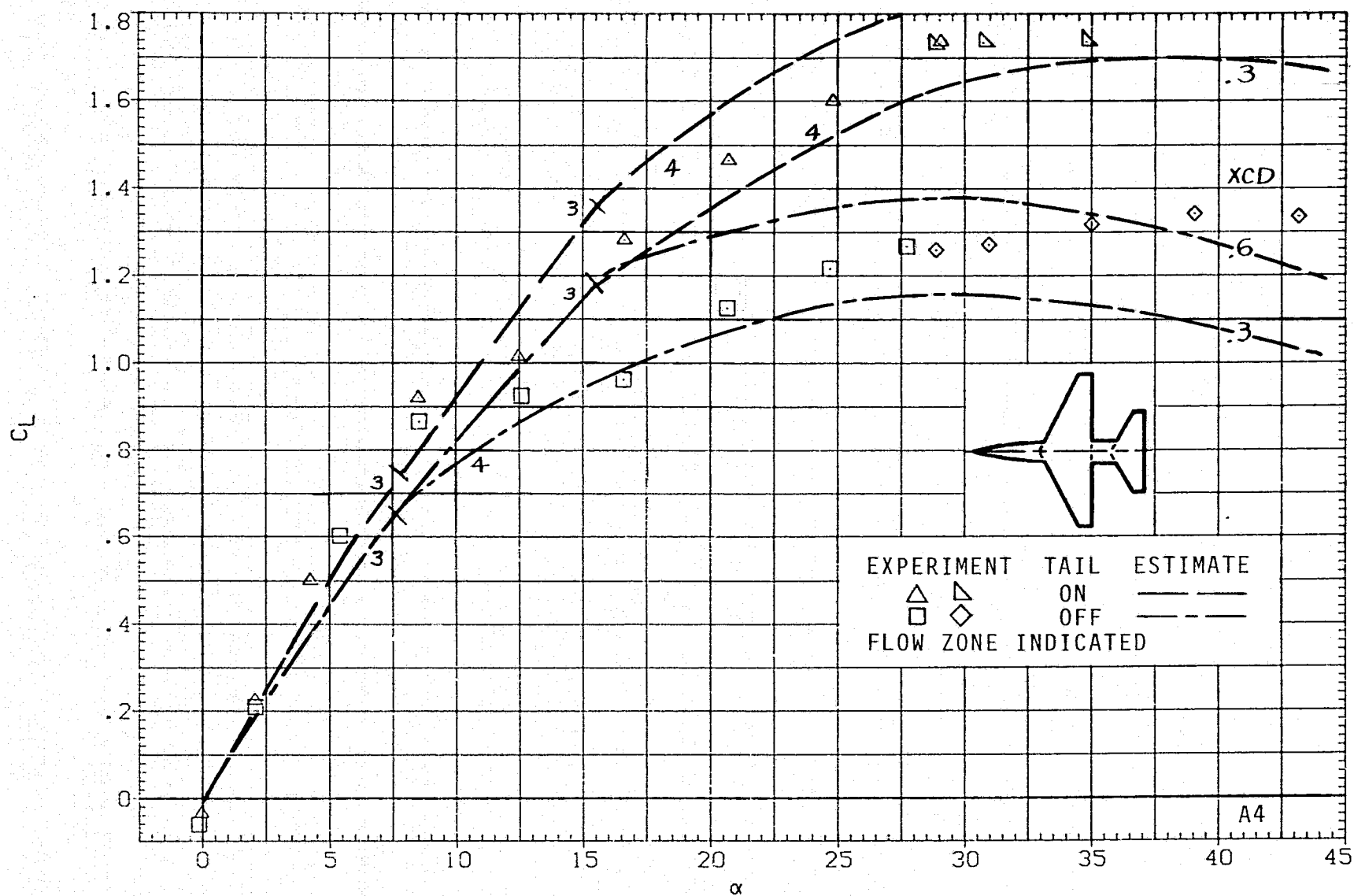
(b) C_L VERSUS C_D ; $M = 0.6$, $J = 1$.

FIGURE 8.- CONTINUED.



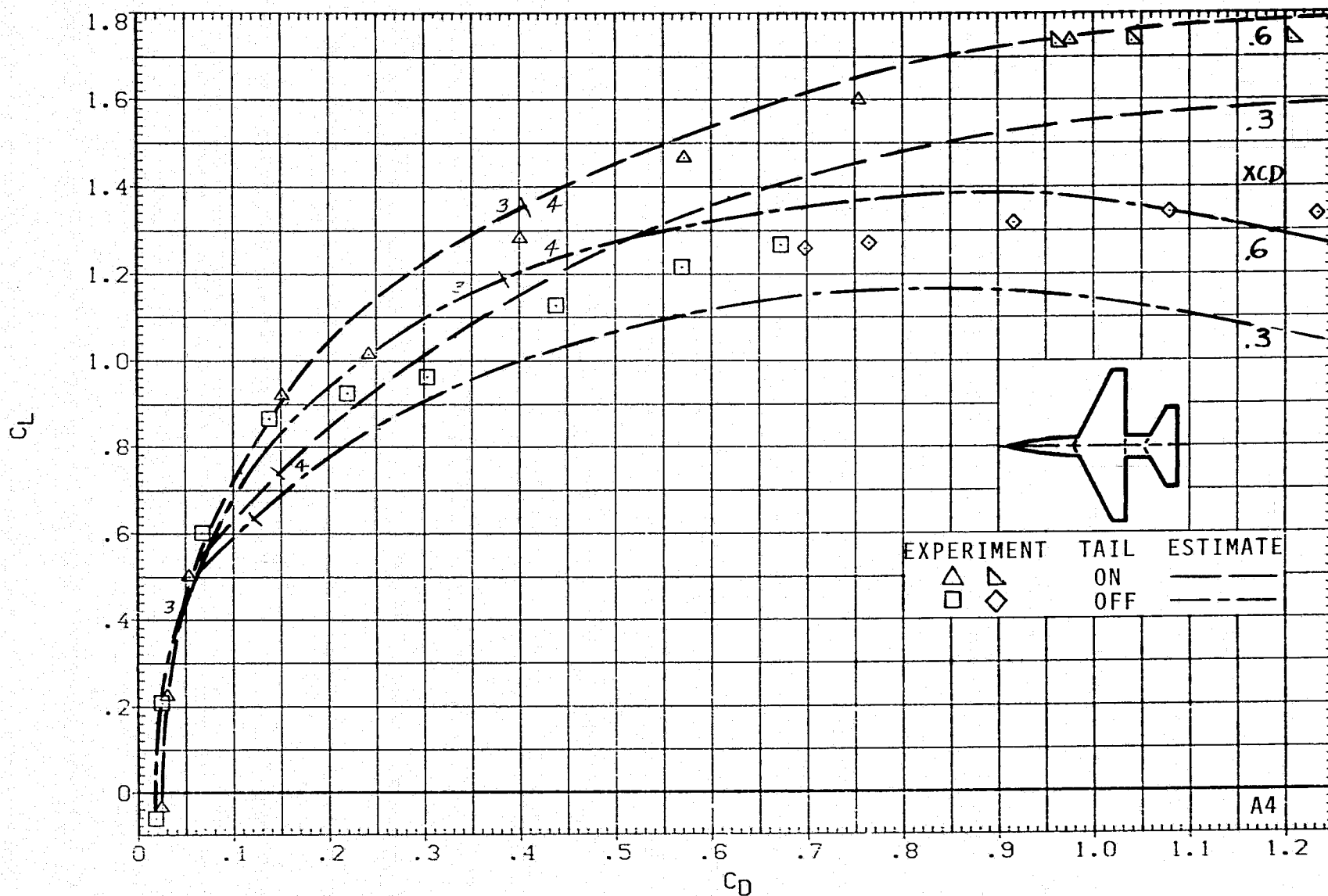
(c) C_L VERSUS C_m ; $M = 0.6$, $J = 1$.

FIGURE 8.- CONTINUED.



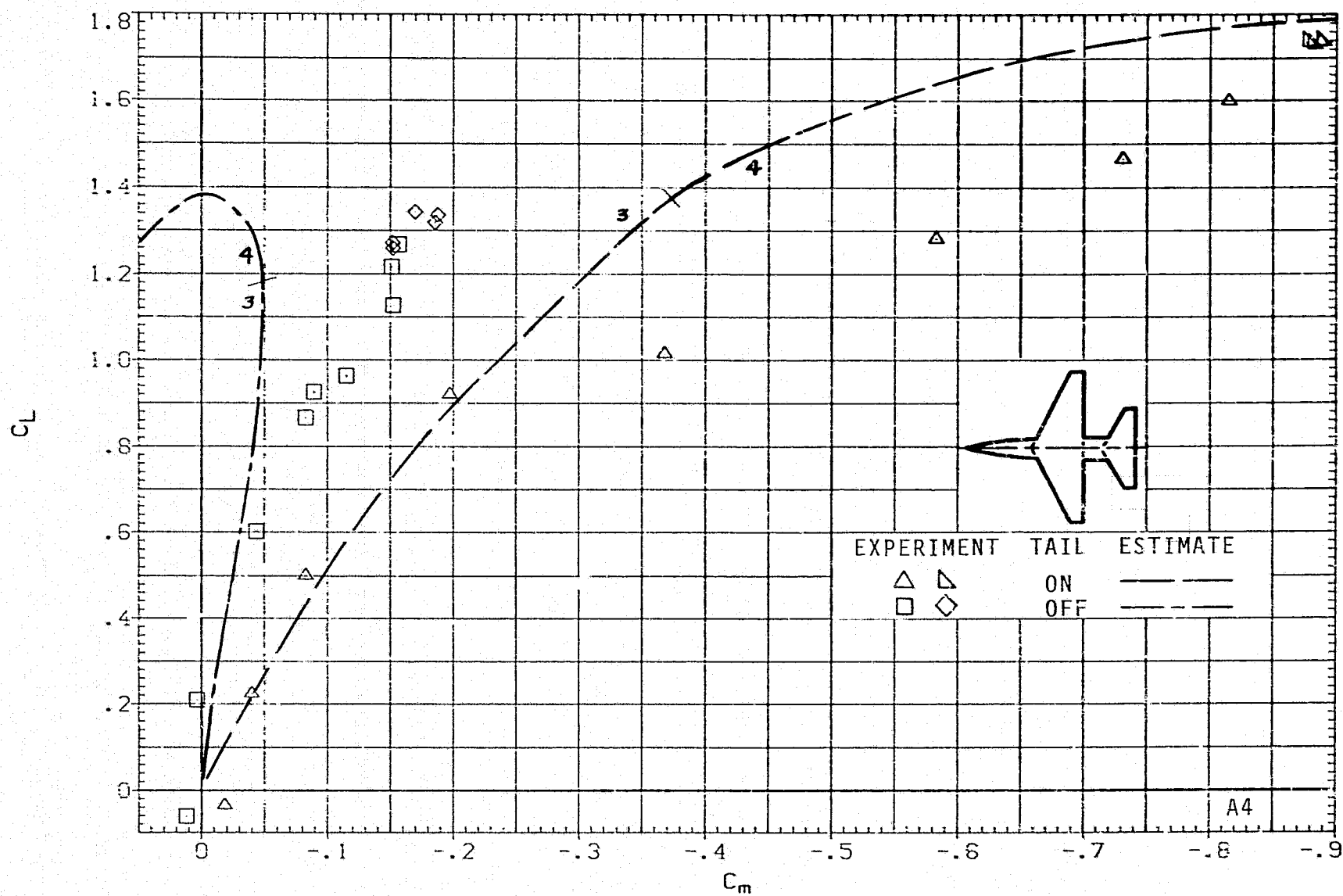
(d) C_L VERSUS α ; $M = 0.9$, $J = 1$.

FIGURE 8.- CONTINUED.



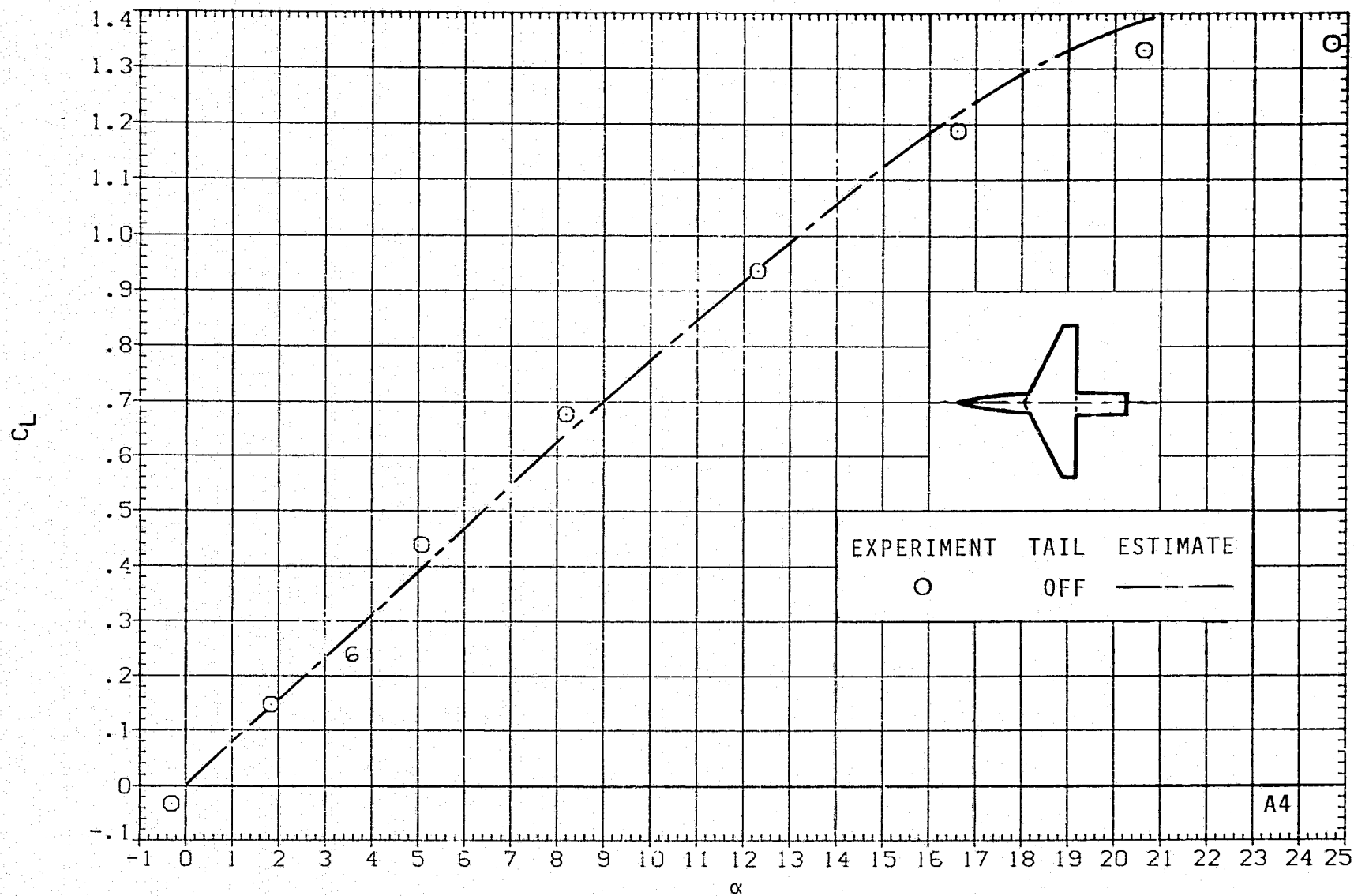
(e) C_L VERSUS C_D ; $M = 0.9$, $J = 1$.

FIGURE 8.- CONTINUED.



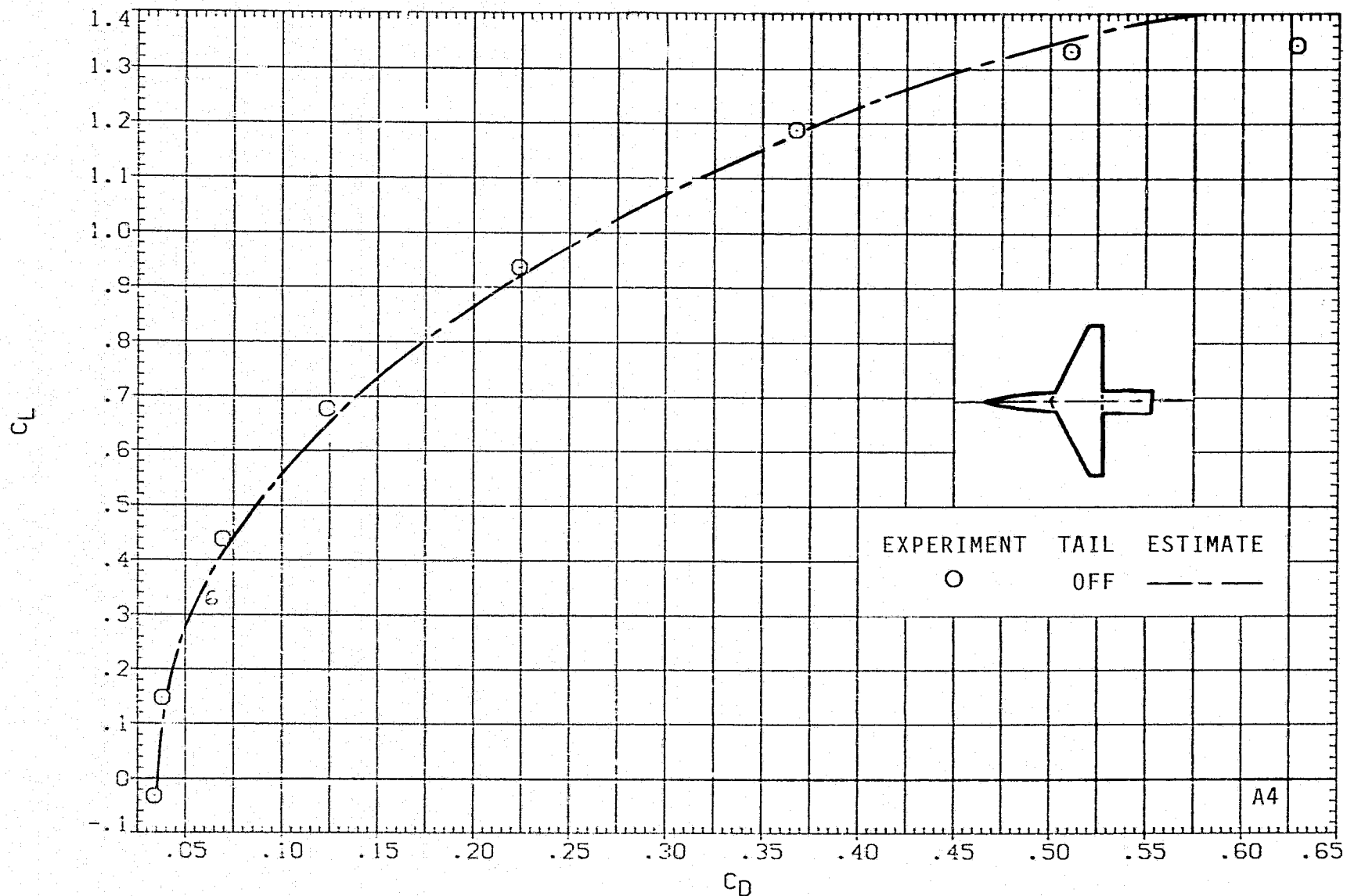
(f) C_L VERSUS C_m ; $M = 0.9$, $J = 1$.

FIGURE 8.- CONTINUED.



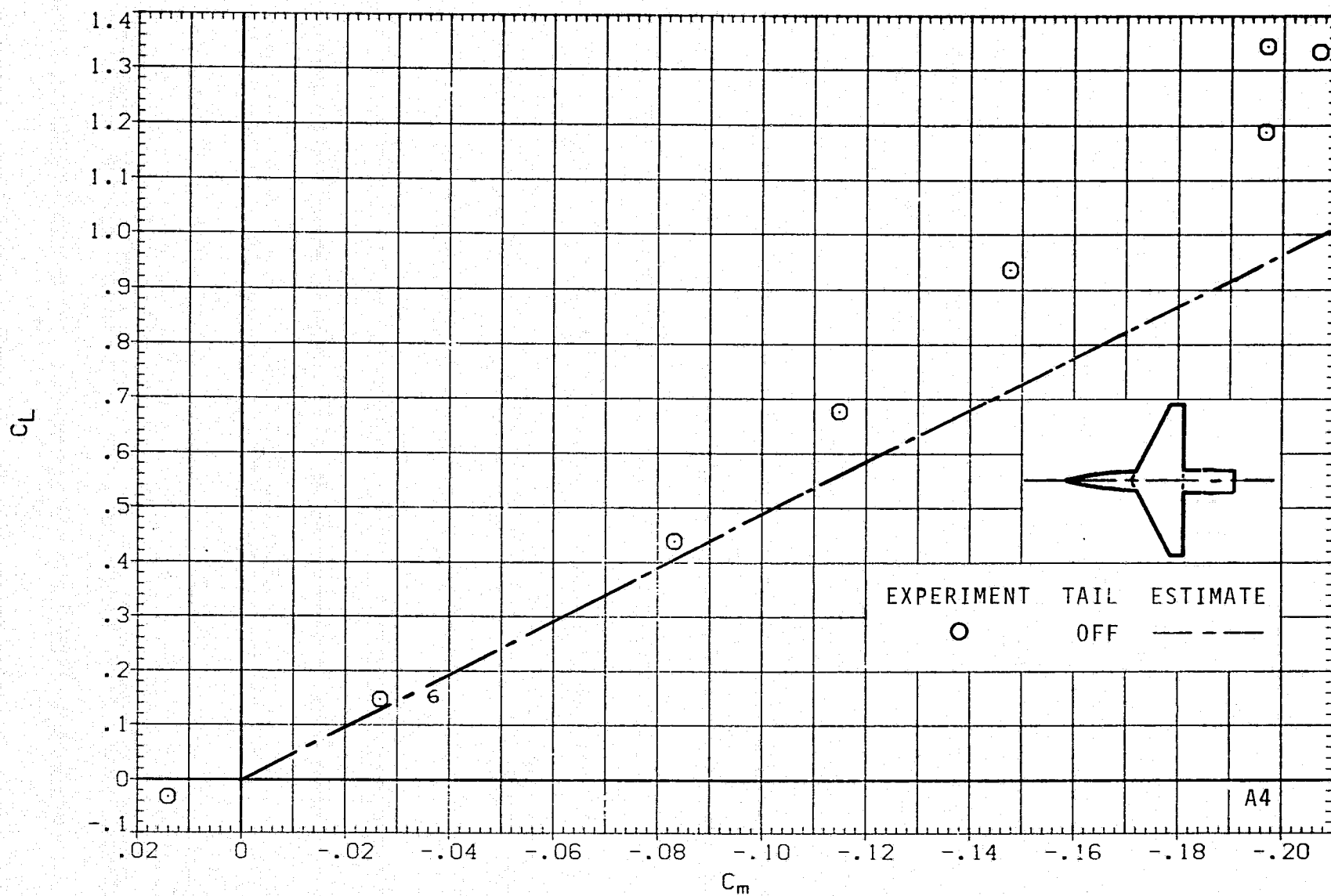
(g) C_L VERSUS α ; $M = 1.2$, $J = 5$.

FIGURE 8.- CONTINUED.



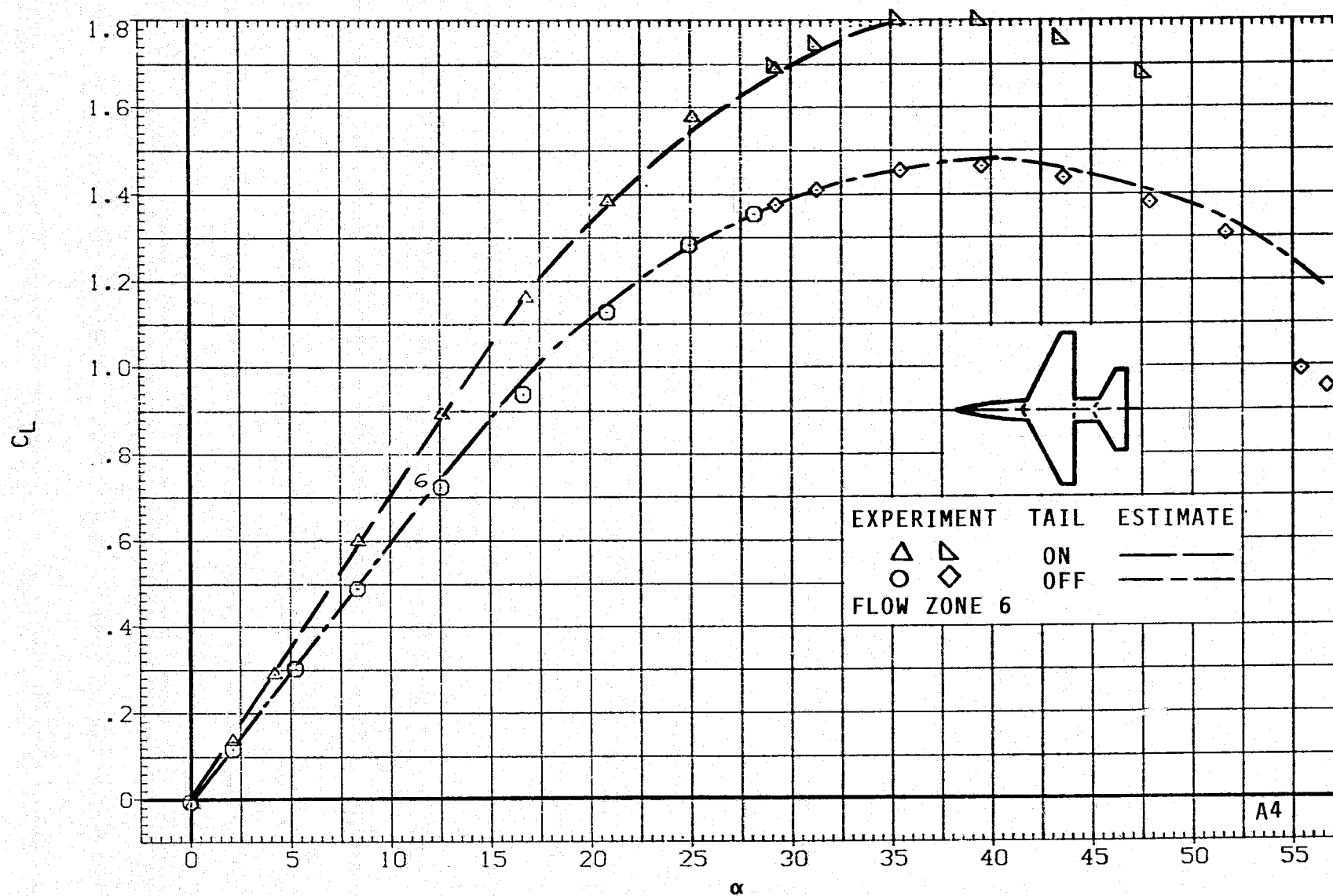
(h) C_L VERSUS C_D ; $M = 1.2$, $J = 5$.

FIGURE 8.- CONTINUED.



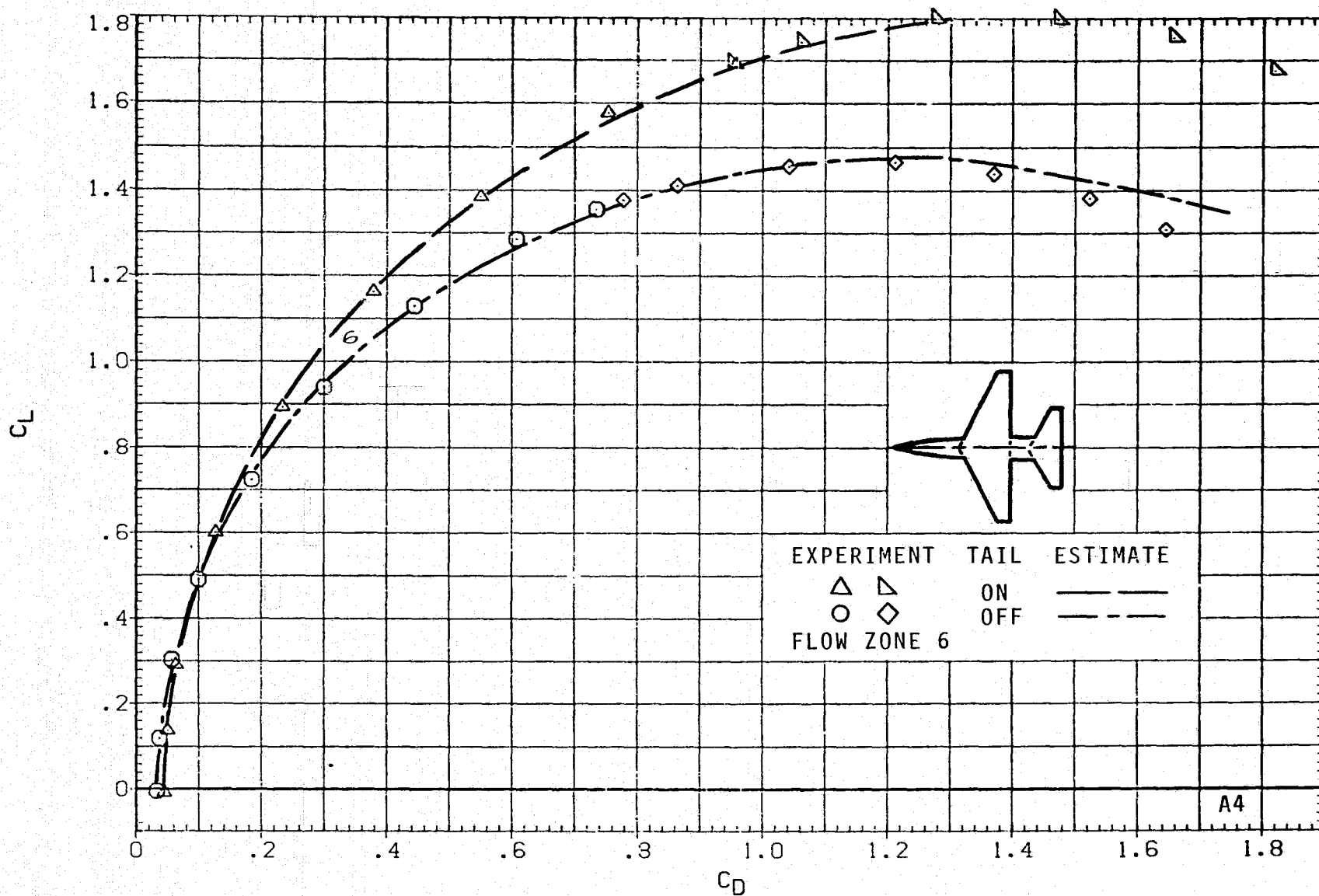
(i) C_L VERSUS C_m ; $M = 1.2$, $J = 5$.

FIGURE 8.- CONTINUED.



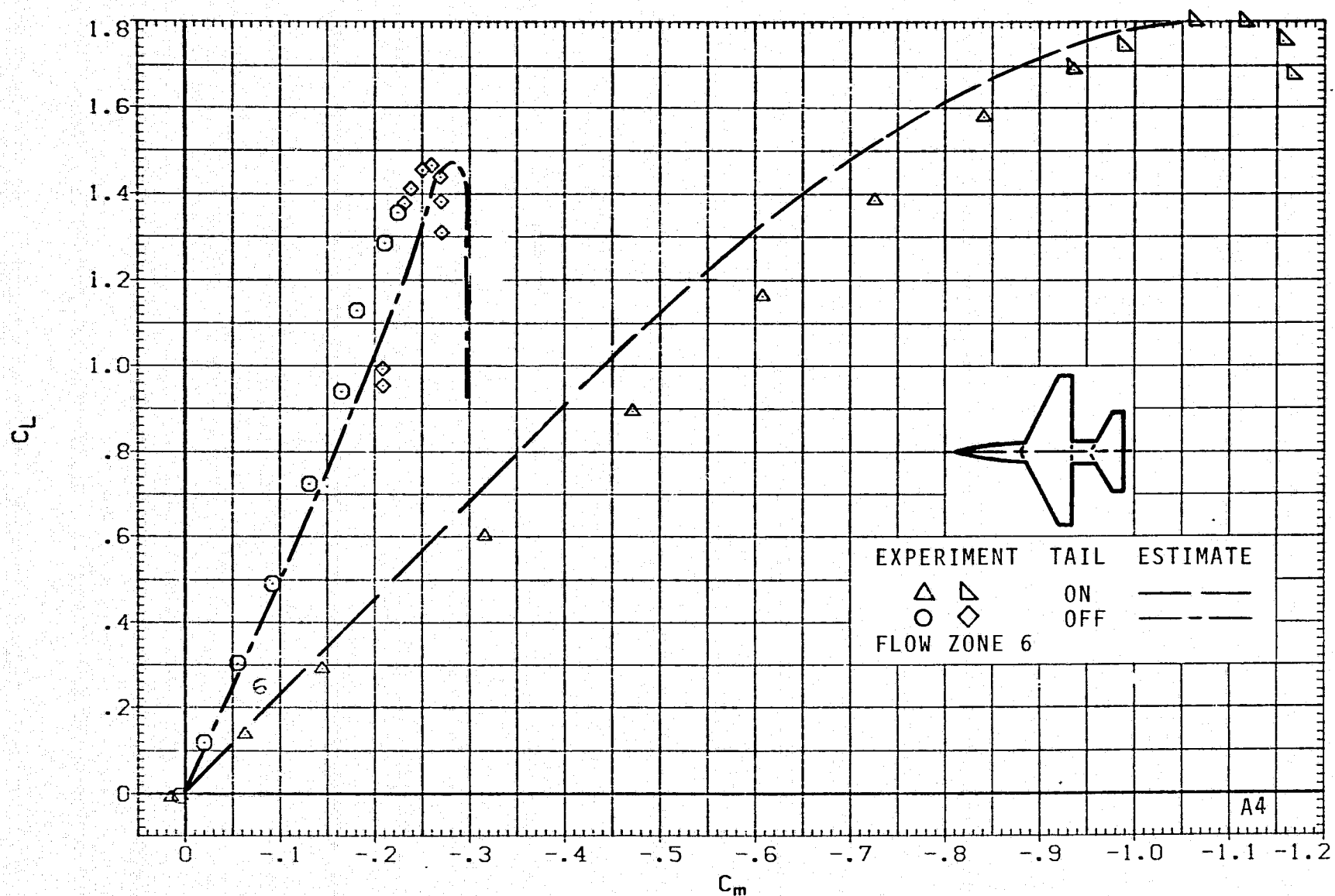
(j) C_L VERSUS α ; $M = 1.5$, $J = 5$.

FIGURE 8.- CONTINUED.



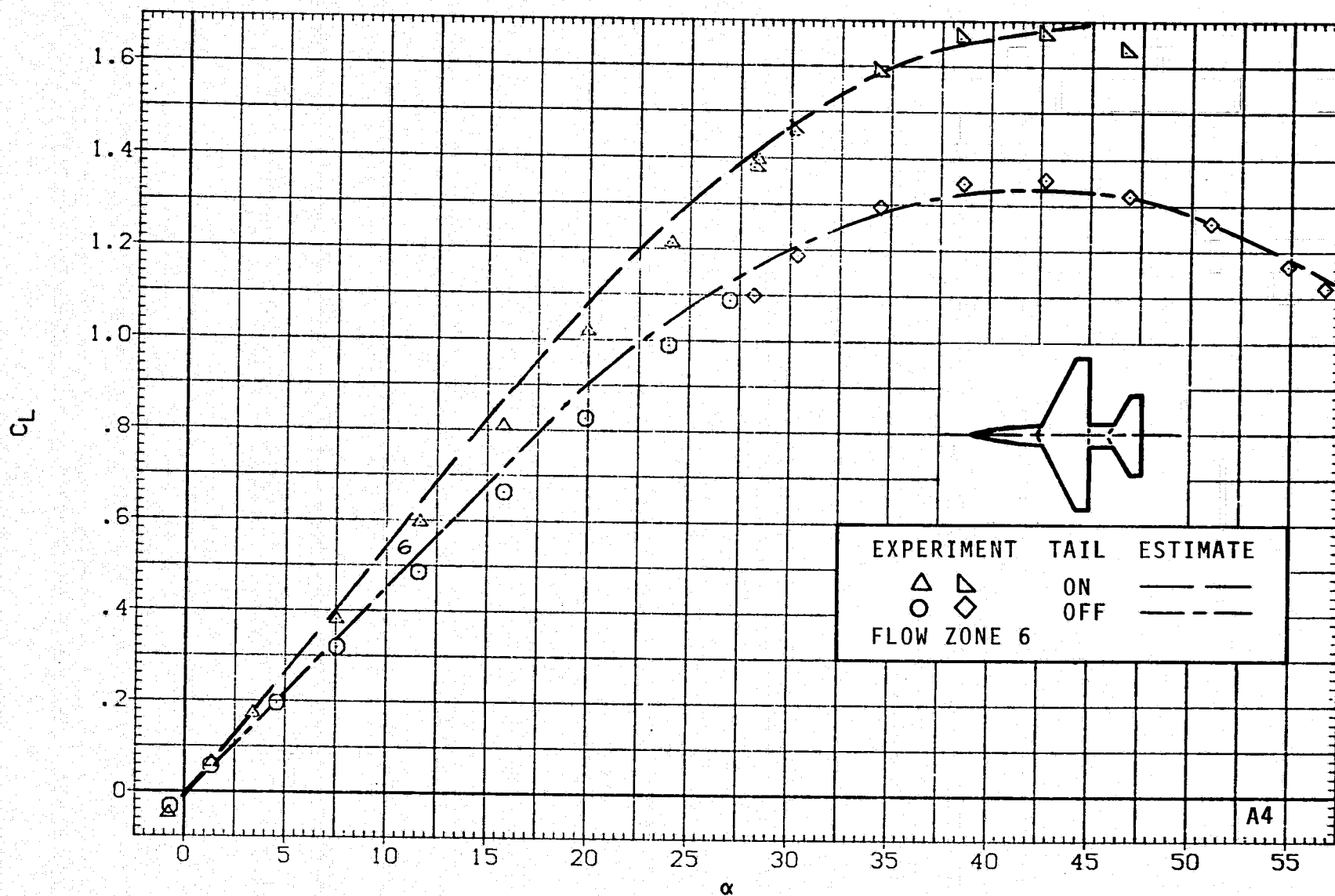
(k) C_L VERSUS C_D ; $M = 1.5$, $J = 5$.

FIGURE 8.- CONTINUED.



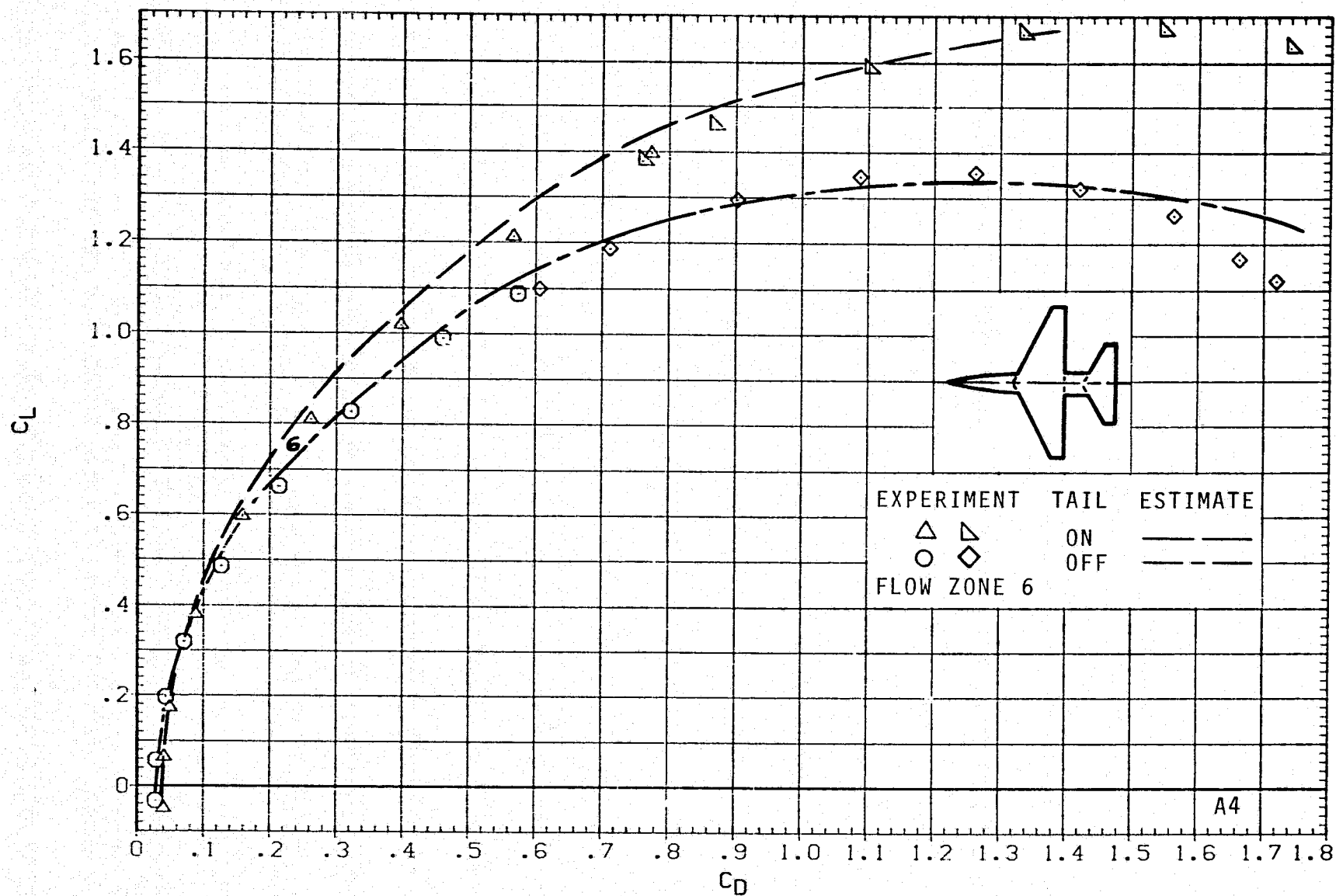
(1) C_L VERSUS C_m ; $M = 1.5$, $J = 5$.

FIGURE 8.- CONTINUED.



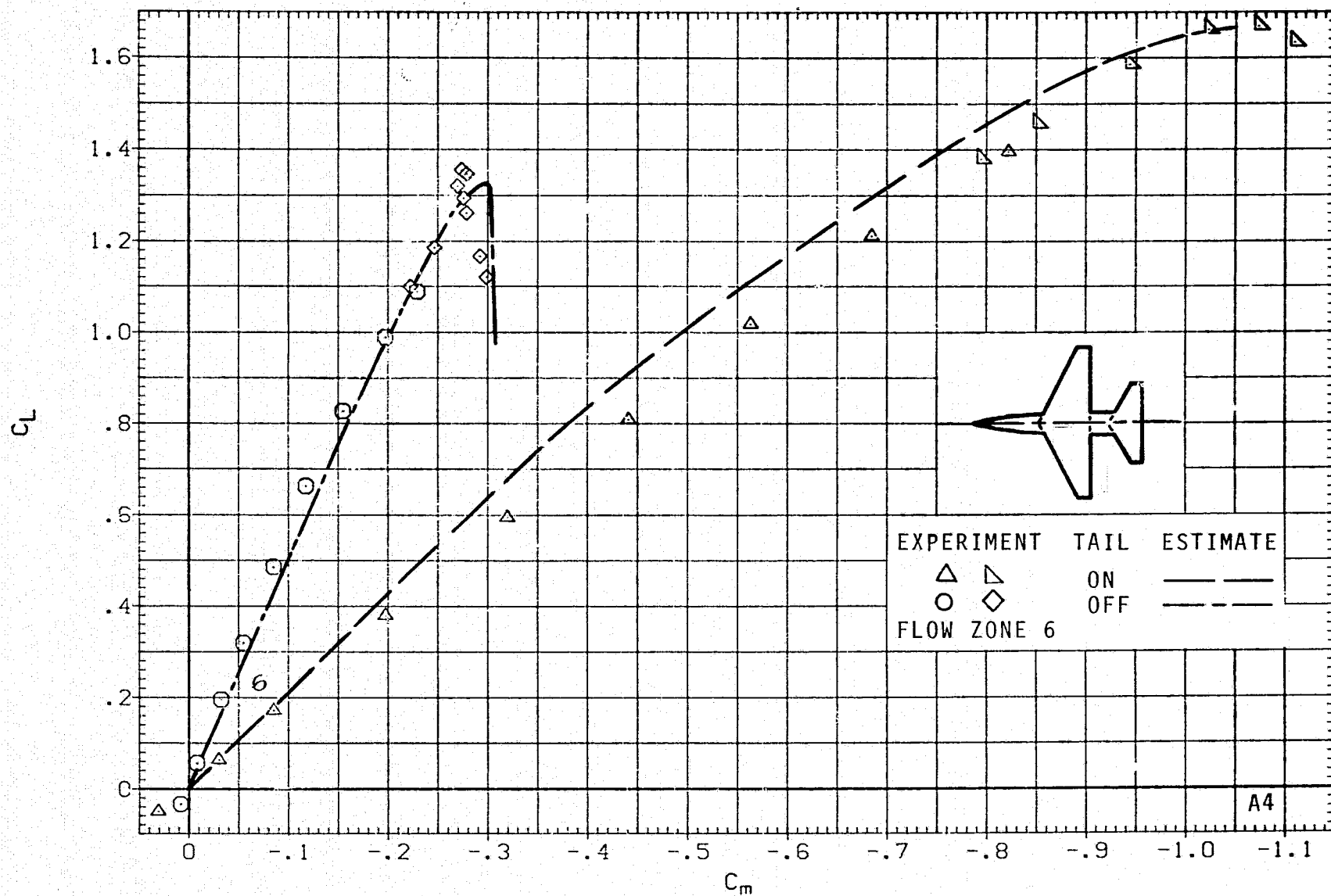
(m) C_L VERSUS α ; $M = 2.0$, $J = 5$.

FIGURE 8.- CONTINUED.



(n) C_L VERSUS C_D ; $M = 2.0$, $J = 5$.

FIGURE 8.- CONTINUED.

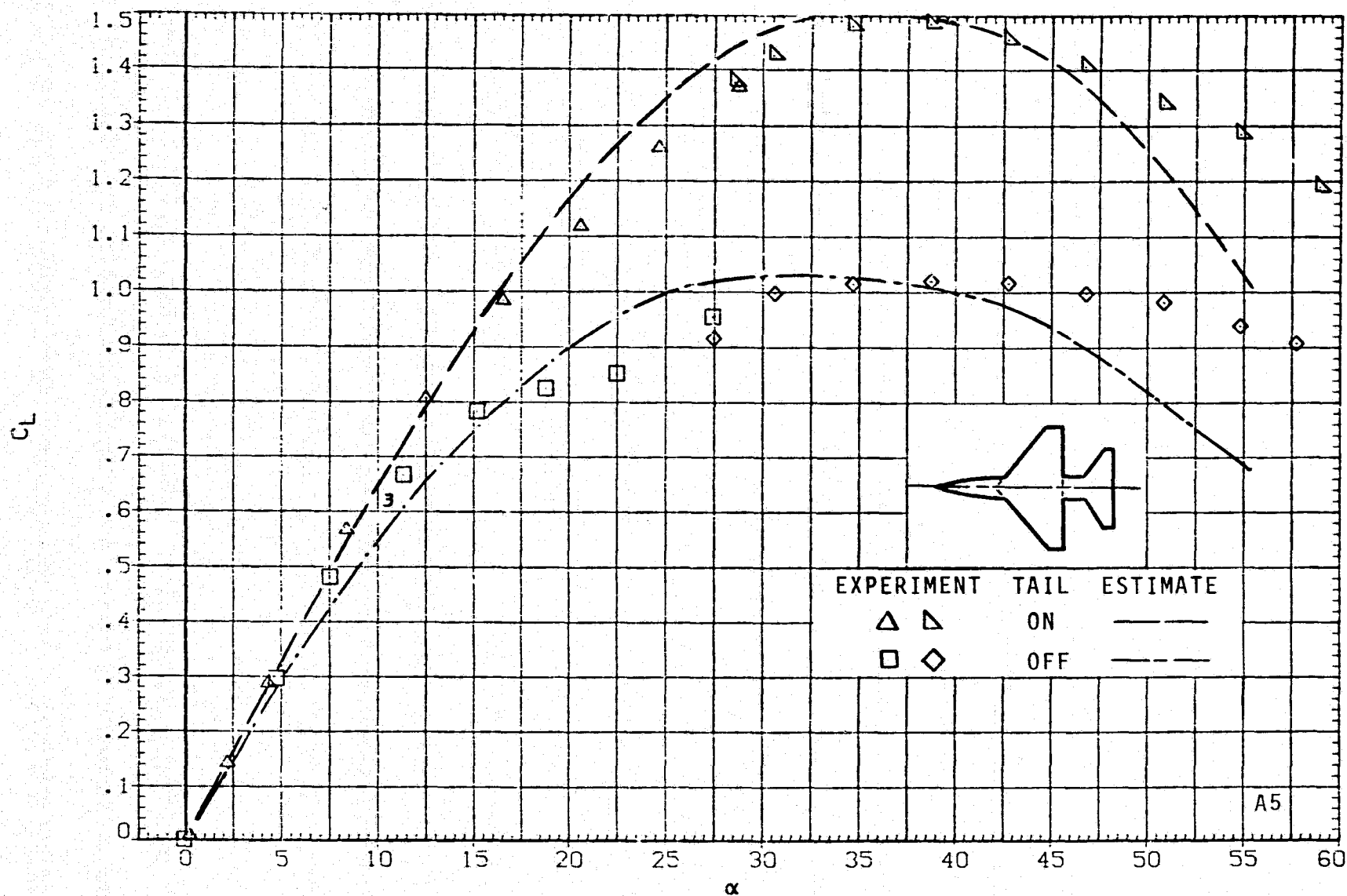


(o) C_L VERSUS C_m ; $M = 2.0$, $J = 5$.

FIGURE 8.- CONCLUDED.

RESEARCH MODEL

$M = 0.60$

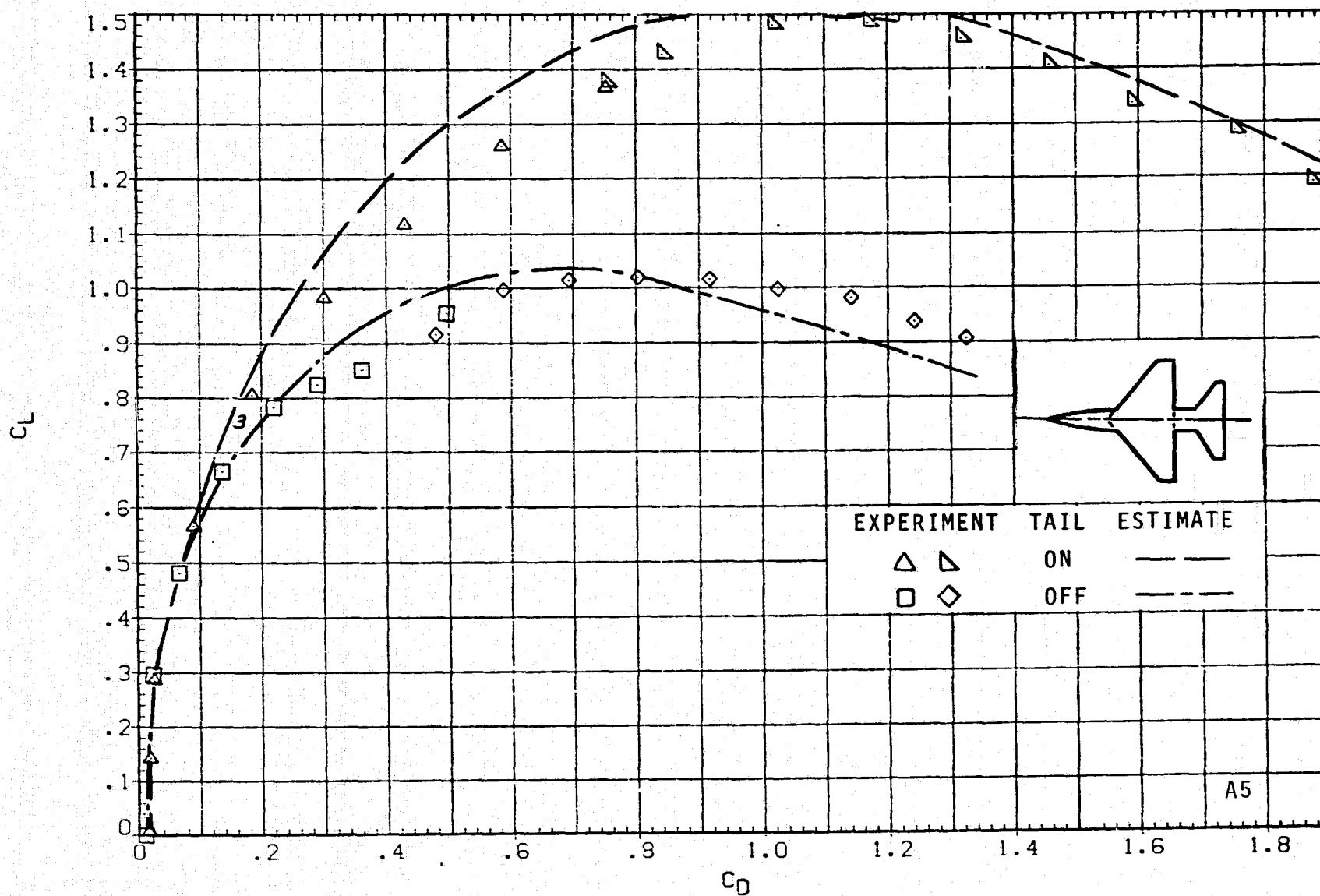


(a) C_L VERSUS α ; $M = 0.6$, $J = 1$.

FIGURE 9.- AERODYNAMICS FOR MODEL A5; ARW = 3, TRW = 0.25.

RESEARCH MODEL

$M = 0.60$

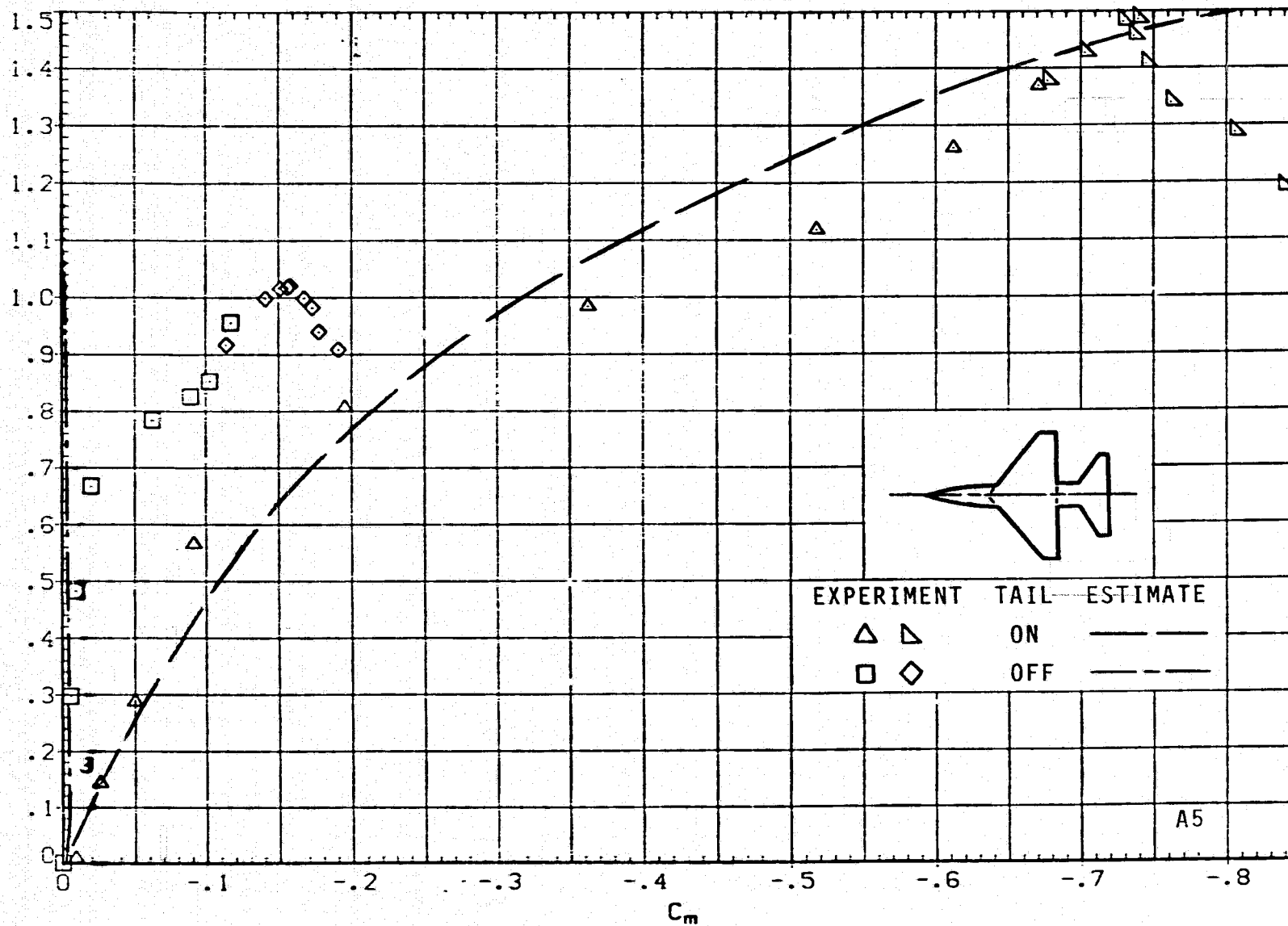


(b) C_L VERSUS C_D ; $M = 0.6$, $J = 1$.

FIGURE 9.- CONTINUED.

RESEARCH MODEL

$M = 0.60$



(c) C_L VERSUS C_m ; $M = 0.6$, $J = 1$.

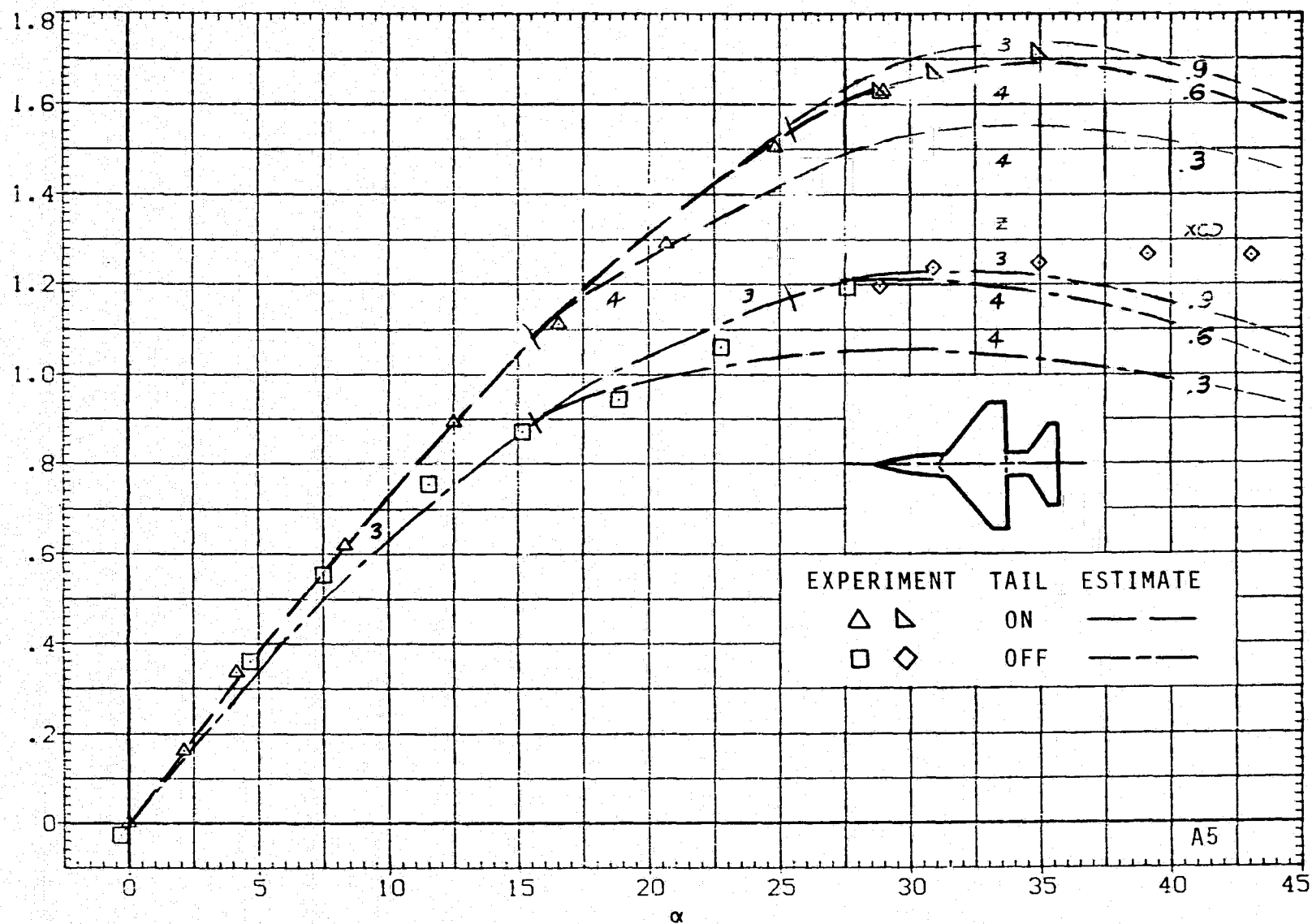
FIGURE 9.- CONTINUED.

RESEARCH MODEL

$M = 0.90$

105

C_L



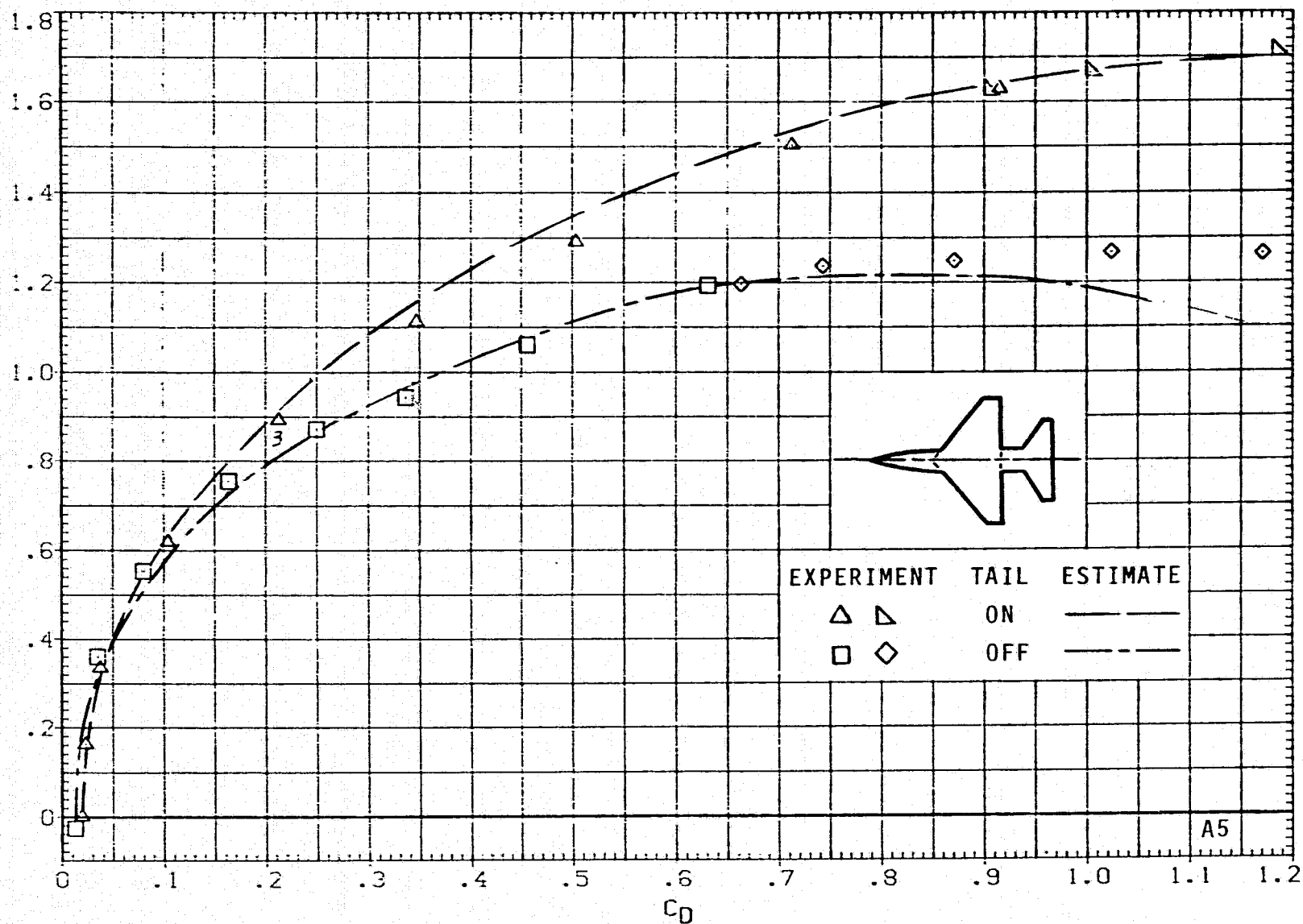
(d) C_L VERSUS α ; $M = 0.9$, $J = 1$.

FIGURE 9.- CONTINUED.

RESEARCH MODEL

$M = 0.90$

106
 C_L



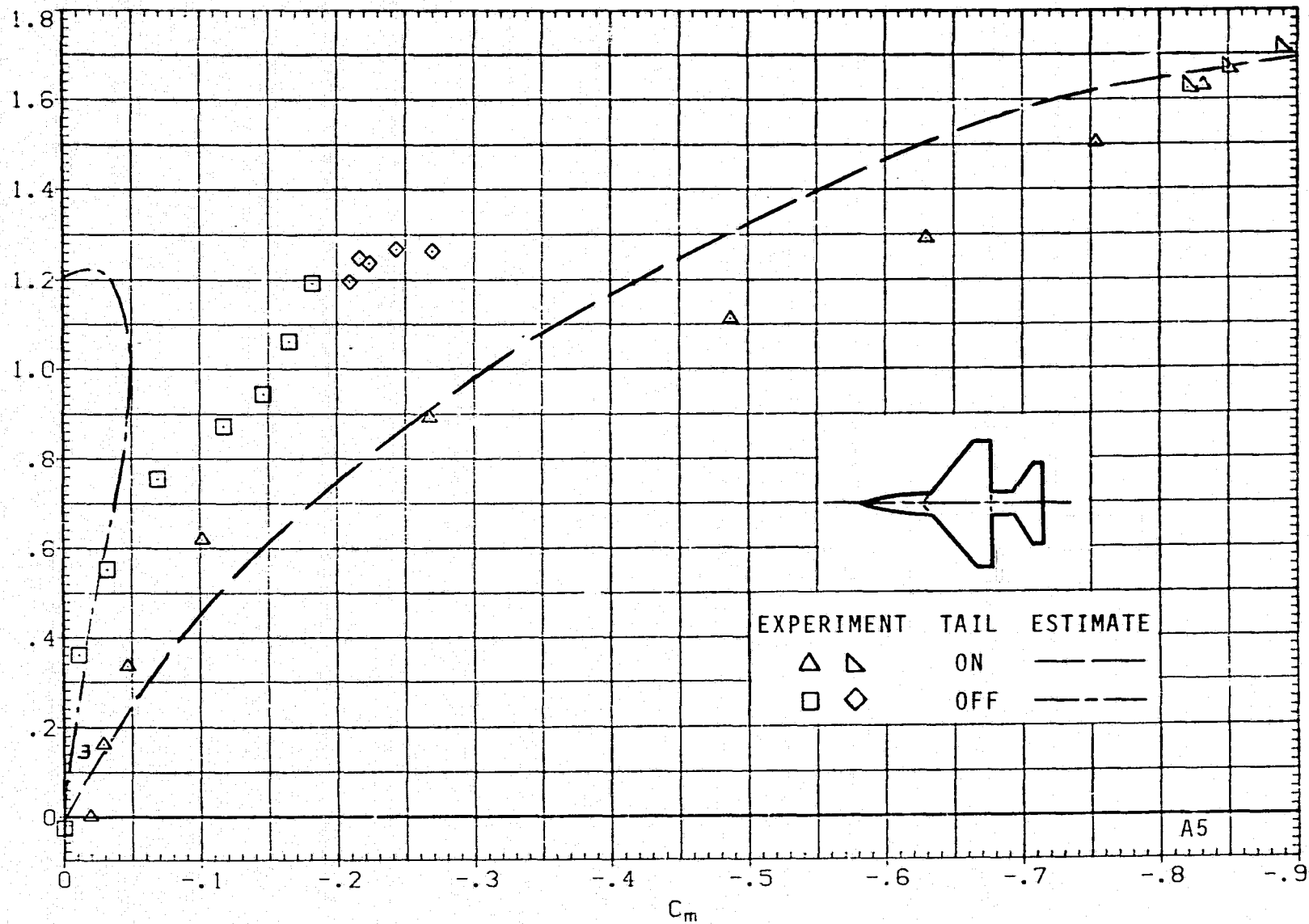
(e) C_L VERSUS C_D ; $M = 0.9$, $J = 1$.

FIGURE 9.- CONTINUED.

A5

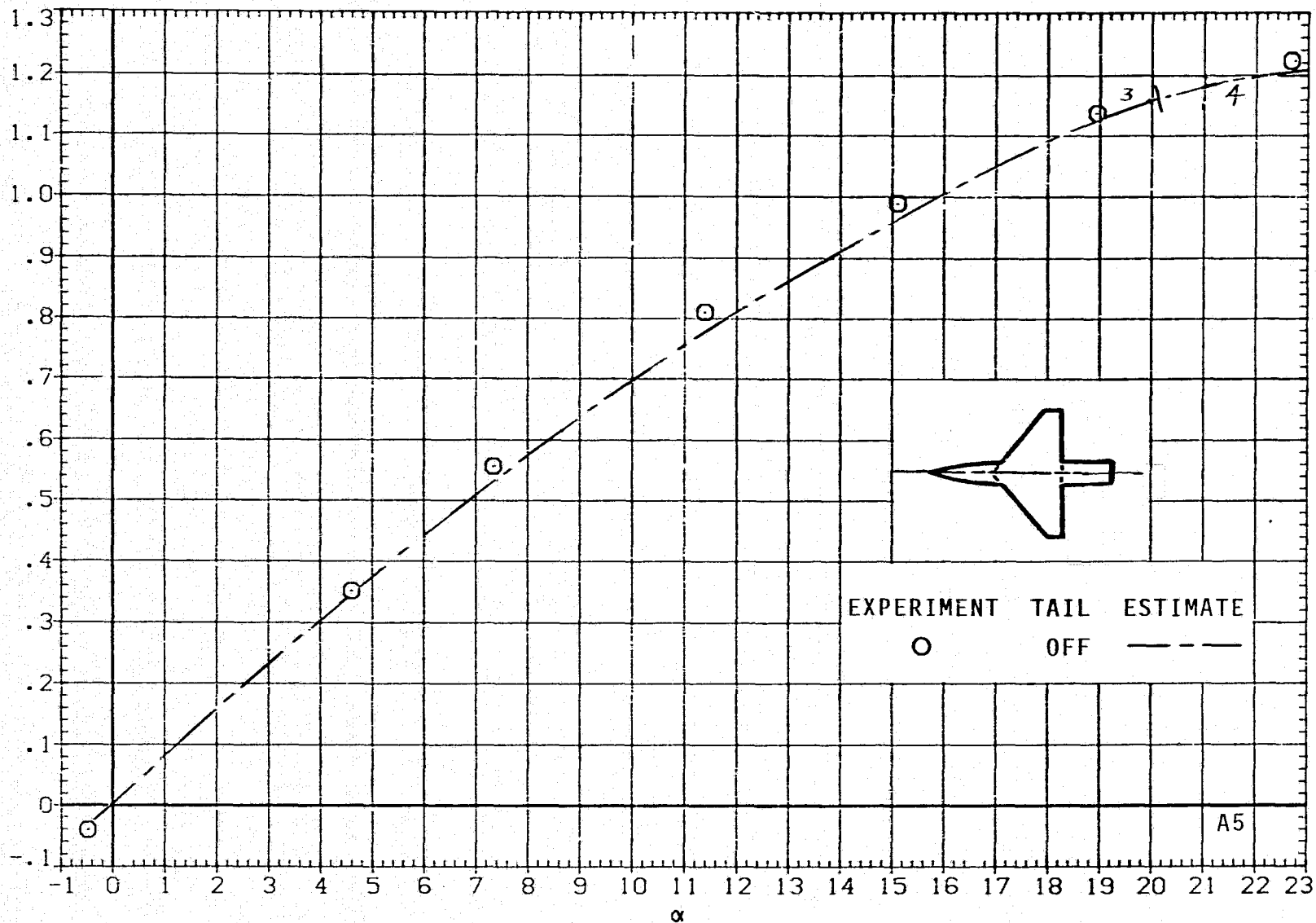
RESEARCH MODEL

$M = 0.90$



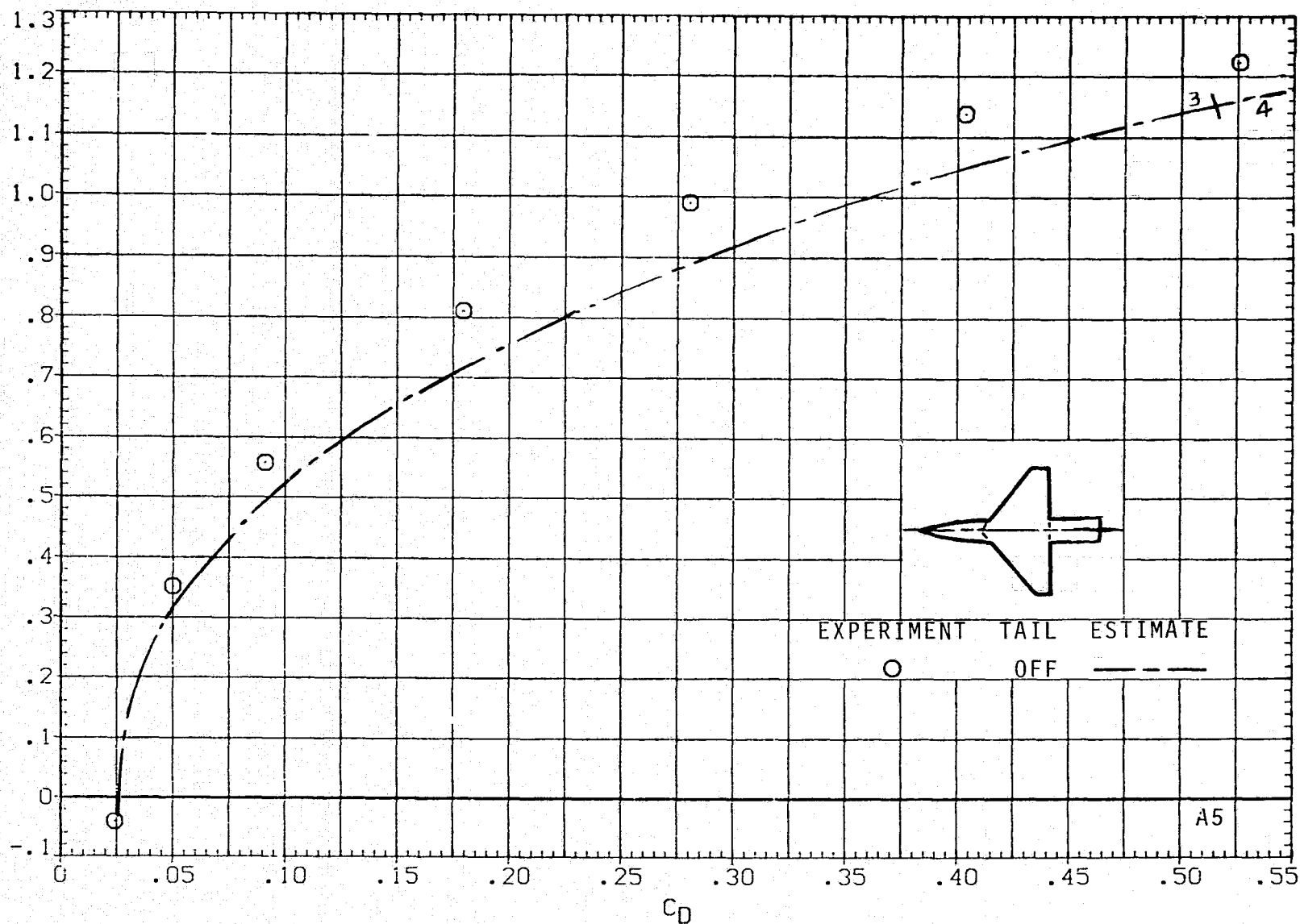
(f) C_L VERSUS C_m ; $M = 0.9$, $J = 1$.

FIGURE 9.- CONTINUED.



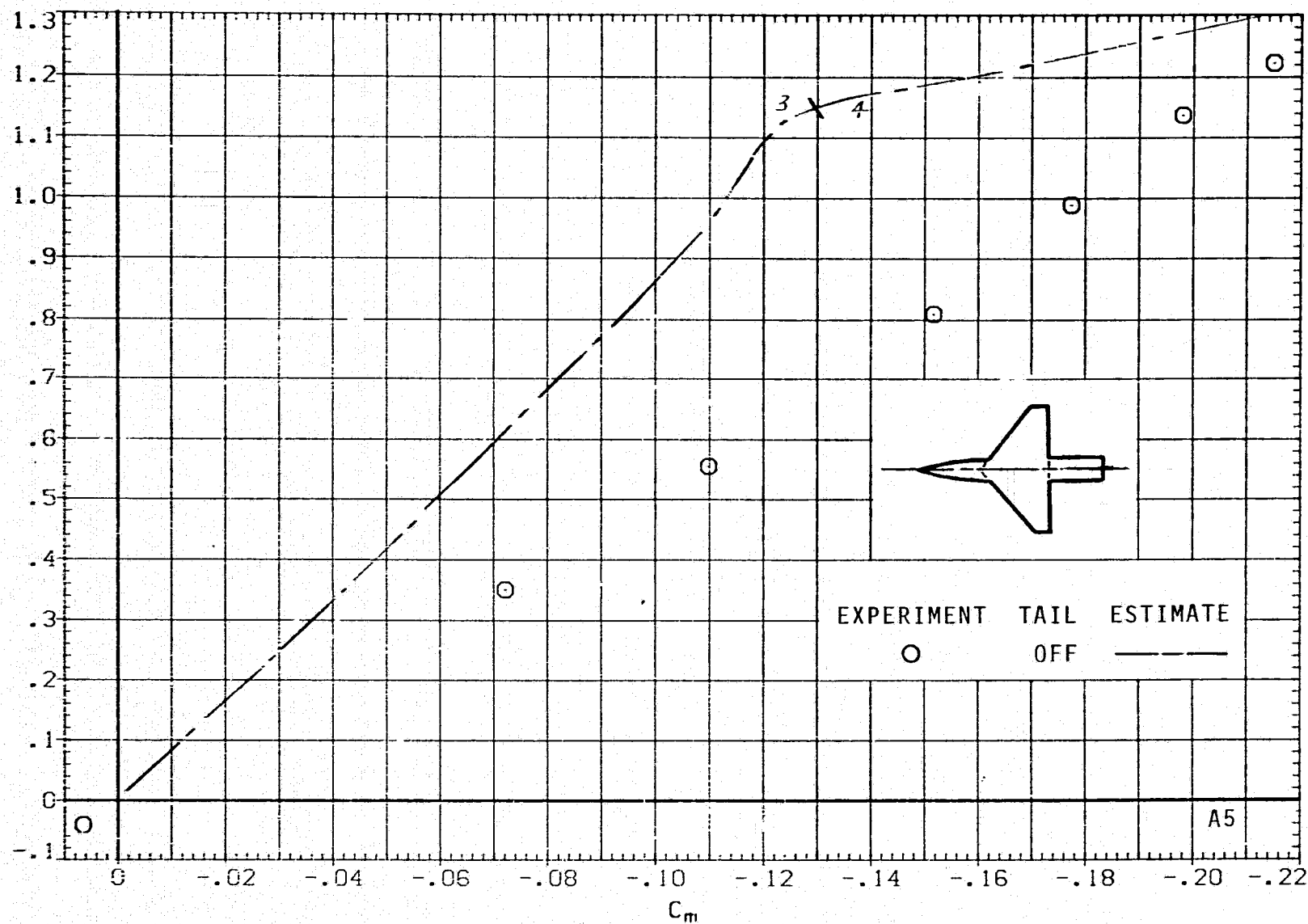
(g) C_L VERSUS α ; $M = 1.2$, $J = 1$.

FIGURE 9.- CONTINUED.



(h) C_L VERSUS C_D ; $M = 1.2$, $J = 1$.

FIGURE 9.- CONTINUED.

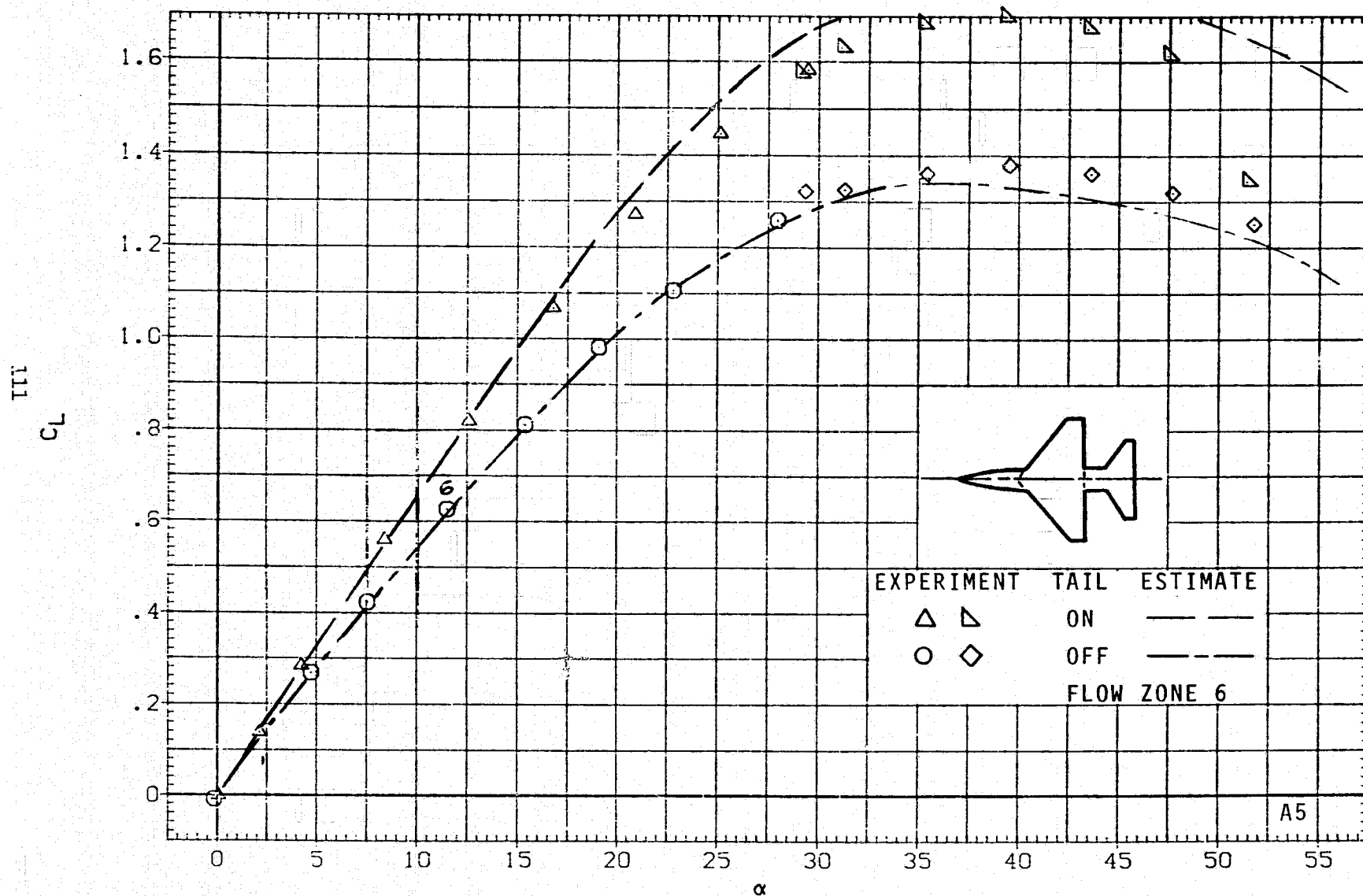


(i) C_L VERSUS C_m ; $M = 1.2$, $J = 1$.

FIGURE 9.- CONTINUED.

RESEARCH MODEL

M = 1.50

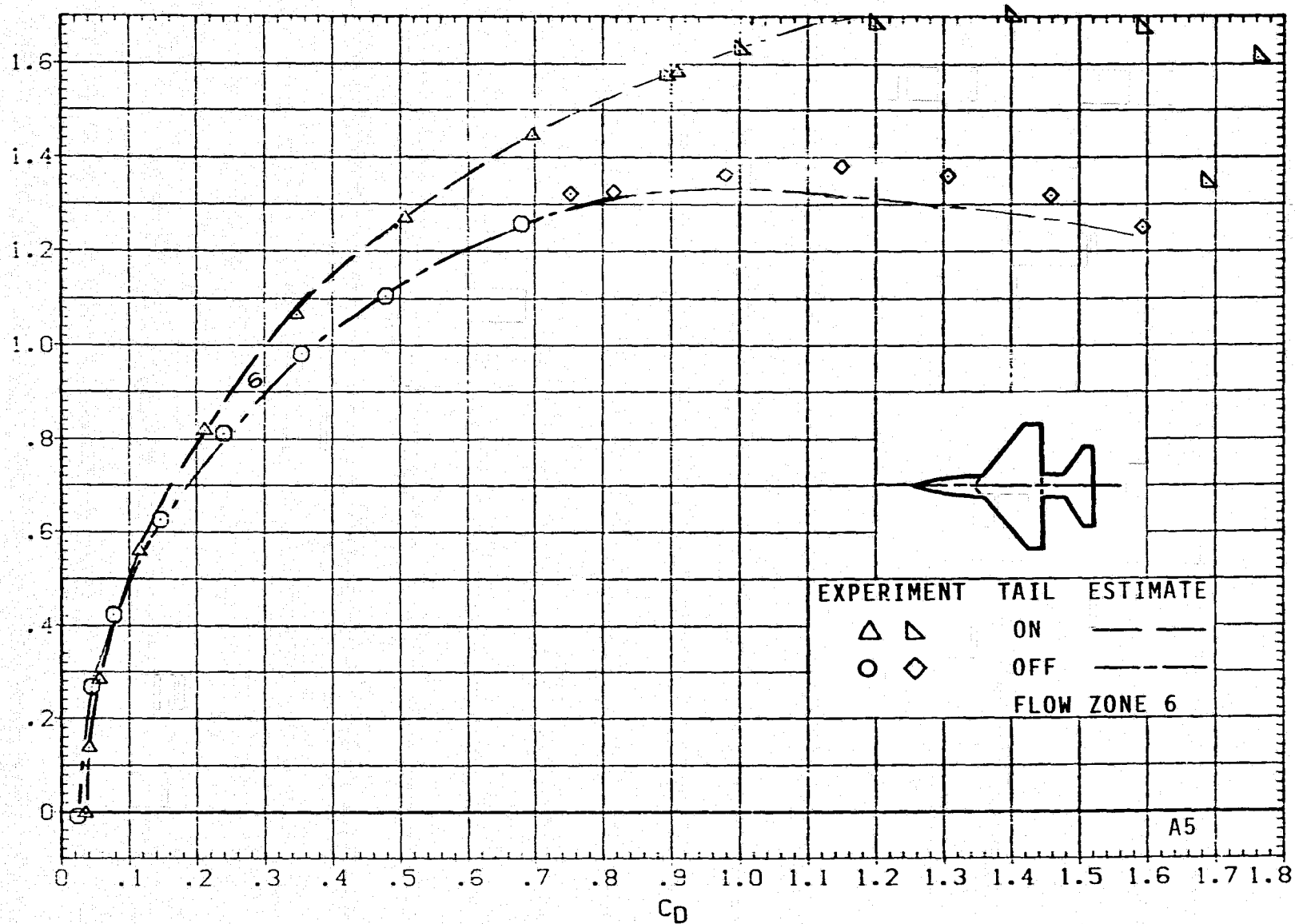


(j) C_L VERSUS α ; M = 1.5, J = 5.

FIGURE 9.- CONTINUED.

RESEARCH MODEL

$M = 1.50$

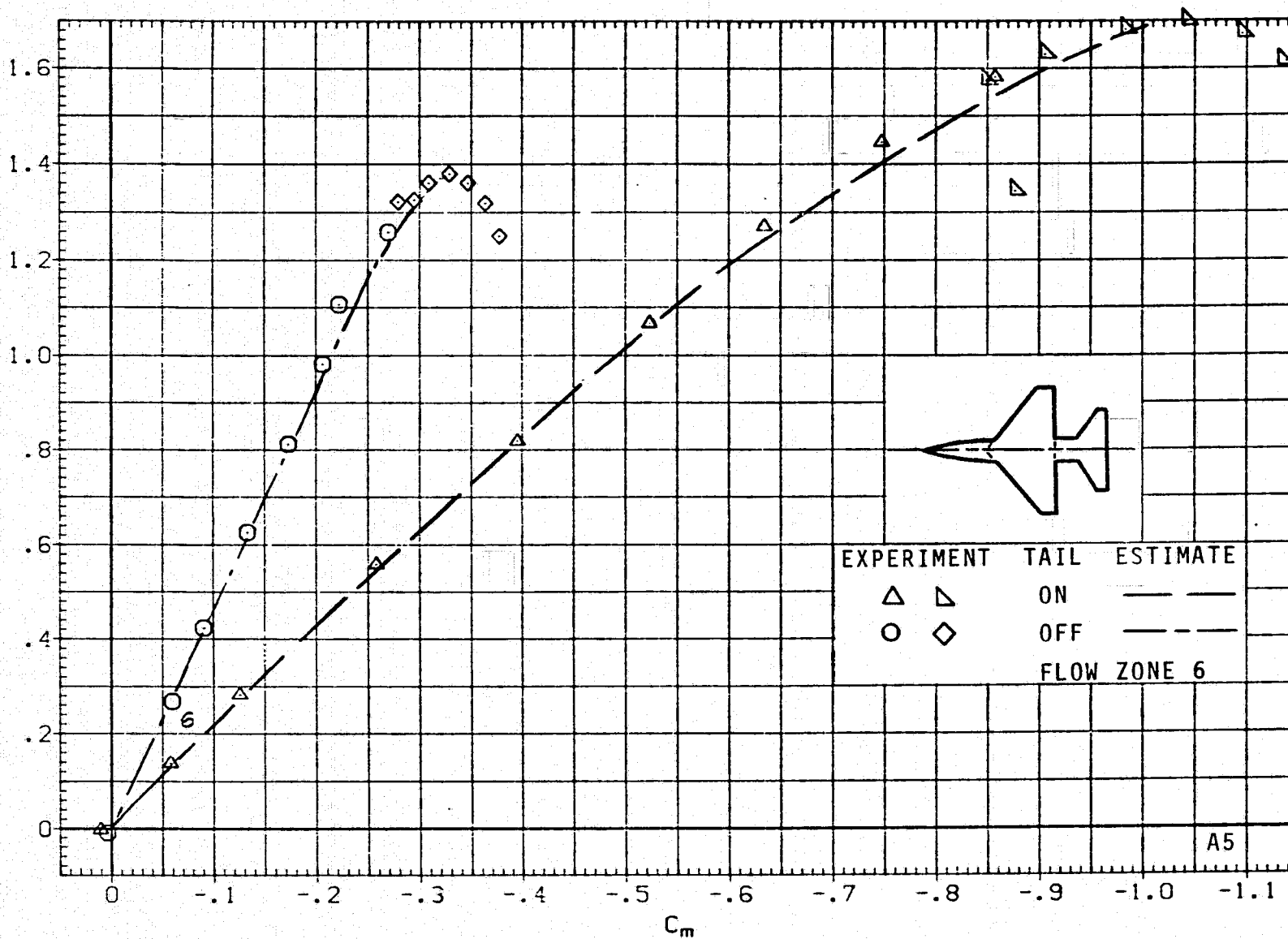


(k) C_L VERSUS C_D ; $M = 1.5$, $J = 5$.

FIGURE 9.- CONTINUED.

RESEARCH MODEL

$M = 1.50$

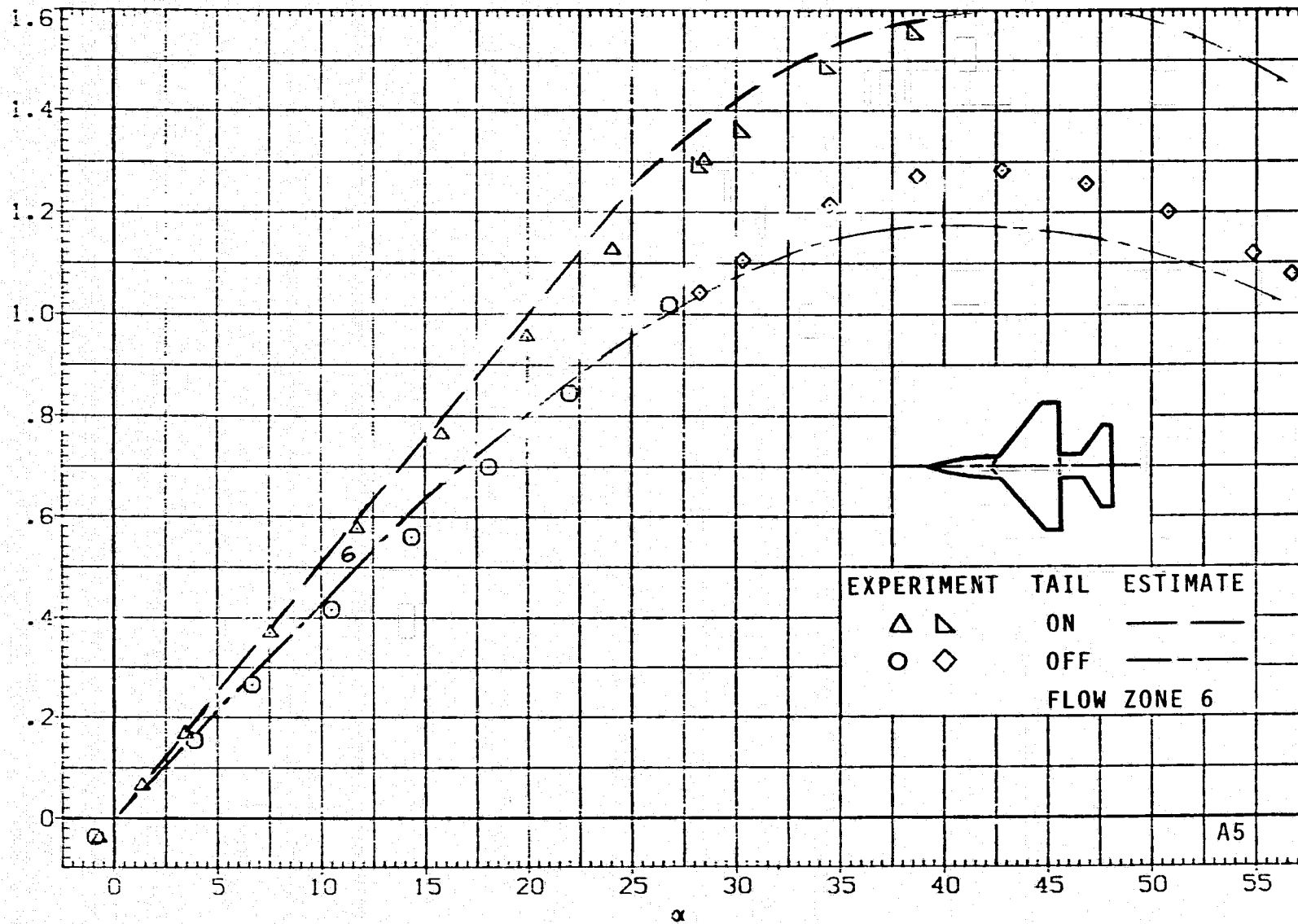


(1) C_L VERSUS C_m ; $M = 1.5$, $\beta = 5$.

FIGURE 9.- CONTINUED.

RESEARCH MODEL

$M = 2.0$

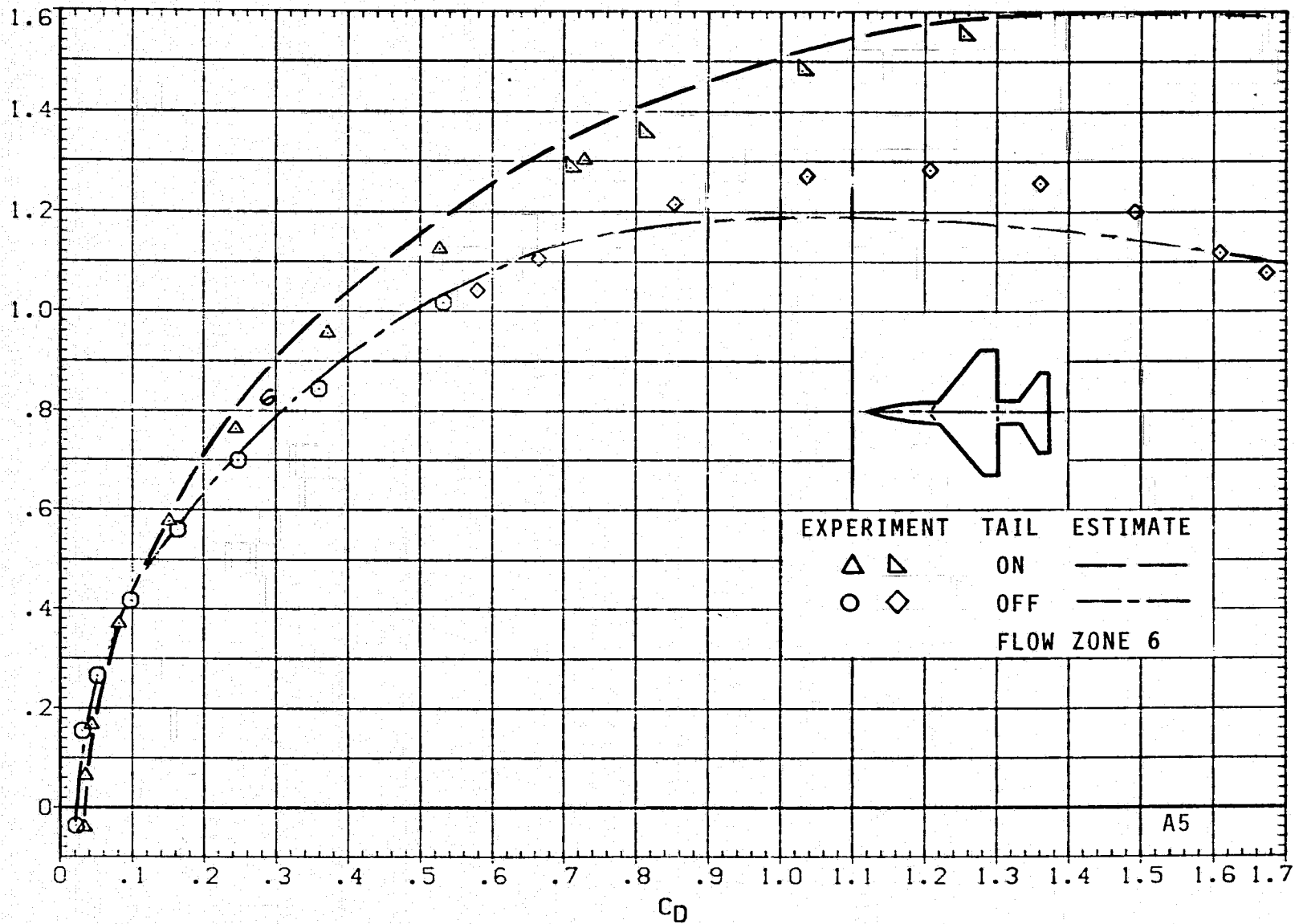


(m) C_L VERSUS α ; $M = 2.0$, $J = 5$.

FIGURE 9.- CONTINUED.

RESEARCH MODEL

$M = 2.0$

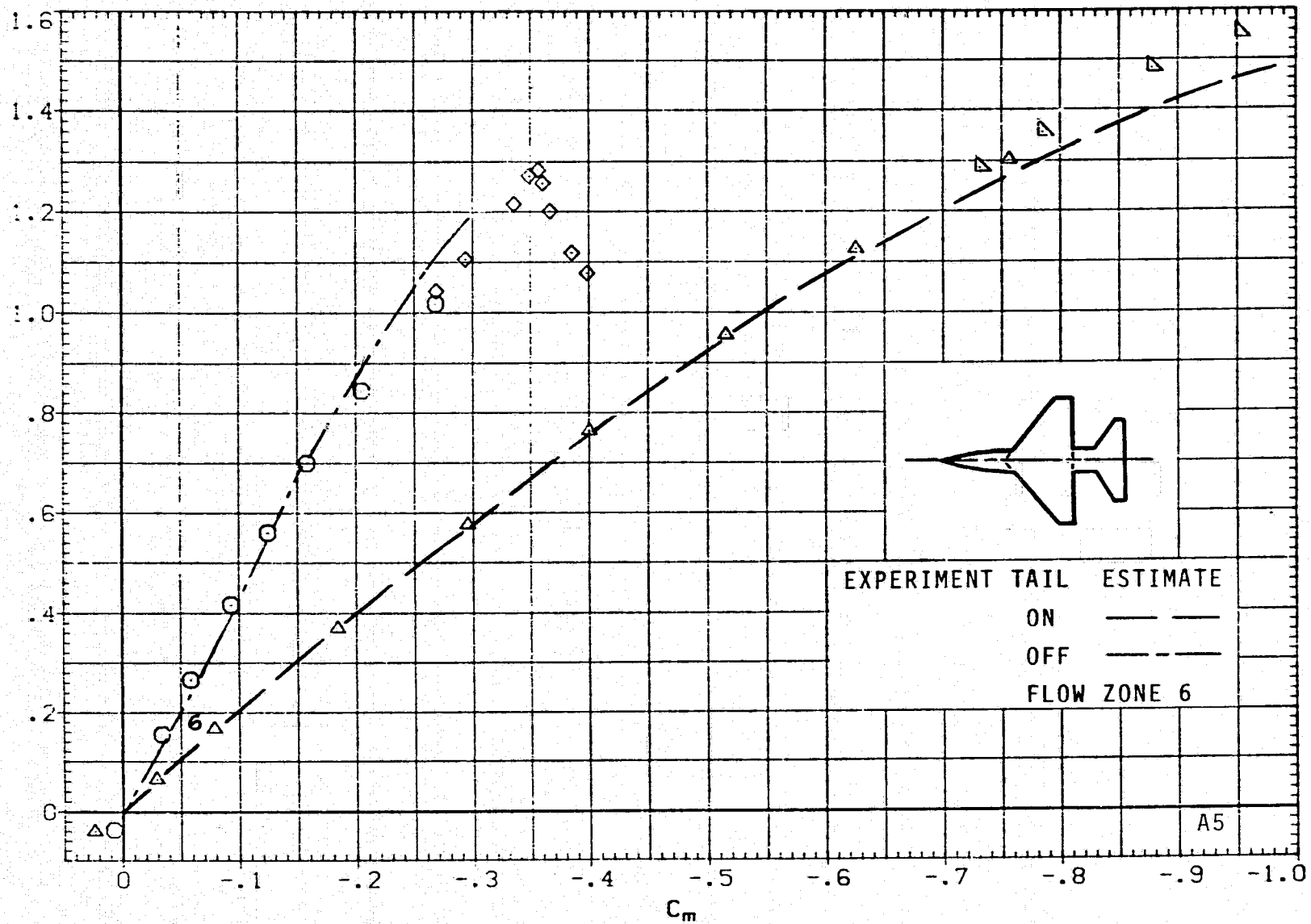


(n) C_L VERSUS C_D ; $M = 2.0$, $J = 5$.

FIGURE 9.- CONTINUED.

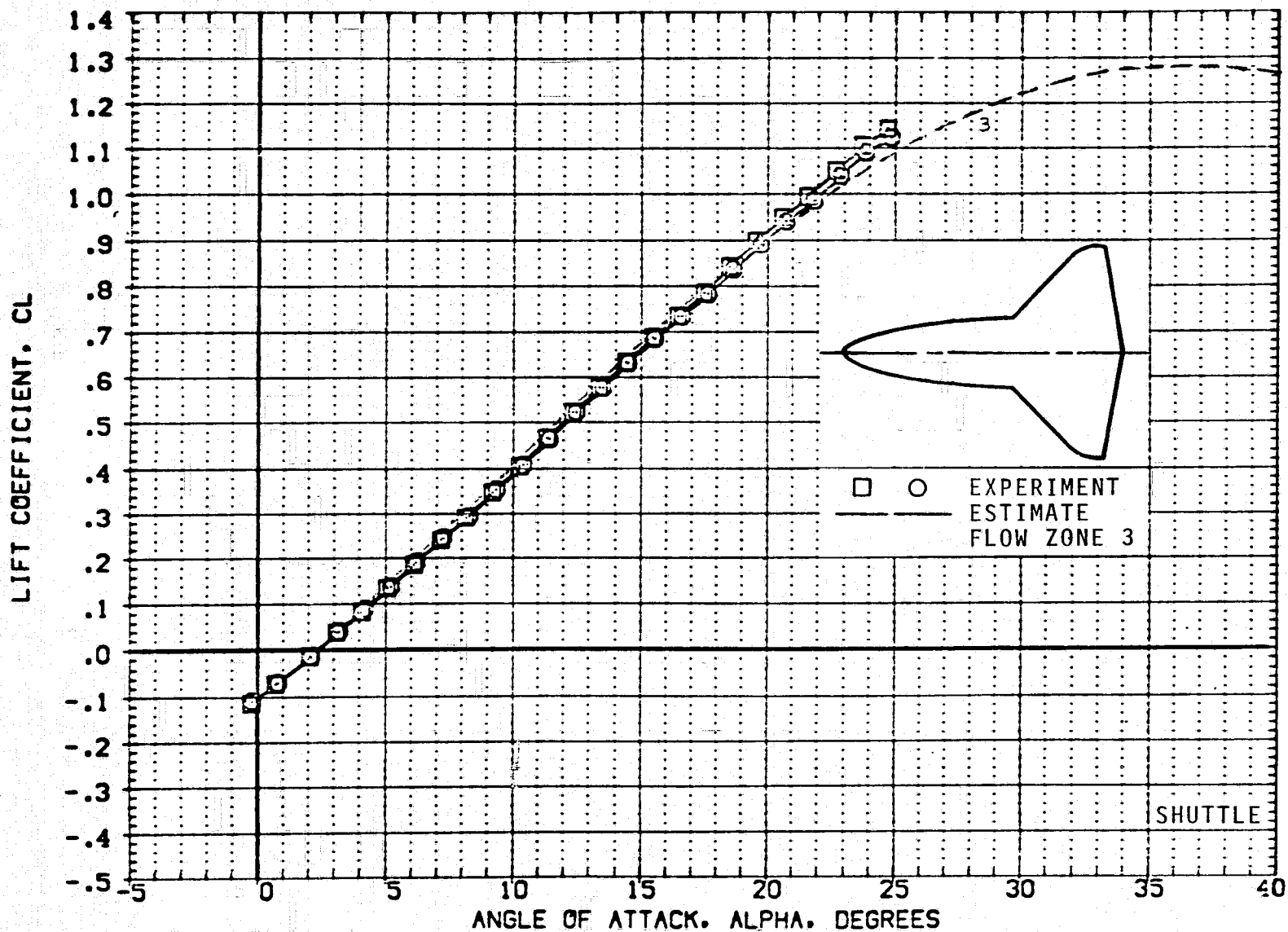
RESEARCH MODEL

$M = 2.0$



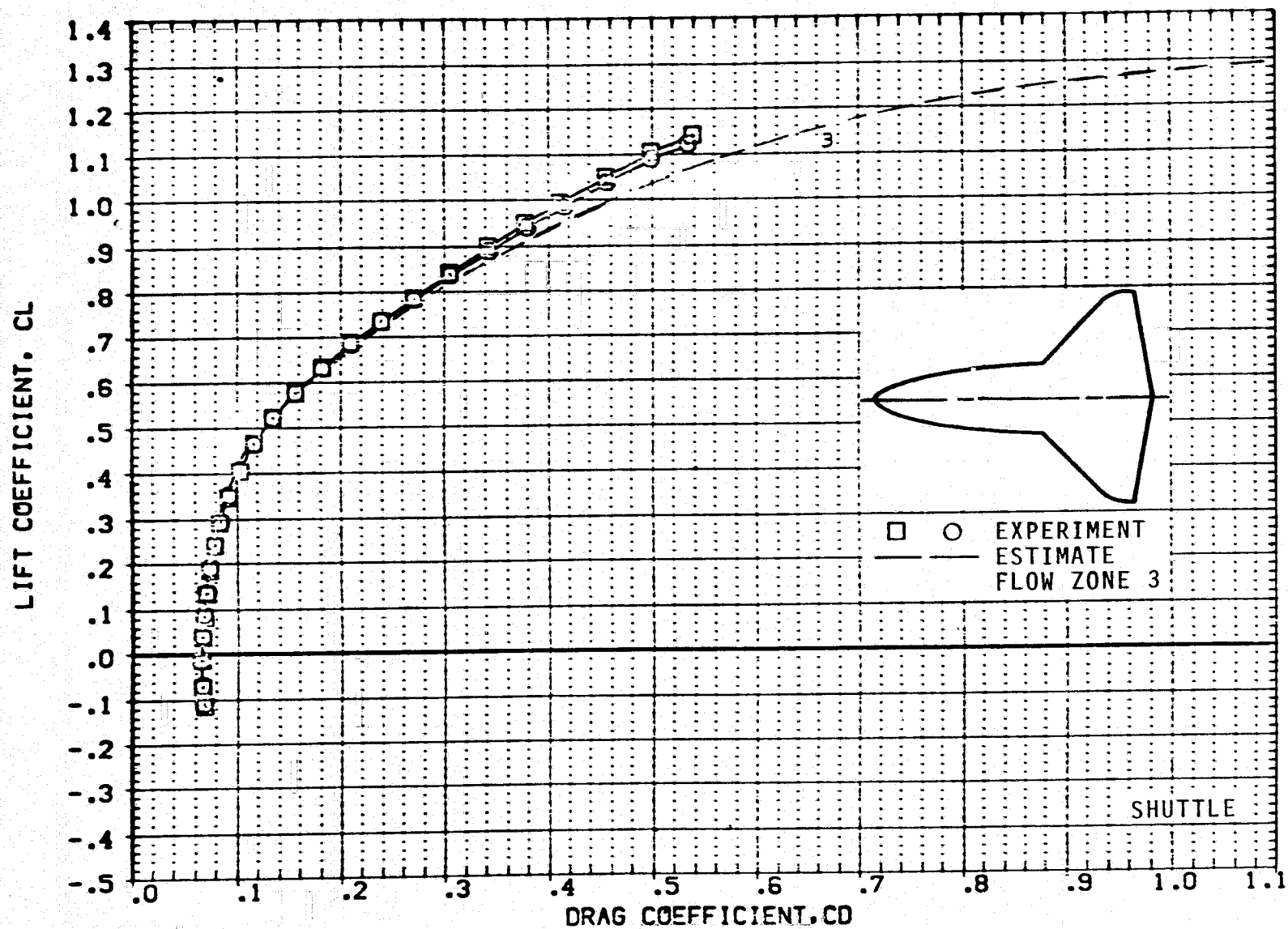
(o) C_L VERSUS C_m ; $M = 2.0$, $J = 5$.

FIGURE 9.- CONCLUDED.



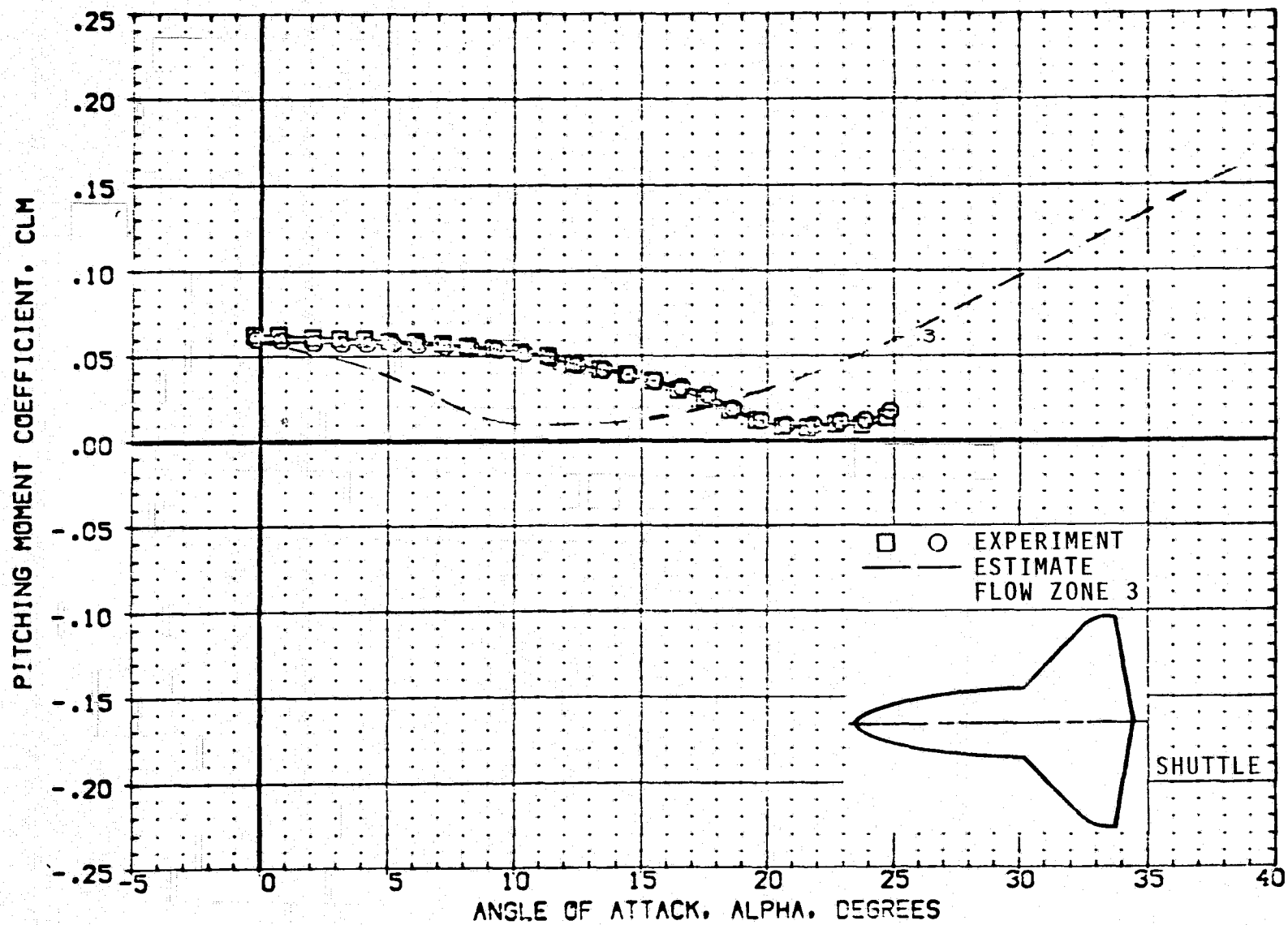
(a) C_L VERSUS α ; $M = 0.6$.

FIGURE 10.- AERODYNAMICS FOR SHUTTLE ORBITER; $J = 2$.



(b) C_L VERSUS C_D ; $M = 0.6$.

FIGURE 10.- CONTINUED.



(c) C_m VERSUS α ; $M = 0.6$.

FIGURE 10.- CONTINUED.

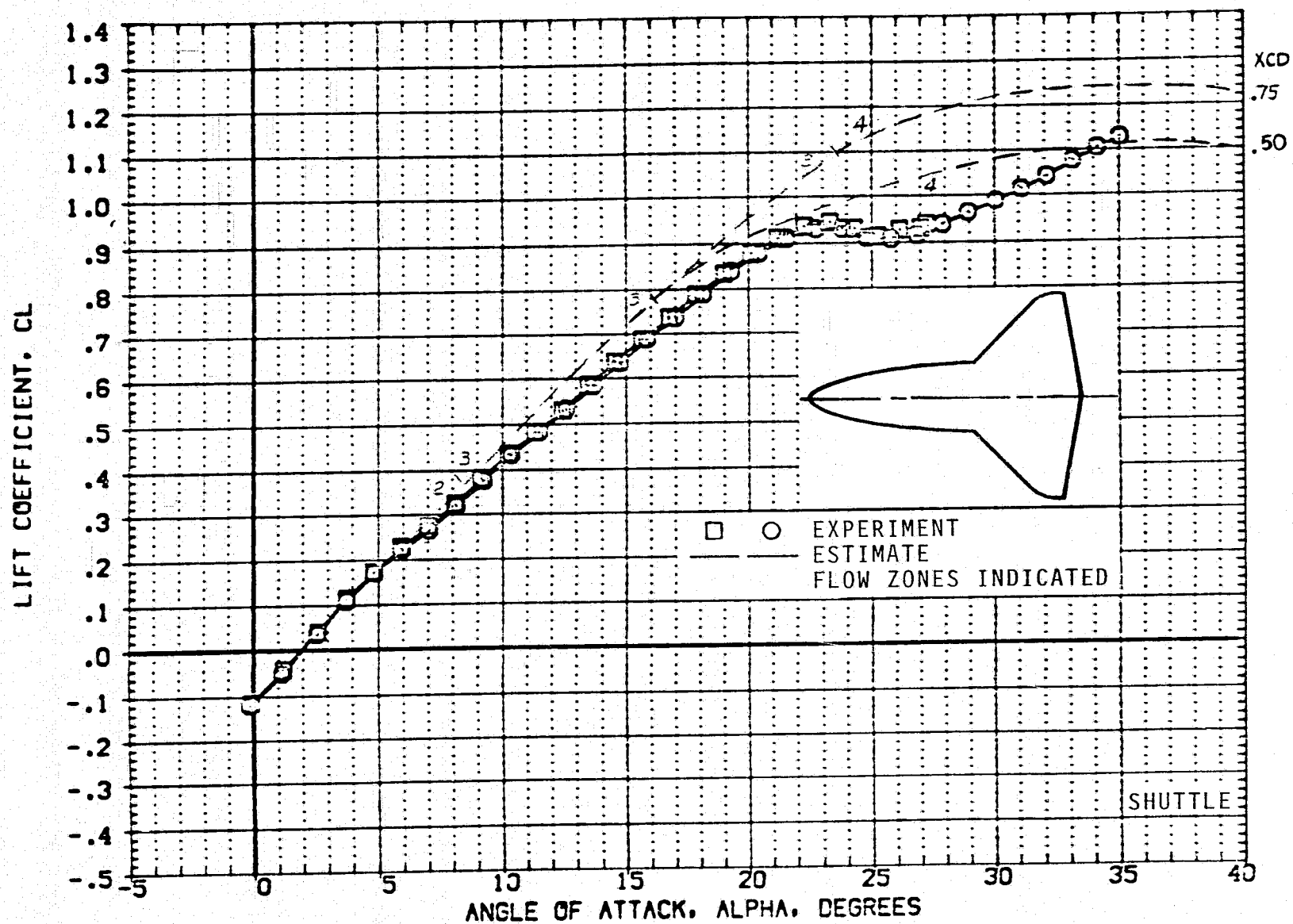
(d) C_L VERSUS α ; $M = 0.9$.

FIGURE 10.- CONTINUED.

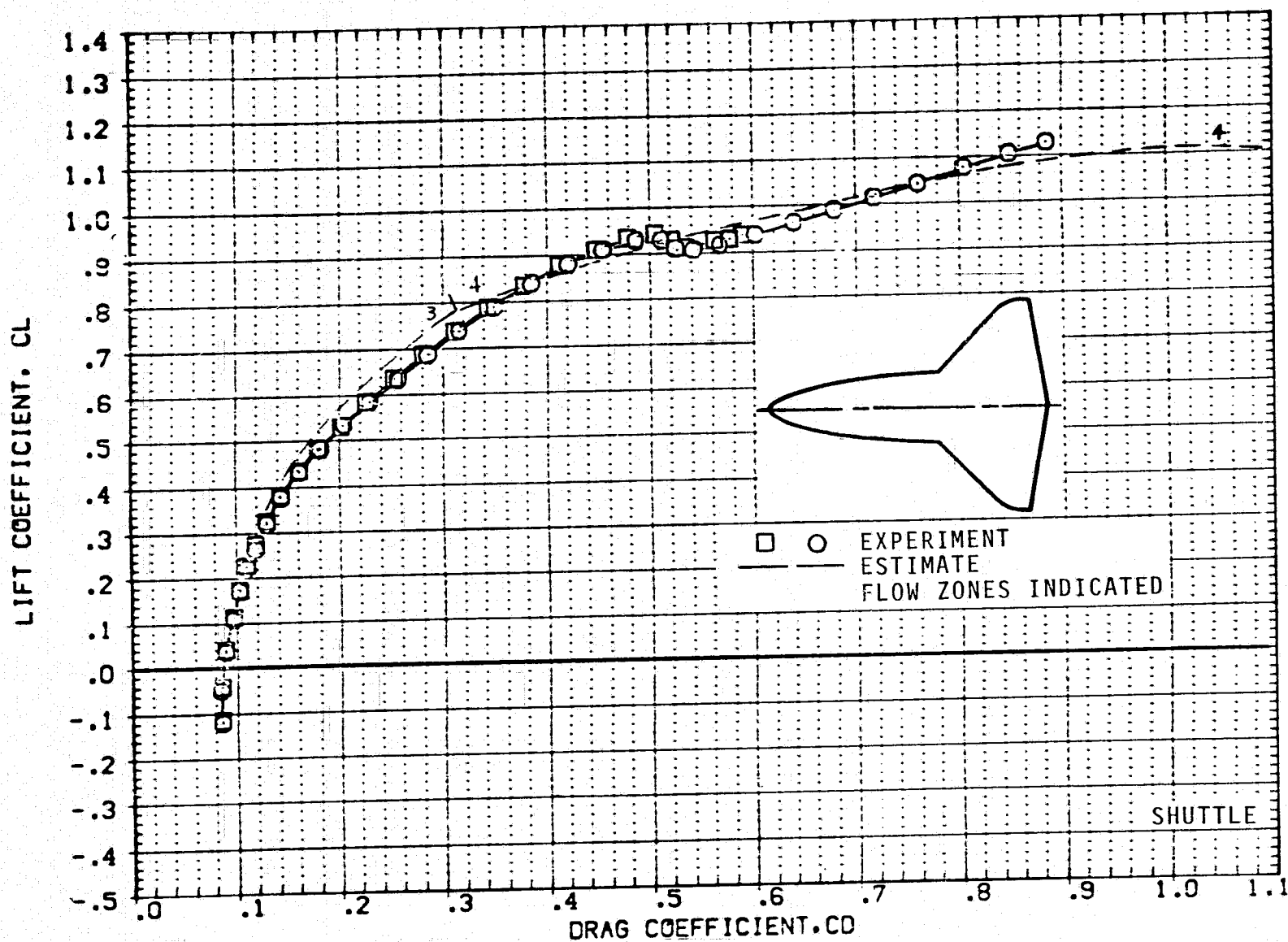
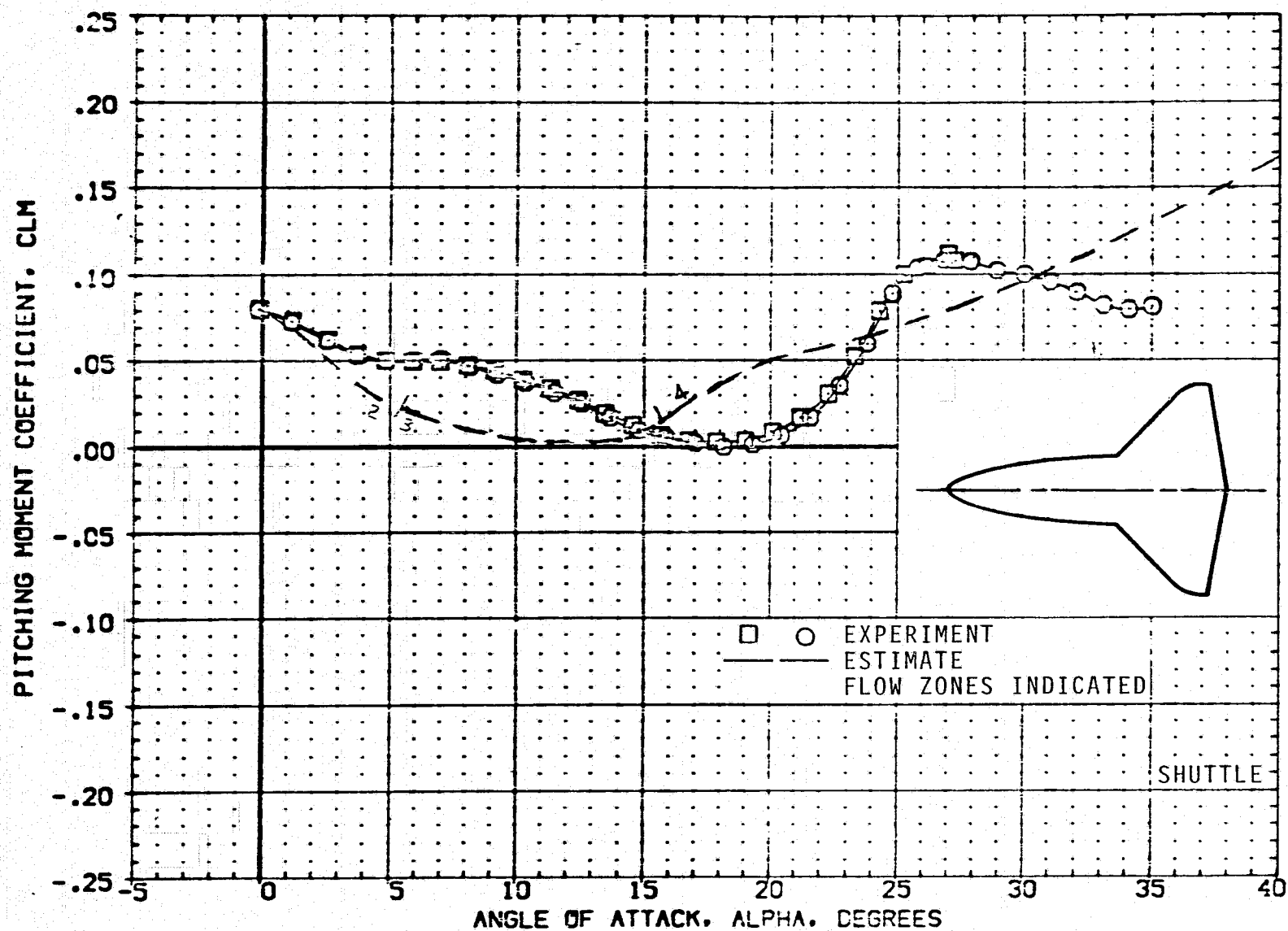
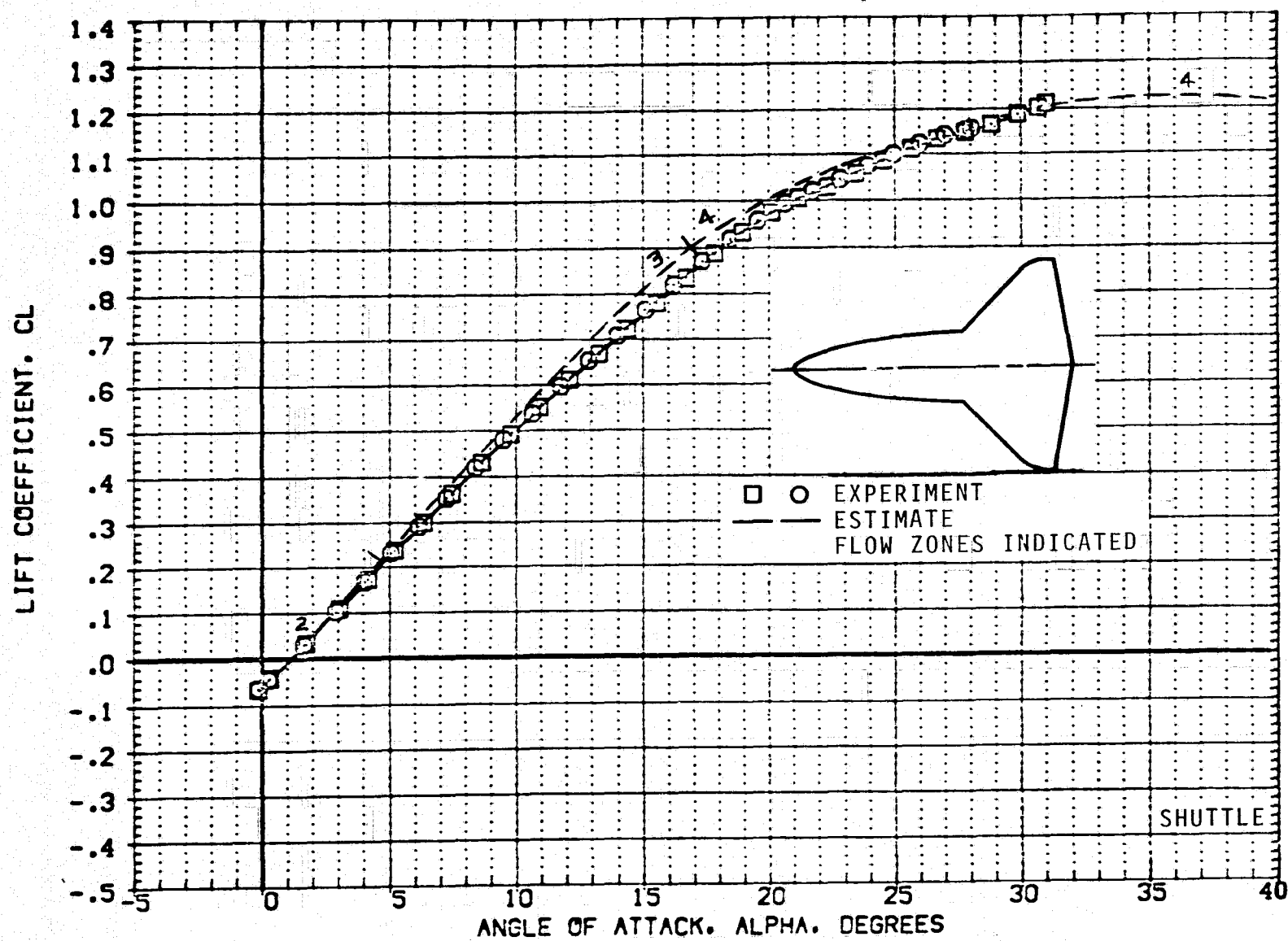
(e) C_L VERSUS C_D ; $M = 0.9$.

FIGURE 10.- CONTINUED.



(f) C_m VERSUS α ; $M = 0.9$.

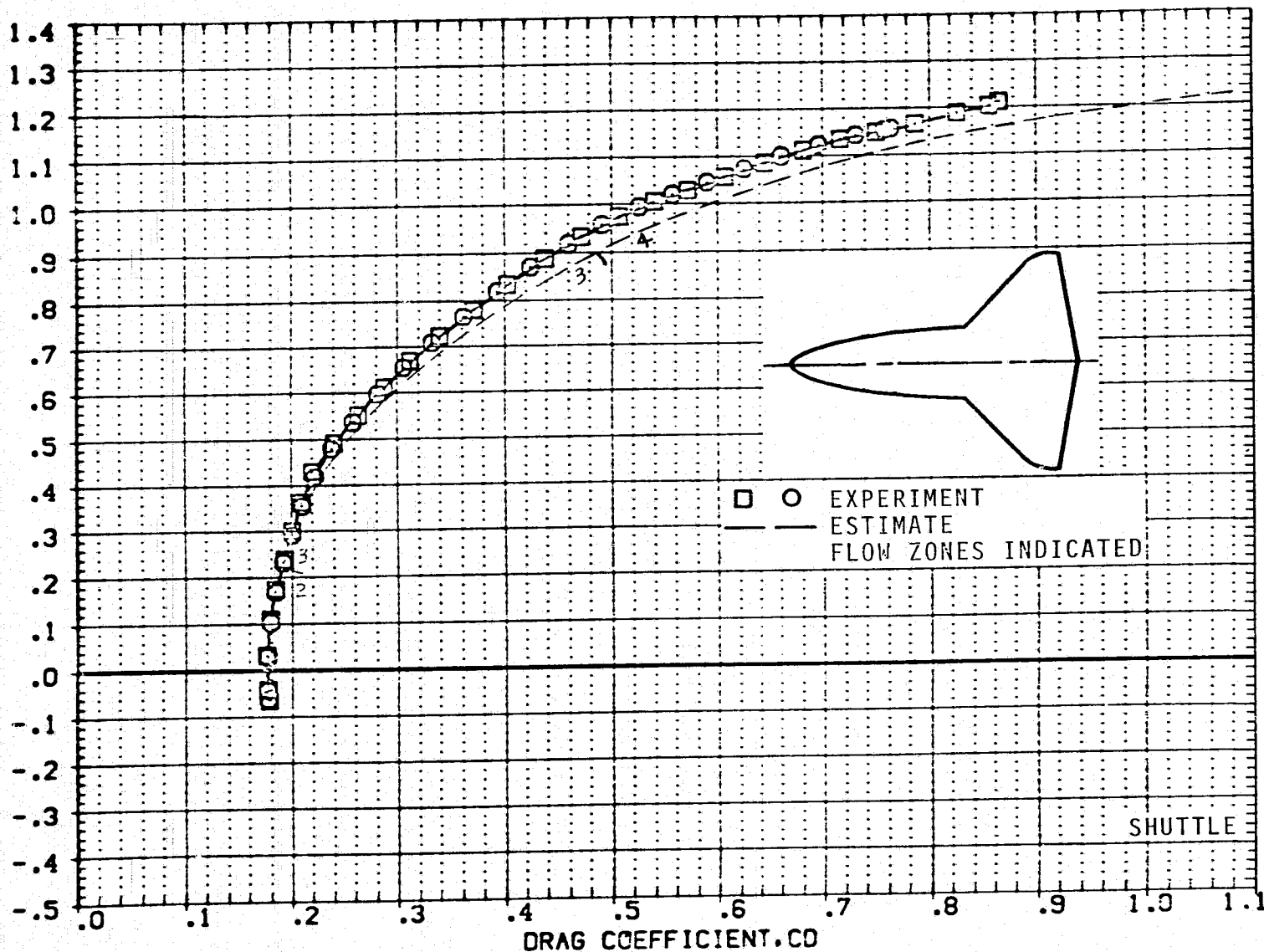
FIGURE 10.- CONTINUED.



(g) C_L VERSUS α ; $M = 1.2$.

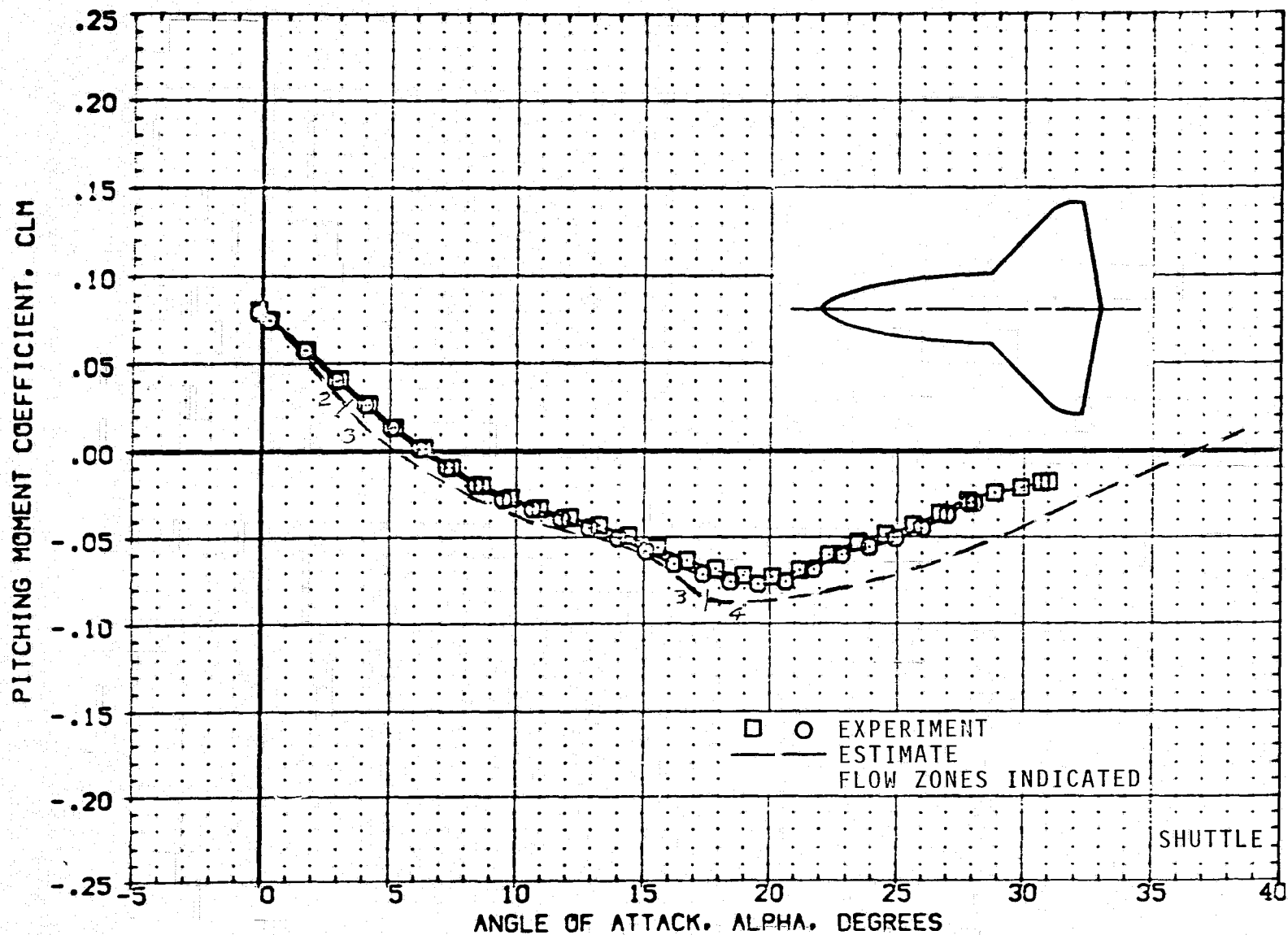
FIGURE 10.- CONTINUED.

LIFT COEFFICIENT, C_L



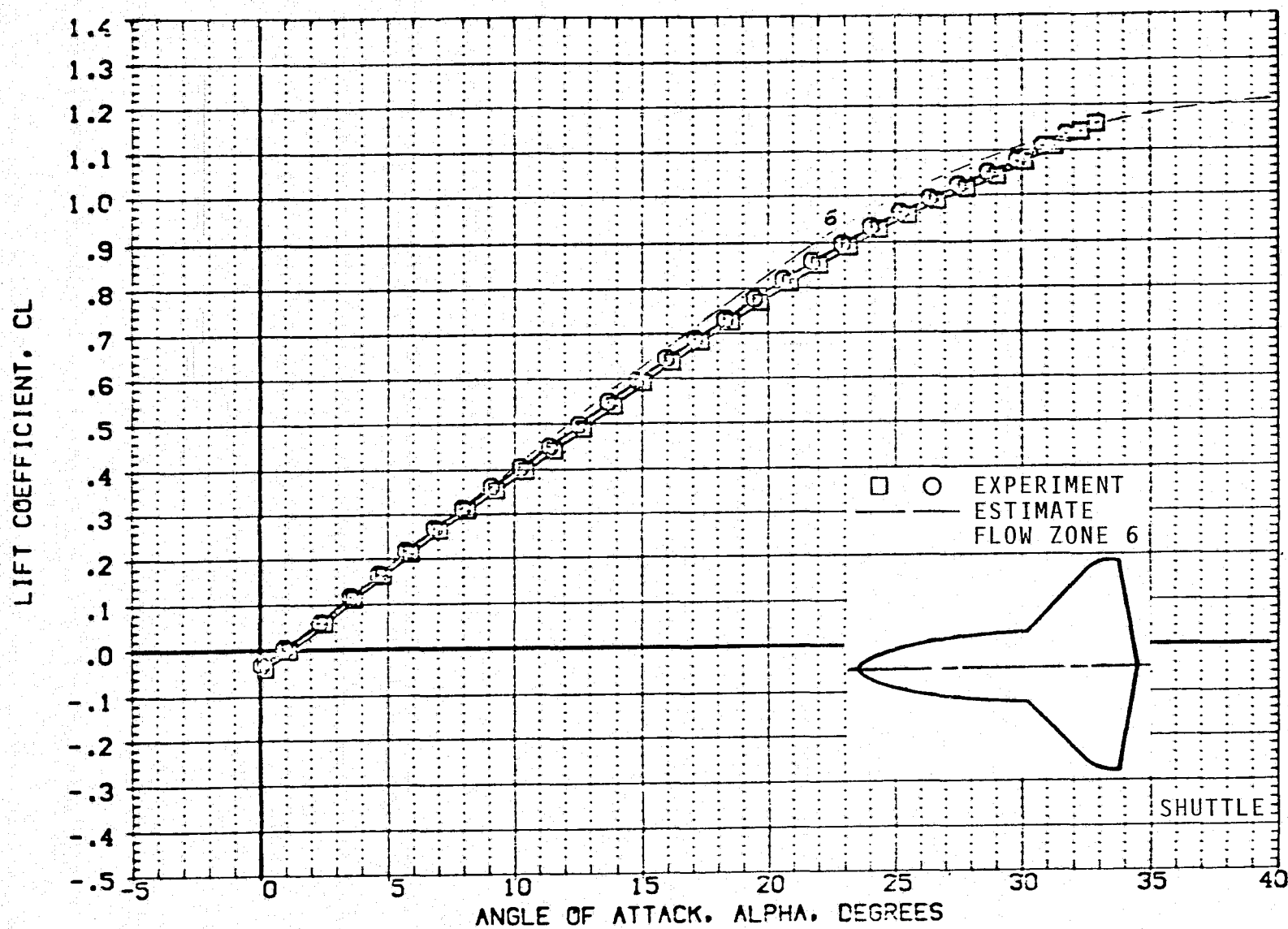
(h) C_L VERSUS C_D ; $M = 1.2$.

FIGURE 10.- CONTINUED.



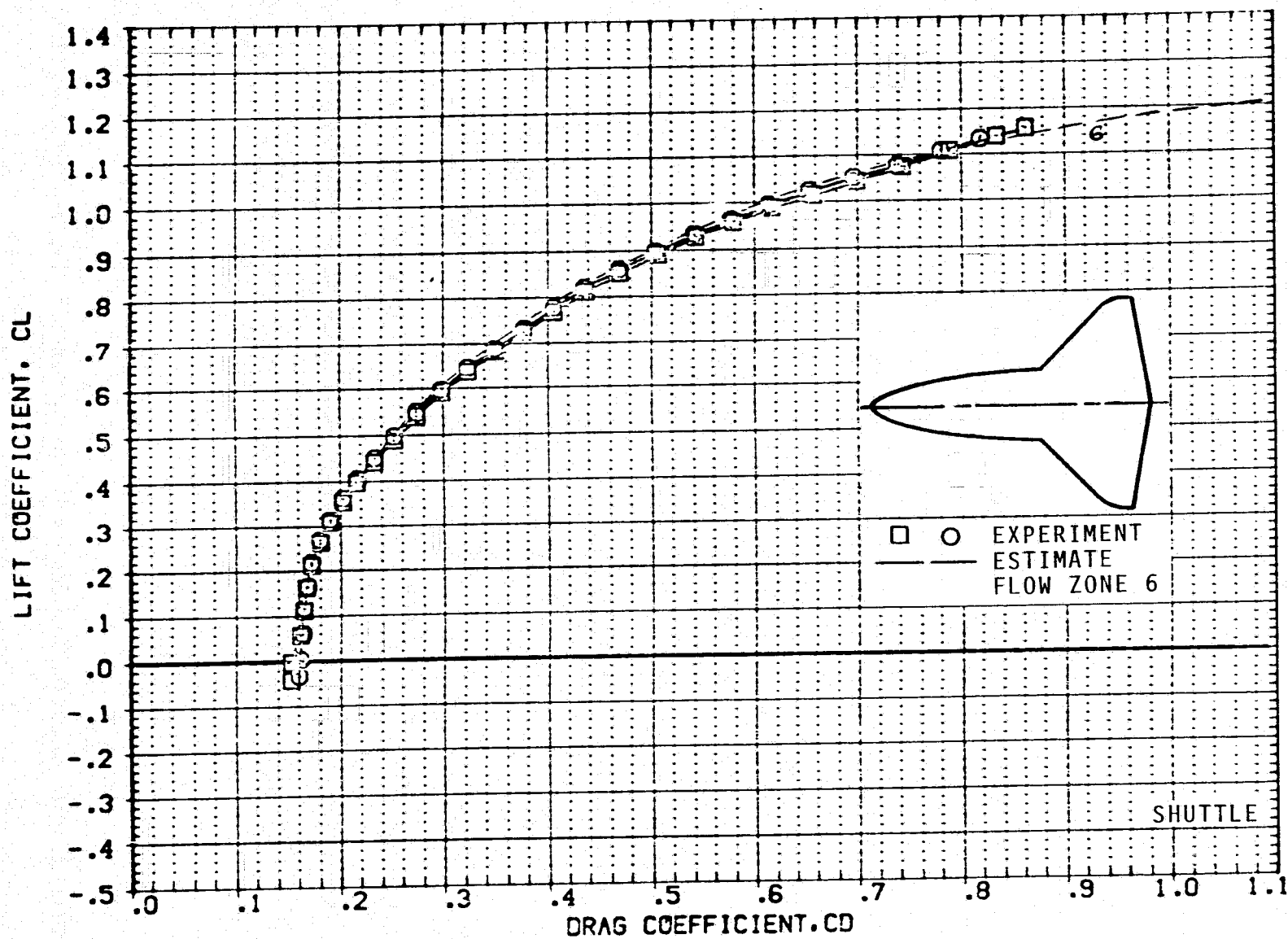
(i) C_m VERSUS α ; $M = 1.2$.

FIGURE 10.- CONTINUED.



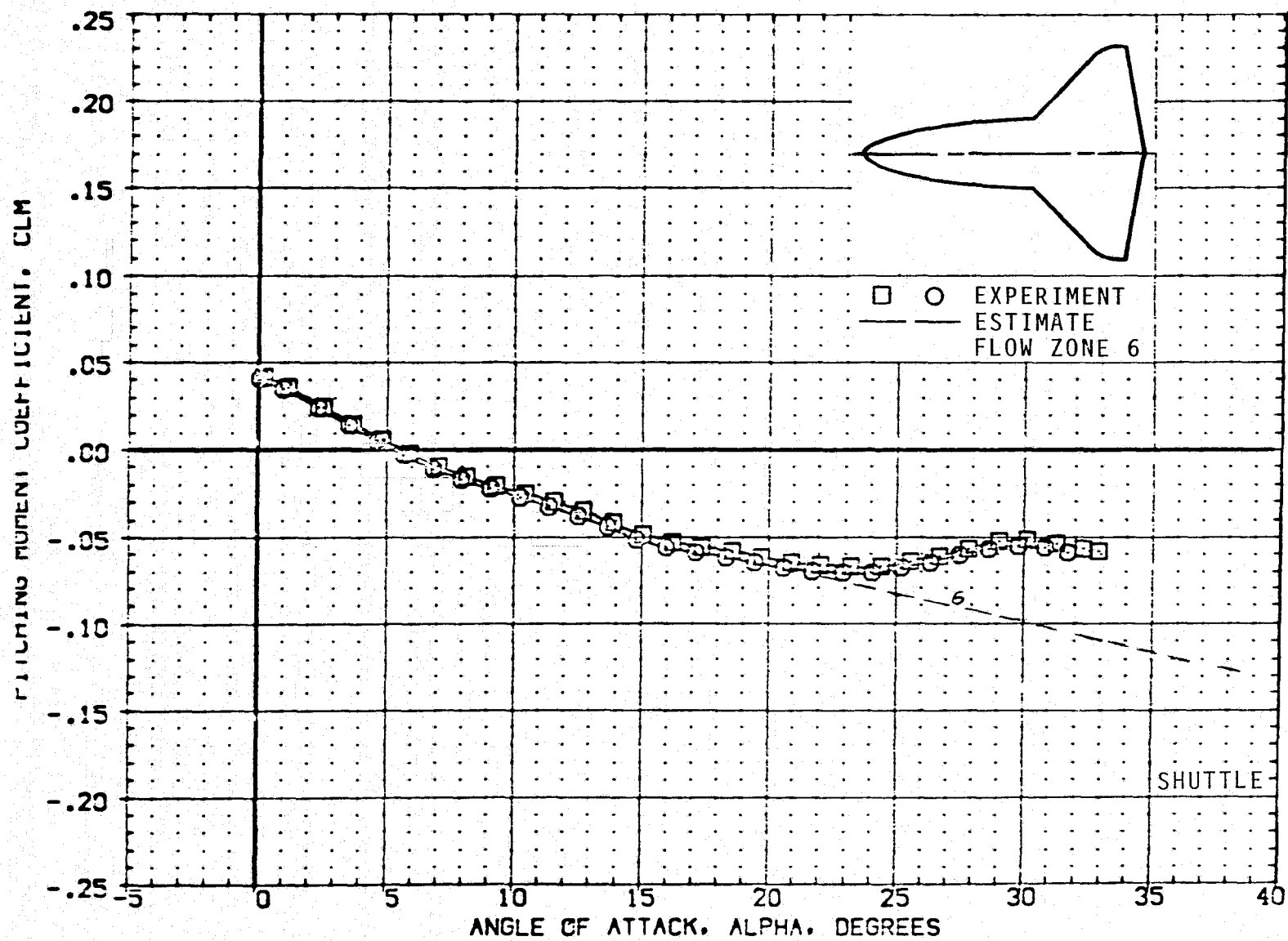
(j) C_L VERSUS α ; $M = 1.6$.

FIGURE 10.- CONTINUED.



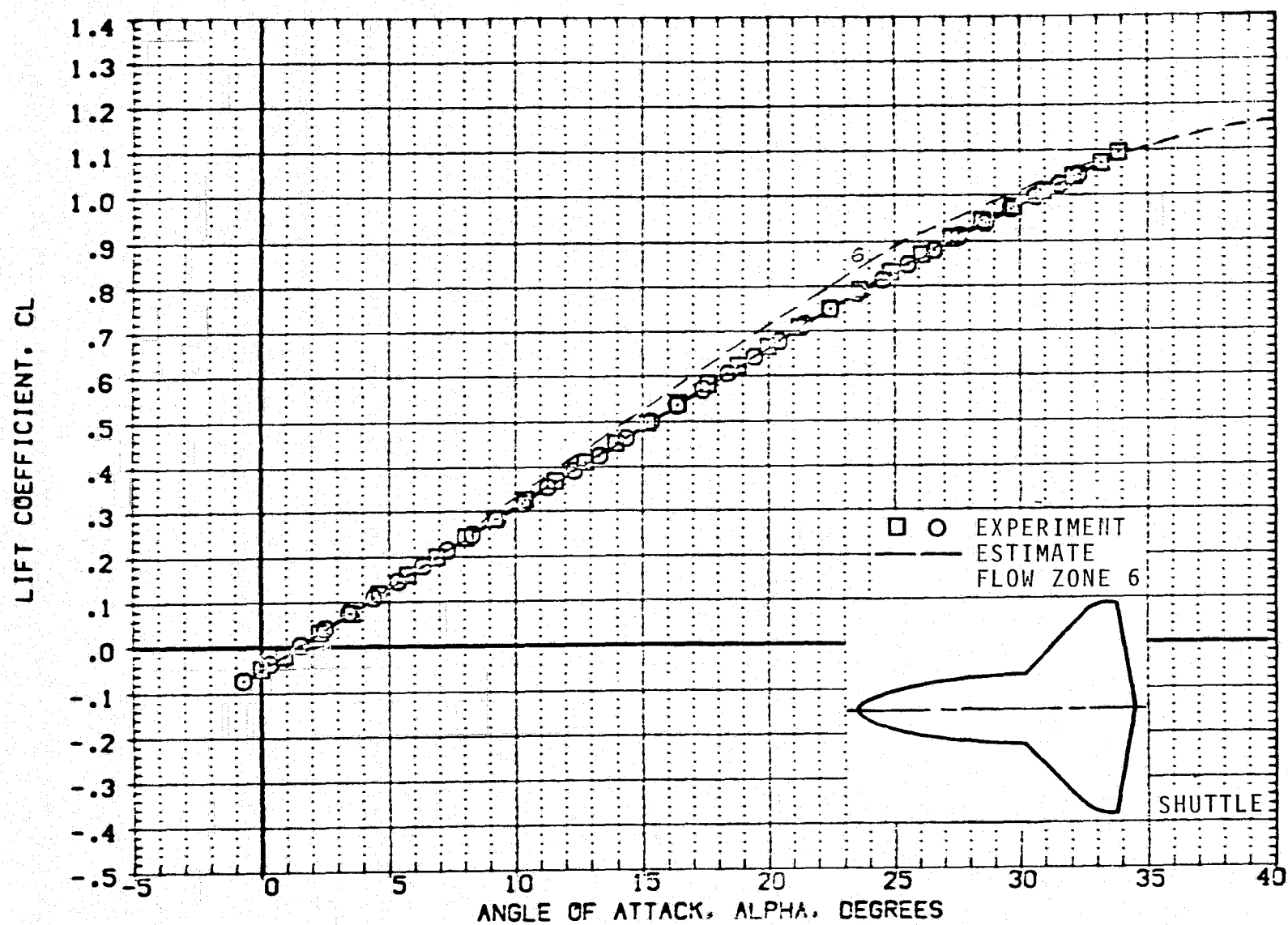
(k) C_L VERSUS C_D ; $M = 1.6$.

FIGURE 10.- CONTINUED.



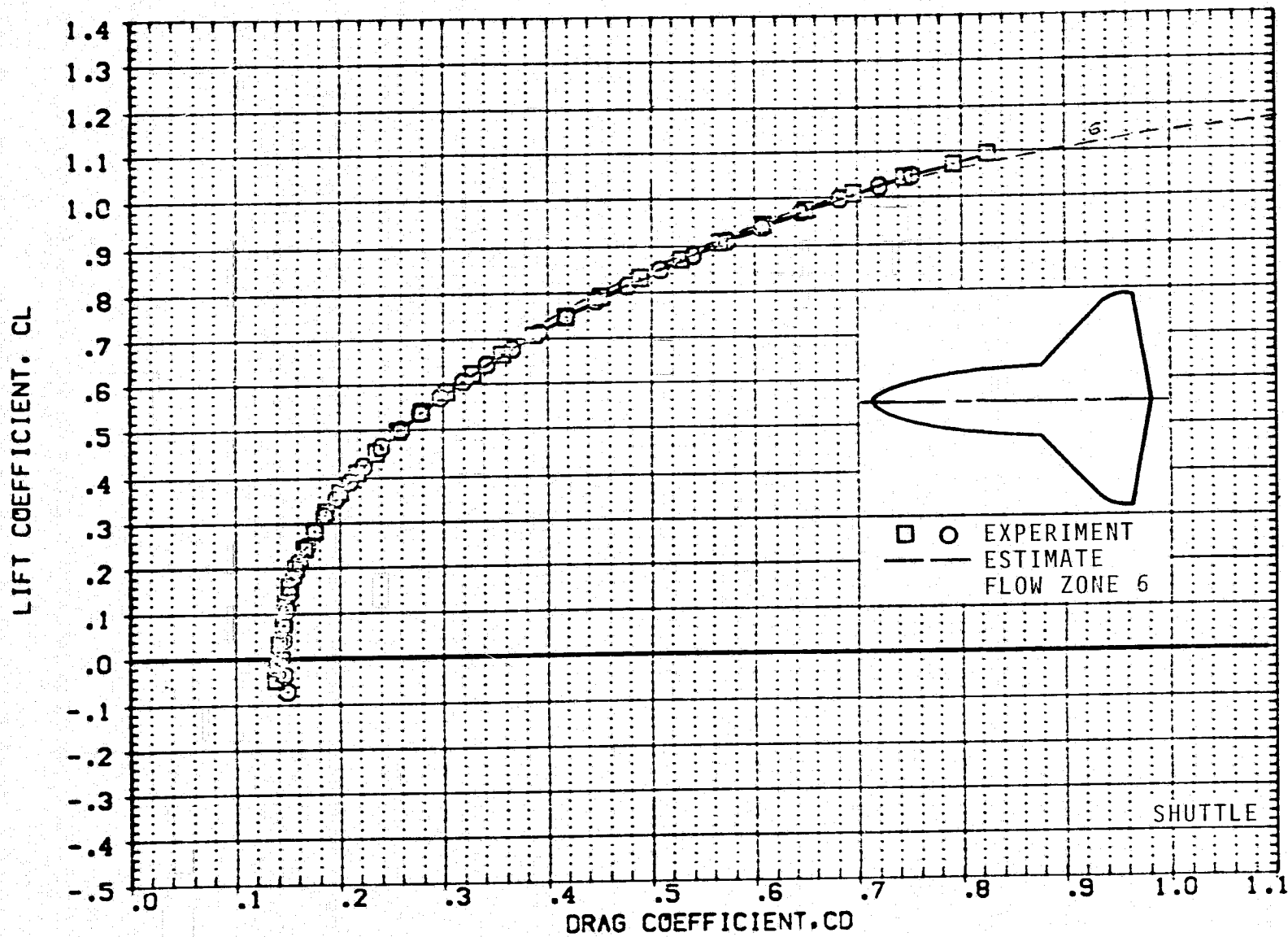
(1) C_m VERSUS α ; $M = 1.6$.

FIGURE 10.- CONTINUED.



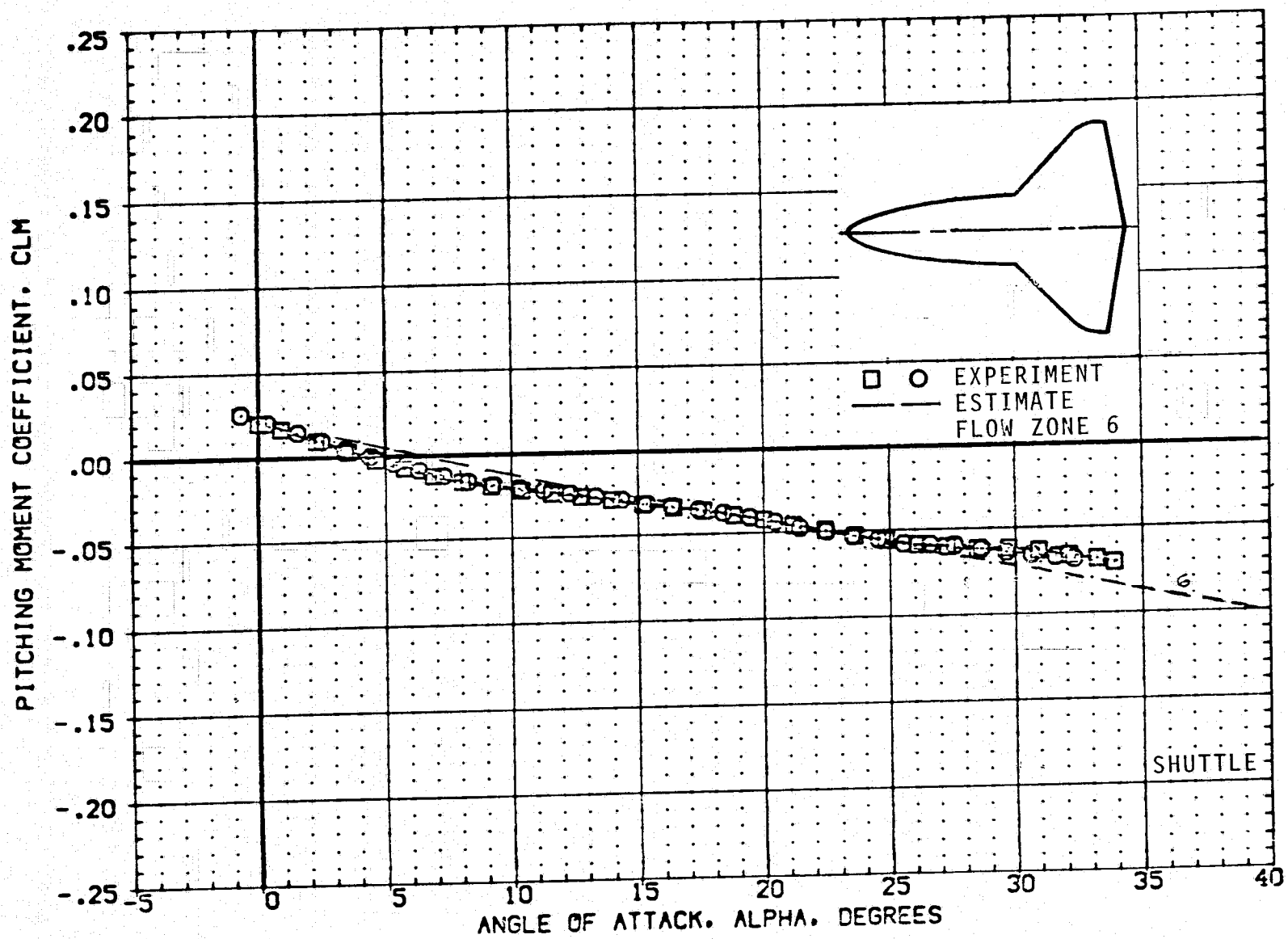
(m) C_L VERSUS α ; $M = 2.0$.

FIGURE 10.- CONTINUED.



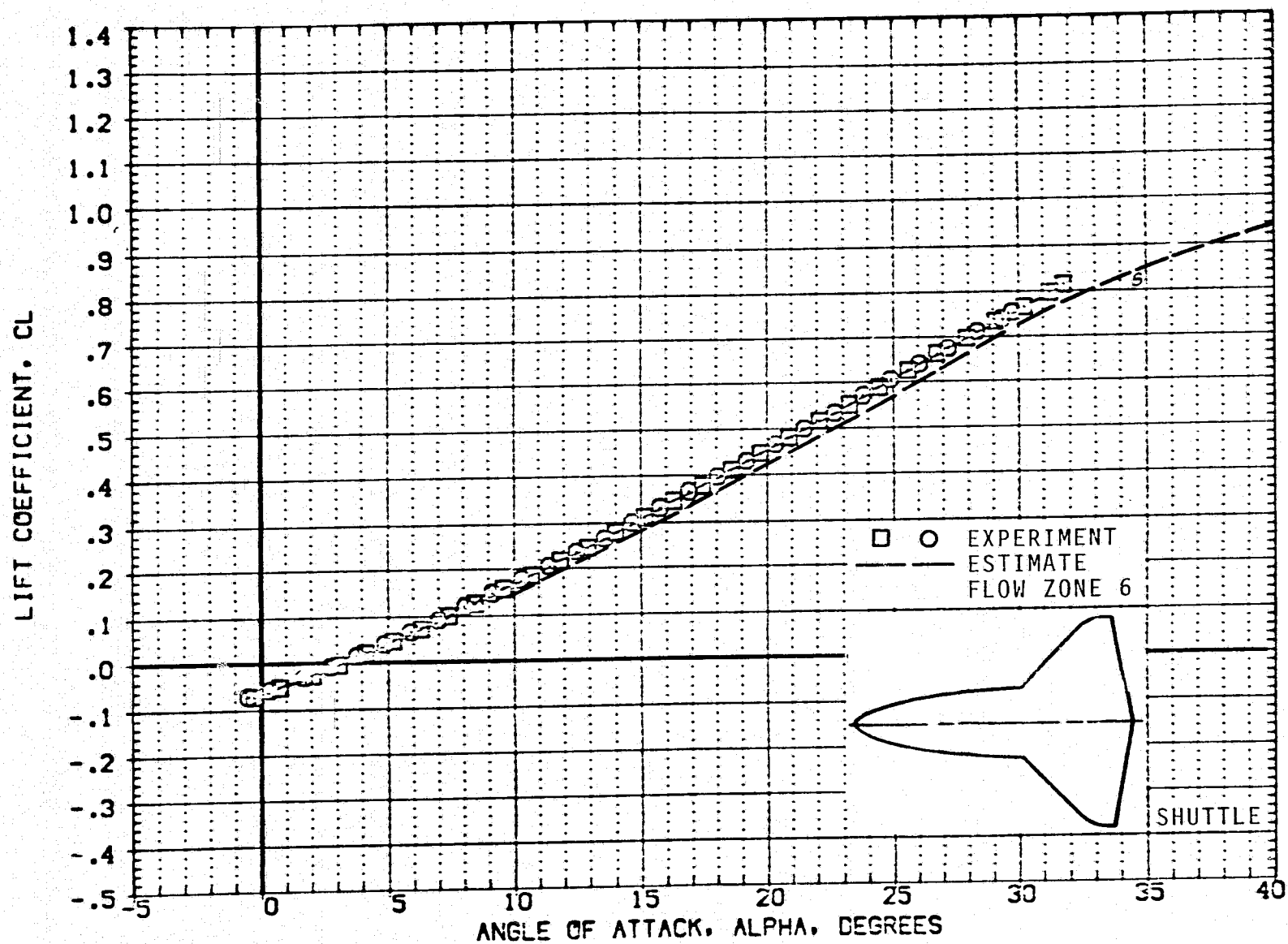
(n) C_L VERSUS C_D ; $M = 2.0$.

FIGURE 10.- CONTINUED.



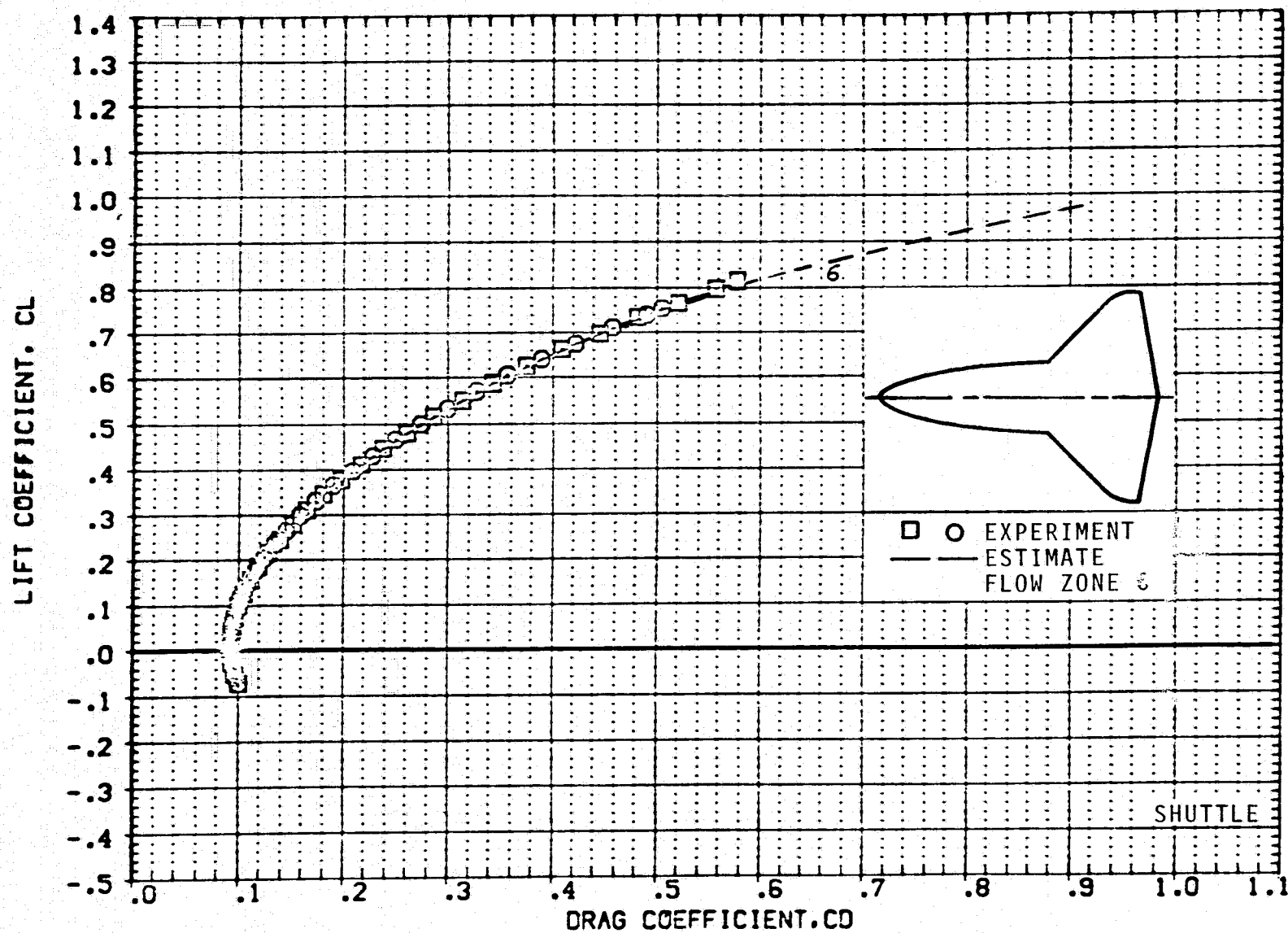
(o) C_m VERSUS α ; $M = 2.0$.

FIGURE 10.- CONTINUED.



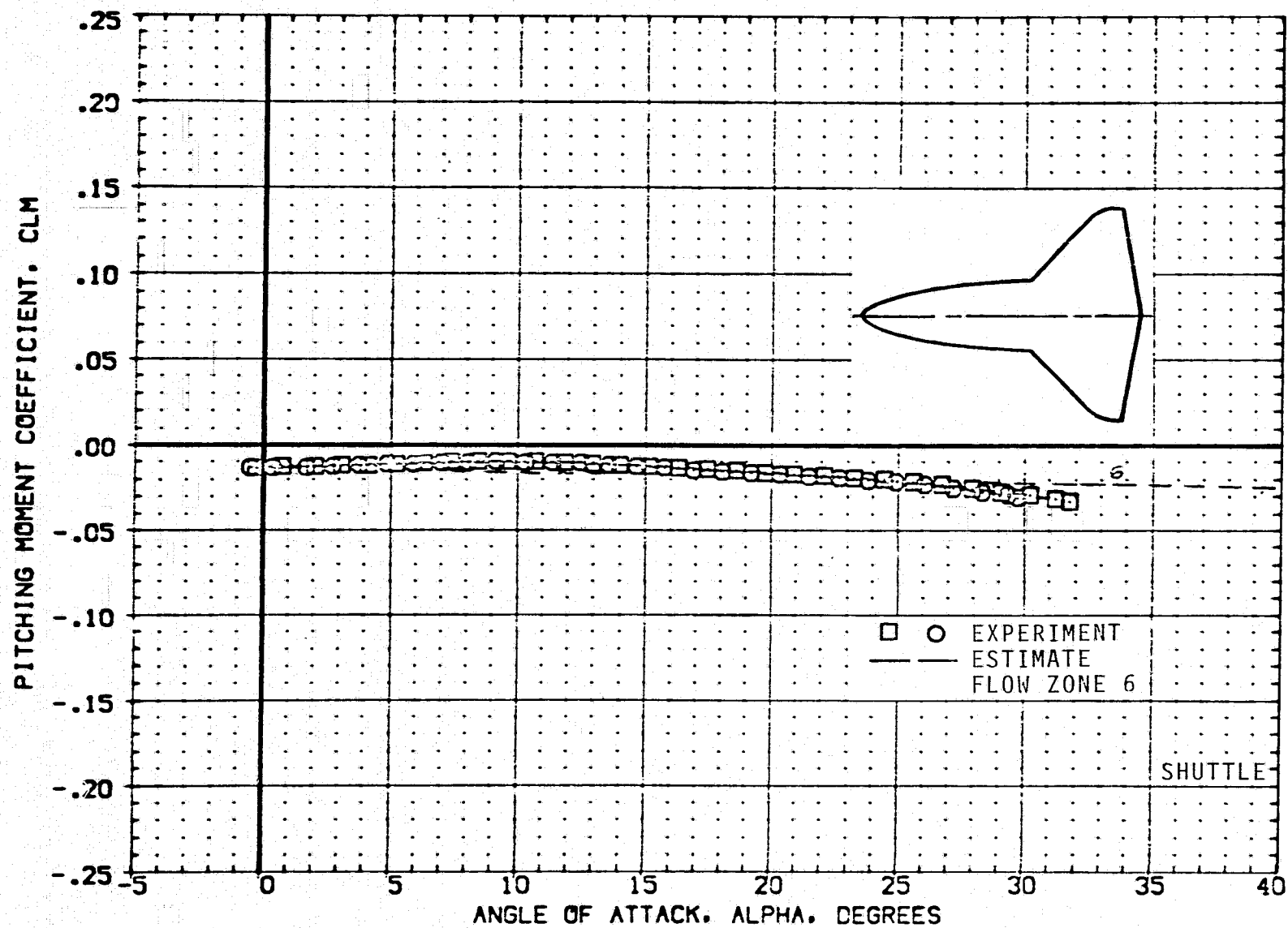
(p) C_L VERSUS α ; $M = 4.0$.

FIGURE 10.- CONTINUED.



(q) C_L VERSUS C_D ; $M = 4.0$.

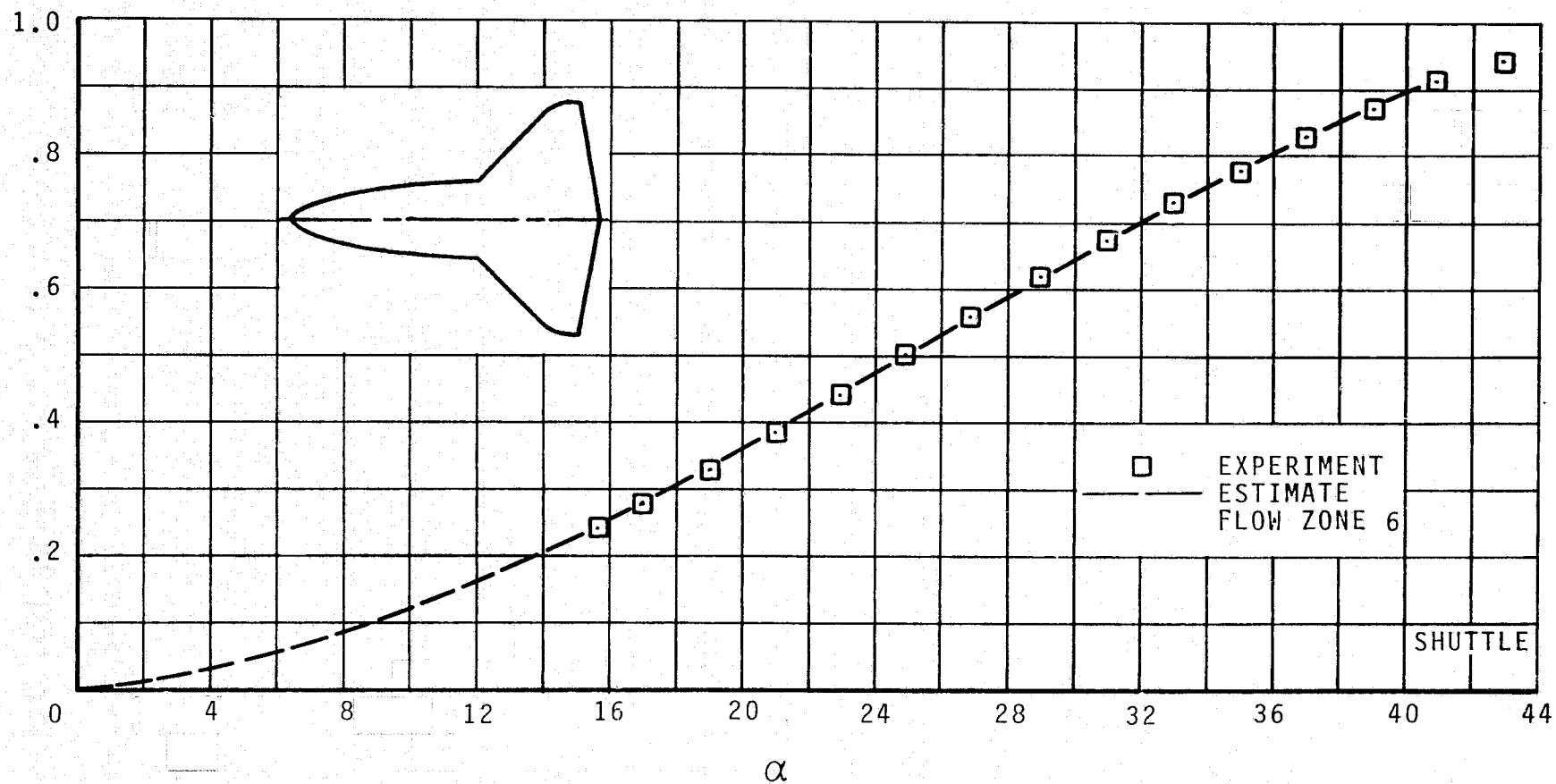
FIGURE 10.- CONTINUED.



(r) C_m VERSUS α ; $M = 4.0$.

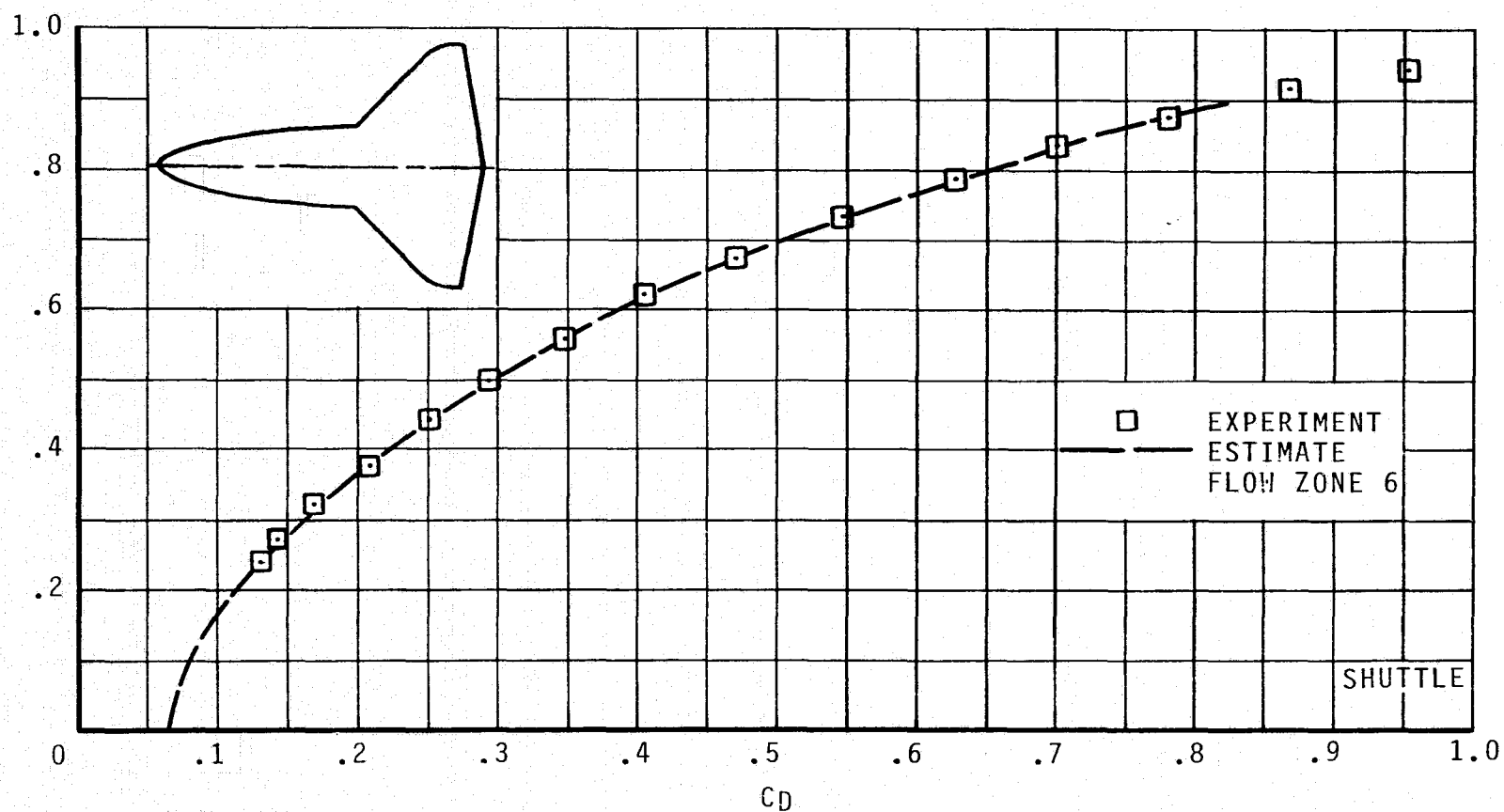
FIGURE 10.- CONTINUED.

135



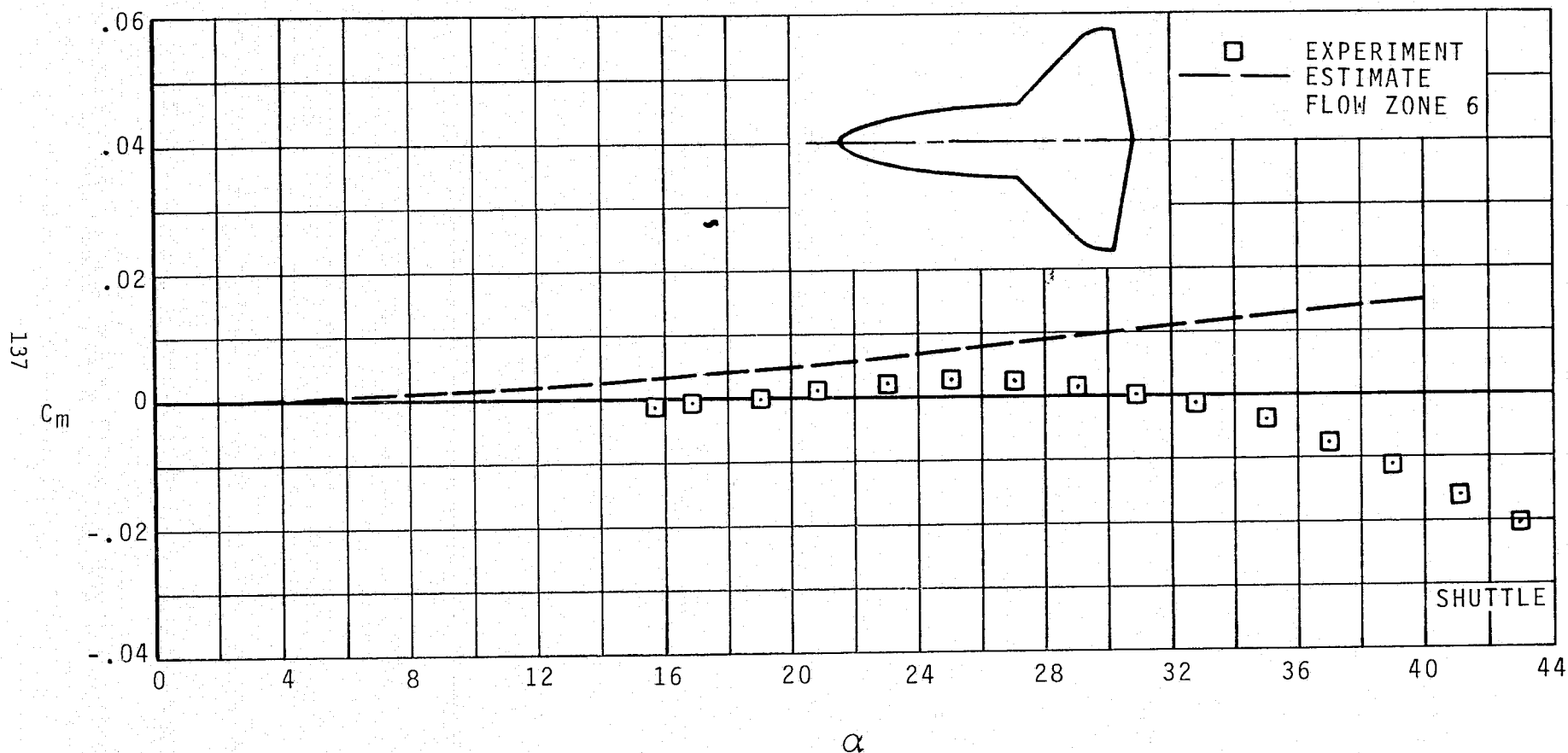
(s) C_L VERSUS α ; $M = 8.0$.

FIGURE 10.- CONTINUED.



(t) C_L VERSUS C_D : $M = 8.0$.

FIGURE 10.- CONTINUED.



(u) C_m VERSUS α ; $M = 8.0$.

FIGURE 10.- CONCLUDED.